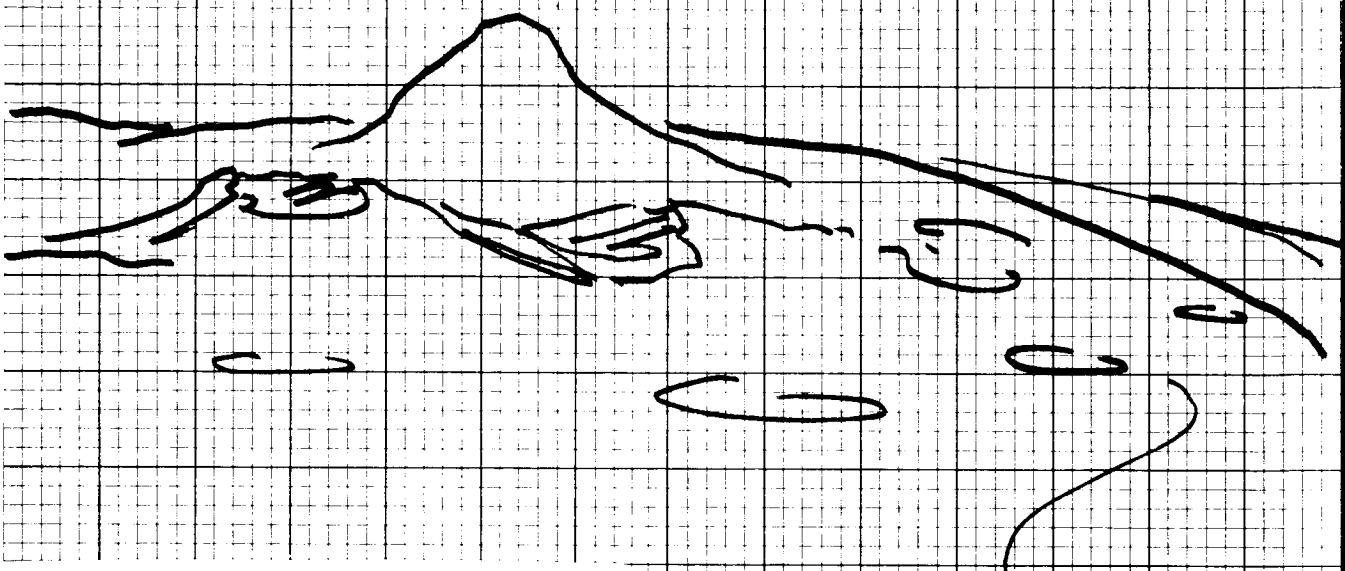

DUAL-MODE LUNAR ROVING VEHICLE NAVIGATION SYSTEMS (FINAL REPORT)

PRINCIPAL INVESTIGATOR: J. C. HUNG

JANUARY 20, 1970

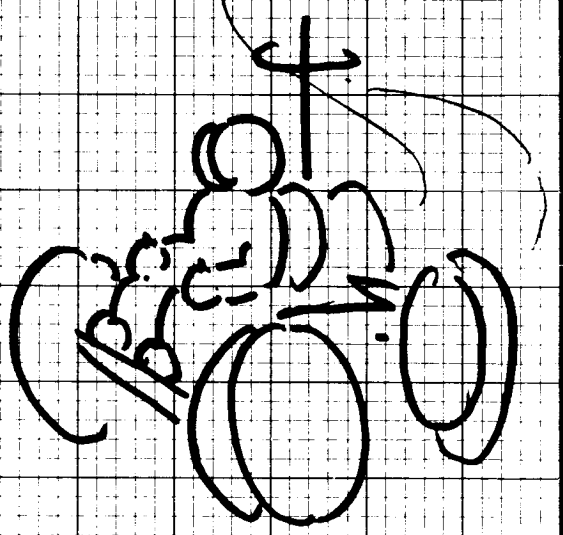

PREPARED FOR GEORGE C. MARSHALL SPACE FLIGHT CENTER, NATIONAL AERONAUTICS AND SPACE ADMINISTRATION, UNDER CONTRACT NAS8-24858/DCN 1-X-40-90850 (1F).

THE UNIVERSITY OF TENNESSEE
DEPARTMENT OF ELECTRICAL ENGINEERING • SYSTEMS RESEARCH

Copy No. 000082

Scientific Report No. 20

Systems Research

DUAL-MODE LUNAR ROVING VEHICLE NAVIGATION SYSTEMS

(FINAL REPORT)

Prepared for George C. Marshall Space Flight Center
National Aeronautics and Space Administration
under Contract NAS8-24858/DCN 1-X-40-90850 (1F)

January 20, 1970

Principal Investigator: James C. Hung

Department of Electrical Engineering
The University of Tennessee
Knoxville, Tennessee 37916

ACKNOWLEDGEMENT

The material contained in this report represents the combined effort of members of the staff at the University of Tennessee and at the NASA Marshall Space Flight Center. The progress of this study was made possible by the generous assistance of Mr. N. Neudatschin of the Astrionics Laboratory, MSFC.

The major contributors to the project activity at the University of Tennessee are:

Dr. J. C. Hung, Principal Investigator
Mr. J. S. Miller
Mr. J. E. Bennett
Mr. C. Chen

Others, who have contributed directly to the project, include:

Mr. H. Holley
Mr. S. C. Sung
Mr. P. F. Bhavsar
Mr. J. D. Barton

The skillful preparation of the manuscript by Mrs. Anne Bateson is appreciated.

TABLE OF CONTENTS

LIST OF FIGURES

LIST OF FIGURES (Continued)

LIST OF FIGURES (Continued)

LIST OF TABLES

CHAPTER 1

INTRODUCTION

This is the final report on the study of navigation systems for the Dual-Mode Lunar Roving Vehicle (DLRV). The study was initiated by the National Aeronautics and Space Administration, and was performed at the University of Tennessee over a period of seven months.

1-1 Project Objectives

NASA's Lunar Roving Vehicle (LRV) program is a logical step in man's exploration of space and the earth's celestial neighbors. The historic Apollo adventures have dramatically put man's footprints on the moon. Now NASA's Apollo Application program will assure that the technological advancements which made possible this epic voyage will be fully exploited. One important part of the Apollo Application program is the LRV. This vehicle is an important tool that will help to maximize one of the returns in our investment in space, namely, new information about lunar environment.

The DLRV, an advanced type of LRV, will have dual mode capability so that it can be operated by astronauts aboard the vehicle or by earth-based remote controllers. The objectives that have been set for the DLRV demand that the vehicle be equipped with an accurate and reliable navigation system. The selection of this navigation system is the subject of the investigation described in this report.

1-2. System Requirements

The requirements for the navigation system to be used on the DLRV are set by the mission planned for the vehicle. At the beginning, the vehicle will leave the Lunar Excursion Module (LEM) and be driven around by astronauts in the manned mode for a short period within 10 kilometers of the LEM. After astronauts return to the earth the vehicle will depart from the LEM for a long distance trip across the lunar surface in the remote-controlled mode. During this journey, the DLRV

will make many stops to collect scientifically important lunar samples by automatic means. At the end of this translunar trip, it will be met by astronauts who will unload the samples from the vehicle for scientific analysis.

Clearly, it is necessary to know the position of the DLRV if the astronauts must return to the LEM in the manned mode and if the astronauts are going to meet the vehicle at the end of its translunar trip. The navigation system will also support the scientific experiments performed during the lunar sorties. It will be possible to use navigation data to record, for any collected sample, the exact location where it was obtained. The reduction of the information generated by the navigation system will also add a new and valuable technique for accurate mapping of the lunar surface. As a matter of fact, scientists planning the experiments that will be carried on the LRV desire a precise measure of the vehicle position.

A list of considerations for the DLRV navigation system is shown below:

1. A maximum travel distance of 1,000 km during a one year period
2. A maximum manned speed of 15 km per hour and a maximum unmanned speed of 2 km per hour
3. A desired navigation accuracy of 10 meters in the horizontal directions and 1 meter in altitude with respect to a given lunar map or a given lunar landmark.
4. The knowledge of DLRV at all times (implying a continuous navigation.)
5. A maximum weight of 7 kg.
6. Reliability consideration
7. Volume consideration
8. Human factor consideration
9. Power consideration

To meet the continuous navigation requirement, a dead reckoning navigator must be employed. However, on the long DLRV mission, the error accumulated with time when a dead reckoning navigator is used would be prohibitively large. Therefore some type of position fixing scheme will be needed to periodically update the position provided by the dead reckoning navigator. As a result, the DLRV navigation system will consist of both a dead reckoning and a position fix navigator.

1-3. The Report

Although navigation is an old art, there still is need for the development of new concepts and better techniques to suit various, particular applications. This report contains many considerations, new concepts, and attractive techniques which have not appeared elsewhere. These new developments are scattered in Chapters 4 to 7 of the report.

A preliminary review of possible navigation components for the DLRV is given in Chapter 2. Components which are obviously unsuitable for DLRV application will be eliminated from study.

The formulation of two sets of navigation equations using lunar coordinates are contained in Chapter 3. Equations needed for the study of navigation errors caused by hardware imperfection are provided for each set.

Chapter 4 considers the usefulness of a pure odometer navigation system for measuring not only the distance traveled by the LRV but also the LRV heading.

Chapter 5 discusses the problems associated with the mechanization of dead reckoning navigation systems using various kinds of sensors. Several new ways of using the components are suggested.

Chapter 6 presents six position fix schemes, two of them make use of celestial bodies with known ephemerides and the others require the use of a lunar satellite. Sensitivity analyses and computation equations for all schemes are provided.

Chapter 7 suggests several new methods of using landmarks for LRV navigation. Only angle measurements are required in these methods. The attractiveness of the methods is discussed in detail.

Comparisons of various types of navigation systems are given in Chapter 8. For the purpose of comparison, a base-line system is proposed as a comparison standard.

A summary of this report and a list of recommended future activities are included in Chapter 9.

The final attachments to the report include a list of references and eight appendices. The appendices contain all the lengthy derivations of the equations shown in the text.

1-4. Coordinate Systems

Three coordinate systems will be used in this report. They and their respective unit vectors are defined in Table 1-1 and shown in Fig. 1-1.

Coordinate System	Origin	Set of Unit Vectors
S1, vehicle centered and vehicle oriented	Vehicle	$\hat{i}_1$ - Along vehicle's forward axis $\hat{j}_1$ - Completing the right hand triad $\hat{k}_1$ - Along vehicle's rightward axis
S2, vehicle centered and lunar coordinate oriented	Vehicle	$\hat{i}_2$ - Eastward along constant latitude line $\hat{j}_2$ - Northward along lunar meridian $\hat{k}_2$ - Completing the right-hand triad (radially outward)
S3, lunar centered and inertially oriented	Lunar Center	$\hat{i}_3$ - Passing through the lunar equator $\hat{j}_3$ - Passing through the lunar equator $\hat{k}_3$ - Passing through the lunar north pole

Coordinate Systems

Table 1-1

S2 and S3

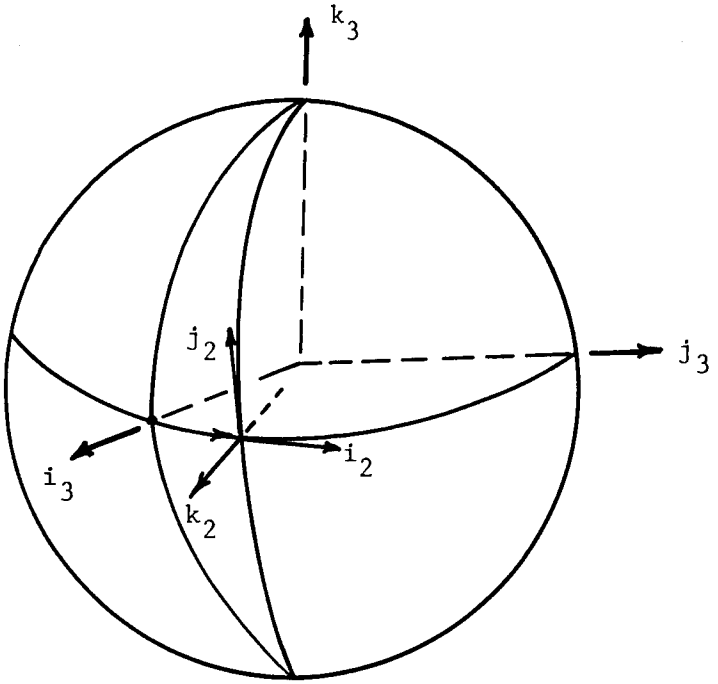

S1

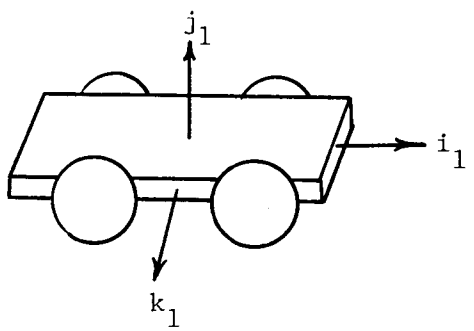

Coordinate Systems and Their Unit Vectors

Fig. 1-1

CHAPTER 2

NAVIGATION SYSTEM COMPONENTS

2-1. Navigation Components

Hardware components such as gyros, radars, accelerometers, and computers are the building blocks that make up navigation systems. The job of the system designer is to use these building blocks to organize and design a system of blocks that is the best solution to the problem at hand. A large collection of building blocks is available for consideration by the designer of a navigation system. What follows is a listing of some of these components. The hardware components are classified according to the function that they perform.

Table II-1 also lists several of these components and gives some pertinent data about them. The information in this table is from reference number 4.

2-2. Velocity Determination

Doppler Radar

The doppler radar is a single beam device that would be mounted on the LRV so that a radar beam would be transmitted forward along the vehicle longitudinal axis. The return signal reflected from stationary lunar objects would be received and compared with the transmitted signal. The doppler frequency shift between the transmitted and received signals would be proportional to the component of LRV velocity along the vehicle longitudinal axis. Other components of the velocity would be approximated as zero.

The doppler radar appears unsuited to the LRV application for two reasons. First, the error in velocity measurement for the doppler radar is independent of the vehicle speed. For the slow speeds expected for the unmanned DLRV this characteristic tends to cause measurement errors that are a large percent of the vehicle speed. Second, the present on-the-shelf doppler radar is too heavy. However, there are means to get around these difficulties. Therefore radar is considered a candidate.

Sensor	Weight kg	Volume cm	Power Watts	Three Sigma Accuracy State of the Art
Doppler radar	12	20000	125	0.01 km/hr.
Accelerometer	1	164	5	null 4×10^{-8} earth g; linearity of gain 10^{-6}
Odometer	0.2	--	--	0.01%
Pendulous inclinometer	0.2	150	15	0.01 degree
Vertical Gyro	2	1000	20	null 0.01 degree; drift 0.01 deg/hr; linearity of gain 0.0003
Directional Gyro	1.5	500	12	null 0.1 degree; drift 0.005 deg/hr.
Sun Tracker	2	1400	10	null error 0.25 degree
Star Tracker	5	16000	15	null error 0.001 degree

Navigation Sensor Data

Table 2-1

Accelerometers

Accelerometers mounted on the LRV can be used to measure the components of the vehicle acceleration along the LRV axes. This acceleration can be resolved along some fixed axes and then twice integrated to determine the LRV position.

The accelerometer null bias and linear error both contribute to the navigation inaccuracy. The effect of the accelerometer bias can be reduced by including a simple logic circuit that will stop the integration of the accelerometer signal when the wheel odometers indicate that the vehicle is parked.

Because of the accuracy of state of the art devices and their light weight (1 kg.) inertial accelerometers are worthy of consideration for LRV navigation.

Odometers

Odometers measuring the angular rate of the LRV wheels are obvious candidates for determining the vehicle velocity. They are especially attractive because the odometer signals are available from the electric motors that are used to drive the LRV. Consequently no weight is charged to the navigation system for the inclusion of odometers. An important source of error is wheel slipping.

2-3. Vertical Determination

Inclinometer

The most obvious method for determining the vertical is with a pendulous inclinometer. This vertical sensing instrument is either an electrolytic or electromagnetic, liquid damped pendulum device. It is lightweight - - only about 0.2 kg.

One potentially degrading feature of a pendulous inclinometer is that it will swing when the vehicle accelerates. This disadvantage can be avoided by using a heavier vertical gyro.

Vertical Gyro

A vertical gyro is a second technique for determining the local vertical. This instrument consists of a gyro with its spin axis maintained parallel to

the local gravity vertical by a gravity sensitive device. The advantage of a vertical gyro is that the vertical gyro is not disturbed by vehicle acceleration. A weight penalty must be paid to achieve this advantage. The vertical gyro weighs about 2 kg, ten times as much as a simple inclinometer.

The vertical gyro's insensitivity to vehicle acceleration is achieved by disconnecting the gyro from the vertical reference signal whenever it is recognized that the vehicle is accelerating. On the LRV the wheel odometer signals could be used to sense acceleration and cause the gyro to be disconnected from the pendulous vertical reference. Or the vertical reference could be applied to the gyro only during those periods when the LRV is stopped. During the time when it is disconnected from the vertical gravity reference the gyroscope maintains the vertical direction because of its gyroscopic characteristics.

Both the pendulous inclinometer and the vertical gyro are gravity sensitive devices. Neither of them will compensate for local gravity anomalies in order to provide the geometric vertical. Although this will probably cause serious difficulties for those DLRV position fixing schemes that require the local vertical, this gravity anomaly problem is not expected to have a serious impact on the dead reckoning schemes.

2-4. Azimuth Determination

Directional Gyro

A directional gyro can be used for azimuth determination. This is a two degree of freedom instrument with the spin axis maintained in the horizontal plane. Precisely determined torques must be applied to the gyro in order to keep the spin axis in the horizontal plane as the horizontal plane rotates in inertial space because of the lunar rotation and vehicle motion across the lunar surface. This method of azimuth determination is attractive because it is self-contained and because many years of evolutionary refinement have been devoted to this navigational technique.

Sun Sensor

A celestial reference such as the sun provides a second technique for azimuth determination. The measured line of sight from the vehicle to the sun can be projected into the measured horizontal plane. The lunar ephemeris

will locate $\hat{i}_2$ in the horizontal plane relative to this projected celestial line of sight if the navigator knows the time and lunar region where the LRV is located.

It is encouraging to notice that the moon rotational rate is much less than the earth's. During a three hour LRV sortie the moon will rotate only about 1.5°. Consequently it might be possible to use the same ephemeris data for the duration of a sortie rather than continuously updating the ephemeris.

One mission restriction imposed by the use of the sun line of sight for azimuth determination is that the LRV must not go behind any objects that would obstruct the vehicle to sun line of sight. Obviously such a device could not function during the lunar night.

One instrument for measuring the line of sight to the sun is a sun aspect sensor. In this device the pattern of a reticle shadow is observed by an array of photoelectric cells and electronically translated into a measurement of the sun line of sight direction. This device is attractive because it is fixed on the LRV and does not require moving gimbals as would a conventional sun tracker. It is expected that a sun aspect sensor would weigh less than 2.5 kg and could provide about one arc minute angular resolution.

An alternate technique for determining the line of sight from the vehicle to the sun is to use a gimbaled sun tracker that would utilize a photoelectric device as a sensor and a closed tracking loop to keep the axis of the device pointed at the sun. This technique is unattractive because the required gimbals would probably be heavier than the digital sun aspect sensor.

2-5. Position Fixing - Line of Sight Devices

Celestial Trackers

In order to use star sightings to generate a position fix for the LRV it is necessary to measure the direction to known stars. This measurement is performed using an optical star tracker. It is also possible that this device could be used to measure the direction to an artificial lunar satellite.

Doppler Radar

One method of determining a position fix involves measuring the range for a navigation satellite as it passes overhead. A doppler radar is used for this measurement.

Radar

Conventional radars that measure the time delay for the reflection of a transmitted signal could be used to measure the distance and direction from the LRV to an artificial lunar satellite. These measurements could be used to establish a position fix.

Laser

A laser tracker offers an alternate method of measuring the direction of an artificial satellite. The primary advantage of a laser is its very narrow beam width.

Transit

Lunar landmarks can be used for navigation. Clearly, landmarks that are shown on available lunar maps could be used to help establish a position fix for the LRV. A transit can be used to make angular measurements. The required accuracy and the corresponding size and weight of the transit will depend upon the role that is assigned to landmark navigation techniques. If landmark navigation is used as a primary system for establishing precise position fixes, then a very accurate transit will be required. If, on the other hand, landmark navigation is reserved as a simple, reliable, back-up navigation system, then the accuracy requirements can be relaxed. Some of the schemes discussed in Chapter 8 could provide valuable guidance information to an astronaut even if he were forced to walk back to the LEM from a disabled LRV. The transit suited to this purpose could be so simple and lightweight that it would be carried in a pocket of the astronaut's suit.

2-6. Orientation Determination

The level of detail at which a system designer is working determines what he considers to be components of his system. Here, gyroscopes and odometers have been listed as components that are used in navigation systems. However, the designer of a gyroscope might very well list the rotor and the gimbals as components of his design. Similarly, a system designer studying the problem of optimally integrating the information obtained from dead reckoning and position fix navigation techniques might very well consider a complete inertial platform as one component in the overall navigation scheme. Two different types of inertial platforms are available: gimbaled platforms and strapdown or computational platforms. Both types of platform have the same purpose. They measure the vehicle orientation in space.

Gimbaled Platform

The classic inertial platform that has been used for many years is a gimbaled inertial platform. In this mechanism the signals from gyros are used to stabilize in space the orientation of a mechanical gimbal. The gyroscopes are mounted on the gimbals of a gimbal system that has two or more degrees of freedom. One of the gimbals is fixed to the vehicle. Signals from the gyroscopes drive torque motors that apply to the gimbals whatever torques are required to stabilize in space the gimbal that is the actual inertial platform. The gimbal angles provide a measure of the vehicle orientation relative to the stabilized gimbal and, consequently, provide a measure of the vehicle orientation relative to space.

The mechanical gimbals required for this type of platform are heavy. Therefore the gimbaled platform is unsuited to the LRV application.

Strapdown or Computational Platform

An alternate way to determine the vehicle orientation is with a strapdown or computational platform. The instruments used in a strapdown platform are rate gyros with their sensitive axes mounted along three orthogonal vehicle axes. By resolving the measured angular rate of the vehicle into an inertial coordinate system and then integrating the angular rate, a continuous measure of the vehicle orientation is generated. The resolution and integration of the angular

rate is performed by a special purpose digital computer. This type of platform is simpler from the instrument standpoint and thus can be lighter and smaller than a gimbaled inertial platform.

CHAPTER 3

DEAD RECKONING NAVIGATION EQUATIONS

3-1. Dead Reckoning

Dead reckoning is the technique of integrating a vehicle's velocity vector with respect to time in order to maintain a continuous measure of the vehicle position. Fig. 3-1 is a block diagram description of the dead reckoning navigation concept. The dead reckoning schemes considered here measure, resolve, and integrate the velocity vector in three steps.

1. The LRV velocity vector is measured and the LRV orientation relative to lunar navigation coordinates is also measured.
2. The information measured in step 1 is used to resolve the LRV velocity along lunar fixed navigation coordinates.
3. The LRV velocity components are integrated with respect to time to determine the LRV position.

In this chapter the sets of navigation equations relating the velocity vector of the LRV to its position on the lunar surface are presented. A position on the lunar surface is defined by a triad including the longitude, the latitude, and the distance from the lunar center. Two sets of navigation equations are discussed. The first one assumes a spherical lunar surface. The second one is an approximation of the first. The simplified equations are accurate enough for LRV navigation if its excursion range is small.

3-2. Navigation Equation Set No. 1

This section presents a set of navigation equations where no approximation is made. Navigation is considered in east, north, and vertical directions. No assumptions are imposed on the lunar terrain nor on the LRV excursion range.

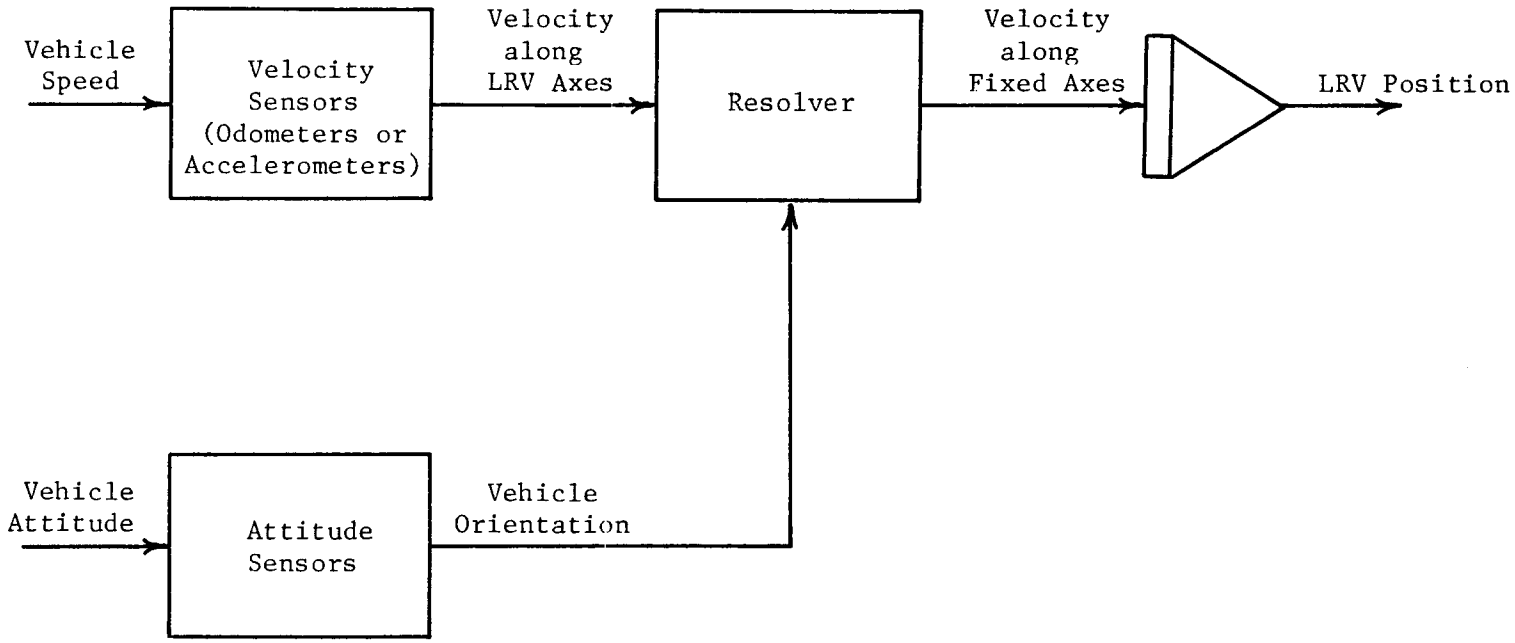

Dead Reckoning Navigation Concept

Fig. 3-1

Navigation Equations

The geometry of special lunar coordinates is depicted in Fig. 3-2. In this figure there are latitude L, longitude λ, horizontal distance H, eastward distance E, northward distance N, radial distance R, and ΔX for the increment of any variable X. V represents the velocity of a reference point on the LRV, Ψ is the heading angle of V and θ is the elevation angle of V.

Let S be the linear distance, then we have the following incremental quantities.

ΔS = incremental distance

ΔH = incremental horizontal distance

$= \Delta S \cos\theta = V \cos\theta \, \Delta t$

ΔR = incremental radial distance

$= \Delta S \sin\theta = V \sin\theta \, \Delta t$

ΔL = incremental latitude change

$$= \frac{\Delta H \cos\Psi}{R} = \frac{V \cos\theta \cos\Psi}{R} \Delta t$$

$\Delta\lambda$ = incremental longitude change

$$= \frac{\Delta H \sin\Psi}{R \cos L} = \frac{V \cos\theta \sin\Psi}{R \cos L} \Delta t$$

Taking limits gives the following rate equations.

$$V_H = \dot{H} = V \cos\theta \,, \quad \text{horizontal speed} \qquad (3\text{-}1)$$

$$V_R = \dot{R} = V \sin\theta \,, \quad \text{vertical speed} \qquad (3\text{-}2)$$

$$\Omega_L = \dot{L} = \frac{V_H \cos\Psi}{R} \,, \quad \text{latitude rate} \qquad (3\text{-}3)$$

$$\Omega_\lambda = \dot{\lambda} = \frac{V_H \sin\Psi}{R \cos L} \,, \quad \text{longitude rate} \qquad (3\text{-}4)$$

Integrating the last three equations yields

$$\text{Latitude } L = L_o + \int \Omega_L \, dt$$

$$= L_o + \int \frac{V \cos\theta \cos\Psi}{R} \, dt \qquad (3\text{-}5)$$

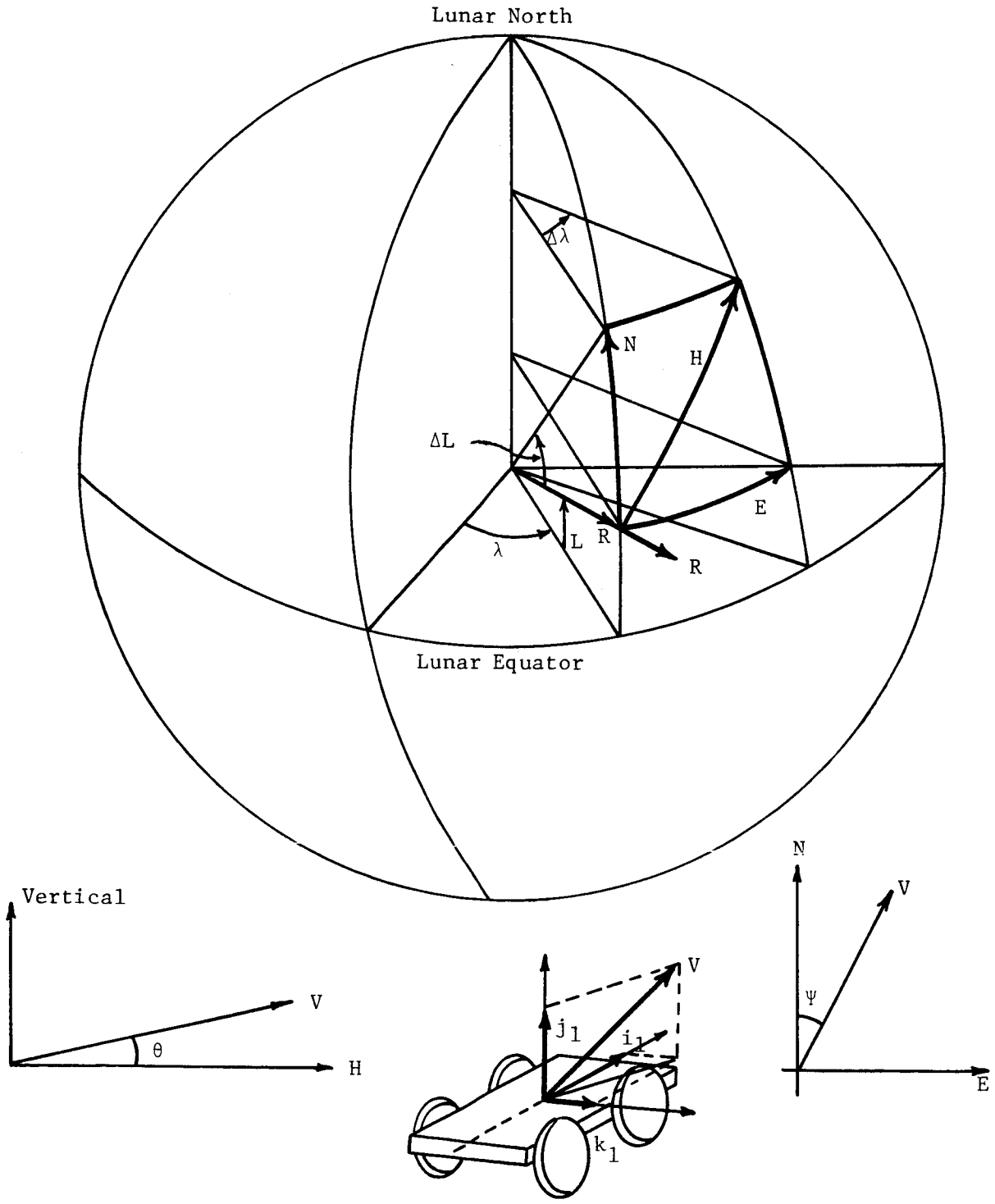

Geometry of Lunar Coordinates

Fig. 3-2

$$\text{Longitude } \lambda = \lambda_o + \int \Omega_\lambda \, dt$$

$$= \lambda_o + \int \frac{V \cos \theta \sin \Psi}{R \cos L} \qquad (3\text{-}6)$$

$$\text{Altitude } R = R_o + \int V_R \, dt$$

$$= R_o + \int V \sin \theta \, dt \qquad (3\text{-}7)$$

The above three equations give the position of the LRV in terms of lunar coordinates. The computations involved in these equations are shown in block diagram, Fig. 3-3.

Error Analysis

Because of the imperfection of sensors the measured quantities always differ from actual quantities. The differences lead to errors in navigation.

Let ε_X denote the errors in X', the measured value of X. Then we have

$\theta' = \theta + \varepsilon_\theta$ = measured pitch angle

$\Psi' = \Psi + \varepsilon_\Psi$ = measured heading

$V' = V + \varepsilon_V$ = measured speed.

Then

$$V_H' = V' \sin \theta' = (V + \varepsilon_V) \sin (\theta + \varepsilon_\theta)$$

$$V_R' = V' \cos \theta' = (V + \varepsilon_V) \cos (\theta + \varepsilon_\theta)$$

$$\Omega'_L = \frac{V'_H \cos \Psi'}{R'} = \frac{(V + \varepsilon_V) \sin (\theta + \varepsilon_\theta) \cos (\Psi + \varepsilon_\Psi)}{R + \varepsilon_R}$$

$$\Omega'_\lambda = \frac{V'_H \sin \Psi'}{R' \cos L'} = \frac{(V + \varepsilon_V) \sin (\theta + \varepsilon_\theta) \sin (\Psi + \varepsilon_\Psi)}{(R + \varepsilon_R) \cos (L + \varepsilon_L)}$$

Integrating the last three equations gives

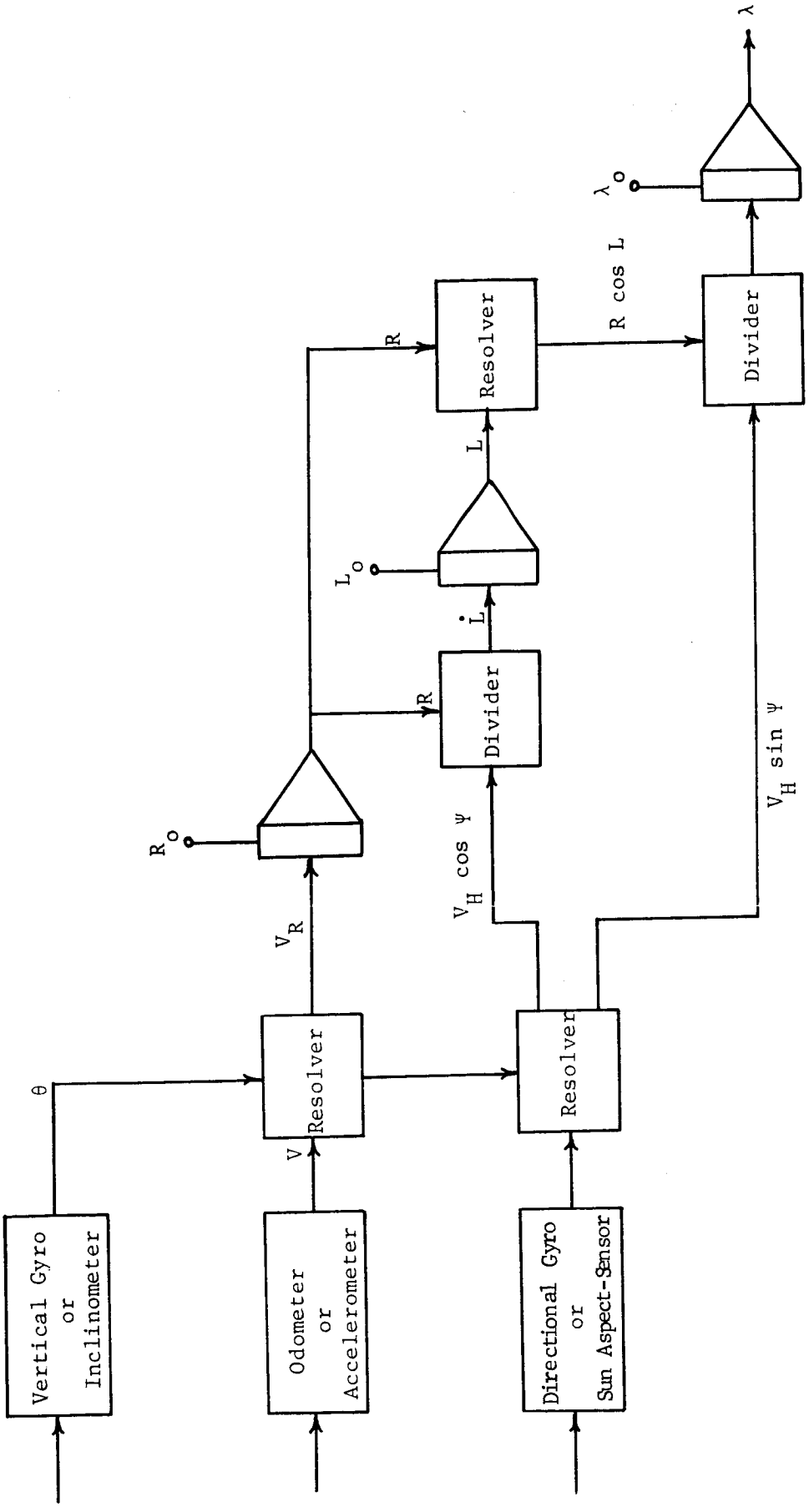

Computational Block Diagram

Fig. 3-3

$$L' = L + \varepsilon_L$$

$$= L_o + \varepsilon_{L_o} + \int \frac{(V + \varepsilon_V) \sin (\theta + \varepsilon_\theta) \cos (\Psi + \varepsilon_\Psi)}{R + \varepsilon_R} \, dt \quad (3\text{-}8)$$

$$\lambda' = \lambda + \varepsilon_\lambda$$

$$= \lambda_o + \varepsilon_{\lambda o} + \int \frac{(V + \varepsilon_V) \sin (\theta + \varepsilon_\theta) \sin (\Psi + \varepsilon_\Psi)}{(R + \varepsilon_R) \cos (L + \varepsilon_L)} \, dt \quad (3\text{-}9)$$

$$R' = R + \varepsilon_R$$

$$= R_o + \varepsilon_{R_o} + \int (V + \varepsilon_V) \cos (\theta + \varepsilon_\theta) \, dt \quad (3\text{-}10)$$

Subtracting (3-5), (3-6), (3-7) from (3-8), (3-9), (3-10), respectively, we obtain the following error equations for LRV navigation.

$$\varepsilon_L = \varepsilon_{L_o} + \int \frac{(V + \varepsilon_V) \sin (\theta + \varepsilon_\theta) \cos (\Psi + \varepsilon_\Psi)}{R + \varepsilon_R} \, dt$$

$$- \int \frac{V \cos \theta \cos \Psi}{R} \, dt \quad (3\text{-}11)$$

$$\varepsilon_\lambda = \varepsilon_{\lambda_o} + \int \frac{(V + \varepsilon_V) \sin (\theta + \varepsilon_\theta) \sin (\Psi + \varepsilon_\Psi)}{(R + \varepsilon_R) \cos (L + \varepsilon_L)} \, dt$$

$$- \int \frac{V \cos \theta \sin \Psi}{R \cos L} \, dt \quad (3\text{-}12)$$

$$\varepsilon_R = \varepsilon_{R_o} + \int (V + \varepsilon_V) \cos (\theta + \varepsilon_\theta) \, dt - \int V \cos \theta \, dt \quad (3\text{-}13)$$

The above equations show that navigation errors are a nonlinear function of measurement errors. To study the effect of measurement errors on navigation, these equations can be simulated by digital computers.

3-3. Navigation Equation Set No. 2

When the excursion range of the LRV is small, a set of simplified navigation equations can be used. Two approximations are made, namely

i) $R = R_o$, a constant, in Equations (3-5) and (3-6)

ii) $\cos L = \cos L_o$, a constant, in Equation (3-6)

Consider the MLRV mission where the excursion range will be less than 5 km. The maximum change in latitude is

$$\Delta L_{max} = \frac{5}{1738} = 0.00288 \text{ radian} = 0.16°$$

where 1738 is the lunar radius in km. Within $\pm$ 20° of lunar equator the maximum change in cos L for 5 km excursion is

$$\left|\cos 20° - \cos 19.84°\right| = \left|-0.93969 + 0.94068\right| = 0.00099.$$

This contributes to a maximum final position error of about 0.099%.

Navigation Equations

Applying the two approximations mentioned above, Equations (3-5), (3-6), and (3-7) become

$$\text{Latitude } L = L_o + \frac{1}{R_o}\int V \cos\theta \cos\Psi \, dt \qquad (3\text{-}14)$$

$$\text{Longitude } \lambda = \lambda_o + \frac{1}{R_o \cos L_o}\int V \cos\theta \sin\Psi \, dt \qquad (3\text{-}15)$$

$$\text{Altitude } R = R_o + \int V \sin\theta \, dt \qquad (3\text{-}16)$$

The computation block diagram for this simplified set of navigation equations is shown in Figure 3-4. Comparing this set to the previous set we see that the divisions by variables are eliminated.

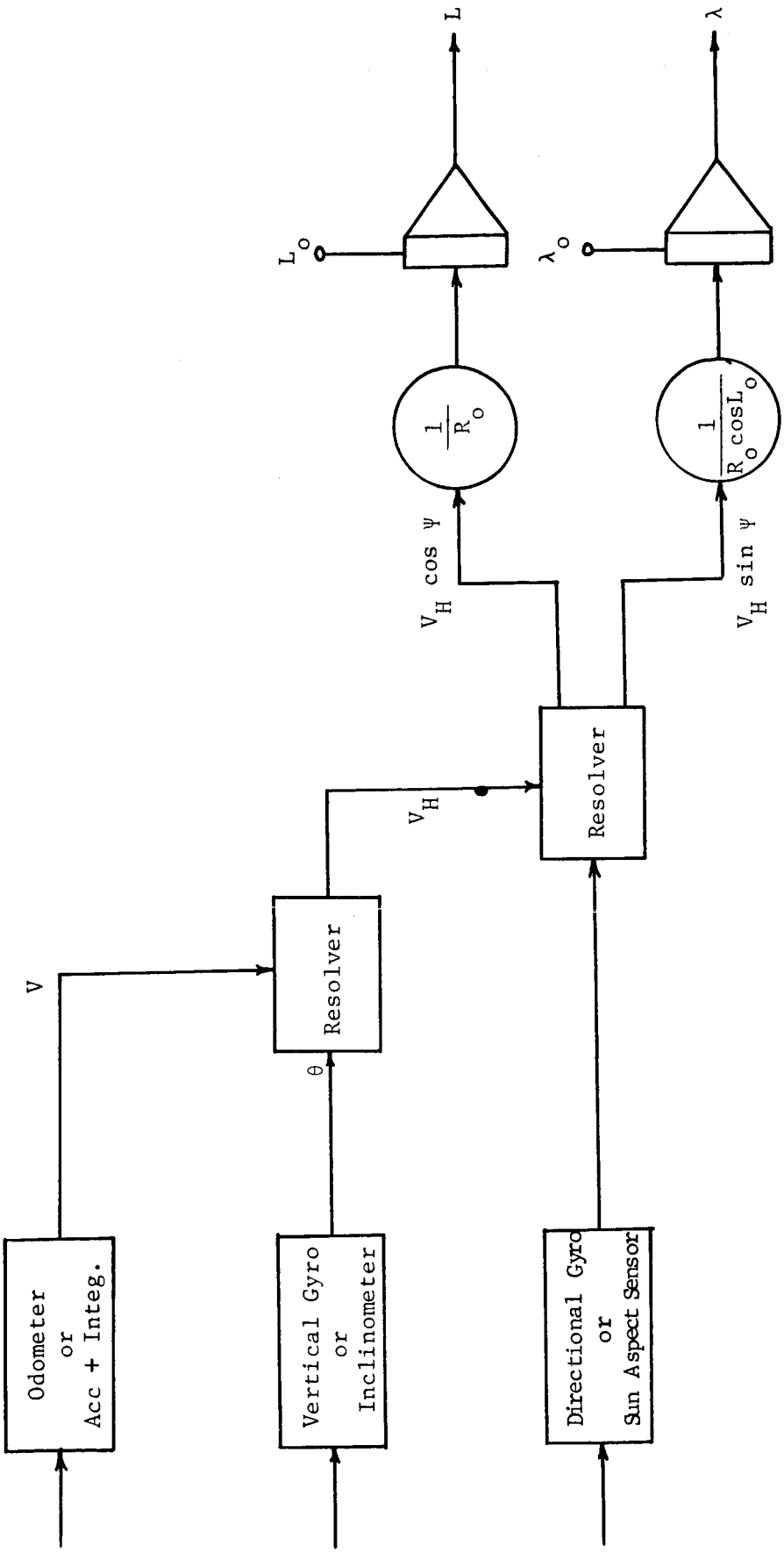

Computation of Eqs. (10) (11) (12)

Fig. 3-4

Error Analysis

Two kinds of errors are involved in using this set of navigation equations. The first kind is the system error which is due to the use of two approximations. The second kind is due to measurement errors.

Replacing variables in (3-14), (3-15), and (3-16) by their measured value and then comparing the resulting equations to (3-5), (3-6), and (3-7), respectively, we obtain the following set of equations for error simulation.

$$\varepsilon_L = \varepsilon_{L_o} + \frac{1}{R_o} \int (V + \varepsilon_V) \cos (\theta + \varepsilon_\theta) \cos (\Psi + \varepsilon_\Psi)\, dt - \int \frac{V \cos \theta \cos \Psi}{R}\, dt \qquad (3\text{-}17)$$

$$\varepsilon_\lambda = \varepsilon_{\lambda_o} + \frac{1}{R_o \cos L_o} \int (V + \varepsilon_V) \cos (\theta + \varepsilon_\theta) \sin (\Psi + \varepsilon_\Psi)\, dt - \int \frac{V \cos \theta \sin \Psi}{R \cos L}\, dt \qquad (3\text{-}18)$$

$$\varepsilon_R = \varepsilon_{R_o} + \int (V + \varepsilon_V) \sin (\theta + \varepsilon_\theta)\, dt - \int V \sin \theta\, dt \qquad (3\text{-}19)$$

CHAPTER 4

ODOMETER NAVIGATION SYSTEM

It is known that there will be an odometer mounted on each wheel of the LRV as part of the wheel package. The odometer used will have angular rate output as well as angular displacement output. Furthermore, the weight of odometers will not be charged to the allowed weight of the navigation system. Therefore, it is very desirable that the navigation system take advantage of the available odometer output.

In the following development it is assumed that the LRV frame consists of two T-frames, as shown in Fig. 4-1, hinged at the feet of the two T's. Four wheels are attached to the arms of T's. Only two front wheel odometers are used in the following development.

4-1. Pure Odometer Navigation System

In principle, when the ground is level, two odometers alone can provide exact coordinates of the LRV if the initial position and heading of the vehicle are known, and can provide the relative position with respect to the initial position if the initial coordinates are not known. A pure odometer navigation system for the level surface is developed here.

Let X(t) and Y(t) be the distance measured eastward and northward, respectively. The LRV position and heading at any time is given by (see Fig. 4-2)

$$X(t) = X_o + \int_o^t V(t_1) \sin \Psi (t_1)\, dt_1$$
$$Y(t) = Y_o + \int_o^t V(t_1) \cos \Psi (t_1)\, dt_1 \qquad (4\text{-}1)$$

and

$$\Psi(t) = \Psi_o + \int_o^t \omega(t_1)\, dt_1 \qquad (4\text{-}2)$$

where

X_o, Y_o, Ψ_o = initial value of X, Y, and Ψ, respectively.

V = LRV linear velocity

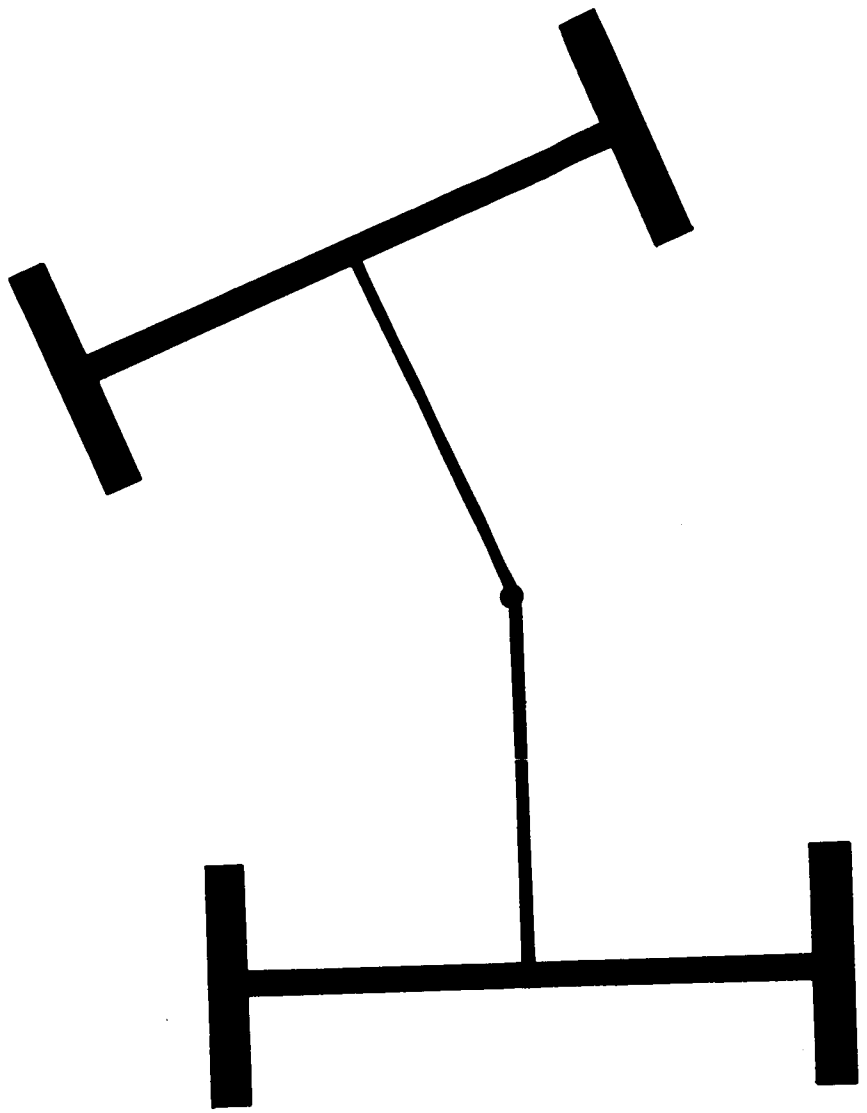

A LRV Frame

Fig. 4-1

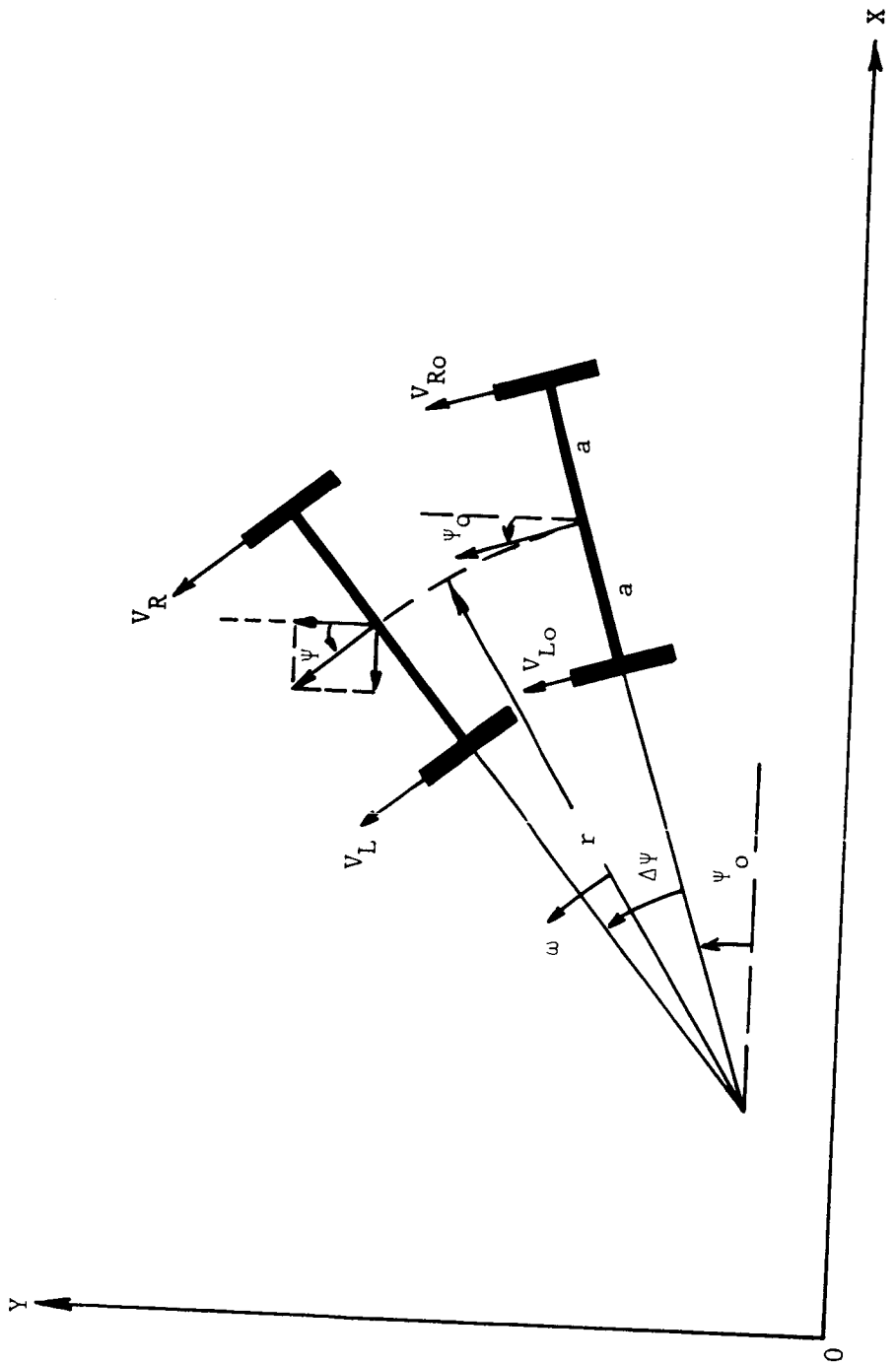

LRV Front Wheel Frame

Fig. 4-2

ω = angular velocity of the wheel axis about its instantaneous center of curvature.

The velocities of the left and right front wheels are

$$V_L = \omega (r - a) \tag{4-3}$$

$$V_R = \omega (r + a)$$

where

r = instantaneous radius of curvature

a = half axial length

Hence,

$$\omega = \frac{V_R - V_L}{2a} . \tag{4-4}$$

Also,

$$V = \frac{V_R + V_L}{2} \tag{4-5}$$

Substituting (4-2), (4-3), (4-4), and (4-5) into (4-1) yields

$$\begin{aligned} X(t) &= X_o + \int_o^t \frac{V_R(t_1) + V_L(t_1)}{2} \sin \left(\Psi_o + \int_o^{t_1} \frac{V_R(t_2) - V_L(t_2)}{2a} dt_2\right) dt_1 \\ Y(t) &= Y_o + \int_o^t \frac{V_R(t_1) + V_L(t_1)}{2} \cos \left(\Psi_o + \int_o^{t_1} \frac{V_R(t_2) - V_L(t_2)}{2a} dt_2\right) dt_1 \end{aligned} \tag{4-6}$$

Equations (4-6) and (4-2) give the LRV's position and heading at any time t. An instrumentation block diagram of the navigation system is shown in Fig. 4-3, which is fairly simple.

4-2. Remarks and Simulation

The merit of this scheme is its simplicity. However, it has the disadvantage that it is sensitive to wheel-slip and wheel-lock. Any slipping or locking of a wheel will generate both permanent heading and distance error. The possibility of a permanent heading error is a very serious disadvantage.

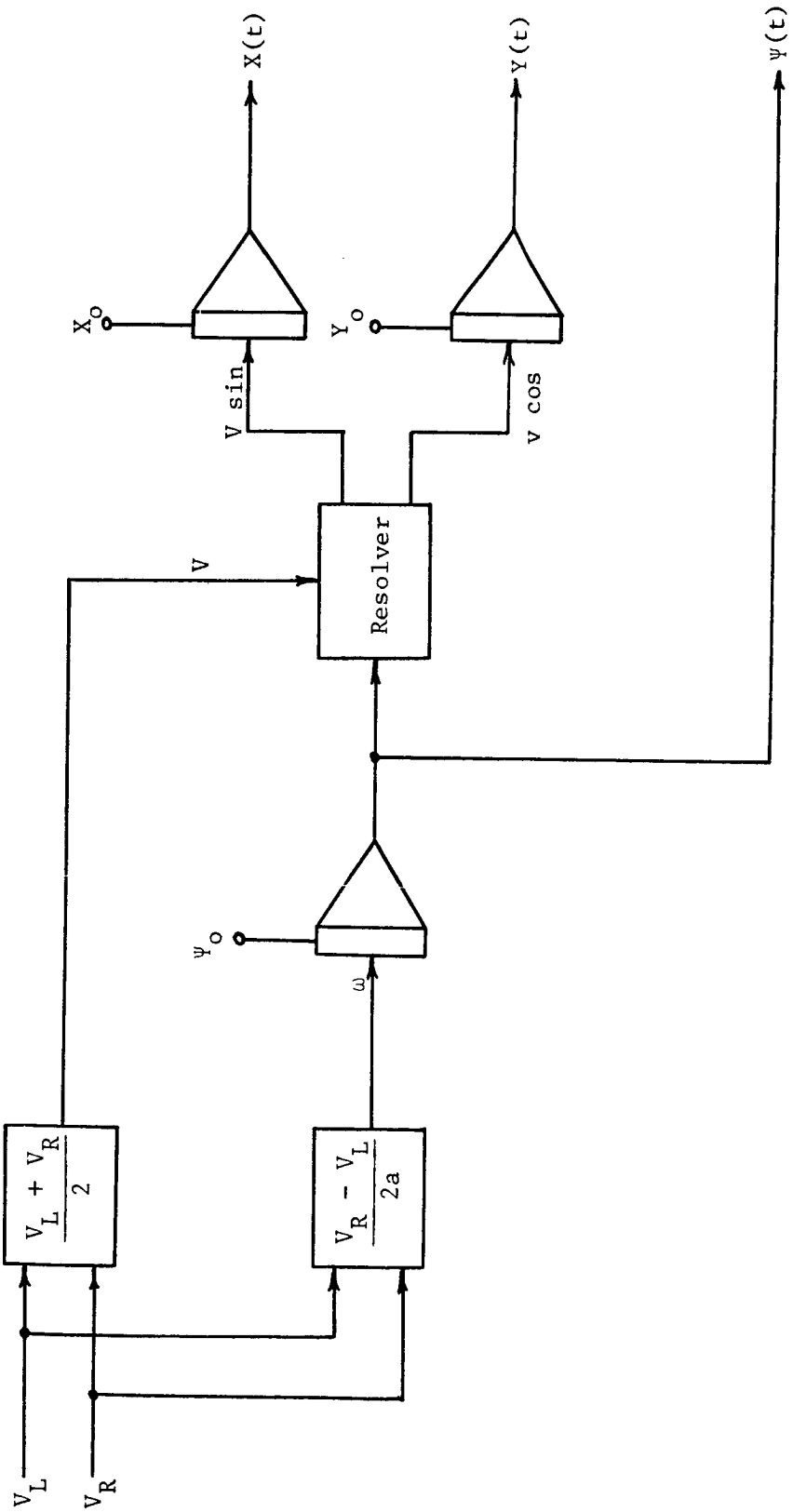

Instrumentation Block Diagram

Fig. 4-3

Heading angle $\Psi = -45°$
LRV velocity 10 meters per second

Tilt angle of flat surface	Actual horizontal distance	Approximate horizontal distance by pure odometer navigation	% Error
$\alpha = \beta = 0$	5.0	5.0	0
$\alpha = \beta = 5°$	49.622	5.0	0.755
$\alpha = \beta = 10°$	48.515	5.0	2.97

Simulation of Odometer Navigation Systems (Fig. 4-4)

Zero Heading Rate

Table 4-1

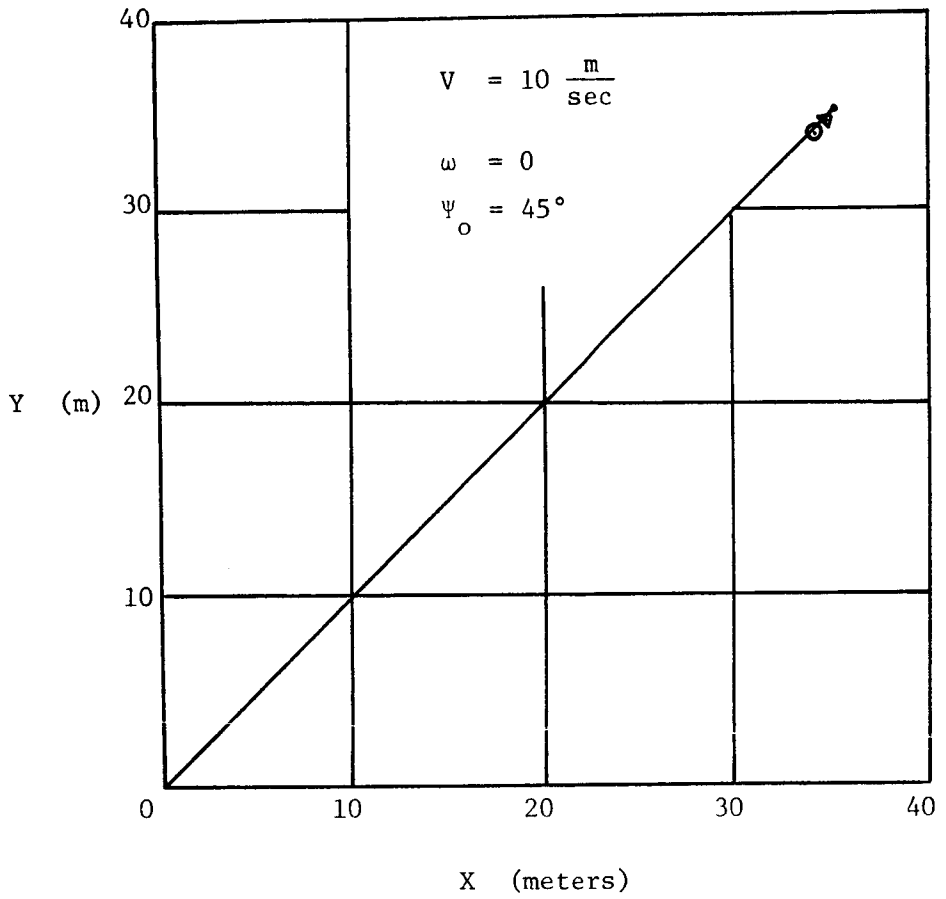

[•] : $\alpha = 0°, \beta = 0°$

[Δ] : $\alpha = 5°, \beta = 5°$

[⊙] : $\alpha = 10°, \beta = 10°$

Simulation of Pure Odometer Navigator (Table 4-1)

Fig. 4-4

Heading rate $\omega = \dot{\Psi} = -\sin 2t$
Flat Surface Tilt angle $\alpha = \beta = 5°$
LRV velocity V = 10 meters per second
Initial heading angle $\Psi_o = 0°$

Time	LRV Horizontal Position					
	Actual		Pure Odometer Approximation			
	X(m)	Y(m)	X(m)	Y-error (%)	Y(m)	Y-error (%)
0	0	0	0		0	
$\pi/10$	1.0127×10^{-1}	3.1387	8.6672×10^{-2}		2.9702	
$2\pi/10$	7.5721×10^{-1}	6.2025	7.5435×10^{-1}		6.1732	
$3\pi/10$	2.2573	8.9484	7.2488		8.8913	
$4\pi/10$	4.4810	1.1156x10	4.4641		1.1079x10	
$5\pi/10$	7.0674	1.2937x10	7.0407	0.378	1.2834x10	0.796
$6\pi/10$	9.6537	1.4717x10	9.6173		1.4588x10	
$7\pi/10$	1.1877x10	1.6925x10	1.1832x10		1.6770x10	
$8\pi/10$	1.3377x10	1.9670x10	1.3327x10		1.9494x10	
$9\pi/10$	1.4033x10	2.2734x10	1.3780x10		2.2541x10	
π	1.4134x10	2.5872x10	1.4081x10	0.375	2.5667x10	0.792
$11\pi/10$	1.4235x10	2.9011x10	1.4181x10		2.8793x10	
$12\pi/10$	1.4891x10	3.2075x10	1.4835x10		3.1840x10	
$13\pi/10$	1.6391x10	3.4820x10	1.6329x10		3.4564x10	
$14\pi/10$	1.8614x10	3.7028x10	1.8544x10		3.6746x10	
$15\pi/10$	2.1200x10	3.8808x10	2.1120x10	0.377	3.8500x10	0.794
$16\pi/10$	2.3787x10	4.0589x10	2.3697x10		4.0255x10	
$17\pi/10$	2.6010x10	4.27797x10	2.5912x10		4.2437x10	
$18\pi/10$	2.7510x10	4.5542x10	2.7406x10		4.5161x10	
$19\pi/10$	2.8166x10	4.8606x10	2.8059x10		4.8208x10	
2π	2.8267x10	5.1744x10	2.8160x10	0.379	5.1334x10	0.792

Simulation of Odometer Navigation Systems (Fig. 4-5)

Non-Zero Heading Rate

Table 4-2

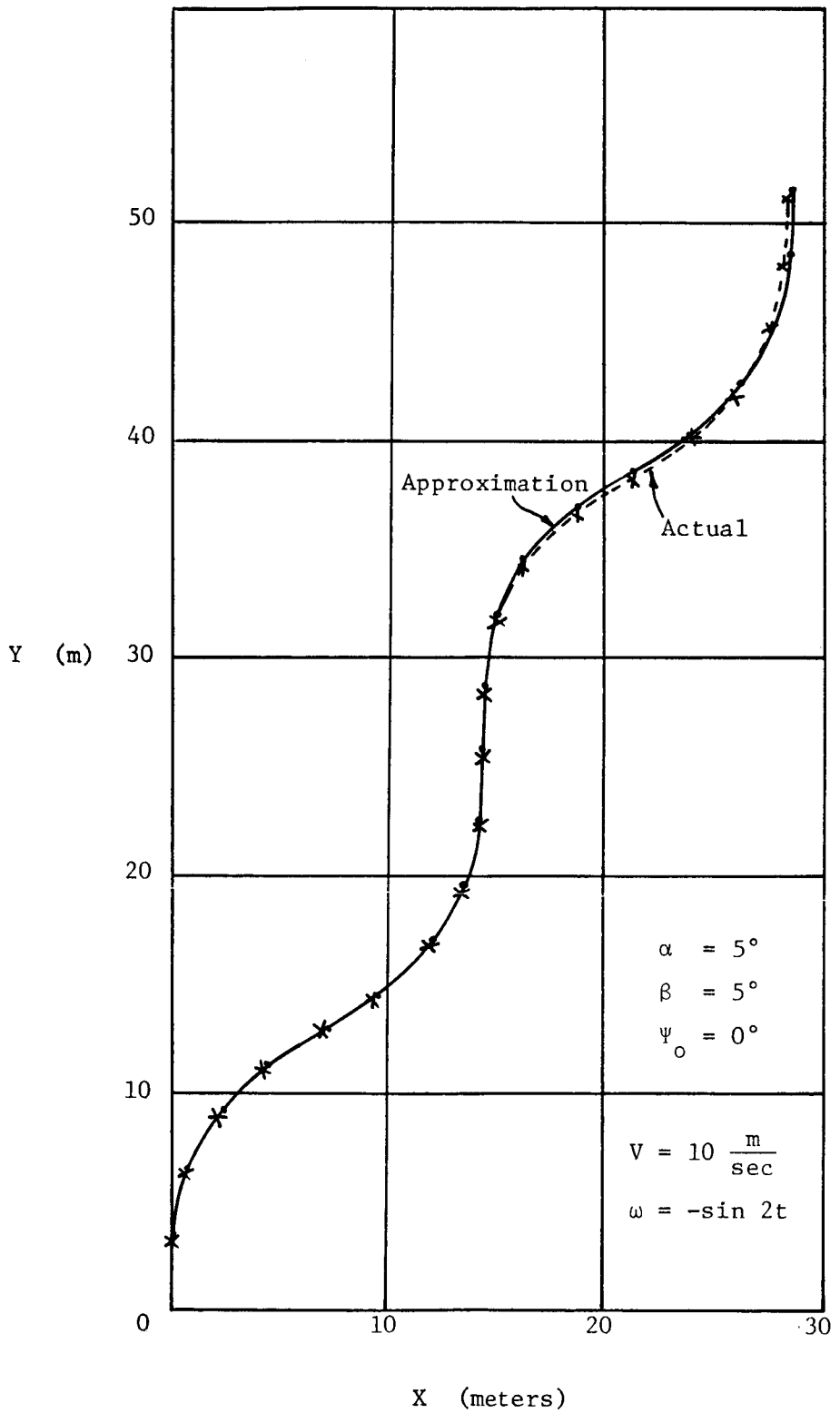

Simulation of Pure Odometer Navigator (Table 4-2)

Fig. 4-5

Heading rate $\omega = \dot{\Psi} = \sin 2t$
Flat Surface Tilt angle $\alpha = \beta = 5°$
LRV velocity 10 meters per second
Initial heading angle $\Psi_o = -45°$

Time	LRV Horizontal Position					
	Actual		Pure Odometer Approximation			
	X(m)	Y(m)	X(m)	Y-error	Y(m)	Y-error
0	0	0	0		0	
$\pi/10$	2.2910	2.1478	2.2823		2.1222	
$2\pi/10$	4.9213	3.8504	4.9027		3.7985	
$3\pi/10$	7.9236	4.7313	7.8937		4.6533	
$4\pi/10$	1.1057x10	4.7197	1.1015x10		4.6181	
$5\pi/10$	1.4145x10	4.1503	1.4092x10	0.375%	4.0274	2.961%
$6\pi/10$	1.7233x10	3.5808	1.7168x10		3.4368	
$7\pi/10$	2.0366x10	3.5693	2.0290x10		3.4016	
$8\pi/10$	2.3369x10	4.4502	2.3281x10		4.2564	
$9\pi/10$	2.5999x10	6.1509	2.5901x10		5.9327	
π	2.8290x10	8.3006	2.8183x10	0.378	8.0549	2.960
$11\pi/10$	3.0581x10	1.0448x10	3.0465x10		1.0177x10	
$12\pi/10$	3.3211x10	1.2151x10	3.3086x10		1.1853x10	
$13\pi/10$	3.6214x10	1.3032x10	3.6077x10		1.2708x10	
$14\pi/10$	3.9347x10	1.3020x10	3.9198x10		1.2673x10	
$15\pi/10$	4.2435x10	1.2451x10	4.2275x10	0.377	1.2082x10	2.964
$16\pi/10$	4.5523x10	1.1881x10	4.5351x10		1.1492x10	
$17\pi/10$	4.8656x10	1.1870x10	4.8473x10		1.2311x10	
$18\pi/10$	5.1659x10	1.2751x10	5.1464x10		1.2311x10	
$19\pi/10$	5.4289x10	1.4454x10	5.4084x10		1.3988x10	
2π	5.6580x10	1.6601x10	5.6366x10	0.378	1.6110x10	2.958

Simulation of Odometer Navigation Systems (Fig. 4-6).

Non-Zero Heading Rate

Table 4-3

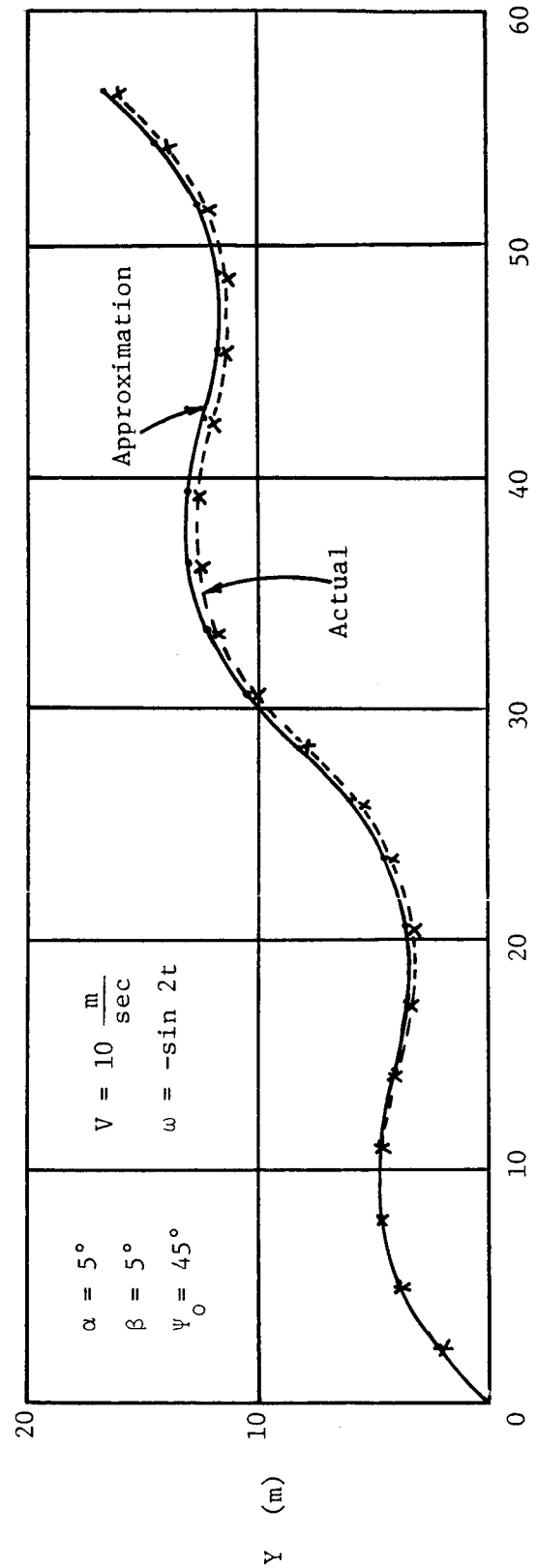

Simulation of Pure Odometer Navigator (Table 4-3)

Fig. 4-6

Heading rate $\omega = \dot{\Psi} = -\sin 2t$
Flat Surface Tilt angle $\alpha = \beta = 10°$
LRV velocity 10 meters per second
Initial heading angle $\Psi_o = 0°$

Time	LRV Horizontal Position					
	Actual		Pure Odometer Approximation			
	X(m)	Y(m)	X(m)	Y-error (%)	Y(m)	Y-error (%)
0	0	0	0		0	
$\pi/10$	1.0127×10^{-1}	3.1387	9.9773×10^{-2}		3.0880	
$2\pi/10$	7.5721×10^{-1}	6.2025	7.4604×10^{-1}		6.0858	
$3\pi/10$	2.2573	8.9484	2.2240		8.7454	
$4\pi/10$	4.4810	1.1145x10	4.4149		1.0835x10	
$5\pi/10$	7.0674	1.2937x10	6.9632	1.474	1.2530x10	3.146
$6\pi/10$	9.6537	1.4717x10	9.5114		1.4207x10	
$7\pi/10$	1.1877x10	1.6925x10	1.1702x10		1.6315x10	
$8\pi/10$	1.3377x10	1.9670x10	1.3180x10		1.8974x10	
$9\pi/10$	1.4033x10	2.2734x10	1.3826x10		2.1972x10	
π	1.4134x10	2.5872x10	1.3926x10	1.472	2.5060x10	3.139
$10\pi/10$	1.4235x10	2.9011x10	1.4025x10		2.8147x10	
$12\pi/10$	1.4891x10	3.2075x10	1.4670x10		3.1145x10	
$13\pi/10$	1.6391x10	3.4820x10	1.6149x10		3.3805x10	
$14\pi/10$	1.8614x10	3.7028x10	1.4834x10		3.5912x10	
$15\pi/10$	2.1200x10	3.8808x10	2.0888x10	1.472	3.7589x10	3.141
$16\pi/10$	2.3787x10	4.0589x10	2.3436x10		3.9266x10	
$17\pi/10$	2.6010x10	4.2797x10	2.5627x10		4.1374x10	
$18\pi/10$	2.7510x10	4.5542x10	2.7104x10		4.4033x10	
$19\pi/10$	2.8166x10	4.8606x10	2.7750x10		4.7031x10	
2π	2.8267x10	5.1744x10	2.7850x10	1.475	5.0119x10	3.140

Simulation of Odometer Navigation Systems (Fig. 4-7).

Non-Zero Heading Rate

Table 4-4

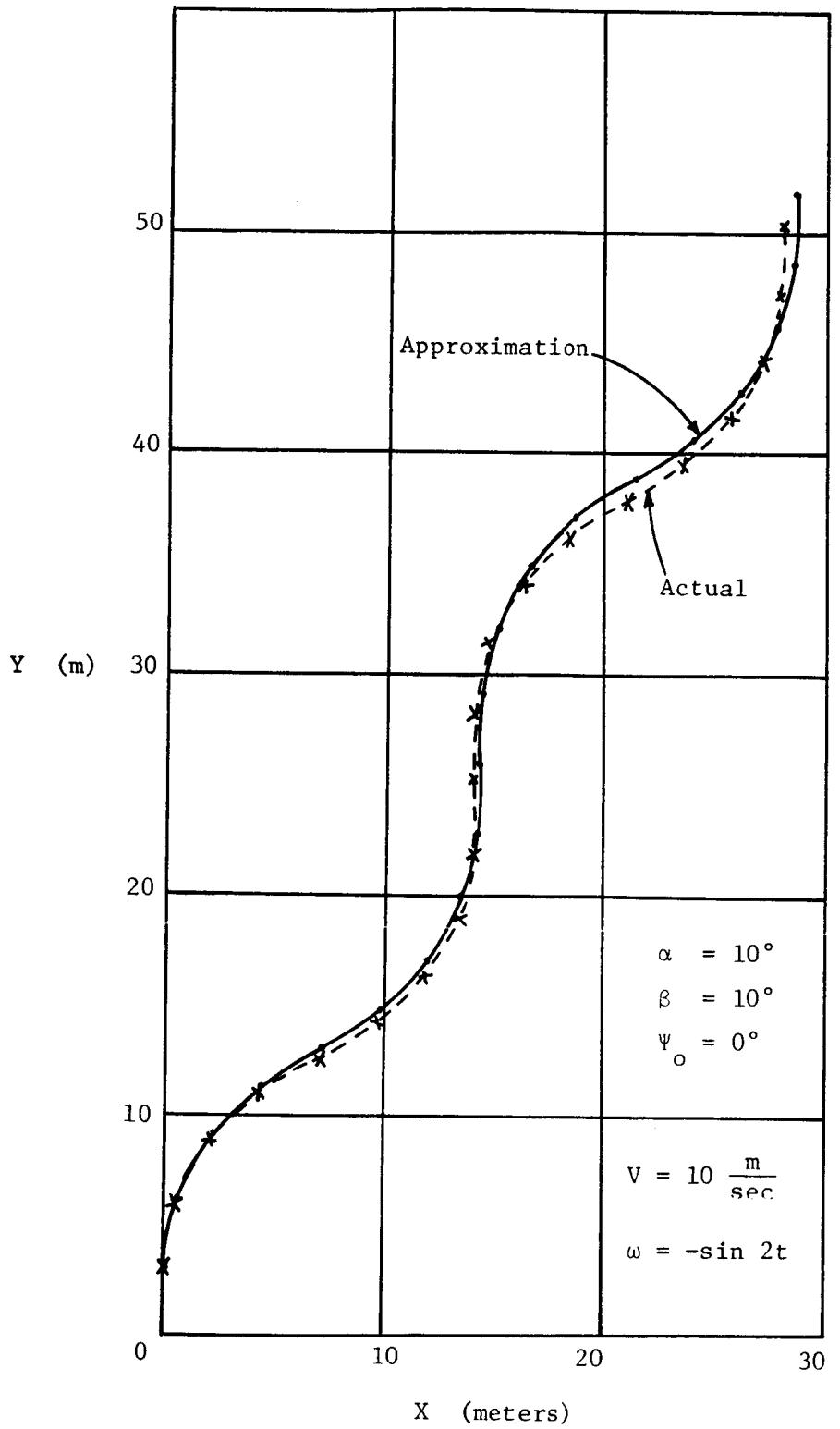

Simulation of Pure Odometer Navigator (Table 4-4)

Fig. 4-7

Heading rate $\omega = \dot{\Psi} = -\sin 2t$
Flat Surface Tilt angle $\alpha = \beta = 10°$
LRV velocity 10 meters per second
Initial heading 40 = -45°

Time	LRV Horizontal Position					
	Actual		Pure Odometer Approximation			
	X(m)	Y(m)	X(m)	Y-error (%)	Y(m)	Y-error (%)
0	0	0	0			
$\pi/10$	2.2910	2.1478	2.2572		2.0470	
$2\pi/10$	4.9213	3.8504	4.8487		3.6457	
$3\pi/10$	7.9236	4.7313	7.8068		4.4240	
$4\pi/10$	1.1057x10	4.7197	1.0894x10		4.3195	
$5\pi/10$	1.4145x10	4.1503	1.3936x10	1.478	3.6670	11.638
$6\pi/10$	1.3233x10	3.5808	1.6979x10		3.0145	
$7\pi/10$	2.0366x10	3.5693	2.0066x10		2.9100	
$8\pi/10$	2.3369x10	4.4502	2.3024x10		3.6884	
$9\pi/10$	2.5999x10	6.1529	2.5616x10		5.2870	
π	2.8290x10	8.3006	2.7873x10	1.474	7.3341	11.638
$11\pi/10$	3.0581x10	1.0448x10	3.0130x10		9.3811	
$12\pi/10$	3.3211x10	1.2151x10	3.2722x10		1.0980x10	
$13\pi/10$	3.6214x10	1.3032x10	2.5680x10		1.1758x10	
$14\pi/10$	3.9347x10	1.3020x10	3.8767x10		1.1653x10	
$15\pi/10$	4.2435x10	1.2451x10	4.1809x10	1.475	1.1001x10	11.646
$16\pi/10$	4.5523x10	1.1881x10	4.4852x10		1.0349x10	
$17\pi/10$	4.8656x10	1.1870x10	4.7939x10		1.0244x10	
$18\pi/10$	5.1659x10	1.2751x10	5.0897x10		1.1023x10	
$19\pi/10$	5.4289x10	1.4454x10	5.3489x10		1.2621x10	
2π	5.6580x10	1.6601x10	5.5746x10	1.474	1.4668x10	11.644

Simulation of Odometer Navigation Systems (Fig. 4- 8).

Non-Zero Heading Rate

Table 4-5

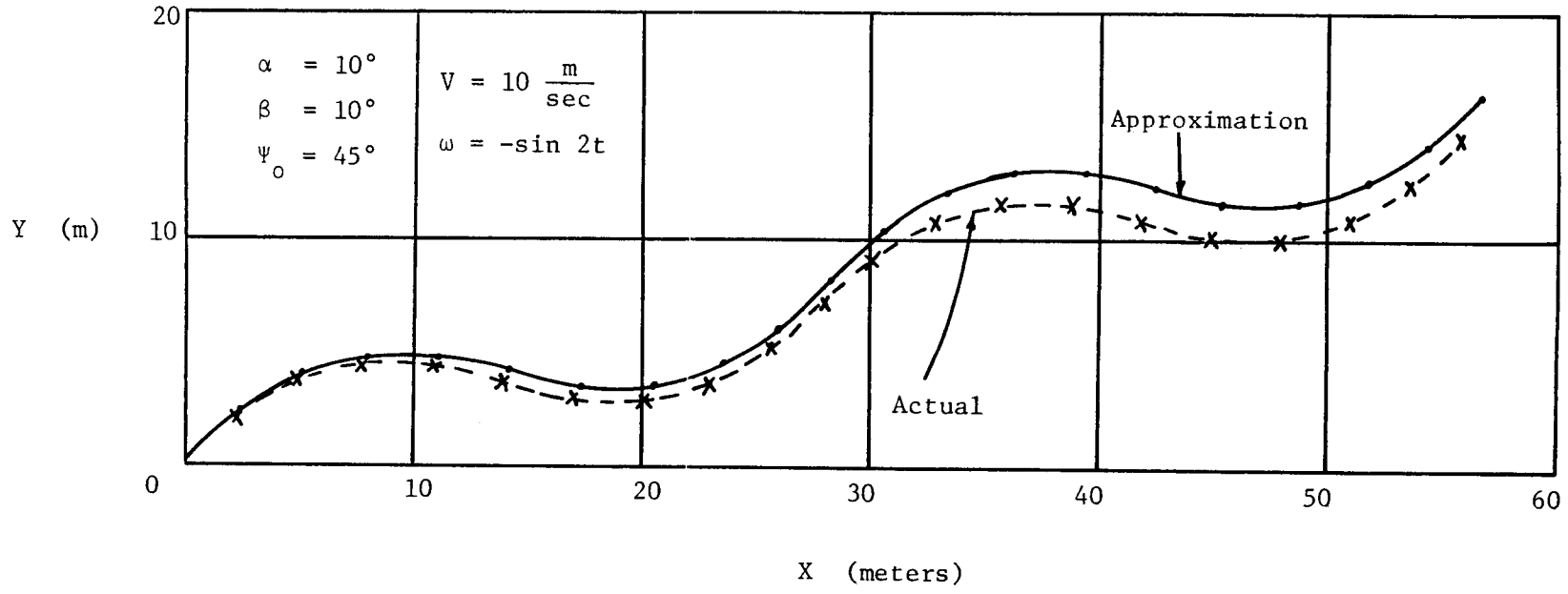

Simulation of Pure Odometer Navigator (Table 4-5)

Fig. 4-8

It has been noted that these navigation equations are valid only when the terrain is flat and level. Any attempt to extend them to account for tilted terrain will add a vertical and a directional sensor to the list of required hardware. These are the same sensors required for the navigation equations described in Chapter 5. Even if these sensors are added, the system that is produced by extending this odometer navigation concept is inferior to the system described in Chapter 5. Clearly, the odometer navigation scheme looses its attractive simplicity when it is pushed beyond the flat and level terrain.

However, a digital computer simulation was built to determine how well a system using the equations for flat and level terrain would perform if it were used on terrain that is actually tilted. Appendix A describes a technique for simulating this problem. The results of this simulation are listed in Tables 4-1 through 4-5 and shown in Figs. 4-4 through 4-8.

In these tables and figures the angles α and β are used to define the tilted plane. Let the level plane have orthogonal axes, x and y. Let the tilted plane have orthogonal axes, x' and y'. Picture a line that is the intersection of the x'y' tilted plane with a vertical plane that includes the x axis. α is the angle between the x axis and this line. β is the angle between the y axis and the y' axis (Fig. 4-9).

The heading angle, Ψ, is the angle between the x' axis and the vehicle velocity vector. The sign of this angle is defined by noting that Ψ is between 0 to 90° if both the x' and y' components of the velocity are positive.

These simulation results show that the simple odometer navigation system can be useful even when it is used on terrain with moderate tilt. In particular, it appears that this scheme could provide a valuable back-up to a more complete dead reckoning system that might be temporarily disabled. For example, a dead reckoning package that obtains its direction reference by watching the sun would be temporarily disabled if it were shadowed. The odometer navigation system could be used until the primary dead reckoning system is able to see the sun again and thus regain its directional reference.

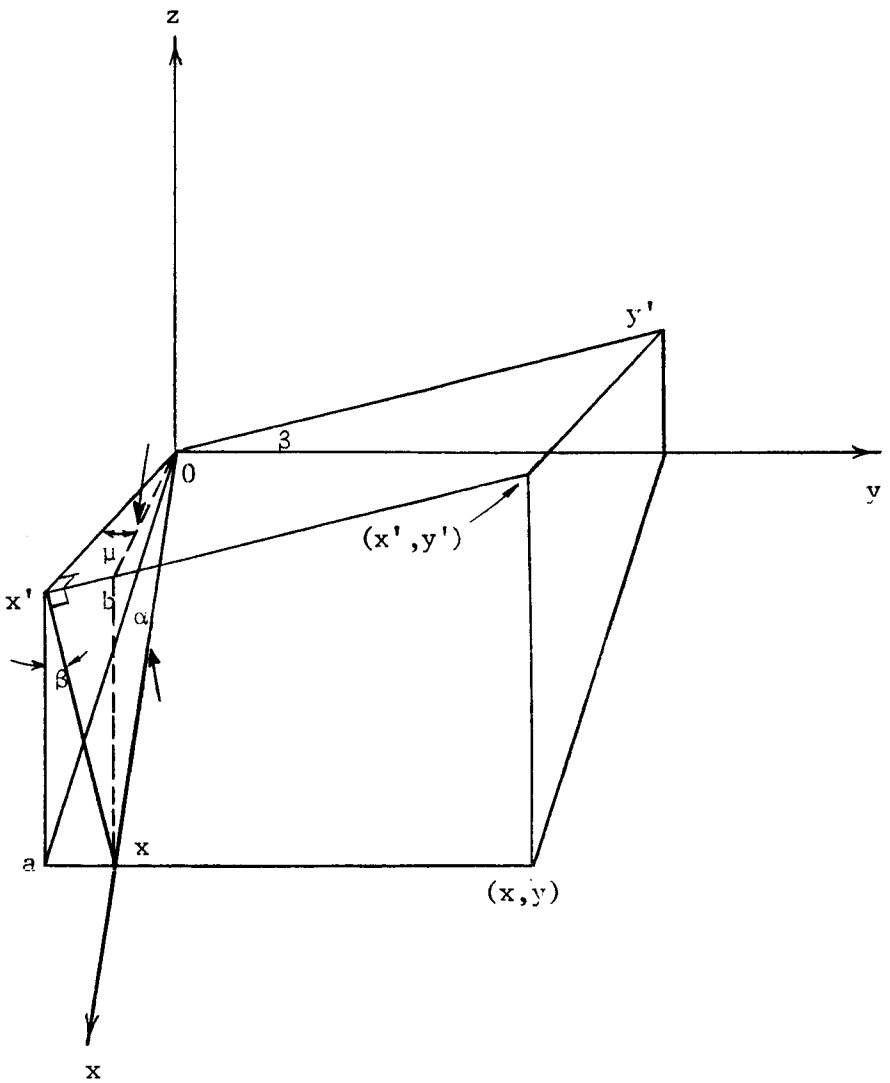

Definition of Angles α and β

Fig. 4-9

CHAPTER 5

DEAD RECKONING MECHANIZATION PROBLEMS

In Chapter 3 the navigation equations for dead reckoning were examined. These equations show that in order to instrument a dead reckoning navigation scheme it is necessary to measure various quantities that can be combined to determine the vehicle vector. These quantities include the forward speed of the vehicle and the angles that define the vehicle orientation relative to some fixed navigation coordinate system. Some of the hardware components that are available to the system designer for making these measurements have been listed. The following is a closer look at the ways that these instruments can be used and at some of the problems associated with their use.

5.1. Odometers

If odometers are used to measure velocity a couple of interesting, potential problems arise. The most straight-forward approach to measuring the velocity vector is to assume that is is parallel to the vehicle longitudinal axis and that its magnitude is proportional to the measured wheel rates. Unfortunately this approach does not measure the velocity precisely when the LRV encounters an irregular lunar surface where it must climb over obstacles or whenever it turns to the right or left.

Fig. 5-1a shows the LRV climbing over a block. In this case the velocities of the front and rear wheels are not even colinear. Neither of these velocities are along the vehicle axis. Fig. 5-1b shows another situation where neither the velocity of the front nor rear wheels is along the longitudinal axis. Here the LRV is traveling over rolling hills represented by a sine profile.

Fig. 5-2 shows another troublesome situation. When the LRV is going around a turn the odometer for the outside wheel indicates a larger speed than the odometer for the inside wheel. The selection of which signal to use must be done carefully.

The pertinent question is "How do these discrepancies affect navigation accuracy?" A feel for the answer to this question can be developed by considering some special cases that represent the problems described above.

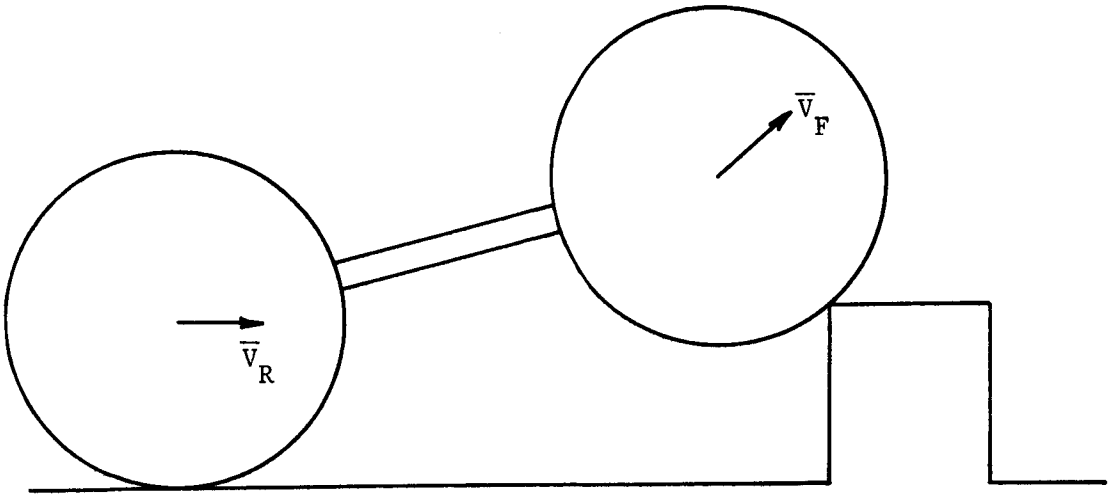

(a)

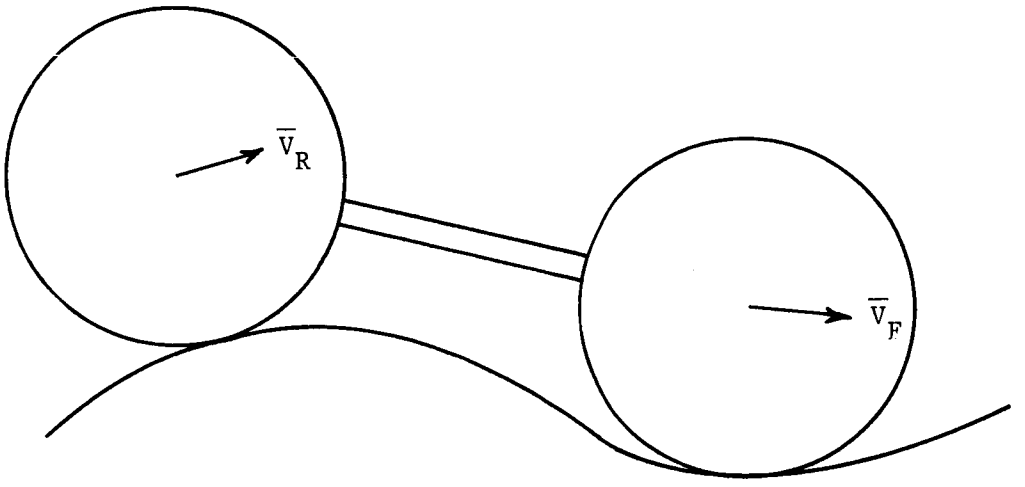

(b)

LRV Traveling Over Irregular Surface

Fig. 5-1

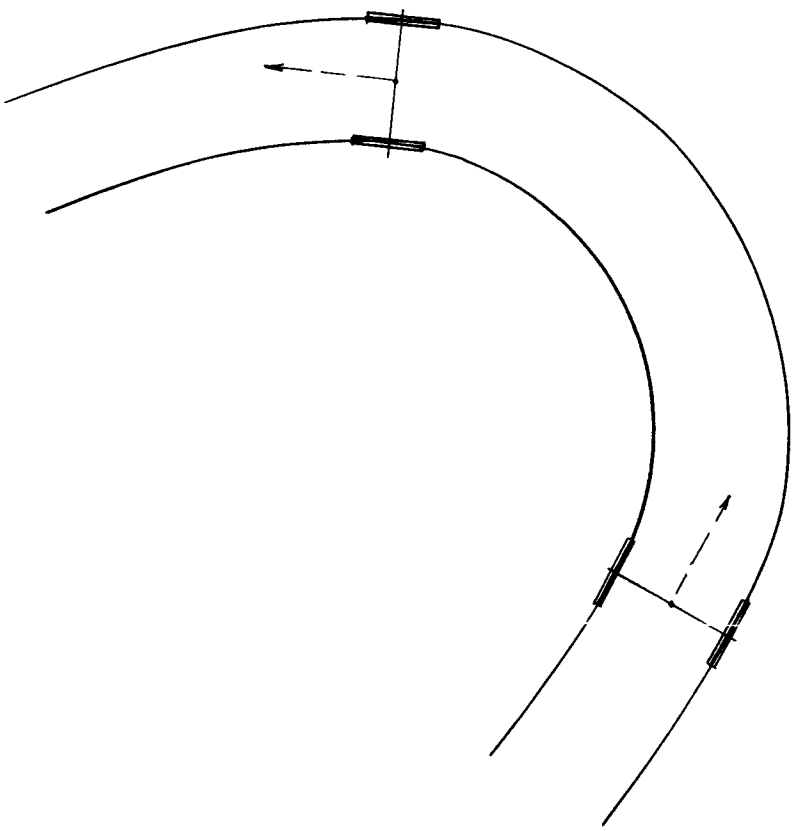

Turning of a Pair of LRV Wheels

Fig. 5-2

Going Over an Obstacle

First the problem of going over an obstacle will be considered. In Fig. 5-3 the vehicle is going over a spike that is as tall as the wheel radius. Two different types of errors are generated when the LRV rolls over a block. One type of error is generated while the LRV rolls up onto the block and back off of the block. A second type of error is generated while the LRV rolls across the top surface of the block. Considering a spike rather than a block focuses our attention on the first type of error.

The actual distance traveled by the vehicle while it is rolling over the spike is X = 2R. If the front wheel odometers were used to measure velocity then X', the computed horizontal travel would be

$$X' = \int R\dot{a}' \cos\theta \, dt \qquad (5\text{-}1)$$

where a' is the measured a, by odometer. But

$$\dot{a}' = \dot{a} + \dot{\theta}$$

$$X' = R \int \dot{a}' \cos\theta \, dt + R \int \dot{\theta} \cos\theta \, dt$$

$$= R \int \cos\theta \, da + R \int \cos\theta \, d\theta$$

Because of symmetry the value of the second integral for the period when the wheel is going up is exactly cancelled by the integral for the period when the wheel is going down. Now

$$X' = R \int_0^{\pi} \cos\theta \, da$$

From Fig. 5-3 it is seen that

$$L \sin\theta + R \sin a$$

so that

$$\cos\theta = \sqrt{1 - \frac{R^2}{L^2} \sin^2 a}$$

Now

$$X' = R \int_0^{\pi} \sqrt{1 - \frac{R^2}{L^2} \sin^2 a} \, da$$

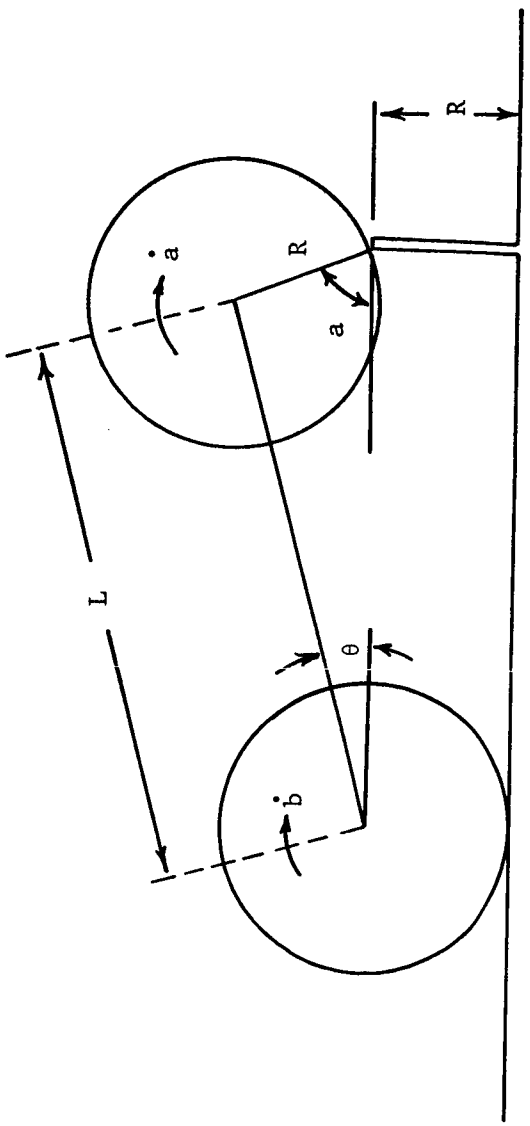

LRV Climbing over a Spike

Fig. 5-3

For an extreme case when R/L = 1/2, X' = 2.93R. Therefore the navigation error accumulated while climbing over this spike is 0.93R.

This brief example demonstrates a problem that is present not only when the vehicle is going over blocks or spikes but also whenever the vehicle encounters smooth, but rolling hills.

Curved Paths

Another problem in the use of odometers is wheel slip. Obviously if the wheels slip this can lead to an erroneous measure of the distance traveled. One possible way to try to alleviate this problem is to use the odometer reading from that wheel that is turning most slowly. In this way the signals from a slipping, overspeeding wheel are ignored. However, this solution to one problem can lead to another kind of trouble as shown in Fig. 5-4.

Here the vehicle is traveling on a smooth flat surface. The trajectory consists of a series of arcs of circles of equal radii, r. The actual distance traveled for one half cycle of this trajectory is

$$X = 2r \sin \frac{\gamma}{2} \tag{5-2}$$

A navigation scheme that uses the odometer signals from the slowest wheel will select the wheels on the inside of the turn. Consequently the computed distance traveled is

$$X' = \int (r - \tfrac{d}{2}) \dot{\Psi} \cos \Psi \, dt$$

For one half cycle of travel

$$X' = \int_{-\gamma/2}^{\gamma/2} (r - \tfrac{d}{2}) \cos\Psi \, d\Psi$$

$$X' = (2r - d) \sin \gamma/2$$

The resulting navigation error is

$$e = X' - X = (2r - d) \sin \frac{\gamma}{2} - 2r \sin \frac{\gamma}{2}$$

$$e = - d \sin \frac{\gamma}{2} \tag{5-3}$$

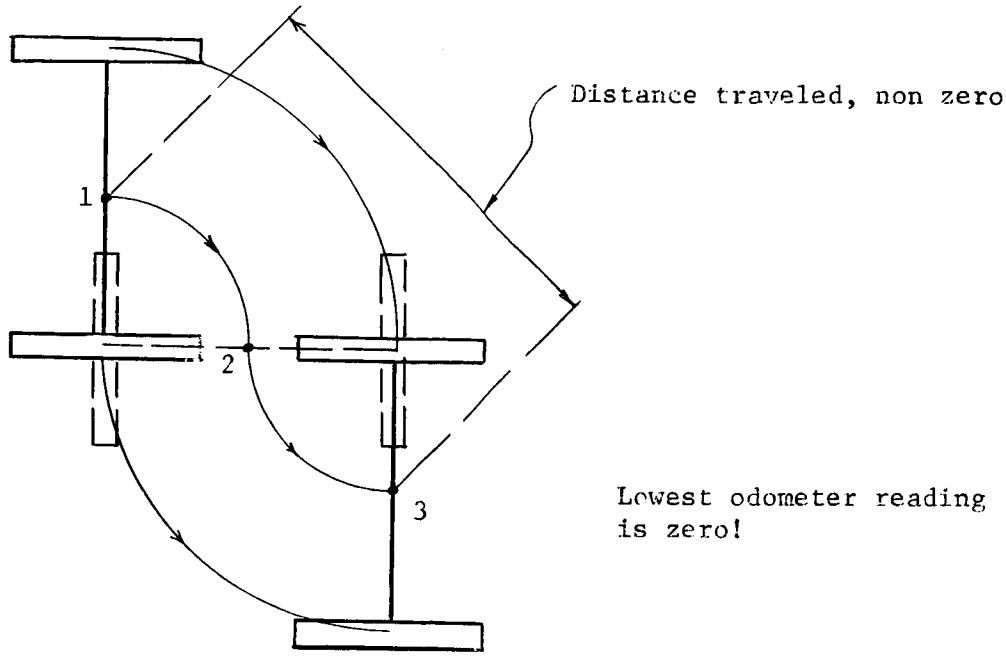

(a)

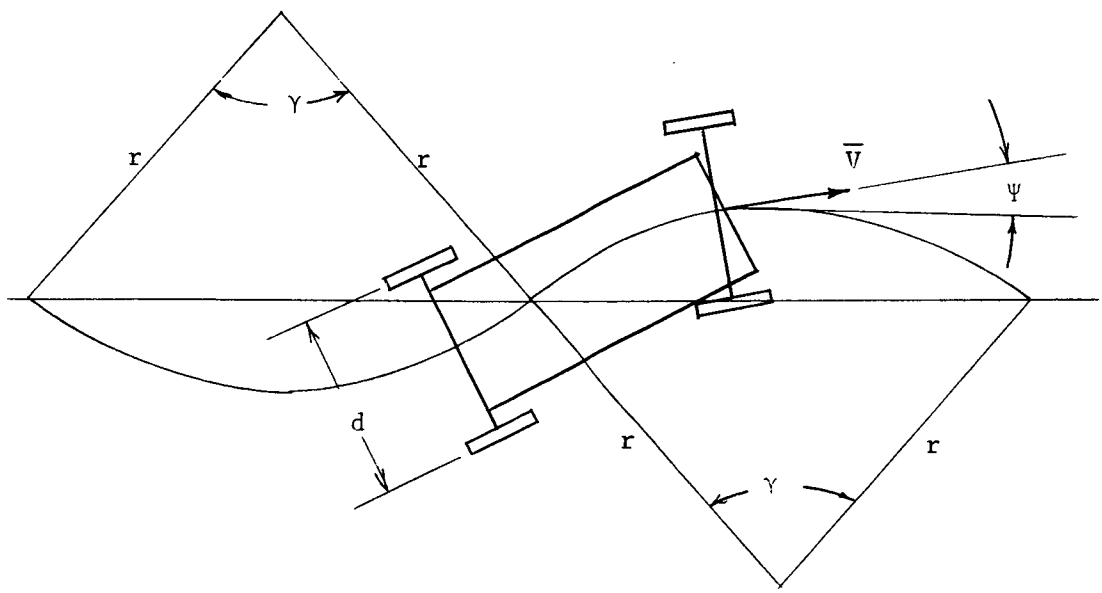

(b)

LRV Following Curved Path

Fig. 5-4

For an extreme case when the trajectory is a sequence of half circles so that $\gamma = \pi$ radians, then

$$e = -d.$$

These simple examples show that any navigation system that uses odometers must be carefully designed. These sources of error must be recognized and examined to determine if they are small enough to be tolerable. If they cannot be tolerated some plan must be devised to eliminate them. What follows is a description of a scheme that could be used to eliminate the error in the velocity measurement that is caused by going over an irregular surface.

Velocity Measurement Technique

The signals from an inclinometer can be used, in conjunction with odometers, to determine the velocity accurately. Again refer to Fig. 5-3. Let $\dot{a}$ and $\dot{b}$ be the angular rates of the front and rear wheels relative to space. Then the measured values of $\dot{a}$ and $\dot{b}$ will be

$$\left.\begin{aligned} \dot{a}' &= \dot{\theta} + \dot{a} \\ \dot{b}' &= \dot{\theta} + \dot{b}' \end{aligned}\right\} \qquad (5\text{-}4)$$

So that

$$\left.\begin{aligned} \dot{a} &= \dot{a}' - \dot{\theta} \\ \dot{b} &= \dot{b}' - \dot{\theta} \end{aligned}\right\} \qquad (5\text{-}5)$$

The quantities on the right of (5-5) can be measured and $\dot{a}$ and $\dot{b}$ can be easily computed. Now

$$\left.\begin{aligned} \left|\overline{V}_F\right| &= R\,\dot{a} \\ \left|\overline{V}_R\right| &= R\,\dot{b} \end{aligned}\right\} \qquad (5\text{-}6)$$

The axle separation is constant. Therefore

$$\overline{V}_F \cdot \hat{i}_1 = \overline{V}_R \cdot \hat{i}_1 \qquad (5\text{-}7)$$

$$(\overline{V}_F - \overline{V}_R) \cdot \hat{i}_1 = 0 \qquad (5\text{-}8)$$

The angular rate of the chassis is

$$\dot{\theta} = \frac{1}{L} \left| (\hat{i}_1 \times \overline{V}_F - \hat{i}_1 \times \overline{V}_R) \right| \tag{5-9}$$

$$\dot{\theta}L = \left| \hat{i}_1 \times (\overline{V}_F - \overline{V}_R) \right| \tag{5-10}$$

and $\overline{V}_F$ and $\overline{V}_R$ can be determined from (5-6), (5-7), and (5-8). Let

$$\left.\begin{aligned} \overline{V}_F &= V_F \cos\alpha \, \hat{i}_1 + V_F \sin\alpha \, \hat{j}_1 \\ \overline{V}_R &= V_R \cos\beta \, \hat{i}_1 + V_R \sin\beta \, \hat{j}_1 \end{aligned}\right\} \tag{5-11}$$

Combining (5-7) and (5-11) produces

$$V_F \cos\alpha = V_R \cos\beta \tag{5-12}$$

Combining (5-10) and (5-11) gives

$$\dot{\theta}L = \left| \hat{i}_1 \times [(V_F \cos - V_R \cos \beta) \, \hat{i}_1 + (V_F \sin - V_R \sin \beta) \, \hat{j}_1] \right| \tag{5-13}$$

From (5-11)

$$\dot{\theta}L = (V_F \sin\alpha - V_R \sin \beta) \tag{5-14}$$

Taking $\dot{\theta}$ as positive for counter clockwise motion gives

$$\dot{\theta}L = V_F \sin\alpha - V_R \sin\beta \tag{5-15}$$

$$\dot{\theta}L = V_F \sqrt{\left\{ 1 - \left(\frac{V_R}{V_F}\right)^2 \cos^2 \beta \right\}} - V_R \sin \beta \tag{5-16}$$

$$(\dot{\theta}L)^2 + \dot{\theta}L \, V_R \sin \beta + V_R^2 \sin^2 \beta = V_F^2 - V_F^2 \cos^2 \beta \tag{5-17}$$

$$2\dot{\theta}L\ V_R \sin\beta = V_F^2 - V_R^2 - (\dot{\theta}L)^2 \qquad (5\text{-}18)$$

$$\beta = \sin^{-1}\left[\frac{V_F^2 - V_R^2 - (\dot{\theta}L)^2}{2\dot{\theta}L\ V_R}\right] \qquad (5\text{-}19)$$

Similarly (5-12) and (5-15) can be manipulated to show that

$$\alpha = \sin^{-1}\left[\frac{V_F^2 - V_R^2 + (\dot{\theta}L)^2}{2\ V_F\ \dot{\theta}L}\right] \qquad (5\text{-}20)$$

Now equations are available for computing the wheel velocities. (5-5) gives the magnitudes of the wheel velocities; (5-19) and (5-20) give the directions of the velocities.

Unfortunately (5-19) and (5-20) fail when the velocities are equal vectors. In this case $\dot{\theta}$ is zero and the right sides of (5-19) and (5-20) are indeterminate.

It might be tempting to say that the velocities must be directed along the vehicle axis if the vehicle axis is not rotating so that $\dot{\theta}$ is zero. However, Fig. 5-5b illustrates a case that violates such an assumption. The odometer and inclinometer signals will be identical for the situations shown in Fig. 5-5a and 5-5b.

A second technique for determining the LRV velocity that does not suffer from this ambiguity requires the addition of another sensing device, a ground contact sensor. However, it does not use any measurement of the vehicle axis angular rate as did the previously discussed method.

The ground contact sensor would measure the angle between the LRV axis, $\hat{i}_1$, and the radius to that part of the wheel that is in contact with the ground. This angle is labeled C in Fig. 5-6. One possible way to instrument this sensor might be the use of an array of strain gages mounted on the inside perimeter of the LRV wheels. The strain gage that is in that part of the wheel that is in contact with the surface would sense the resulting deformation of the wheel. Another device, either mechanical or photoelectric, would measure the attitude of the wheel relative to the LRV axis. The signals from these two devices could be combined to generate the angle C.

If C can be measured then the velocity can be resolved along the vehicle axes.

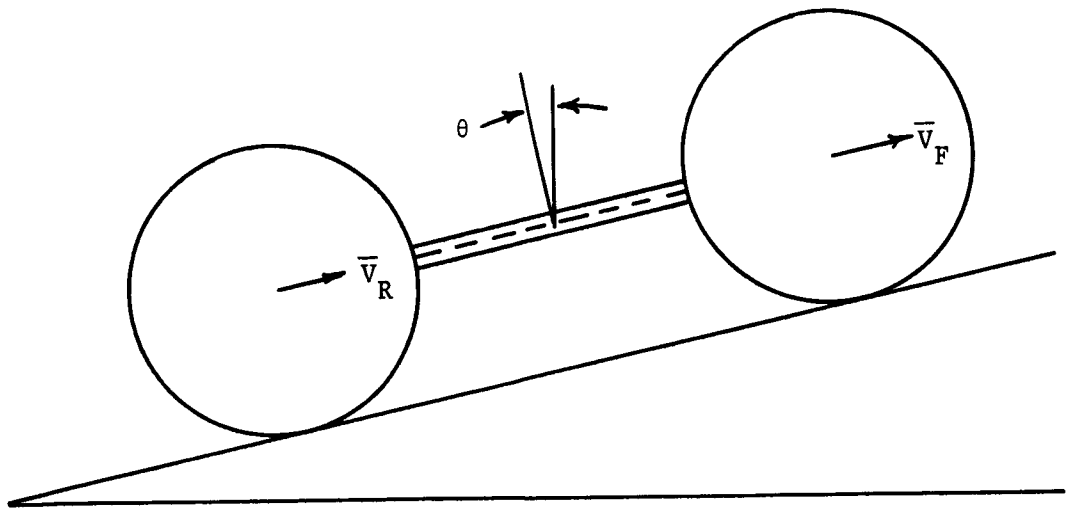

(a)

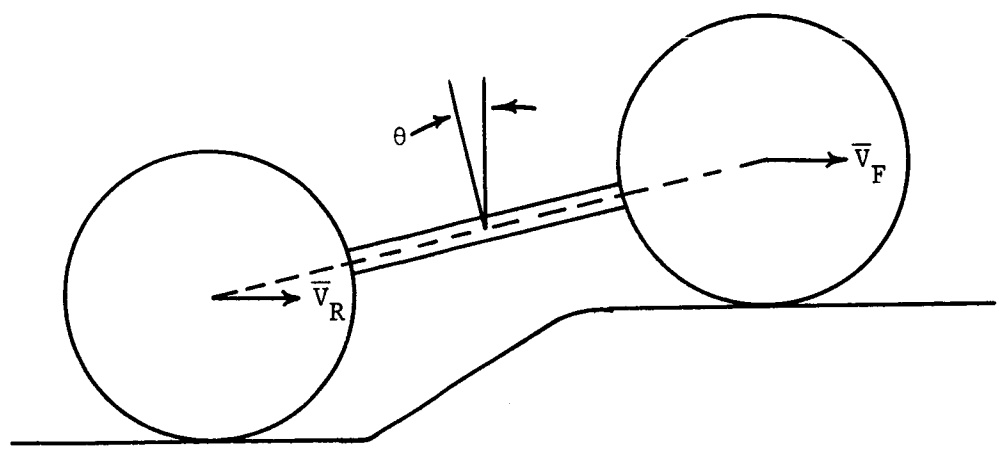

(b)

Two Cases with Zero Angular Rate and Equal Elevation

Fig. 5-5

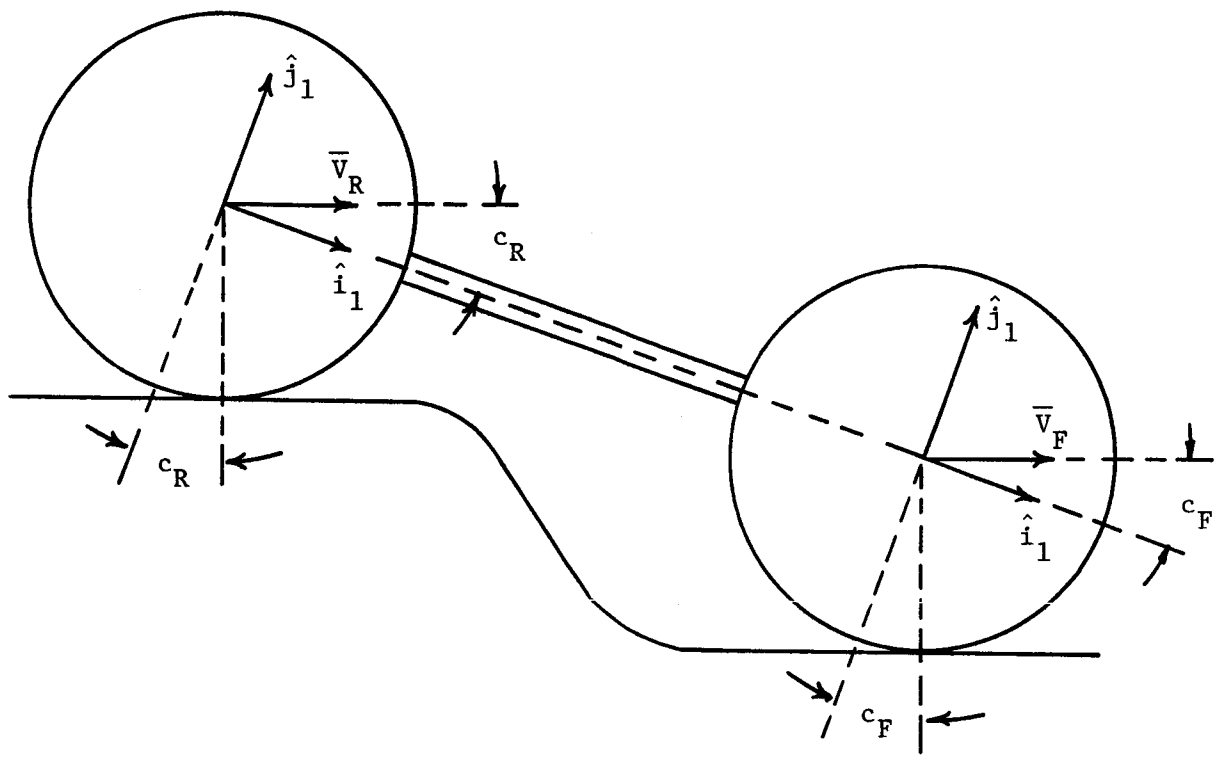

Ground Contact Sensor Geometry

Fig. 5-6

$$\overline{V}_F = R\dot{\phi}\,[\cos C_F\,\hat{i}_1 + \sin C_F\,\hat{j}_1] \qquad (5\text{-}21)$$

$$V_F = R\dot{\theta}\,[\cos C_R\,\hat{i}_1 + \sin C_R\,\hat{j}_1] \qquad (5\text{-}22)$$

5-2. Accelerometers

An accelerometer is used to measure translational acceleration. Modern accelerometers that are used in aerospace systems today are sophisticated refinements of the simple concept illustrated in Fig. 5-7. If the accelerometer case in Fig. 5-7 is accelerated along the sensitive axis this mechanical system will obey Newton's laws. The spring will be stretched so that its change in length is proportional to the applied acceleration. Therefore, this reaction to the applied acceleration can be used to measure the acceleration.

Two possible uses for accelerometers in dead reckoning navigation systems will be discussed. First, it will be shown that accelerometers can be used to instrument a strapped-down vertical sensor that will measure the roll and elevation angles of the platform on which they are mounted. Secondly, it will be shown how accelerometers should be used to determine the translational motion of a strapped-down platform.

Strapped-Down Vertical Sensor

Consider two accelerometers mounted on the LRV chassis with normal sensitive axes as shown in Fig. 5-8. If the vehicle is not accelerating then the instrument outputs will be

$$\text{Accelerometer No. 1 output} = a_g \sin\theta$$

$$\text{Accelerometer No. 2 output} = -a_g \cos\theta \sin\phi$$

where a_g is the local acceleration of gravity. Clearly these equations can be used to determine θ and ϕ from the accelerometer signals.

Measurement of Translational Motion

Accelerometers can also be used to measure translational motion. Three accelerometers mounted on the LRV chassis with their sensitive axes along the vehicle axes sense the acceleration of the point at which they are mounted.

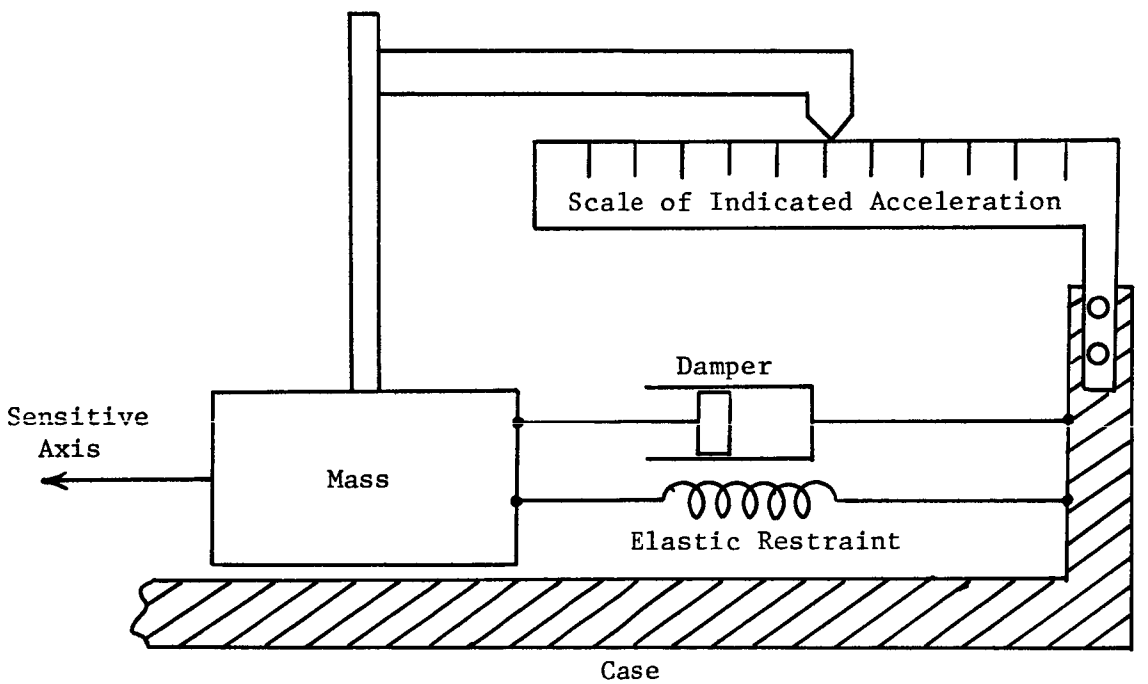

Simple Form of Accelerometer

Fig. 5-7

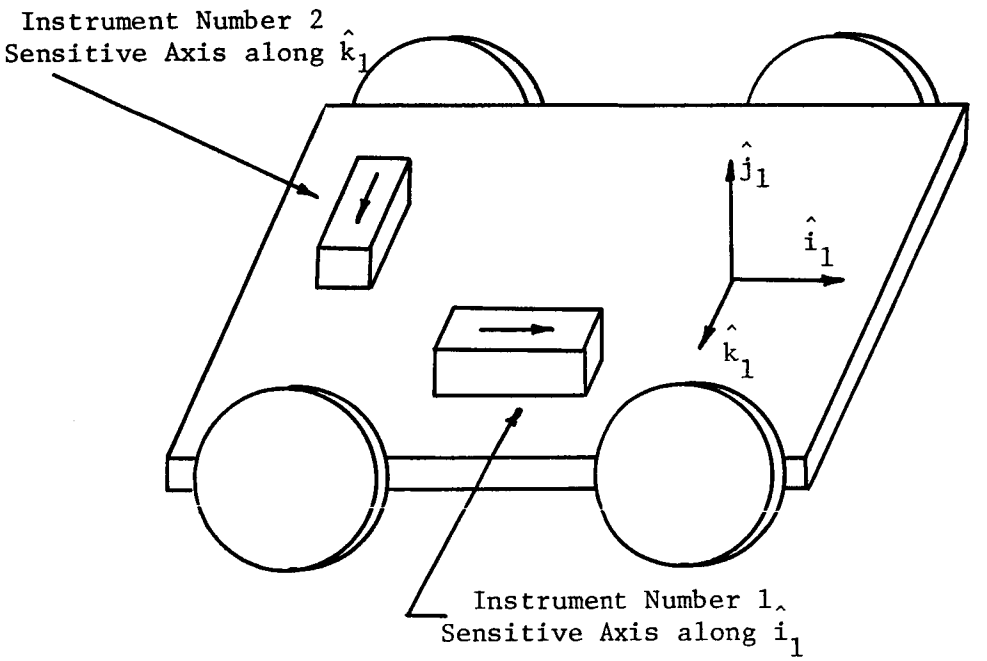

Two Strapped Down Accelerometers Used as a Vertical Sensor

Fig. 5-8

The accelerometers signals can be used to write the acceleration vector of that point as follows:

$$\bar{a} = a_{i1}\hat{i}_1 + a_{j1}\hat{j}_1 + a_{k1}\hat{k}_1$$

where $\hat{i}_1$, $\hat{j}_1$, and $\hat{k}_1$ are unit vectors along the vehicle axes and a_{i1}, a_{j1}, and a_{k1} are the signals from the accelerometers that have their sensitive axes along these unit vectors.

This acceleration vector can be integrated twice in order to determine the change in the vehicle position. However, it is important to notice that

$$\text{change in position} \neq \hat{i}_1 \int\int a_{i1}\, dt + \hat{j}_1 \int\int a_{j1}\, dt + \hat{k}_1 \int\int a_{k1}\, dt.$$

This is because the vehicle axes, $\hat{i}_1$, $\hat{j}_1$, and $\hat{k}_1$, are not fixed in space and for this reason they cannot be brought out of the integration as is attempted above.

The correct way to double integrate the acceleration vector is first to use the direction cosines that relate the S1, vehicle fixed coordinates, to the S2 coordinates that are fixed in space and resolve the acceleration vector along the fixed coordinates. Then the acceleration vector can be written as follows:

$$\bar{a} = a_{i2}\hat{i}_2 + a_{j2}\hat{j}_2 + a_{k2}\hat{k}_2$$

Now since $\hat{i}_2$, $\hat{j}_2$, and $\hat{k}_2$ are fixed in space the unit vectors can be brought outside the integration so that

$$\text{change in position} = \hat{i}_2 \int\int a_{i2}\, dt + \hat{j}_2 \int\int a_{j2}\, dt + \hat{k}_2 \int\int a_{k2}\, dt.$$

5-3. Two-Degree-of-Freedom Gyros

A two-degree-of-freedom gyro consists of a rotor supported by two gimbals as shown in Fig. 5-9. This type of gyro can be mounted on a vehicle and used to measure the vehicle orientation relative to some fixed coordinate system.

Ideally, the rotor spin axis direction remains unchanged even though the vehicle rotates. Consequently, the angle between the two gimbals and the angle between the outer gimbal and a reference direction on the vehicle both are functions of vehicle orientation. These angles can be measured and the resulting

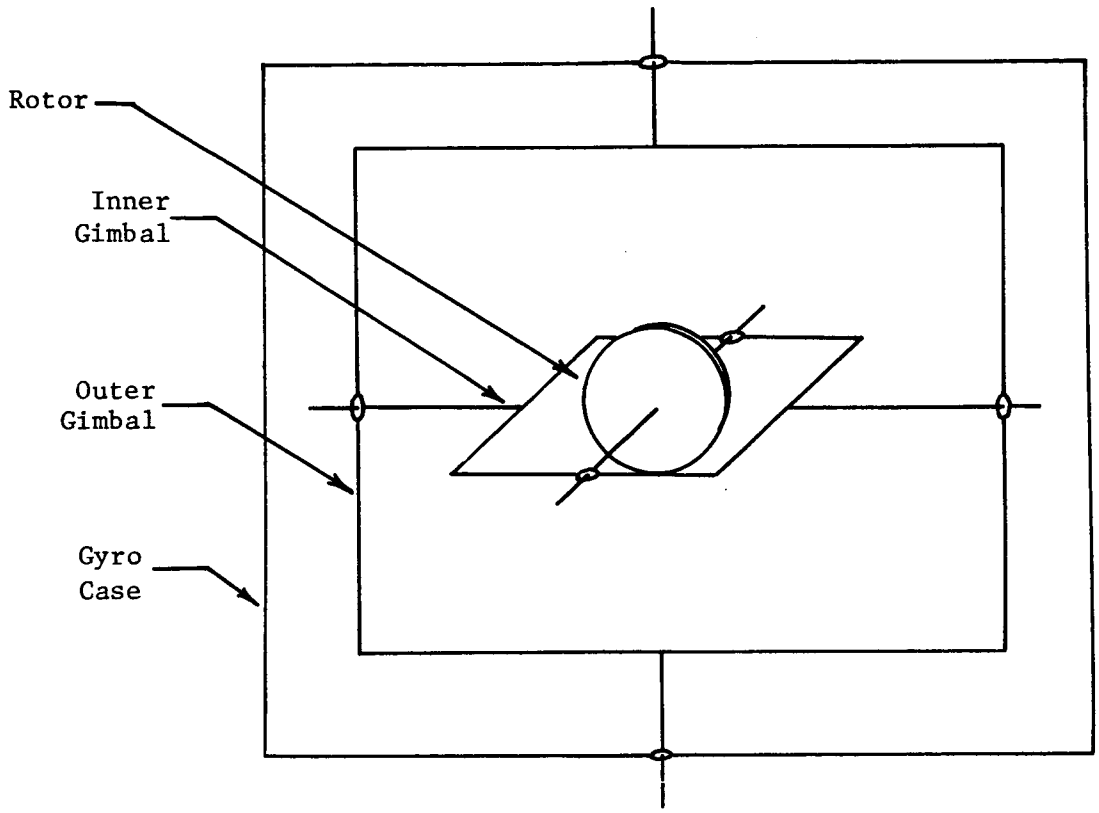

Two-Degree-of-Freedom Gyro

Fig. 5-9

measurement signals can be processed to determine the vehicle orientation.

The vehicle orientation will be described by a conventional set of three Euler angles. The functions relating these Euler angles and the measured gimbal angles are determined by the choice of the spin axis direction and the gimbal arrangement. Interestingly enough, these functions are much more complicated for some spin axis-gimbal combinations than for others. Therefore, prudent choice of the gyro arrangement can greatly reduce the computation that is required to determine the vehicle orientation from the measured gimbal angles. Here this point will be demonstrated by comparing the nature of the gimbal angles for six different combinations of spin axes and gimbals.

Next some of the factors involved in the selection of gimbal arrangements will be illustrated by an example. Instruments will be selected to determine the orientation of a vehicle for which the roll and elevation angles are restricted while the heading is unrestricted.

Coordinate Systems

Two right-hand coordinate systems S1 and S2, introducted in Section 1-5, will be used in this discussion. S2 is a fixed, reference system; S1 is the vehicle coordinate system and it rotates in space with the vehicle. The Euler angles Ψ, θ, and ϕ shown in Fig. 5-10 describe the vehicle orientation relative to the S2 coordinate system. $\hat{j}_2$ will be taken as upward and $\hat{i}_1$ will be taken as the vehicle longitudinal axis. Then Ψ, θ, and ϕ conveniently become heading, elevation, and roll angles.

Gimbal Arrangements

Fig. 5-11 shows six different spin-axis-gimbal arrangements. These six combinations were generated by pointing the rotor spin axis along each of the three coordinates of the fixed S2 coordinate system. For each of these spin axis directions there are two ways to arrange the gimbals. This produces the six combinations shown.

One angle that can be measured on the gimbals will be called the inner angle (IA). This angle is between the planes of the inner and outer gimbals. The sides of this angle are shown for each gimbal arrangement.

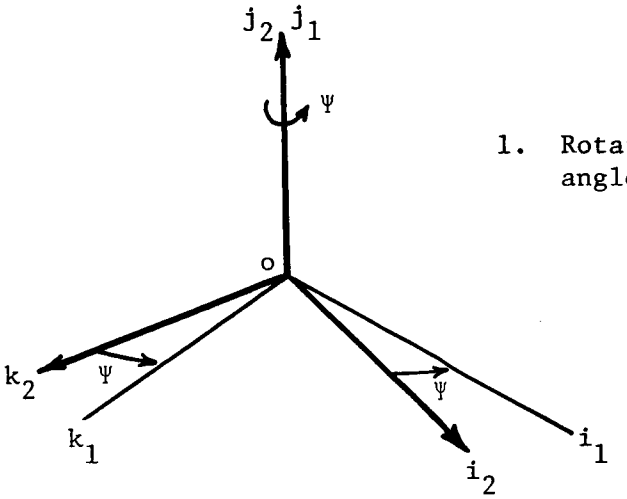

1. Rotate S1 through the angle Ψ about j_3.

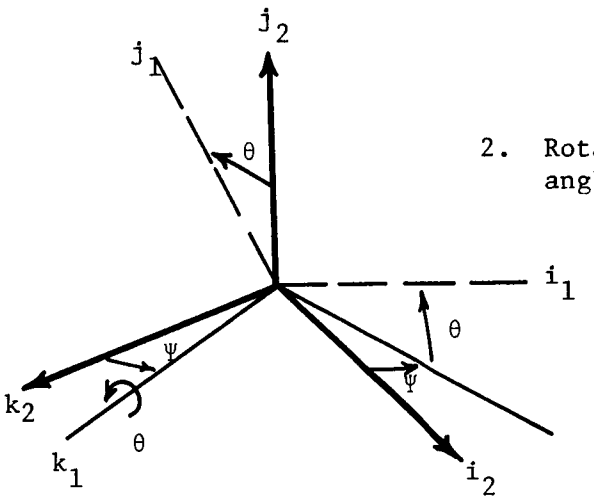

2. Rotate S1 through the angle θ about k_1.

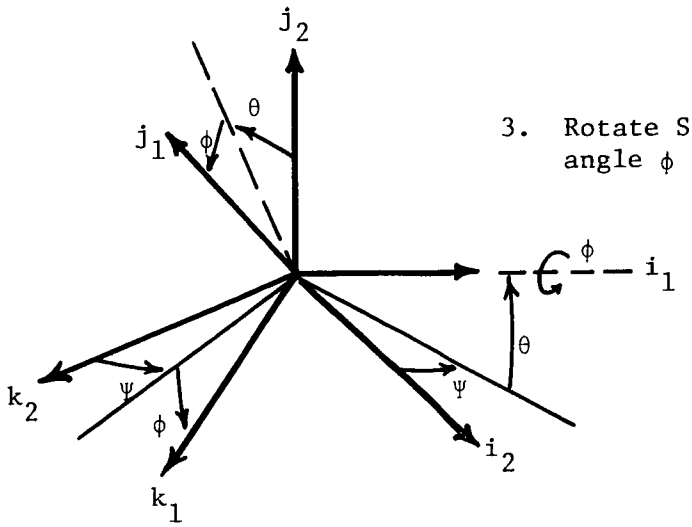

3. Rotate S1 through the angle ϕ about i_1.

Definition of Euler Angles

Fig. 5-10

(i) Arrangement 1

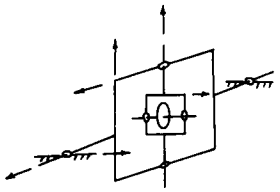

Spin axis is along $\hat{i}_2$

Inner gimbal plane: $\hat{i}_2$, $\hat{i}_2 \times \hat{k}_1$

Inner Angle between $\hat{i}_2$ and $\hat{k}_1$

Outer angle between $\hat{i}_1$ and $\hat{k}_1 \times \hat{i}_2$

Cos IA = sin θ cos Ψ sin ϕ + sin Ψ cos ϕ

$$\text{Cos OA} = \frac{\cos\phi \sin\theta \cos\Psi - \sin\phi \sin\Psi}{\sqrt{(\cos\theta \cos\Psi)^2 + (\cos\phi \sin\theta \cos\Psi - \sin\phi \sin\Psi)^2}}$$

Yaw motion causes gimbal lock.

(ii) Arrangement 2

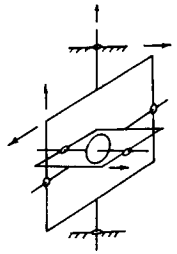

Spin axis is along $\hat{i}_2$

Inner gimbal plane: $\hat{i}_2$, $\hat{i}_2 \times \hat{j}_1$

Inner angle between $\hat{i}_2$ and $\hat{j}_1$

Outer angle between $\hat{i}_1$ and $\hat{i}_2 \times \hat{j}_1$

Cos IA = sin ϕ sin Ψ - cos ϕ sin θ cos Ψ

$$\text{Cos OA} = \frac{-(\sin\theta \sin\phi \cos\Psi + \sin\Psi \cos\phi)}{\sqrt{(\cos\theta \cos\Psi)^2 + (\sin\theta \sin\phi \cos\Psi + \sin\Psi \cos\phi)^2}}$$

Pitch motion causes gimbal lock.

(iii) Arrangement 3

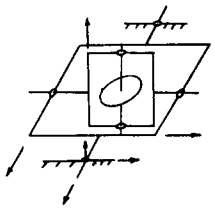

Spin axis is along $\hat{j}_2$

Inner gimbal plane: $\hat{j}_2$, $\hat{j}_2 \times \hat{k}_1$

Inner angle is between $\hat{j}_2$ and $\hat{k}_1$

Outer angle is between $\hat{j}_1$ and $\hat{j}_2 \times \hat{k}_1$

Cos IA = - cos θ sin ϕ

$$\text{Cos OA} = \frac{-\sin\theta}{\sqrt{\sin^2\theta + (\cos\theta \sin\phi)^2}}$$

Roll motion causes gimbal lock.

(iv) Arrangement 4

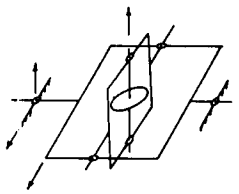

Spin axis is along $\hat{j}_2$

Inner gimbal plane: $\hat{j}_2$, $\hat{j}_2 \times \hat{i}_1$

Inner angle is between $\hat{j}_2$ and $\hat{i}_1$

Outer angle is between $\hat{j}_1$ and $\hat{i}_1 \times \hat{j}_2$

Cos IA = sin θ

Cos OA = sin ϕ

$\epsilon = \pi/2$ - IA

$\phi = \pi/2$ - OA

Convenient for measuring θ and ϕ.

Pitch motion causes gimbal lock.

(v) Arrangement 5

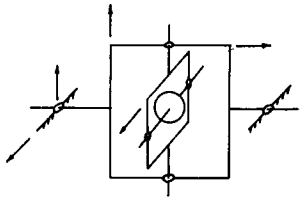

Spin axis is along $\hat{k}_2$

Inner gimbal plane: $\hat{k}_2$, $\hat{k}_2 \times \hat{i}_1$

Inner angle between $\hat{k}_2$ and $\hat{i}_1$

Outer angle between $\hat{k}_1$ and $\hat{k}_2 \times \hat{i}_1$

Cos IA = - sin Ψ cos θ

$$\text{Cos OA} = \frac{-(\cos\phi \sin\theta \sin\Psi + \sin\phi \cos\Psi)}{\sqrt{(\sin\phi \sin\theta \sin\Psi + \cos\phi \cos\Psi)^2 + (\cos\phi \sin\theta \sin\Psi + \sin\phi\cos\Psi)^2}}$$

Yaw motion causes gimbal lock.

(vi) Arrangement 6

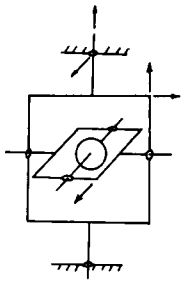

Spin axis is along $\hat{k}_2$

Inner gimbal plane: $\hat{k}_2$, $\hat{j}_1 \times \hat{k}_2$

Inner angle between $\hat{k}_2$ and $\hat{j}_1$

Outer angle between $\hat{k}_1$ and $\hat{j}_1 \times \hat{k}_2$

Cos IA = cos ϕ sin θ sin Ψ + sin ϕ cos Ψ

$$\text{Cos OA} = \frac{\sin\Psi \cos\theta}{\sqrt{(\sin\Psi \cos\theta)^2 + (\cos\phi \cos\Psi - \sin\phi \sin\theta \sin\Psi)^2}}$$

Roll motion causes gimbal lock.

Gimbal Arrangements of Two-Degree-of-Freedom Gyros

Fig. 5-11

The second angle that can be measured will be called the outer angle (OA). This angle is between the plane of the outer gimbal and one of the axes of the vehicle fixed S1 coordinate system. The sides of this angle are shown for each of the gimbal arrangements.

In Fig. 5-11 the cosines of the inner angle and the outer angle are listed as functions of the Euler angles Ψ, θ, and ϕ for each gimbal arrangement. As promised earlier these functions have a wide range of complexity.

The derivation of these expressions is shown in Appendix B.

Gyro Selection

It will be assumed that two two-degree-of-freedom gyros must be selected to measure the vehicle orientation by measuring Ψ, θ, and ϕ.

The first elimination of gimbal arrangements can be made by discarding those that are vulnerable to gimbal lock for the type of rotation anticipated. For example, in many applications such as a land vehicle, a submarine, a commercial airliner, and even a lunar roving vehicle, the elevation and roll angles will never approach 90°. However, for these same applications the heading angle can take on any value. For these applications gimbal arrangements 1 and 5 must be discarded because they will experience gimbal lock unless heading angle is restricted. For other applications different restrictions on vehicle rotation will cause different gimbal arrangements to be vulnerable to gimbal lock.

Of the remaining four gimbal systems, apparently arrangement 4 should be selected as one of the two instruments needed for this job. The inner and outer angles of the gimbals in arrangement 4 are direct measurements of the Euler angles θ and ϕ.

A second instrument must be chosen to determine the heading angle, Ψ. Arrangement 3 is of no use because its gimbal angles are independent of Ψ. Gimbal arrangements 2 and 6 remain. For these systems the cosines of the inner angles are much simpler functions than the cosines of the outer angles. Therefore, the measurement of one of these inner angles should be used. For arrangement 2 and 6 the cosines of the inner angles are equally complex functions of Ψ, θ, and ϕ. Arrangement 6 will be arbitrarily selected to measure the heading angle.

For arrangement 6

$$\cos (IA) = \cos \phi \sin \theta \sin \Psi + \sin \phi \cos \Psi \qquad (5\text{-}23)$$

The size of the inner angle (IA) is measured. ϕ and θ are available from the gyro that was selected with a vertical axis. In order to determine Ψ these known angles must be used in the above equations so that it becomes

$$A = B \sin \Psi + C \cos \Psi \qquad (5\text{-}24)$$

where A, B, and C are known constants. Now this transcendental equation must be solved for Ψ. It seems that this solution might be difficult to instrument.

Neglecting the Roll Angle, ϕ

At this point it is tempting to go back to (5-23) and make the approximation that the roll angke, ϕ, is zero. Certainly for many applications the roll angle is small most of the time. This approximation causes (5-23) to become simply

$$\cos (IA) = \sin \theta \sin \Psi \qquad (5\text{-}25)$$

The effects of this approximation will be examined for two specific cases which will show that this approximation cannot be tolerated.

First consider the case where $\Psi = 0°$, $\theta = 10°$, and $\phi = 10°$.

$$\cos (IA) = \sin 10°$$

Using (5-25) Ψ is computed as follows:

$$\Psi \text{ computed} = \sin^{-1} (\cos (IA)/\sin \theta)$$

$$= \sin^{-1} (\sin 10°/\sin 10°)$$

$$= 90°$$

Even this mild 10° roll angle caused a 90° error in the measure of Ψ.

The second case to be considered is $\Psi = 90°$, $\theta = 10°$, and $\phi = 10°$. From (5-23)

$$\cos (IA) = \sin 10° \cos 10°$$

Using (5-25)

$$\Psi \text{ computed} = \sin^{-1} (\cos (IA)/\sin \theta)$$

$$= 80°$$

This time the error in the computation of Ψ is 10°.

Apparently, approximating the roll angle as zero in (5-23) is an unsatisfactory solution to this problem.

Roll Stabilized Directional Gyro

The requirement to solve the transcendental equation (5-25) can be avoided by using a roll stabilized directional gyro. The outer gimbal of a roll stabilized gyro is not mounted to the vehicle. Instead it is mounted in a third gimbal that is in turn mounted on the vehicle. This is shown in Fig. 5-12.

This third gimbal is slaved to the roll angle measured by the vertical gyro so that the plane of gimbal remains vertical. This is accomplished by using a control loop to force the angle shown as Q in Fig. 5-12 always to be equal to the measured value of ϕ.

Now the directional gyro actually measures the orientation of the third gimbal rather than the orientation of the vehicle. The control loop described above assures that ϕ is zero for the third gimbal. Fortunately, however, the gimbal heading and elevation angles are exactly the same as those for the vehicle. See Fig. 5-12. The fact that the roll angle is zero leads to the following simple equation.

$$\cos (IA) = \sin \Psi \sin \theta \qquad (5\text{-}26)$$

Elevated Inner Gimbal Axis

Now just as things were beginning to look good another problem appears. If the elevation angle, θ is zero the inner angle will be zero regardless of the size of the heading angle, Ψ. Once again, the elusive heading angle has succeeded in hiding itself.

Remember that two gimbal arrangements, 2 and 6 were candidates for the task of determining Ψ. Arrangement 6 was arbitrarily chosen. Perhaps if arrangement 2 were mounted in a roll stabilized gimbal the present difficulty would go away.

Unfortunately, a quick check of Fig. 5-11 shows that arrangement 2 would also be unable to provide an indication of the heading angle when the elevation is zero. Using the inner angle of arrangement 2 leads to the same problem experienced with arrangement 6. Using the outer angle is too complicated. Therefore, there is no good reason to abandon the arbitrarily selected arrangement 6

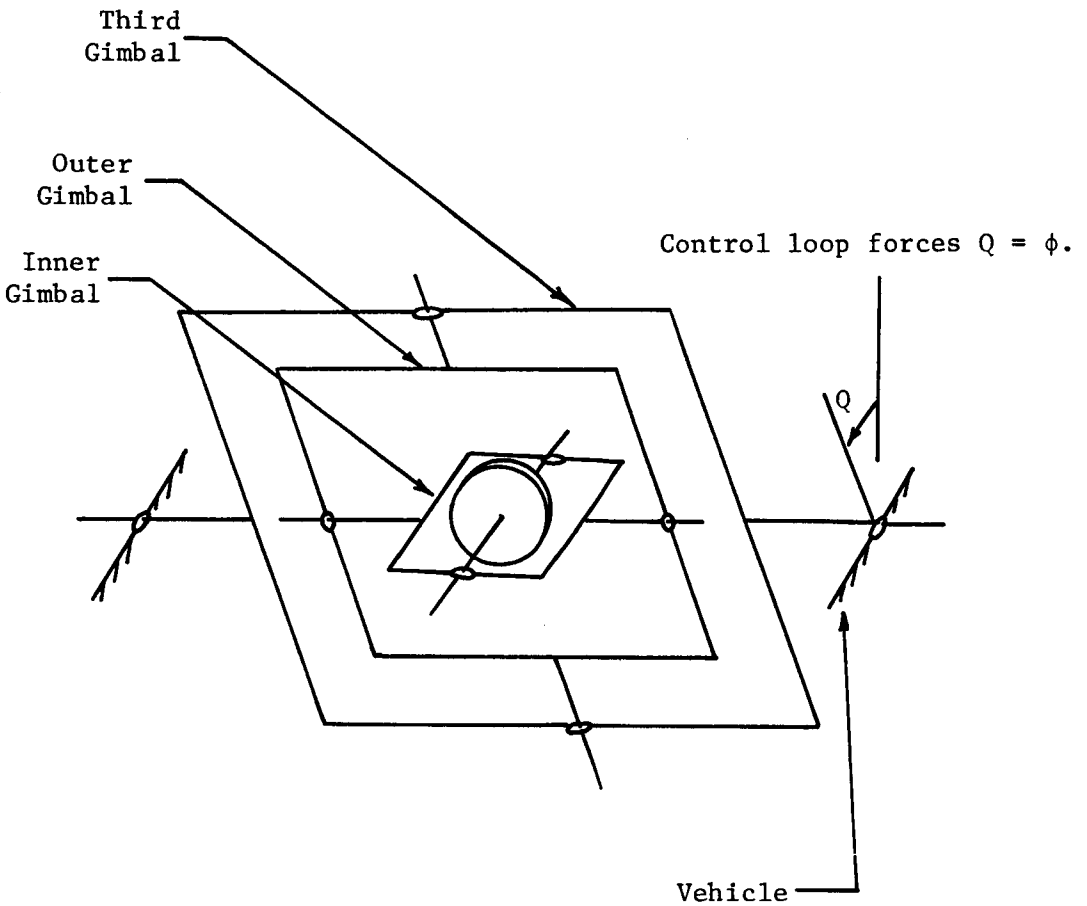

Roll Stabilized Gyro

Fig. 5-12

in favor of arrangement 2.

The correct solution to this current problem is to elevate the outer gimbal relative to the vehicle axis. In this way the undesirable singularity of (5-26) can be shifted so that it will occur only if the vehicle is elevated to an angle that is outside the expected operating range. Fig. 5-13 shows a roll stabilized directional gyro with an elevated outer gimbal. If $\theta_o + 90°$ is the angle between the outer gimbal axis and the vehicle longitudinal axis and θ_g is the elevation angle for the third gimbal then

$$\theta = \theta_g - \theta_o$$

$$\cos (IA) = \sin \theta_g \sin \Psi$$

$$\cos (IA) = \sin (\theta + \theta_o) \sin \Psi$$

$$\Psi = \sin^{-1}(\cos (IA)/\sin (\theta + \theta_o))$$

This last equation will not be indeterminate unless θ goes to $-\theta_o$. Since θ_o will be selected outside the range of expected elevation values this arrangement will successfully measure the heading angle.

Summary

Fig. 5-14 shows the two instruments that have been selected to measure the orientation of a vehicle with restricted elevation and roll angles. The amount of computation that must be performed on the measured angles is indicated.

5-4. Rate Gyros and Computational Platforms

One system that will determine the complete vehicle orientation —— heading, elevation, and roll —— is a strapped down, computational platform. The strapped down platform uses three single-degree-of-freedom rate gyros mounted on the vehicle to measure the rotation of the vehicle about each of its own axes. Before looking at the equations for the strapped down platform, it will be beneficial to study the way in which a single-degree-of-freedom, rate gyro works. The following discussion is found in reference 1.

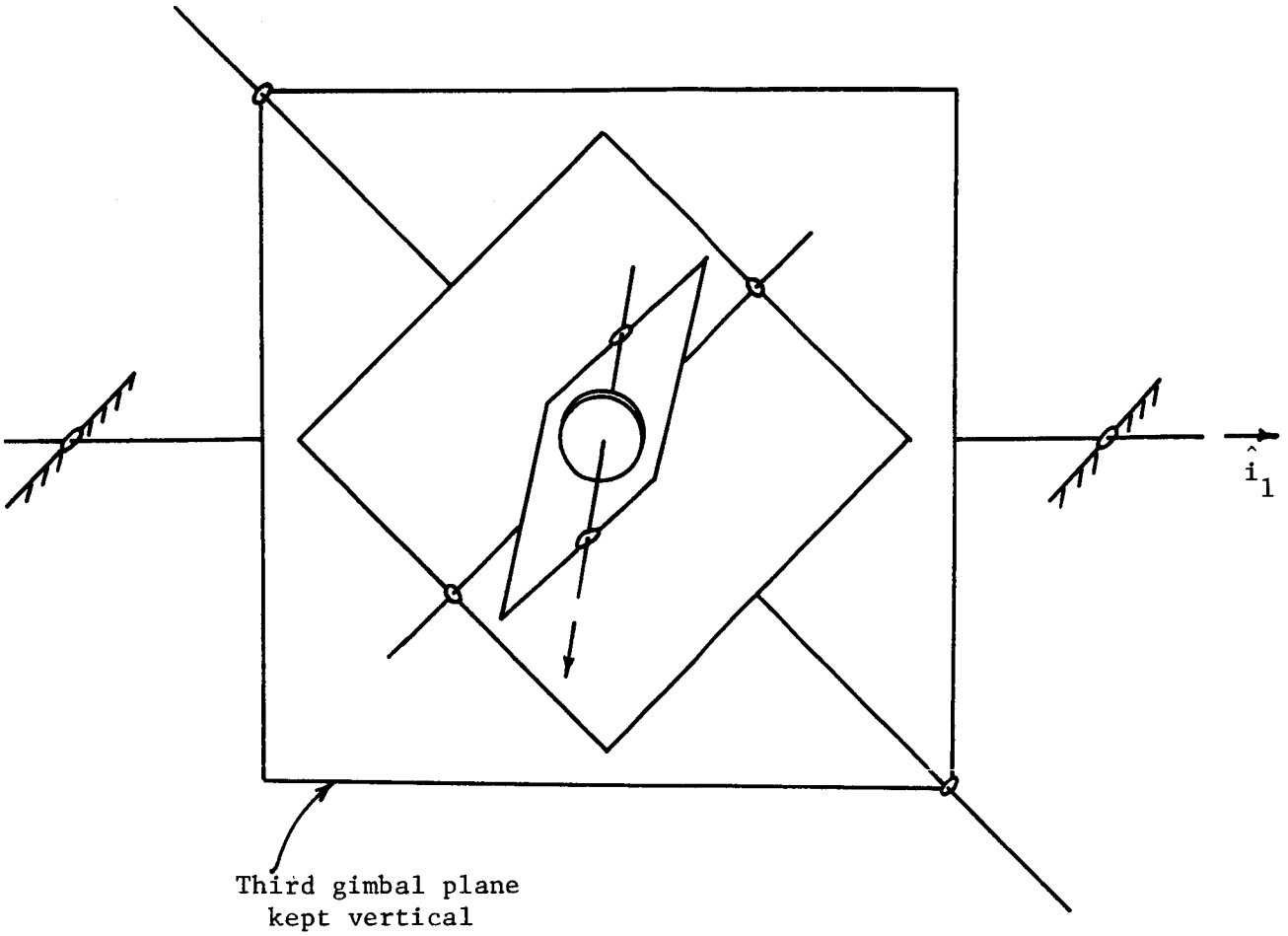

Roll Stabilized Directional Gyro with Elevated Inner Gimbal Axis

Fig. 5-13

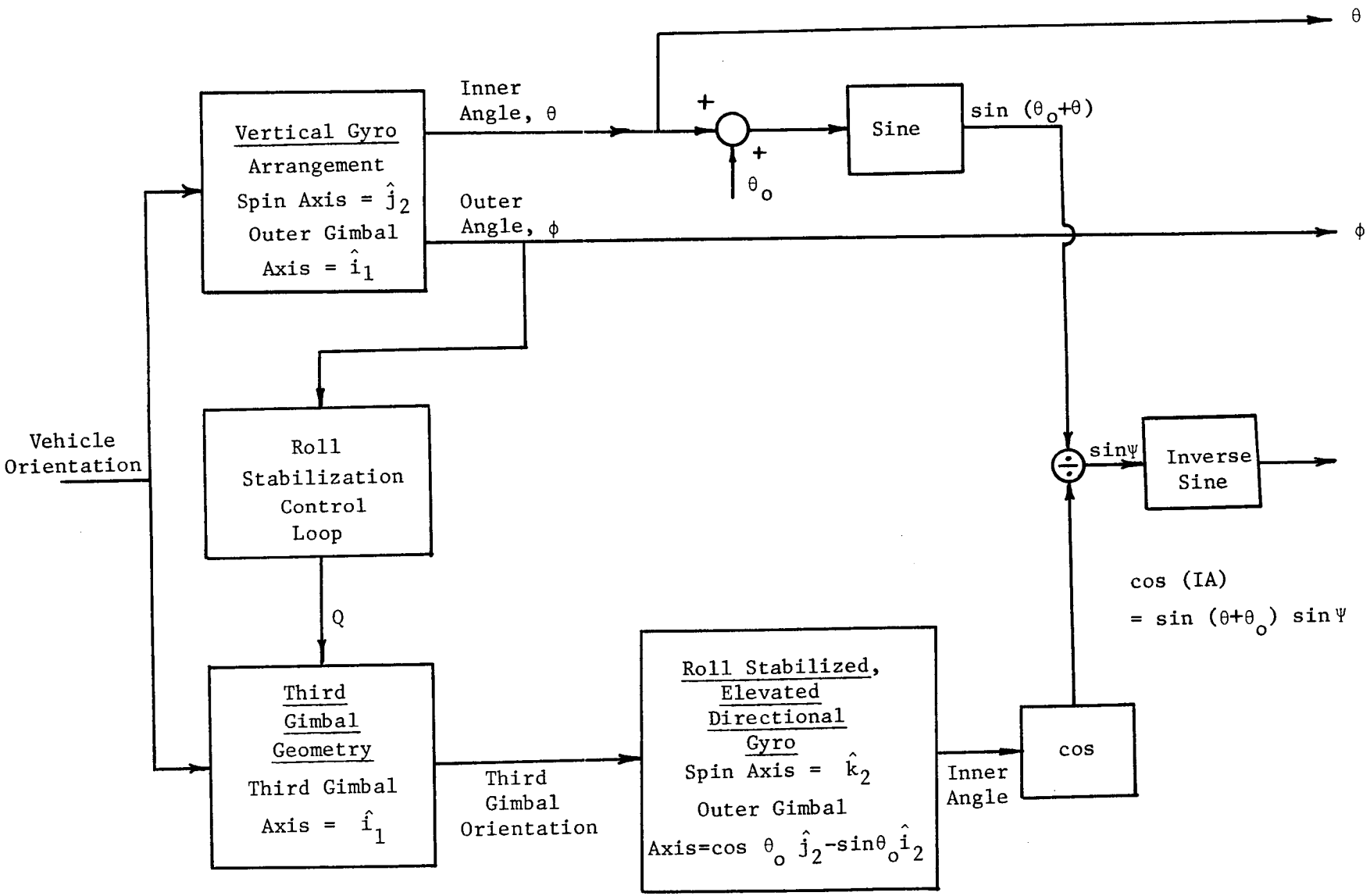

Gyro System Block Diagram

Fig. 5-14

Single-degree-of-freedom gyros

The fundamental relationship describing the motion of a rotating wheel under the influence of an external torque perpendicular to the axis of spin of the body is

$$T = \omega \times I_s\omega'$$

where

T = torque about the input axis

I_s = moment of inertia about the spin axis

ω' = angular velocity about the spin axis

ω = angular velocity about the precession axis

The angular momentum of the wheel is represented by

$$H = I_s\omega'$$

so that

$$T = \omega \times H$$

The relationship between the angular momentum vector, the torque vector, and the precession vector may be seen in Fig. 5-15a.

A similar angular rate about the T-axis would produce a torque about the precession axis. To avoid confusion about whether the input to the gyro is a torque or an angular rate, the axes of a single-degree-of-freedom gyro are usually labeled the spin axis or spin-reference axis (SRA); the input axis (IA); and the precession or output axis (OA). These axes are shown on Fig. 5-15b.

In the single-degree-of-freedom gyro shown in Fig. 5-15b, the spinning wheel with its set of spin bearings has only one additional degree of freedom with respect to the gyro case. An angular rate ω_1 about the input axis (IA) will cause a precession torque about the output axis (OA). The torques opposing any gyroscopic torque about the output axis are due to the inertia, viscous damping, and spring-reaction torques acting on this axis. Thus, the sum of all the torques acting on the OA is

$$T = H\omega_1 = I_o\ddot{\theta} + C\dot{\theta} + K\theta$$

where ω_1 is the rate about the IA, I_o is the inertia about the OA, C is the damping about the OA, K is the spring constant about the OA, and θ is the angular precession or rotation about the OA.

If the spring constant K is made large compared with the inertia and damping, the gyro has the following characteristics:

$$H\omega_1 \approx K\theta$$

thus

$$\theta \approx \frac{H}{K}\omega_1 \qquad (5\text{-}27)$$

or, the output angle is directly proportional to the input rate. Thus, the gyro becomes a rate-measuring instrument. In this configuration, it is known as a spring-restrained rate gyro. Equation (5-27) is exact for low frequencies, but is in error near and above the resonant frequency determined by I_o and K.

Some form of angular position pickoff, shown as signal generator (SG), may be employed to provide an electrical output. A direct visual output in the form of a pointer may also be used, as in the common turn-and-bank indicator employed in aircraft. This type of gyro is commonly used to provide a rate of damping signal to stabilize an autopilot system. For this type of gyro, the common range of input rates varies from a few degrees per minute to hundreds of degrees per second, although in any one instrument the linearity and null errors of the gyro would probably be from 1 to 5 percent of full-scale rate. The typical error sources of this type of gyro are pickoff and spring nulls not exactly aligned, unbalance of the rotor or gimbal, and damping or other highly temperature-dependent characteristics.

Computational Platform

Fig. 5-10 shows that three Euler angles, Ψ, θ, and ϕ, can be used to describe the vehicle orientation. Three of the single-degree-of-freedom gyros described above can be mounted on the LRV with their input axes along the vehicle axes so that they will measure P, Q, and R, the vehicle pitch, yaw, and roll rates. The following equations give the rate of change of the Euler angles as a function of P, Q, and R and the current values of the Euler angles.

$$\dot{\theta} = Q\cos\phi - R\sin\phi$$

$$\dot{\phi} = P + Q\sin\phi\tan\theta + R\cos\phi\tan\theta$$

$$\dot{\Psi} = Q\frac{\sin\phi}{\cos\theta} + R\frac{\cos\phi}{\cos\theta}$$

The Euler angles can be determined by integrating these Euler angle rates. The block diagram in Fig. 5-16 illustrates the mechanization of these equations that will generate a continuous measure of the vehicle orientation.

5-5. Solar Sensors

Photosensitive devices can be used to determine the vehicle's heading angle by measuring the direction to the sun. Here five different ways to instrument this measurement will be described and compared. The five systems that will be examined are distinguished by the type of sensors used and the way in which the sensors are mounted. The five arrangements are:

1. Single axis, wide field of view sensor fixed to the vehicle.
2. Single axis, narrow field of view sensor, pivoted on the vehicle.
3. Single axis, wide field of view sensor, fixed to a level platform.
4. Single axis, narrow field of view sensor, pivoted on a level platform.
5. Two axis, narrow field of view sensor, tracking the solar line of sight.

The trade-off's that must be made in order to select the one system that is best suited for the LRV application will be examined by asking the following questions about each system.

1. Is a single axis or a two axis sensor required?
2. What is the required sensor field of view?
3. How much computation is required?
4. How many mechanical gimbals must be controlled?
5. Must the value of the roll angle, ϕ, be provided by an external source?
6. Must the system be re-aimed at the sun if it is temporarily shadowed by some obstacle?

Table 5-1 summarizes the results of this comparison.

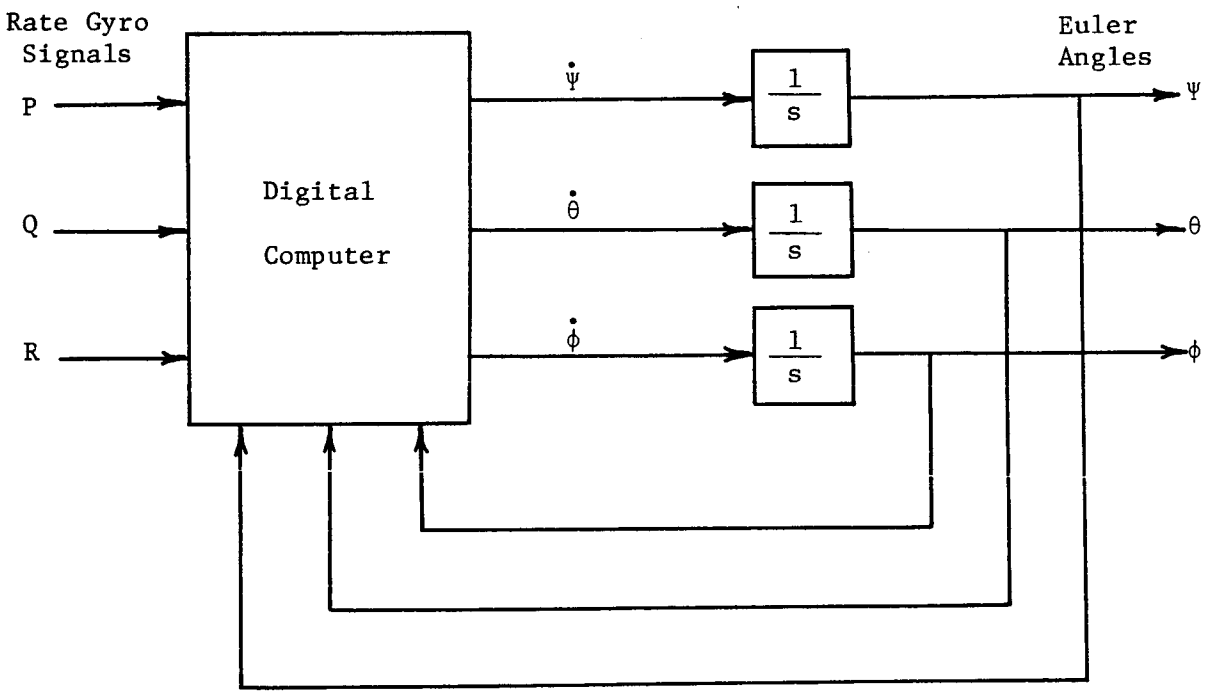

Strapped Down Platform

Fig. 5-16

System Number	Sensor Platform	Number of Angles Photosensitively Measured	Computation Requirements	Number of Controlled Gimbals	Is Roll Angle Needed	Must the System be Re-aimed if the Sensor is shadowed
1	Vehicle	1	High	0	Yes	No
2	Vehicle	1	High	1	Yes	Yes
3	Level Platform	1	None	2	Yes	No
4	Level Platform	1	None	3	Yes	Yes
5	Solar Tracking Platform	2	Low	2	No	Yes

System Comparison

Table 5-1

Sensors

It will be assumed that the same type of sensor will be used to instrument each of the five systems. This basic sensor will consist of a row of photocells that are shielded from the sun by a reticle with a single slot as shown in Fig. 5-17a. The signals from the photocells are a direct indication of the angle between the line of the photocells and the projection of the sun line of sight into the plane normal to the slit. This very simple device would measure the same angle that is measured by the much more sophisticated sun aspect sensors that are produced for aerospace applications. Whether the output signal from the sensor is digital or analog is irrelevant to this current geometric discussion.

For some of the systems that will be discussed sensors with a narrow field of view will be adequate. In these cases a sensor like the one in Fig. 5-17a can be used. Other systems will require that the sensor be able to measure angles from 0 to 360 degrees. This can be accomplished by using an array of sensors as shown in Fig. 5-17b. In the following discussion the array in Fig. 5-17b will be called one sensor with a 360° field of view.

The sensor shown in Fig. 5-17a measures the angle between the photocell line and the projection of the solar direction into the plane normal to the slit. This is a single axis sensor since only one angle is measured. If two sensors are combined so that they measure angles defined by the projections of the sun into two planes that are normal to the slits in the two sensors then this instrument will be called a two-axis sensor.

Solar Direction

A unit vector, $\hat{S}$, along the direction toward the sun can be resolved in the fixed S2 coordinate system and in the vehicle referenced S1 coordinate system.

For convenience let $\hat{i}_2$ be along the projection into the horizontal plane of the LOS from the vehicle to the sun. In this way the heading angle, Ψ, will be zero when the LRV is headed toward the sun.

If b is the elevation angle of the solar LOS above the local horizon then

$$\hat{S} = \cos b\, \hat{i}_2 + \sin b\, \hat{j}_2 \qquad (5\text{-}28)$$

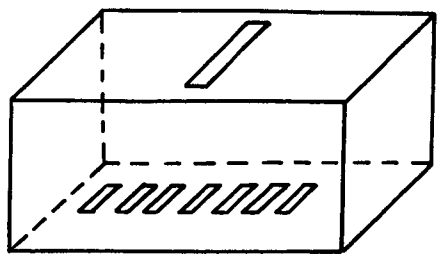

(a) Basic Sun Aspect Sensor

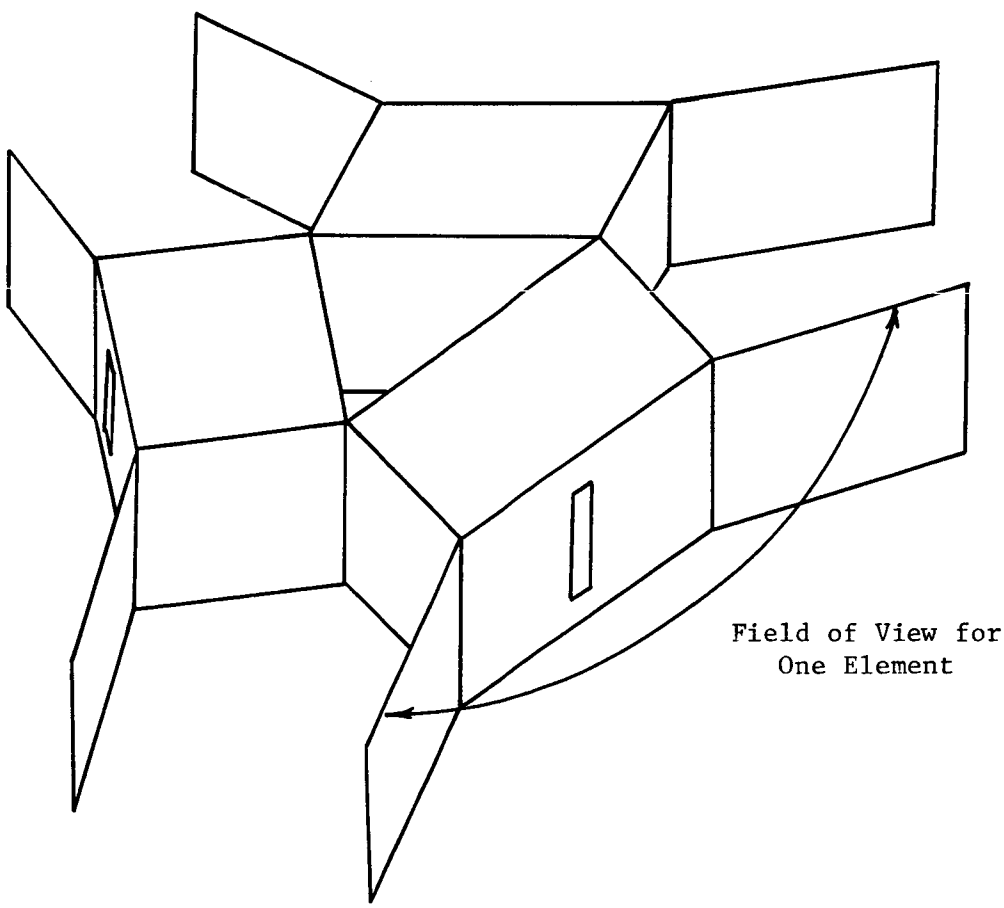

(b) Sensor Array with 360° Field of View

Fig. 5-17

Using the direction cosines that relate the S2 and S1 coordinate systems shows that the solar line of sight resolved along vehicle coordinates is

$$\begin{aligned}\hat{S} = &(\cos b \cos\theta \cos\Psi + \sin b \sin\theta)\,\hat{i}_1 \\ &+(\cos b\,(-\cos\phi \sin\theta \cos\Psi + \sin\phi \sin\Psi) + \sin b \sin\theta \\ &\quad \cos\phi)\,\hat{j}_1 \\ &+(\cos b\,(\sin\theta \cos\Psi \sin\phi + \sin\Psi \cos\phi) - \sin b \cos\theta \\ &\quad \sin\phi)\,\hat{k}_1\end{aligned} \tag{5-29}$$

System 1: One Sensor Fixed to the Vehicle

The first arrangement to be examined will be one sensor fixed to the vehicle. This approach requires that the sensor have a 360° field of view in order to assure that the solar direction can always be measured.

Initially, it will be assumed that the sun aspect sensor will be strapped down to the LRV with the reticle slit and the line of the photocells along two of the vehicle axes. There are six such orientations and they are listed in Table 5-2 along with the cosine of the angle that is measured for each orientation. Equation (5-29) was used to develop these expressions for the measured angle cosines.

Let it be assumed that θ and ϕ are measured with the inclinometer or a vertical gyro and that b, the elevation of the sun, is known from the lunar ephemeris. Still the solution of one of these transcendental expressions is a discouragingly complicated task. Unfortunately, though, one of these expressions must be solved if a strapped down sun sensor is used to measure Ψ.

The sensor has a 360° field of view. Therefore this system will not have to be re-aimed at the sun if the line of sight is temproarily interrupted.

System 2: One Sensor Pivoted on the Vehicle

The second scheme is geometrically very similar to the first. A single axis, narrow field of view sensor is mounted so that it can rotate about an axis normal to the vehicle as shown in Fig. 5-18. This gimbaled sensor is pointed by a tracking loop that uses the sensor signals to keep it pointed at the solar plane. The mechanical gimbal angle is the same as the angle measured by a strapped down

	Slit Direction	Direction of Line of Photocells	Projection Plane	Cosine of Measured Angle
1	i_1	j_1	j_1k_1	$\frac{S_j}{\sqrt{S_j^2 + S_k^2}}$
2	i_1	k_1	j_1k_1	$\frac{S_k}{\sqrt{S_j^2 + S_k^2}}$
3	j_1	k_1	i_1k_1	$\frac{S_k}{\sqrt{S_i^2 + S_k^2}}$
4	j_1	i_1	i_1k_1	$\frac{S_i}{\sqrt{S_i^2 + S_k^2}}$
5	k_1	i_1	i_1j_1	$\frac{S_i}{\sqrt{S_i^2 + S_j^2}}$
6	k_1	j_1	i_1j_1	$\frac{S_j}{\sqrt{S_i^2 + S_j^2}}$

$$S_i = \cos b \cos \theta \cos \Psi + \sin b \sin \theta$$

$$S_j = \cos b [\sin \phi \sin \Psi - \cos \phi \sin \theta] + \sin b \cos \theta \cos \phi$$

$$S_k = \cos b [\sin \theta \cos \Psi \sin \phi + \sin \Psi \cos \phi] - \sin b \cos \theta \sin \phi$$

Cosines of Angles Measured by Strap-Down Sensor

Table 5-2

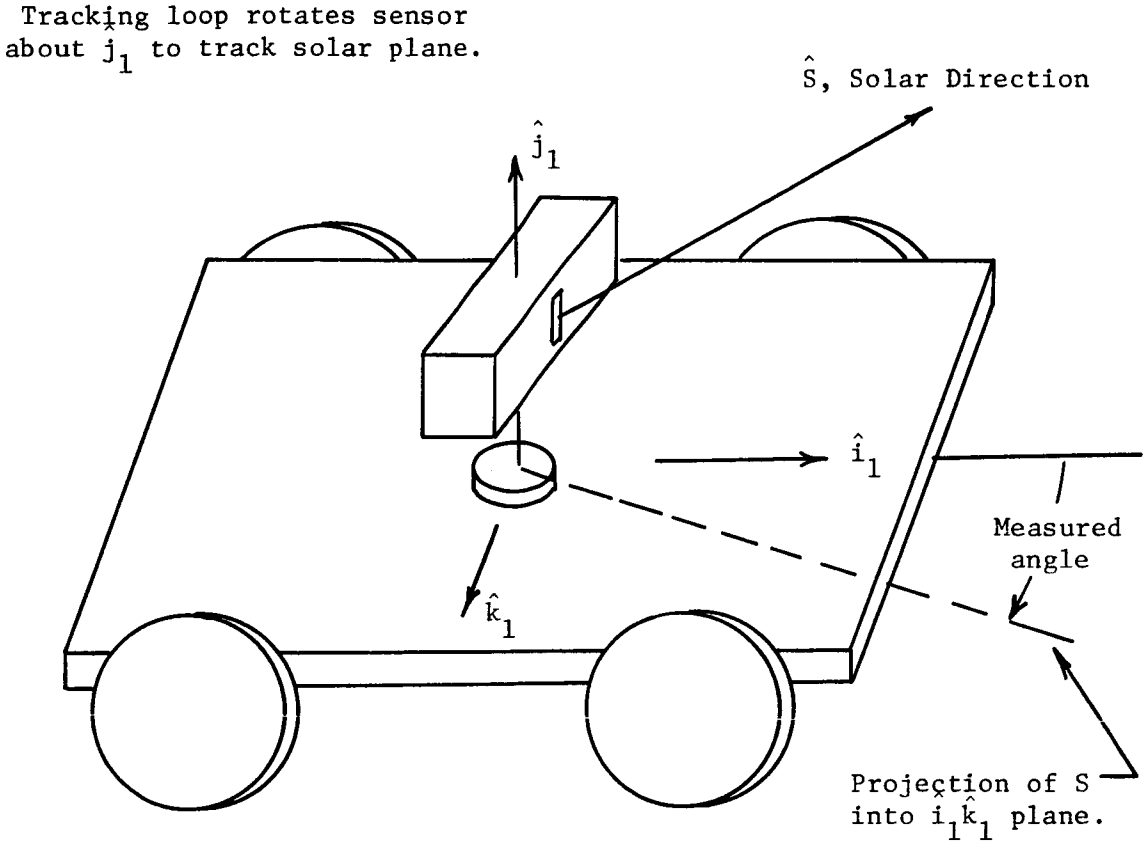

One Sensor Pivoted on Vehicle

Fig. 5-18

sensor with the slit along $\hat{j}_1$ and the photocell line along $\hat{i}_1$, which is number 4 in Table 5-2. Therefore, the solution of a complicated, transcendental function of θ, ϕ, b, and Ψ is still required in order to determine Ψ. If the sensor is shadowed it must be re-aimed at the sun.

System 3: One Sensor Fixed to a Level Platform

One way to avoid the solution of the transcendental equation to get Ψ is to abandon the idea of mounting the sensor to the vehicle and instead mount it on a level platform for which θ and ϕ are zero and for which Ψ is the same as the vehicle heading angle. Fig. 5-19 shows such an arrangement.

It is assumed that the gimbal angles are somehow set so that the platform is level, that is, parallel to the $\hat{i}_2\hat{k}_2$ plane. The discussion of how this can be done will be temporarily postponed. It is not immediately obvious that the constraint that the platform be level will cause the platform heading angle to be the same as the vehicle heading angle. That this is true will now be demonstrated.

The vehicle heading angle is the angle between $\hat{i}_2$ and the projection of $\hat{i}_1$ into the $\hat{i}_2\hat{k}_2$ plane. This projection will be called $\overline{p}$.

$$\overline{p} = (\hat{i}_1 \cdot \hat{i}_2)\, \hat{i}_2 + (\hat{i}_1 \cdot \hat{k}_2)\, \hat{k}_2$$

One edge of the platform in Fig. 5-19 is along $\hat{j}_2 \times (\hat{i}_1 x \hat{j}_2)$. This direction will be considered for the forward direction for the platform. If these cross products are evaluated,

$$\hat{j}_2 \times (\hat{i}_1 \times \hat{j}_2) = (\hat{i}_1 \cdot \hat{i}_2)\, \hat{i}_2 + (\hat{i}_1 \cdot \hat{k}_2)\, \hat{k}_2$$

It is now seen that the platform forward direction along this edge of the platform is the same as the projection of the vehicle forward axis into the $\hat{i}_2\hat{k}_2$ level plane. Therefore, the platform heading angle is the same as the vehicle heading angle.

The sensor shown in Fig. 5-19 will directly measure the angle between platform forward axis and the projection of the solar line of sight into the plane of the level platform. This means that the sensors directly measure the platform heading angle and consequently directly measure the vehicle heading angle.

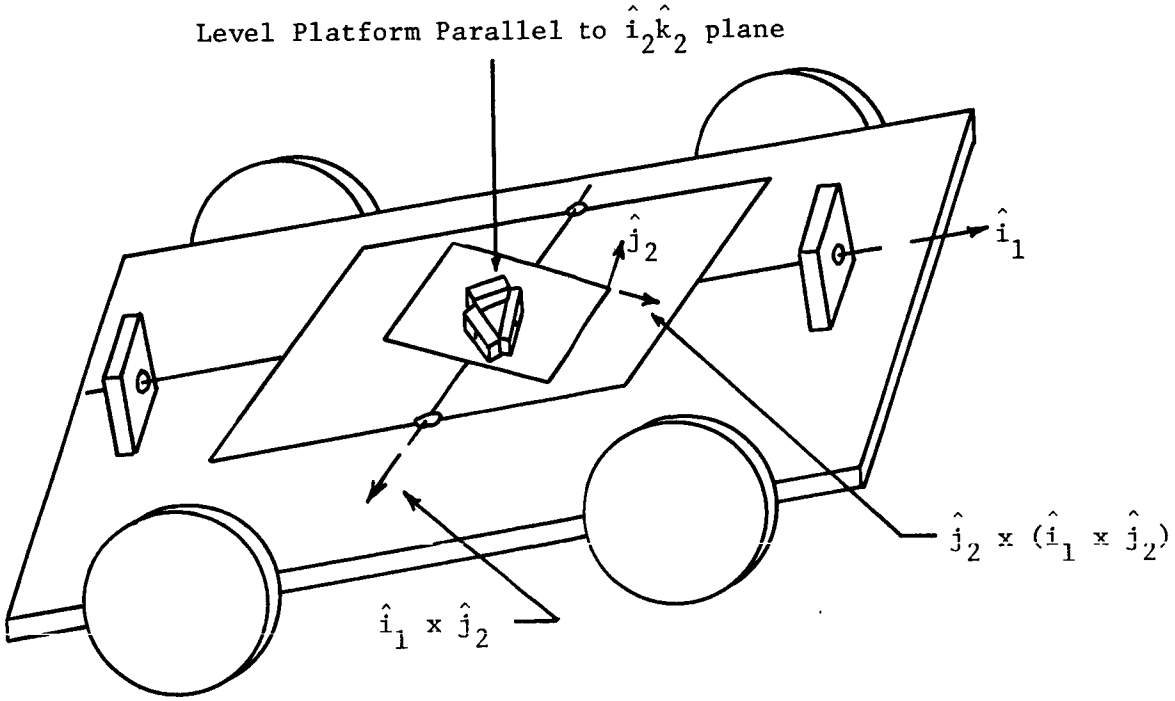

Single Axis Sensor Fixed on a Level Platform

Fig. 5-19

Mounting the sensor on the level platform has eliminated the computation that was required to determine Ψ from the output of a strapped down sensor. In fact, the gimbal system actually serves as a sort of analog angle computer.

Since this system uses a sensor with a 360° field of view it will not need to be re-aimed if the reticle is temporarily shadowed.

System 4: One Sensor Pivoted on a Level Platform

The fourth way to use a solar sensor to determine the LRV heading angle is to mount a single axis, narrow field of view sensor on a level platform so that it can pivot about an axis normal to the platform. Then a closed tracking loop can use the signals from the sensor to keep it pointed at the sun. This is a combination of the tracking loop from system 2 and the level platform of system 3. As in system 3 the vehicle heading angle is measured directly. For this system the heading angle is indicated by the angle of the gimbal driven by the tracking loop.

If the sensor used in this system is temporarily shadowed it will have to be re-aimed at the sun so that the tracking loop can re-acquire its solar target.

Level Platform Mechanization

At least two techniques are available for leveling the gimbaled platform for system 3 and 4. The first approach is to simply hand a plumb bob on the platform. The bob would level the gimbaled platform. This approach suffers from the disadvantage that the platform would swing whenever the vehicle accelerated either laterally or longitudinally.

A second approach eliminates this difficulty. Closed loop control systems can be used to slave the gimbal angles to the elevation and roll angles measured on a vertical gyro. The outer gimbal angle should be maintained equal to the measured value of roll; the inner gimbal angle should be forced to be equal to the measured value of elevation. Such a control loop would cause the platform to remain level as is required.

System 5: Two Sensors Mounted on a Gimbaled Platform that Tracks the Solar Line of Sight

Each of the systems previously discussed used only one sensor and either

measured or tracked the plane defined by the solar line of sight and some reference direction, either the local vertical or the direction normal to the vehicle chassis. This final scheme is different in that two sensors are used and the solar direction is tracked rather than the solar plane. Here two sensors or equivalently one two axis sensor is mounted on a two-degree-of-freedom platform that is supported by an inner and an outer gimbal.

One way to arrange the gimbals is shown in Fig. 5-20. If the outer gimbal axis were normal to the vehicle chassis the system would be vulnerable to gimbal lock when the sun was nearly overhead. The arrangement shown in Fig. 5-20 has the outer gimbal axis parallel to the chassis so that the system does not experience gimbal lock difficulties when the sun is overhead. For this system gimbal lock can occur only when the sun is near the horizon.

For this arrangement the gimbal can be used to measure the angle between the solar line of sight and $\hat{i}_1$. The cosine of this angle is as follows:

$$\cos \text{ (Inner Angle)} = \cos b \cos \theta \cos \Psi + \sin b \sin \theta$$

No other arrangement of two gimbals can produce a gimbal angle that is a simpler function than this one.

Given b and θ the inner angle can be measured and the above linear equation for the cosine of Ψ can be solved to determine Ψ.

Since this system uses narrow field of view instruments it would need to be re-aimed at the sun if the sensors were temporarily shadowed.

Summary

The following five techniques for using solar sensors to determine the vehicle heading angle have been described.

1. Single axis, wide field of view sensor fixed to vehicle.
2. Single axis, narrow field of view sensor, pivoted on vehicle.
3. Single axis, wide field of view sensor, fixed to level platform.
4. Single axis, narrow field of view sensor, pivoted on the level platform.
5. Two axis, narrow field of view sensor, tracking the solar line of sight.

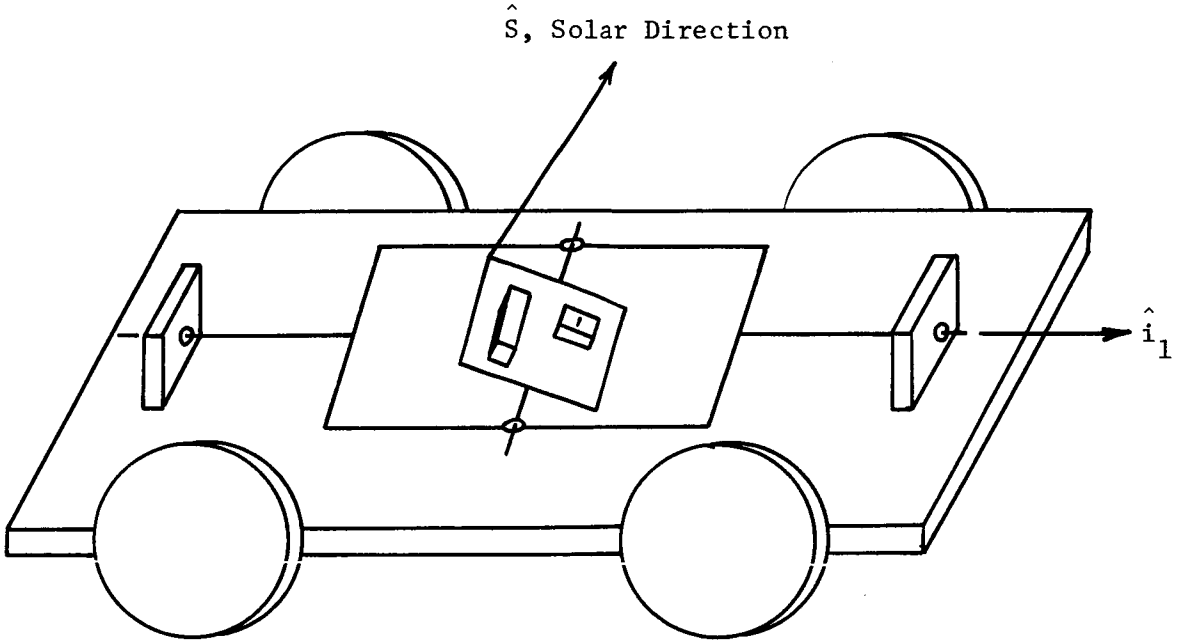

Two Sensors Tracking Solar Line of Sight

Fig. 5-20

The first system is mechanically simple because the sensor is fixed to the vehicle. However, the angles that can be measured by these strapped down sensors are complicated, transcendental functions of Ψ, θ, ϕ, and b. Extracting Ψ from the sensor output would require considerable computation.

The second system is comparable to the first in that it too would require the same computations to determine Ψ from the measured angle. Here, however, the requirement for a wide field of view sensor is eliminated by providing a mechanical tracking loop that enables the narrow field of view sensor to track the solar plane.

System 3 fixes the sensor to a level platform and thereby eliminates the computation that was required to determine Ψ from the sensor signals. Actually the computation task has been traded for the new problem of instrumenting a gimbaled level platform.

System 4 is comparable to system 3. Here too the heading angle is measured directly. Now, however, a narrow field of view sensor is used rather than a wide field of view sensor. A tracking loop is required to keep the sensor pointed at the solar plane.

System 5 is distinguished from the others in that it does not require knowledge of the roll angle, ϕ, from an external source. It is the only system that uses a two-axis sensor. The cosine of the measured angle is linearly related to the cosine of Ψ so that the computational requirements are not as extreme as they were for systems 1 and 2.

Some of the features of these five systems are compared in Table 5-1.

5-6. Pendulous Inclinometer

The most obvious method for determining the vertical is with a pendulous inclinometer. A two-degree-of-freedom pendulum can be used to measure the same roll and elevation angles that are measured by a two-degree-of-freedom vertical gyro. The attractive features of a pendulum are its light weight and its simplicity. However, the pendulous inclinometer suffers from the essential disadvantage that it swings when the LRV accelerates either forward or laterally.

The important question is "How does this swinging affect navigation accuracy?" Some feel for the answer to this question is provided by the following discussion.

Figure 5-21 shows a pendulum mounted on the LRV. For small δ the acceleration along $\hat{i}_1$ of the bob is

$$a_B = a - d\ddot{\delta}$$

The force on the bob along $\hat{i}_1$ is

$$F = mg\delta + \beta\dot{\delta}$$

where β is a measure of the pendulum damping. Consequently,

$$mg\delta + \beta\dot{\delta} = ma - md\ddot{\delta}$$

Using Laplace Transforms

$$\delta(s) = \frac{a(s)}{g} \frac{1}{\frac{s^2}{g/d} + \frac{\beta s}{mg} + 1}$$

If the damping constant, β, is set at $1.41fm\sqrt{gd}$ so that the damping ratio is 0.707 then the deflection caused by a step of acceleration is

$$\delta(t) = \frac{a}{g}\left[1 - 1.414e^{-.707\sqrt{g/d}\ t} \cos .707\sqrt{\frac{g}{d}}\ t\right]$$

For a 10 cm. pendulum and for g = 162 cm/sec^2 on the lunar surface the value of g/d is 4.03 rad/sec. Then

$$\delta(t) = \frac{a}{g}\left[1 - 1.414\ e^{-2.84t} \cos 2.84\ t\right] \qquad (5\text{-}30)$$

If the LRV starts from zero speed and accelerates with constant acceleration to some final speed then the duration of the acceleration and the distance covered while accelerating are given by (5-31) and (5-32).

$$T(\text{sec}) = 0.171\ v/c \qquad (5\text{-}31)$$

$$S(\text{km}) = 2.38 \times 10^{-5}\ \frac{v2}{c} \qquad (5\text{-}32)$$

where

v = LRV final speed in km./hr.

c = ratio of the LRV acceleration to the lunar surface gravity.

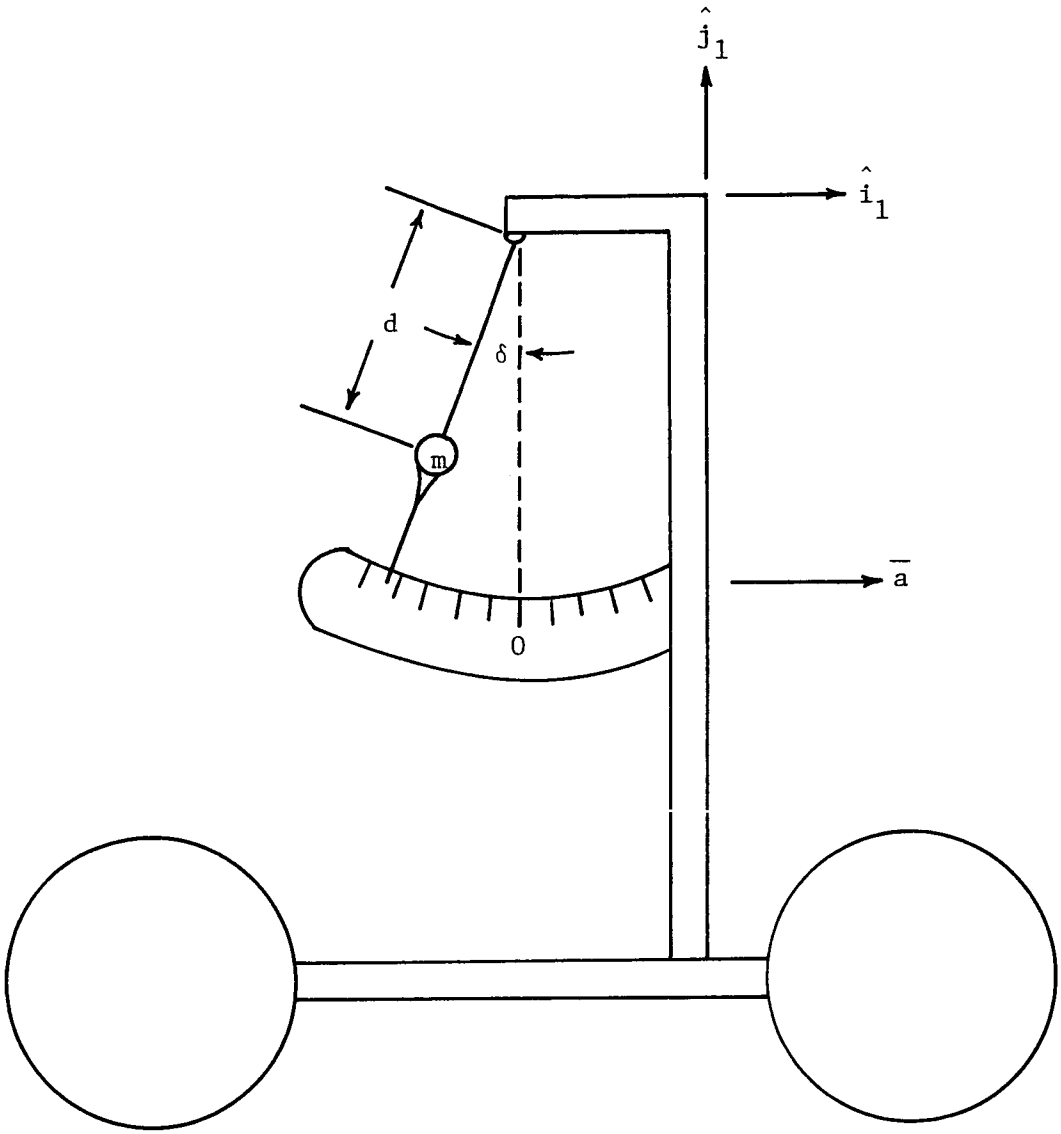

Pendulum Mounted on the LRV

Fig. 5-21

For $v > 10$ km/hr and $c < 1$, T is greater than or equal to 1.71 seconds. Consequently, (5-30) says that for most of the acceleration period δ can be closely approximated as a/g radians.

Assume that the acceleration and velocity are in the horizontal plane. The swinging pendulum will erroneously indicate that the LRV is tilted δ radians relative to the vertical. The resulting dead reckoning navigation errors will be

$$\text{horizontal error} = S\,(1 - \cos\delta)$$

$$\text{vertical error} = S \sin\delta$$

Since δ will be a small angle the first two terms of the cosine series will be used to approximate $\cos\delta$ and the first term of the sine series will be used to approximate $\sin\delta$. Then

$$\text{horizontal error} = \frac{1}{2} S \left(\frac{a^2}{g^2}\right)$$

$$= \frac{1}{2} \left(\frac{1}{2} \frac{v^2}{a}\right) \left(\frac{a^2}{g^2}\right)$$

$$= \frac{1}{4} \frac{v^2 c}{g}$$

$$= 1.19 \times 10^{-3}\, cv^2 \text{ (meters)}$$

$$\text{vertical error} = S \frac{a}{g}$$

$$= \frac{1}{2} \frac{v^2}{a} \frac{a}{g}$$

$$= \frac{1}{2} \frac{v^2}{g}$$

$$= 2.38 \times 10^{-3}\, v^2 \text{ (meters)}$$

where c and v are as defined above.

These equations say that accelerating at 1/5 lunar gravity to 15 km/hr generates 0.0535 meters horizontal error and 0.536 meters vertical error.

5.7. Sensor Combinations for Determining Orientation

This chapter has discussed several individual instruments that can be used in a dead reckoning navigation system to help measure the vehicle orientation. Table 5.3 lists eight potential ways that these instruments might be combined to determine the LRV orientation.

Instruments	Comments
1. One gyro 2. One sun sensor 3. Two sun sensors	None of these will work exactly because there is not enough information in one reference direction to define H. Errors that are a function of the LRV elevation and roll angles will occur if one of these systems are used.
4. Two gyros	Permits determination of vehicle's complete orientation. Gimbal arrangements have been investigated.
5. One gyro and an inclinometer	Geometrically equivalent to two gyro system. Inclinometer replaces vertical gyro.
6. Sun sensor and vertical gyro	Permits determination of vehicle's complete orientation. Mechanization has been investigated.
7. Sun sensor and inclinometer	Geometrically equivalent to sun sensor and vertical gyro system. Inclinometer replaces vertical gyro.
8. Computational platform with three rate gyros fixed to the LRV	Digital computation requirements are high. Equations for mechanization are in Section 5.4.

Heading Angle Determination

Table 5-3

CHAPTER 6

CELESTIAL AND SATELLITE POSITION FIX SCHEMES

6-1. Introduction

A trans-lunar excursion is planned for the DLRV. This explorative journey will take about one year and cover about 1000 km. Astronauts will rendezvous with the LRV after it finishes its trip across the moon. In order to provide the navigation accuracy required for this DLRV mission, periodic position fixes will be needed to update the dead reckoning navigator.

Three possible techniques for position fixing are:

1. Celestial sightings;
2. Satellite sightings;
3. Landmark sightings.

Each of these broad categories of position fixing techniques includes several specific position fixing schemes. What follows is a description and analysis of some celestial and satellite position fix techniques. Techniques based on landmark sightings will be discussed in Chapter 7.

In this description and comparison of several celestial and satellite position fix schemes the assumption will be made that the moon is a smooth sphere. This assumption will significantly simplify the geometry but will not obscure the inherent, geometric advantages and difficulties of the various position fix concepts. Therefore, a meaningful comparison of the position fix techniques can be made under the assumption that the moon is a smooth sphere.

Once the comparison of the schemes has indicated which position fix concepts are best suited to the LRV application then the smooth sphere assumption can be removed and the selected position fix concepts can be examined very precisely.

An important first question in the comparison of lunar position fixing techniques is whether a satisfactory position fix can be established from celestial sightings. The use of celestial sightings is relatively attractive when compared with the use of a navigational satellite simply because it avoids the requirements for having a navigational satellite in lunar orbit.

Two schemes for establishing a position fix based on celestial sightings will be examined here. One scheme uses the measurement of angles between a landmark on the earth and two different stellar directions. The second uses the measurement of angles between the local vertical and two different stellar directions.

TRANSIT, a network of satellites for navigation, has been developed for the U. S. Navy. This navigation satellite system is operational and it does provide precise position fix information to ships at sea. The success of this system suggests that using an artificial satellite in lunar orbit should be considered for the LRV position fixing requirement.

There are several ways to establish a position fix by observing a navigational satellite for which the orbital parameters are known. The satellite's orbital parameters include enough information to completely define that satellite's position and velocity at any instant of time. Any scheme that determines the LRV position relative to this satellite of known position will obviously provide a position fix for the LRV.

Three specific schemes will be described that assume that the orbital parameters are known and available. These schemes are based on measurement of:

1. LRV to satellite range
2. LRV to satellite range rate
3. Angles provided by satellite tracking

The second scheme is the one used for the TRANSIT system.

6-2. Sensitivity Analysis Technique

A mathematical technique described in Battin's Astronautical Guidance will be used here to develop expressions that relate the accuracy of a position fix to the position fix geometry and the precision with which the basic measurements are made. Obviously these equations will help in the selection of advantageous position fix schemes.

In this first analysis the following assumptions will be made:

1. The moon is a smooth sphere.

2. The LRV clock is perfect so that all measurements are made at known instants of time.
3. The lunar ephemeris is known exactly.

Since the moon is assumed to be spherical, the length of $\bar{r}$, the vector from the moon's center to the LRV position, is assumed to be a known constant. Two more parameters are needed to define the direction of $\bar{r}$ and thus complete the description of the LRV position. Consequently, two measurements must be made to establish a position fix. When celestial sightings are used these two measurements are celestial angles. Later the use of a navigation satellite for position fixing is considered. Then the two measurements are either angle, range, or range rate measurements. In any case the two measurements will be named q_1 and q_2.

Clearly the values of q_1 and q_2 depend on $\bar{r}$. It will be shown that if the LRV moves about a reference point in a region that is small enough so that all changes can be taken as first order differentials, that is, small enough so that the relation between the q's and $\bar{r}$ can be linearized then

$$\begin{aligned} \Delta q_1 &= \bar{h}_1 \cdot \Delta\bar{r} \\ \Delta q_2 &= \bar{h}_2 \cdot \Delta\bar{r} \end{aligned} \tag{6-1}$$

$\Delta\bar{r}$ is the deviation of $\bar{r}$ from the reference value $\bar{r}_o$; Δq is the deviation of q from the reference value q_o.

$$\begin{aligned} \Delta\bar{r} &= \bar{r} - \bar{r}_o \\ \Delta q_1 &= q_1 - q_{10} \\ \Delta q_2 &= q_2 - q_{20} \end{aligned} \tag{6-2}$$

Equation (6-1) shows that each measurement establishes the component of $\Delta\bar{r}$ along some vector, either $\bar{h}_1$ or $\bar{h}_2$.

Since $|\Delta\bar{r}|$ is assumed to be small relative to $|\bar{r}|$ it can be further assumed that $\Delta\bar{r}$ is in a plane normal to $\bar{r}_o$ and consequently $\Delta\bar{r}$, $\bar{h}_1$, and $\bar{h}_2$ can be resolved along two normal coordinates, $\hat{\ell}$ and $\hat{m}$ in that plane.

$$\Delta\bar{r} = \Delta r_\ell \hat{\ell} + \Delta r_m \hat{m}$$

$$\bar{h}_1 = h_{1\ell}\hat{\ell} + h_{1m}\hat{m}$$

$$\hat{h}_2 = h_{2\ell}\hat{\ell} + h_{2m}\hat{m}$$

Then

$$\begin{pmatrix} \Delta q_1 \\ \Delta q_2 \end{pmatrix} = \begin{pmatrix} h_{1\ell} & h_{1m} \\ h_{2\ell} & h_{2m} \end{pmatrix} \begin{pmatrix} \Delta r_\ell \\ \Delta r_m \end{pmatrix} \tag{6-3}$$

or

$$\Delta\bar{q} = H\Delta\bar{r} \tag{6-4}$$

The inverse relation is

$$\begin{pmatrix} \Delta r_\ell \\ \Delta r_m \end{pmatrix} = \frac{1}{h_{1\ell}h_{2m} - h_{1m}h_{2\ell}} \begin{pmatrix} h_{2m} & -h_{1m} \\ -h_{2\ell} & h_{1\ell} \end{pmatrix} \begin{pmatrix} \Delta q_1 \\ \Delta q_2 \end{pmatrix} \tag{6-5}$$

or

$$\Delta\bar{r} = H^{-1}\,\Delta\bar{q} \tag{6-6}$$

Thus far the H matrix has been used only to relate differential changes in the angles that are measured to differential changes in the LRV position vector. However, this relation is closely connected to the sensitivity of position fixing accuracy to measurement errors.

In the following equations primed variables represent measured or estimated values.

$$\bar{r} = \bar{r}_o + \Delta\bar{r}$$

$$\bar{r}' = \bar{r}_o + \Delta\bar{r}'$$

$$\bar{e}_r = \Delta\bar{r}' - \Delta\bar{r} = \bar{r}' - \bar{r}$$

$$\bar{q} = \bar{q}_o + \Delta\bar{q}$$

$$\bar{q}' = \bar{q}_o + \Delta\bar{q}'$$

$$\therefore\ \bar{e}_q = \Delta\bar{q}' - \Delta\bar{q} = \bar{q}' - \bar{q}$$

If $\Delta\bar{r}' = H^{-1}\Delta\bar{q}'$ as suggested by (6-6) then

$$\bar{e}_r = \Delta\bar{r}' - \Delta\bar{r}$$

$$= H^{-1} (\Delta\bar{q}' - \Delta\bar{q}) = H^{-1} \bar{e}_q \qquad (6\text{-}7)$$

Looking back it is seen that the H matrix determined for (6-3) is useful because it is later used in (6-7) to relate measurement errors and position fix error.

The magnitude of the position fix error vector is simply the square root of

$$|\bar{e}_r|^2 = \bar{e}_r^T \bar{e}_r = \bar{e}_q^T (H^{-1})^T H^{-1} \bar{e}_q$$

If $(H^{-1})^T H^{-1}$ is denoted by the matrix B as

$$(H^{-1})^T H^{-1} = \begin{pmatrix} b_{11} & b_{12} \\ b_{21} & b_{22} \end{pmatrix}$$

then

$$|\bar{e}_r|^2 = \bar{e}_r^T \bar{e}_r = \bar{e}_q^T (H^{-1})^T H^{-1} \bar{e}_q$$

$$= \begin{pmatrix} e_{q_1} & e_{q_2} \end{pmatrix} \begin{pmatrix} b_{11} & b_{12} \\ b_{21} & b_{22} \end{pmatrix} \begin{pmatrix} e_{q_1} \\ e_{q_2} \end{pmatrix} = b_{11} e_q^2 + b_{22} e_q^2 + (b_{12}+b_{21}) e_{q_1} e_{q_2}$$

If e_{q_1} and e_{q_2} are independent random variables then the expected value of $|e_r|^2$ is

$$E [|\bar{e}_r|^2] = b_{11} E [e_{q1}^2] + b_{22} E [e_{q1}^2]$$

Taking the square root of both sides of the above equation yields

$$RMS [|\bar{e}_r|] = \{b_{11} RMS^2 [e_{q_1}] + b_{22} RMS^2 [e_{q_2}]\}^{1/2}$$

This last equation gives the root mean square of the position fix error in terms of the RMS values of the measurement errors and the position fix geometry. This expression will be valuable for the comparison of various position fixing schemes.

Since H is only a two by two matrix, b_{11} and b_{22} are easily determined:

$$H = \begin{pmatrix} h_{1\ell} & h_{1m} \\ h_{2\ell} & h_{2m} \end{pmatrix} \qquad H^{-1} = \frac{\begin{pmatrix} h_{2m} & -h_{1m} \\ -h_{2\ell} & h_{1\ell} \end{pmatrix}}{D}$$

$$[H^{-1}]^T H^{-1} = \frac{1}{D^2} \begin{pmatrix} h_{2m} & -h_{2\ell} \\ -h_{1m} & h_{1\ell} \end{pmatrix} \begin{pmatrix} h_{2m} & -h_{1m} \\ -h_{2\ell} & h_{1\ell} \end{pmatrix}$$

$$\therefore \quad b_{11} = (h_{2\ell}^2 + h_{2m}^2) \; / \; D^2$$

$$b_{22} = (h_{1\ell}^2 + h_{1m}^2) \; / \; D^2$$

where

$$D = h_{1\ell} \, h_{2m} - h_{2\ell} \, h_{1m}$$

In the following discussion several celestial and satellite position fixing techniques will be compared by examining the H matrix for each of the schemes.

6-3. Celestial Position Fix Scheme I - Earth Landmark and Two Stellar Directions

The angle that a navigator can observe between a known stellar direction and a known landmark on a nearby planet establishes a conical locus of his position in space. By measuring the angle between the same landmark and a second known stellar direction the navigator can establish a second conical locus for his position. These loci are shown in Fig. 6-1. Now the navigator knows that he must be located at the mutual intersection of these two cones and the lunar sphere. There will be at least two such mutual intersections. A priori information can be used to select which intersection is the actual LRV location.

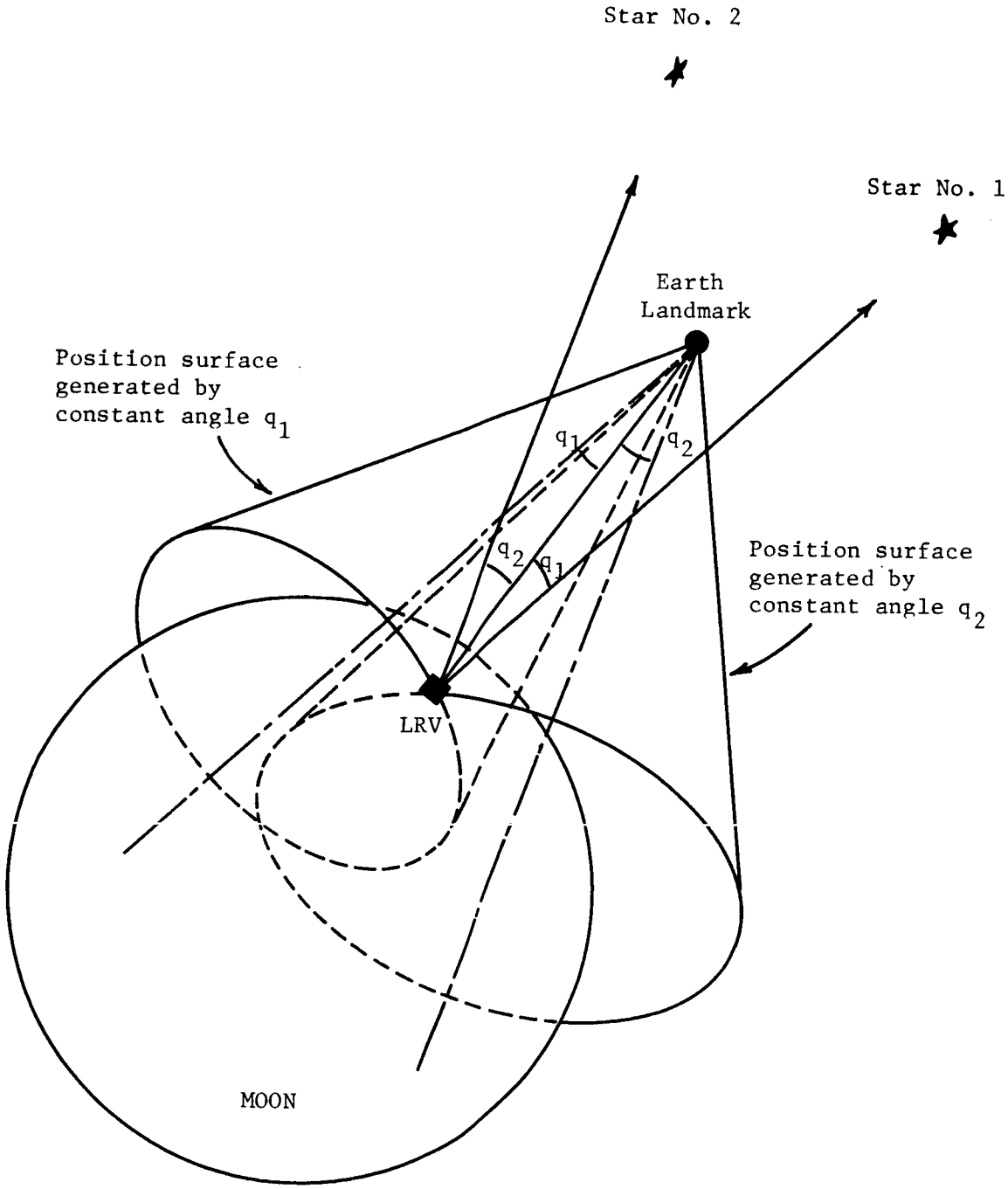

Known: - Position of the earth landmark with respect to the moon
- Stellar ephemeris

Measured: Angles q_1 and q_2.

Positive fix by Earth Landmark & Two Stellar Directions

Fig. 6-1

Sensitivity Analysis

The measured angle between the landmark on a nearby planet and a stellar direction is most sensitive to motion of the LRV when the nearby landmark is nearly above the LRV and the LRV travels in the plane defined by the stellar direction and the line from the center of the moon to the landmark. Unfortunately, even for this case the geometric sensitivity of this sighting is as follows:

$$\Delta q = \frac{|\Delta \bar{r}|}{R-r}$$

where $\Delta \bar{r}$ is a small change in the LRV position vector, Δq is the corresponding small change in the measured angle, r is the radius of the moon, and R is the distance from the center of the moon to the landmark.

If R is taken as 385×10^3 km, the distance from the center of the moon to the earth; and r is taken as 1738 km, the mean radius of the moon, then

$$\Delta q = 2.6 \times 10^{-6} |\Delta \bar{r}|$$

This means that if the LRV moved 5 km, the resulting change in the basic angles that are measured for this scheme would be less than 0.8×10^{-3} degrees. Conversely, a measurement error of only 0.8×10^{-3} degree would cause a position fix error of at least 5 km.

This concept is not attractive for the LRV application because the position fix accuracy is too sensitive to small measurement errors.

The relation between the measured angles and changes in the LRV position is shown below:

$$\begin{pmatrix} \Delta q_1 \\ \Delta q_2 \end{pmatrix} = \begin{pmatrix} \frac{\sin \gamma_1 \cos\alpha_1}{P \sin q_1} & \frac{1}{P \sin q_1}\left(\sin\gamma_1 \sin\alpha_1 - \frac{R}{P} \cos\ _1 \sin\beta\right) \\ \frac{\sin\gamma_2 \cos\alpha_2}{P \sin q_2} & \frac{1}{P \sin q_2}\left(\sin\alpha_2 \sin\alpha_2 - \frac{R}{P} \cos\ _2 \sin\beta\right) \end{pmatrix} \begin{pmatrix} \Delta r_\ell \\ \Delta r_m \end{pmatrix}$$

or

$$\begin{pmatrix} \Delta r_\ell \\ \Delta r_m \end{pmatrix} = \frac{1}{\sin\gamma_1 \sin\gamma_2 \sin(\alpha_2-\alpha_1) + \frac{R}{P}\sin\beta\,(\cos q_1 \sin\gamma_2 \cos\alpha_2 - \cos q_2 \sin\gamma_1 \cos\alpha_1)}$$

$$\begin{pmatrix} P \sin q_1 (\sin\gamma_1 \sin\alpha_2 - \frac{R}{P} \cos q_2 \sin\beta) & -P \sin q_2 \sin\gamma_1 \sin\alpha_1 - \frac{R}{P} \cos q_1 \sin\beta) \\ -P \sin q_1 \sin\gamma_2 \cos\alpha_2 & P \sin q_2 \sin\gamma_1 \cos\alpha_1 \end{pmatrix}$$

$$\begin{pmatrix} \Delta q_1 \\ \Delta q_2 \end{pmatrix}$$

The derivation of these equations is shown in Appendix C. The meaning of the variables in these equations are illustrated in Fig. 6-2.

Position Fix Computation

The following three simultaneous equations can be solved for the LRV coordinates. The angles in these equations are defined in Fig. 6-3. These equations are derived in Appendix D.

$$(x - x_E)^2(1 - \cos^2 L_1 \cos^2\lambda_1 \sec^2 q_1) + (y - y_E)^2(1-\cos^2 L_1 \sin^2\lambda_1 \sec^2 q_1) +$$

$$(z-z_E)^2(1-\sin^2 L_1 \sec^2 q_1)+(x-x_E)(y-y_E)\sin 2\lambda_1(2-\cos^2 L_1 \sec^2 q_1)-(y-y_E)(z-z_E)\sin 2L_1 \sin\lambda_1 \sec^2 q_1 -$$

$$(z-z_E)(x-x_E)\sin 2L_1 \cos\lambda_1 \sec^2 q_1 = 0$$

$$(x-x_E)^2(1-\cos^2 L_2 \cos^2\lambda_2 \sec^2 q_2)+(y-y_E)^2(1-\cos^2 L_2 \sin^2\lambda_2 \sec^2 q_2) +$$

$$(z-z_E)^2(1-\sin^2 L_2 \sec^2 q_2)+(x-x_E)(y-y_E)\sin\lambda_2(2-\cos^2\lambda_2 \sec^2 q_2) -$$

$$(y-y_E)(z-z_E)\sin 2L_2 \sin\lambda_2 \sec^2 q_2-(z-z_E)(x-x_E)\sin 2L_2 \cos\lambda_2 \sec^2 q_2 = 0$$

$$x^2+ y^2+ z^2= r^2$$

where

$$x_E = R \cos\lambda_E \cos L_E$$

$$y_E = R \sin\lambda_E \cos L_E$$

$$z_E = R \sin L_E$$

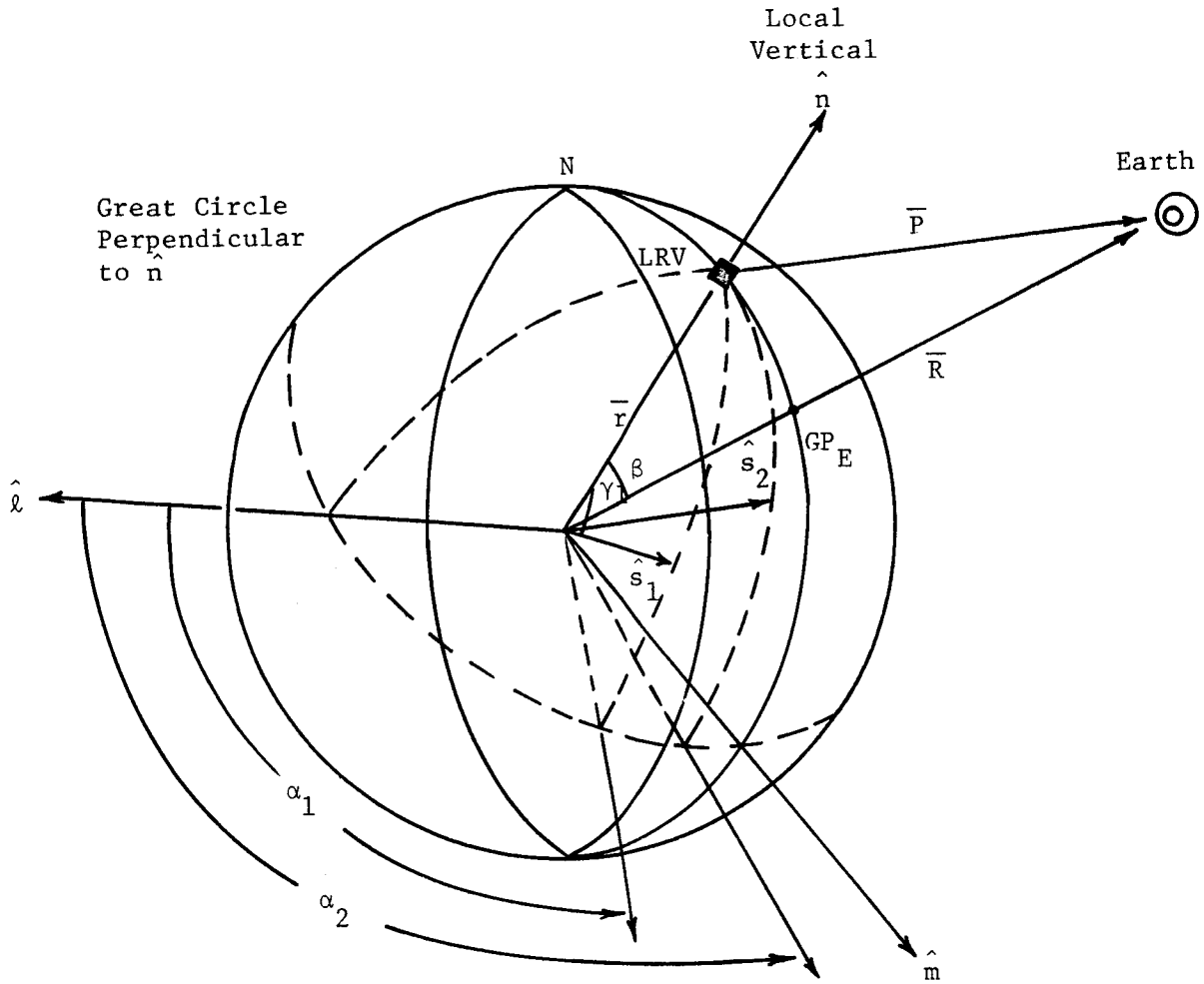

(a)

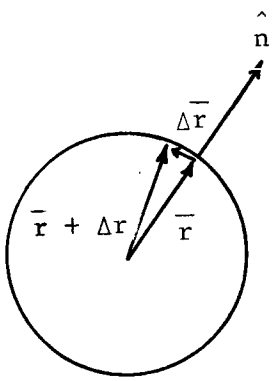

$\Delta\bar{r} \cdot \hat{n} = o$

(b)

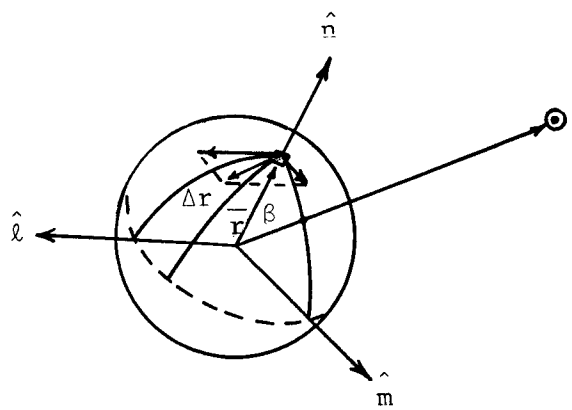

$$-\Delta\beta = \tan^{-1} \frac{\Delta\bar{r} \cdot \hat{m}}{r}$$

$$= \frac{\Delta\bar{r} \cdot \hat{m}}{r}$$

(c)

Earth Landmark and Two Stellar Directions

Fig. 6-2

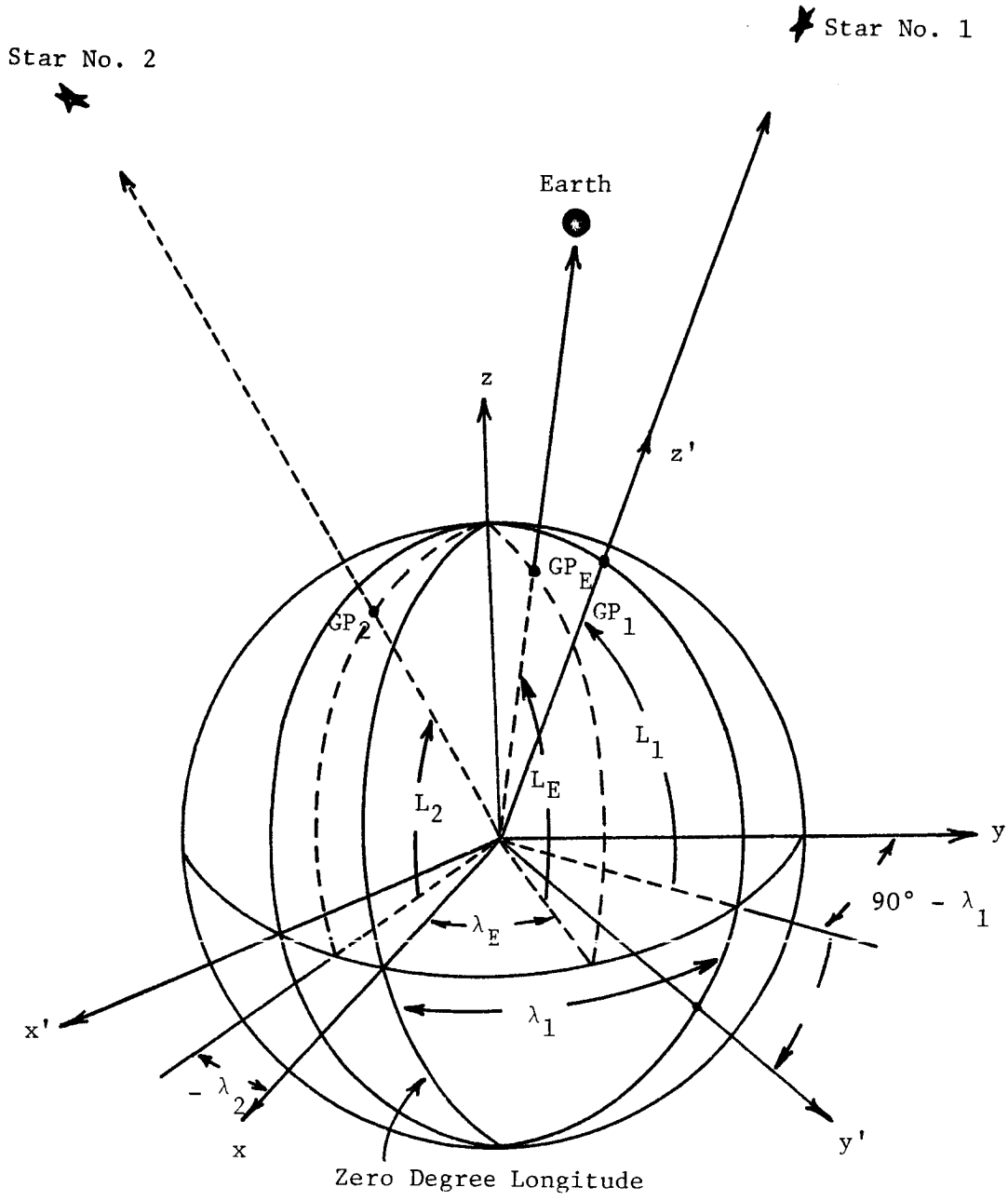

Definition of Angles, A Supplement to Figs. 6-1 and 6-2

Fig. 6-3

Here x, y, and z form a lunar coordinate system with its origin at the moon's center. The z axis passes through the north pole as shown in Fig. 6-3. The x and y axes are in the equatorial plane.

6.4 Celestial Position Fix Scheme II - Local Vertical and Two Stellar Directions

In Fig. 6-4 it is shown that a navigator can establish a circular locus of position on the spherical lunar surface by measuring the angle between the local vertical and a known stellar direction. A second, similar locus of position can be generated by measuring the angle between the local vertical and a second known stellar direction (see Fig. 6-5). The LRV location is at one of the intersections of the two circular loci. The navigator uses the approximate LRV position provided by the dead reckoning system to select the correct intersection.

Sensitivity Analysis

The relation between changes in the LRV position to changes in the measured angles is shown below. The variables are defined in Fig. 6-6. The derivation is in Appendix C.

$$\begin{bmatrix} \Delta q_1 \\ \Delta q_2 \end{bmatrix} = \begin{bmatrix} -\frac{1}{r} & 0 \\ -\frac{1}{r}\cos\alpha & \frac{-\sin\alpha}{r} \end{bmatrix} \begin{bmatrix} \Delta r_\ell \\ \Delta r_m \end{bmatrix}$$

or

$$\begin{bmatrix} \Delta r_\ell \\ \Delta r_m \end{bmatrix} = \begin{bmatrix} -r & 0 \\ r\cot\alpha & -r\csc\alpha \end{bmatrix} \begin{bmatrix} \Delta q_1 \\ \Delta q_2 \end{bmatrix}$$

However,

$$|\Delta\bar{r}|^2 = (\Delta r_\ell)^2 + (\Delta r_m)^2$$

$$= (-r\Delta q_1)^2 + (r\cot\alpha\,\Delta q_1 - r\csc\alpha - \Delta q_2)^2$$

$$|\Delta\bar{r}|^2 = r^2\,(\csc^2\alpha\,\Delta q_1^{\,2} + \csc^2\alpha\,\Delta q_2^{\,2} - 2\cot\alpha\csc\alpha\,\Delta q_1\,\Delta q_2)$$

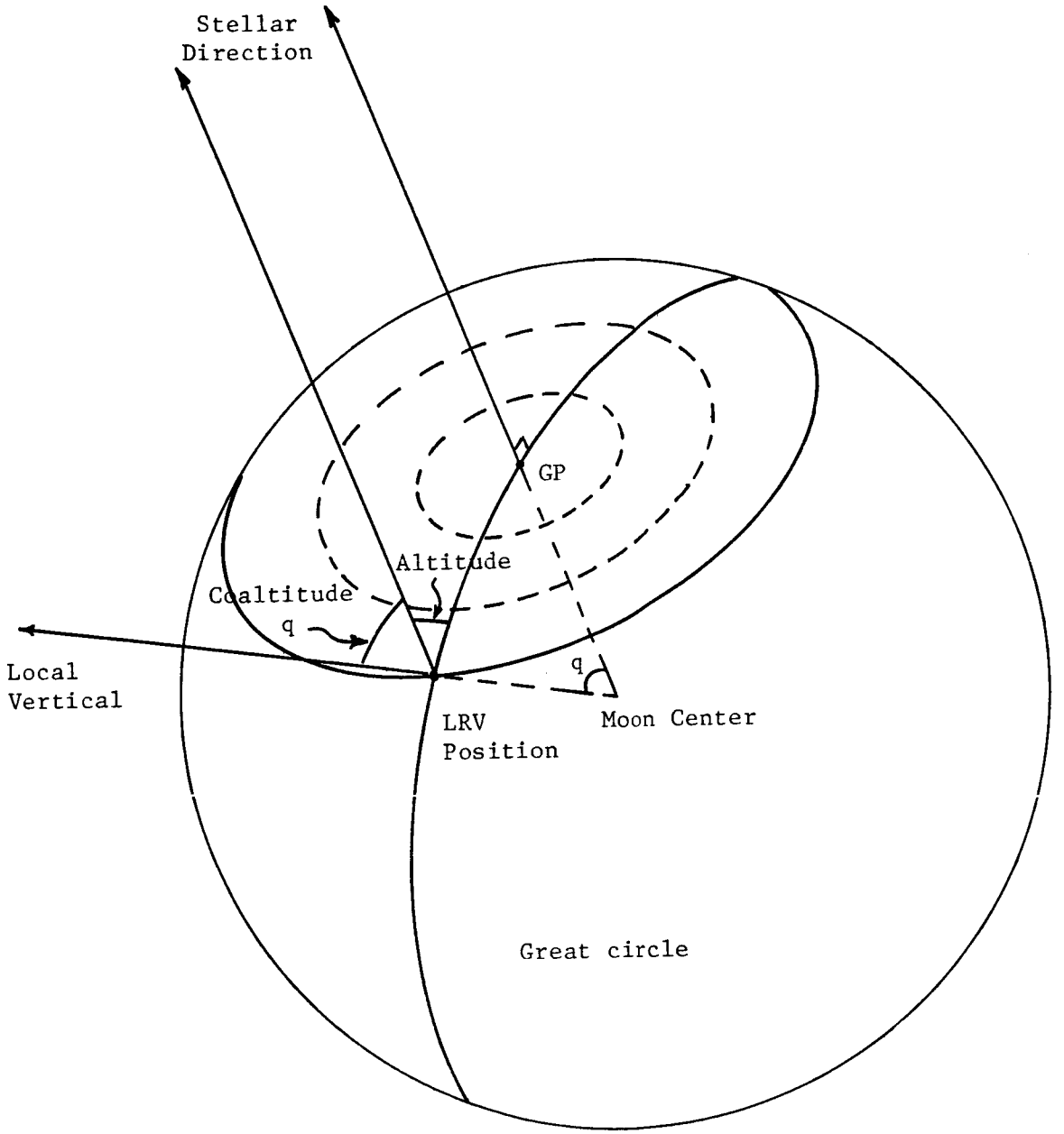

Known: -Local Vertical

-Stellar ephemeris

Measured: Altitude or coaltitude q.

Establishment of a Position Circle

Fig. 6-4

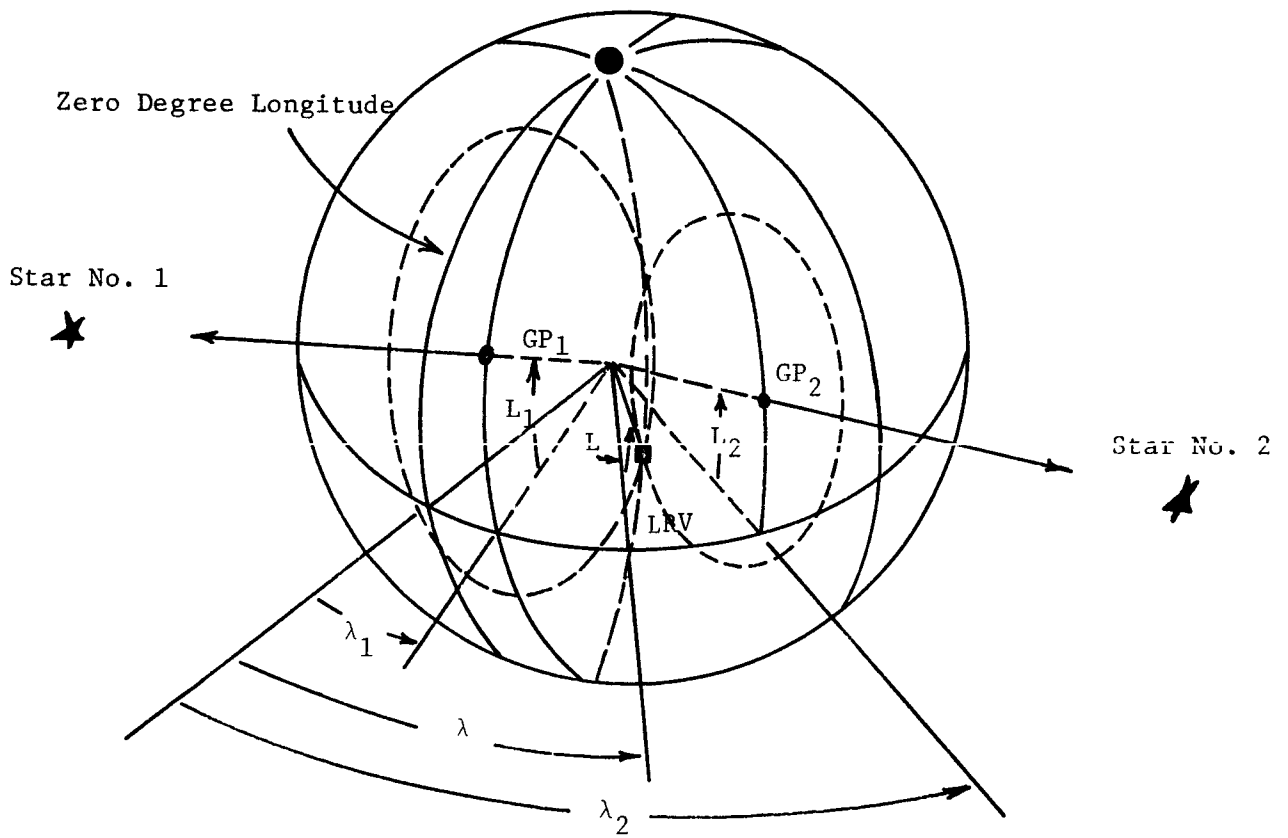

Position Fix by Two Stellar Direction and Local Vertical

Fig. 6-5

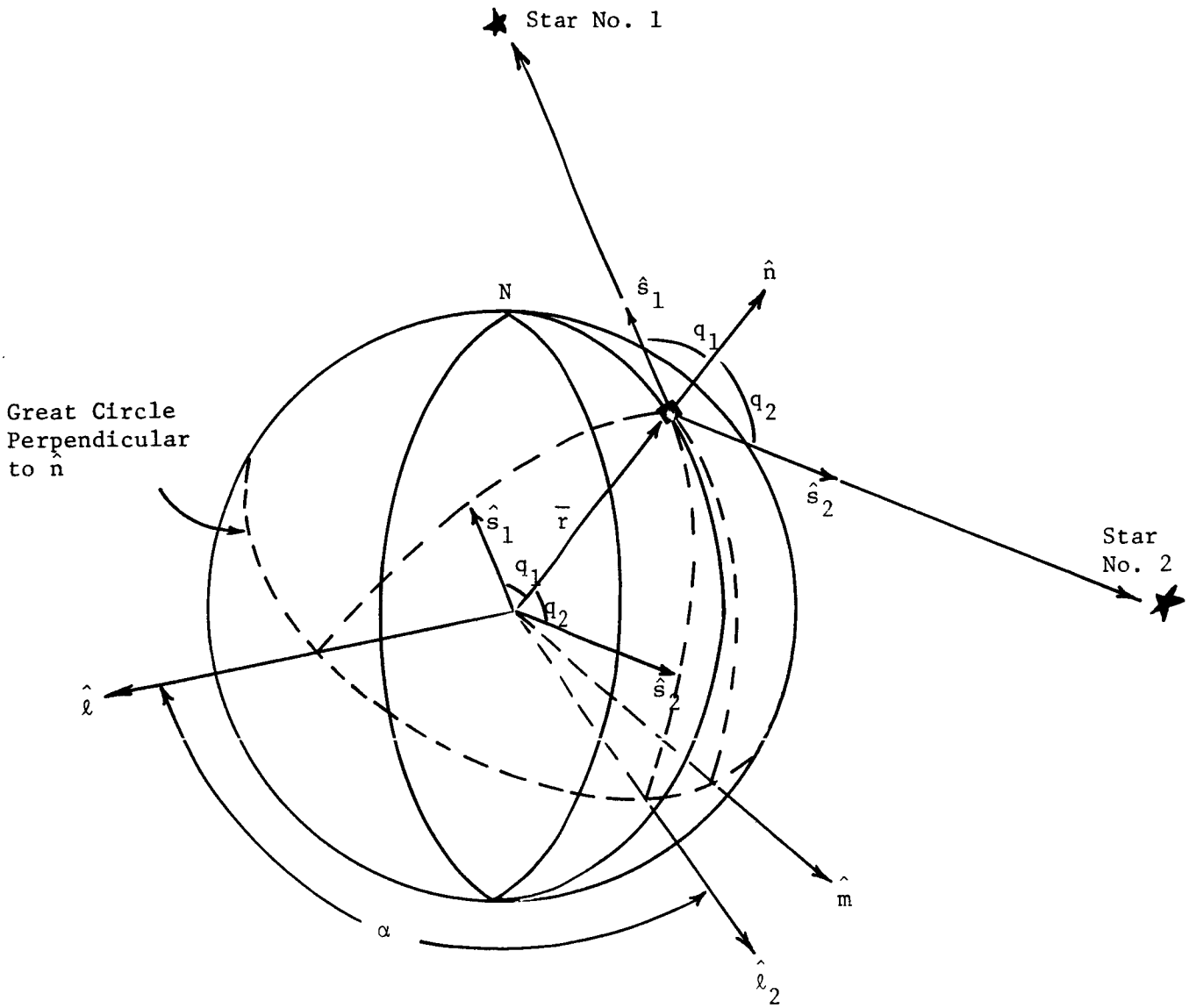

Local Vertical and Two Stellar Directions

Fig. 6-6

If e_{q1} and e_{q2} are independent random variables with equal RMS value, then

$$E\ (\Delta q_1 \quad \Delta q_2) = 0$$

$$\text{RMS}\ (\Delta q_1) = \text{RMS}\ (\Delta q_2) \triangleq \text{RMS}\ (\Delta q)$$

Therefore, the RMS value of $|\Delta\bar{r}|$ is

$$\text{RMS}\ (|\Delta\bar{r}|) = \sqrt{E[r^2(\csc^2\alpha\Delta q_1^{\,2} + \csc^2\alpha\Delta q_2 - 2\cot\alpha\csc\alpha\ \Delta q_1\ \Delta q_2)]}$$

$$= \sqrt{2}\ r\ \csc^2\alpha\ \text{RMS}\ (\Delta q)$$

This is minimized by selecting $\hat{s}_1 \perp \hat{s}_2$, i.e., $\alpha = 90°$; then

$$\text{RMS}\ (|\Delta\bar{r}|) = \sqrt{2}\ r\ \text{RMS}\ (\Delta q)$$

The radius of the moon is 1738 km.

$$\text{RMS}\ (|\Delta\bar{r}|) = 2460\ \text{km} \times \text{RMS}\ (\Delta q)$$

An error in angle measurement, Δq, of 0.05° would give a position fix error, $\Delta\bar{r}$, of 1.5 km.

The most serious problem encountered in trying to make the required measurements of the angles between the stellar directions and the geometric vertical is that the local vertical indicated by the gravity sensitive device will not be the same as the geometric vertical. Reference 4 indicates that the nominal 3σ value of this vertical anomaly is 0.05°, which means that position fix error so caused would be 1.5 km.

Another feature of this position fixing concept should be mentioned. Any attempt to extend this concept and use it to estimate the altitude of the LRV on a non-spherical moon will fail because the angles measured are completely insensitive to the radial distance of the LRV from the center of the moon.

Position Fix Computation

The following equations for the LRV coordinates are derived in Appendix D. The variables used here are shown in Fig. 6-5. The solution of these two equations for λ and L give the LRV position.

$$\lambda_2 - \lambda_1 = \cos^{-1}\left(\frac{\cos q_1 - \sin L_1 \sin L}{\cos L_1 \cos L}\right) + \cos^{-1}\left(\frac{\cos q_2 - \sin L_2 \sin L}{\cos L_2 \cos L}\right)$$

$$\lambda = \lambda_1 + \cos^{-1}\left(\frac{\cos q_1 - \sin L_1 \sin L}{\cos L_1 \cos L}\right)$$

6-5. Navigation Satellite Scheme I - LRV to Satellite Range

If the moon is assumed to be a smooth sphere, then two range measurements made at two different times are sufficient to determine the LRV position. Each measurement of the distance from the LRV to the satellite establishes a circular locus on the lunar surface. These circles have two intersections, one of which is the measured LRV position. The estimate of the LRV position provided by the dead reckoning navigator is used to select the intersection that is the LRV location.

For this position fixing concept the measured parameters, q_1 and q_2, are the ranges measured from the LRV to the satellite at two different instants of time.

Sensitivity Analysis

The equation relates changes in the LRV position to changes in the measured ranges as shown below. The meanings of the variables are illustrated in Fig. 6-7.

$$\begin{pmatrix} \Delta q_1 \\ \Delta q_2 \end{pmatrix} = \begin{pmatrix} \cos E_1 & 0 \\ \cos E_2 \cos\alpha & \cos E_2 \sin\alpha \end{pmatrix} \begin{pmatrix} \Delta r_\ell \\ \Delta r_m \end{pmatrix}$$

or

$$\begin{pmatrix} \Delta r_\ell \\ \Delta r_m \end{pmatrix} = \begin{pmatrix} \sec E_1 & 0 \\ -\cot E_2 \cos\alpha & \cos E_2 \sin\alpha \end{pmatrix} \begin{pmatrix} \Delta r_\ell \\ \Delta r_m \end{pmatrix}$$

The derivations of these equations are in Appendix E, Section E-1.

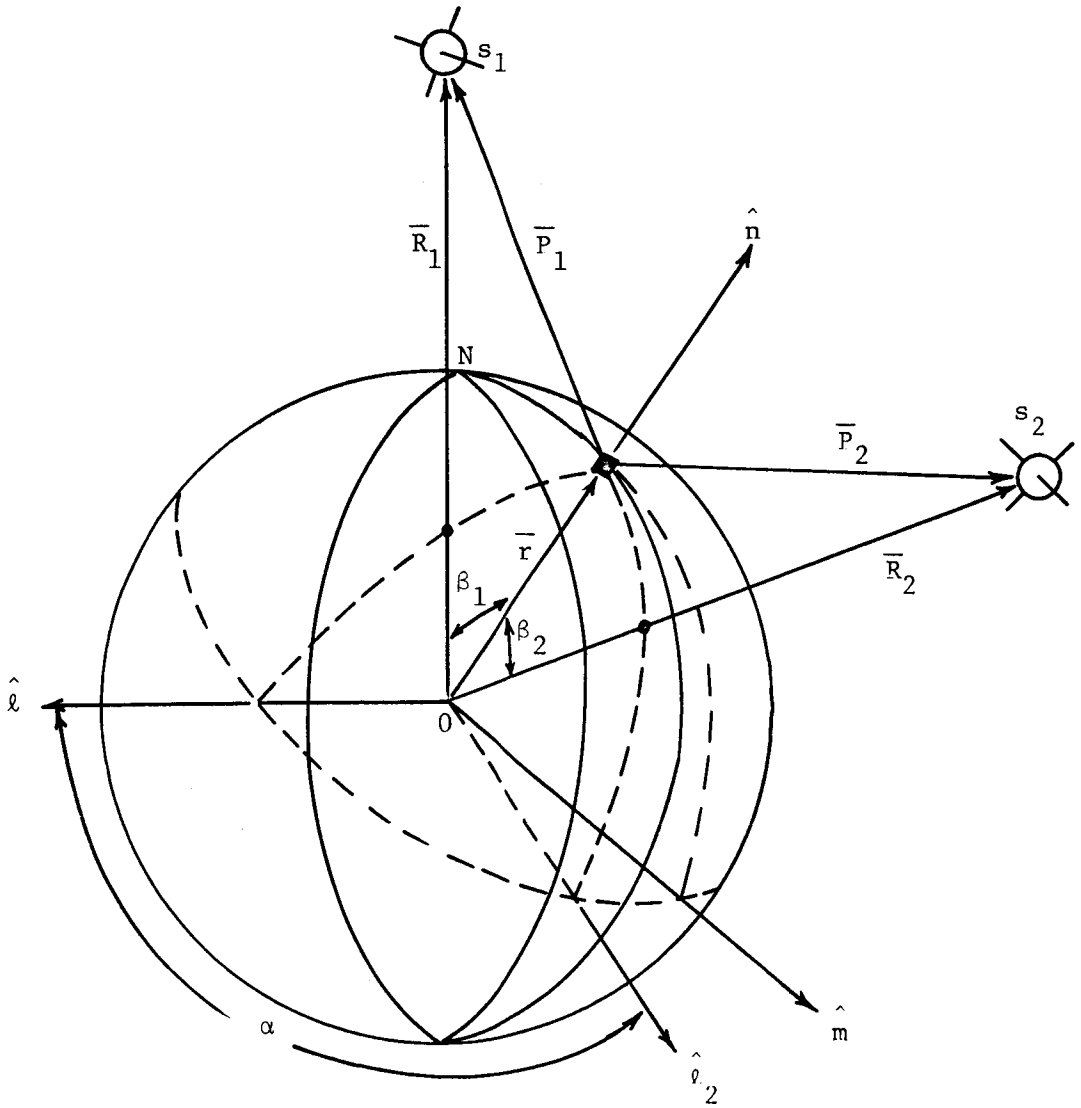

(a)

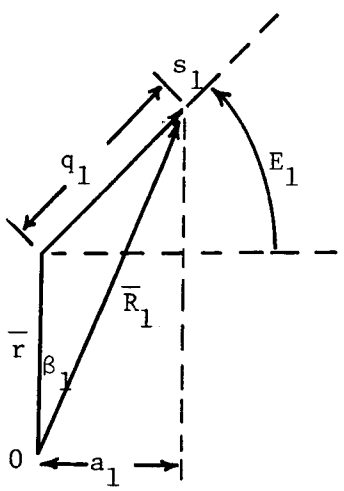

(b)

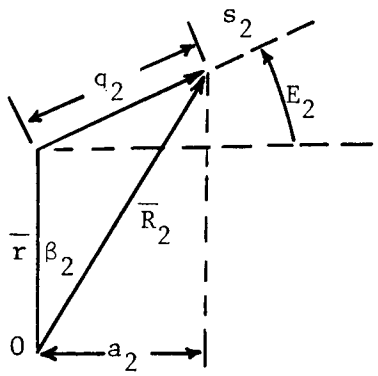

(c)

LRV to Satellite Range

Fig. 6-7

Position Fix Computation

The equations of the position fix for this scheme are shown below. Fig. 6-8 defines the variables that are in these equations.

$$\lambda_2 - \lambda_1 = \cos^{-1} \frac{\cos\beta_1 - \sin L_1 \sin L}{\cos L_1 \cos L} + \cos^{-1} \frac{\cos\beta_2 - \sin L_2 \sin L}{\cos L_2 \cos L}$$

$$\lambda = \lambda_1 + \cos^{-1} \frac{\cos\beta_1 - \sin L_1 \sin L}{\cos L_1 \cos L}$$

where

$$\cos\beta_1 = \frac{r^2 + (r+R_1)^2 - q_1^2}{2r\ (r+R_1)}, \qquad \cos\beta_2 = \frac{r^2 + (r+R_2)^2 - q_2^2}{2r\ (r+R_2)}$$

The LRV position on the lunar surface can be determined by solving these equations for λ and L, the LRV longitude and latitude.

The derivation of these equations is shown in Appendix F, Section F-1.

6-6. Navigation Satellite Scheme II - LRV to Satellite Range Rate

The TRANSIT navigation system uses range rate measurements made with a doppler radar. It is possible to discuss this navigation scheme by deriving equations for the position fix in terms of the doppler beat frequency. However, it is just as easy to look at this navigation concept in terms of the geometric parameters involved. This latter approach is more consistent with the descriptions that have been given here for other position fixing schemes. Fig. 6-9 shows the scheme.

Fig. 6-10 shows the satellite a short time before the time of its closest approach to the LRV. At the time when the navigator detects a silent beat on doppler radar, it is the time that the line of sight to the satellite perpendicular to the satellite path. Let that time be t_o and the distance from LRV to the satellite at t_o be R_o; then the value of R_o can be calculated if we know the second derivative of range R at t_o when the range vector is perpendicular to satellite's orbit.

Known: - Lunar radius r.

- Satellite's orbit with respect to the moon, thus know GP_1, GP_2, R_1 and R_2.

Measured: Ranges q_1 and q_2

Computed: Angles β_1 and β_2

Note: Local vertical not required

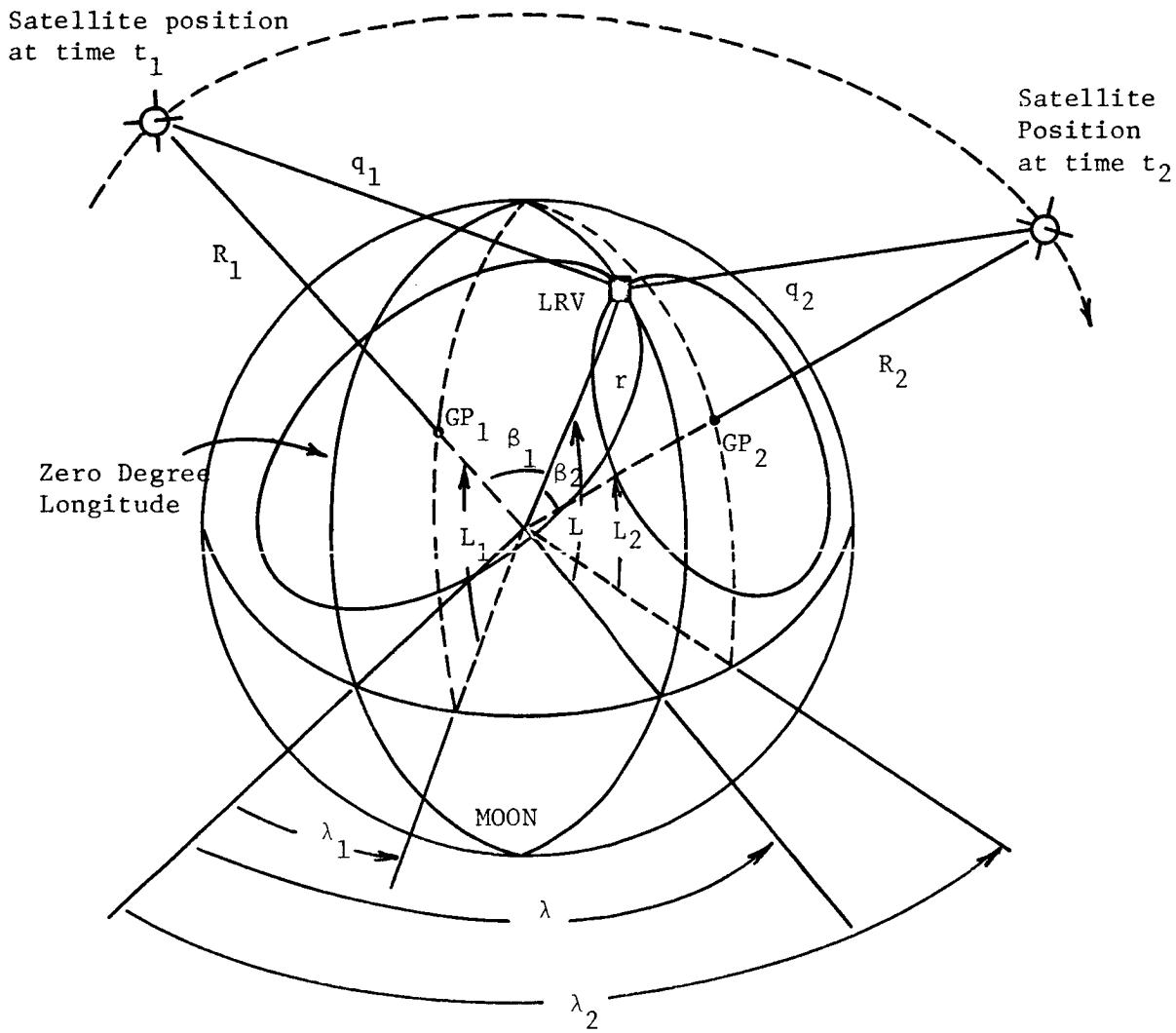

Position Fix by Two Ranges to Satellite

Fig. 6-8

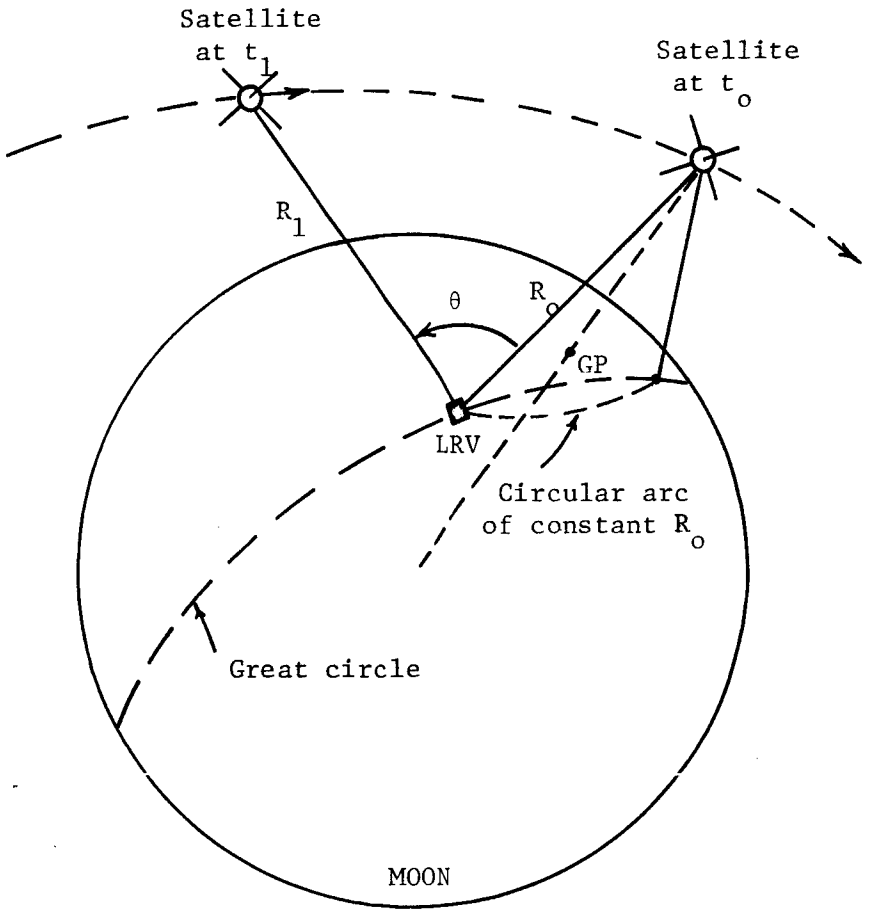

Known: - Satellite's orbit relative to the moon

Measured: - The second derivative of range at time to when the range vector is perpendicular to satellite's orbit

- Time t_o

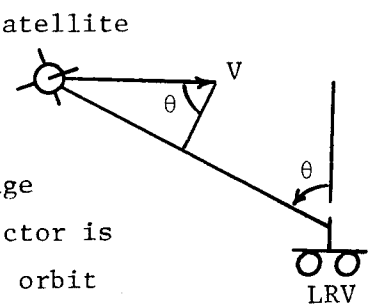

Position Fix by Satellite Range Rate

Fig. 6-9

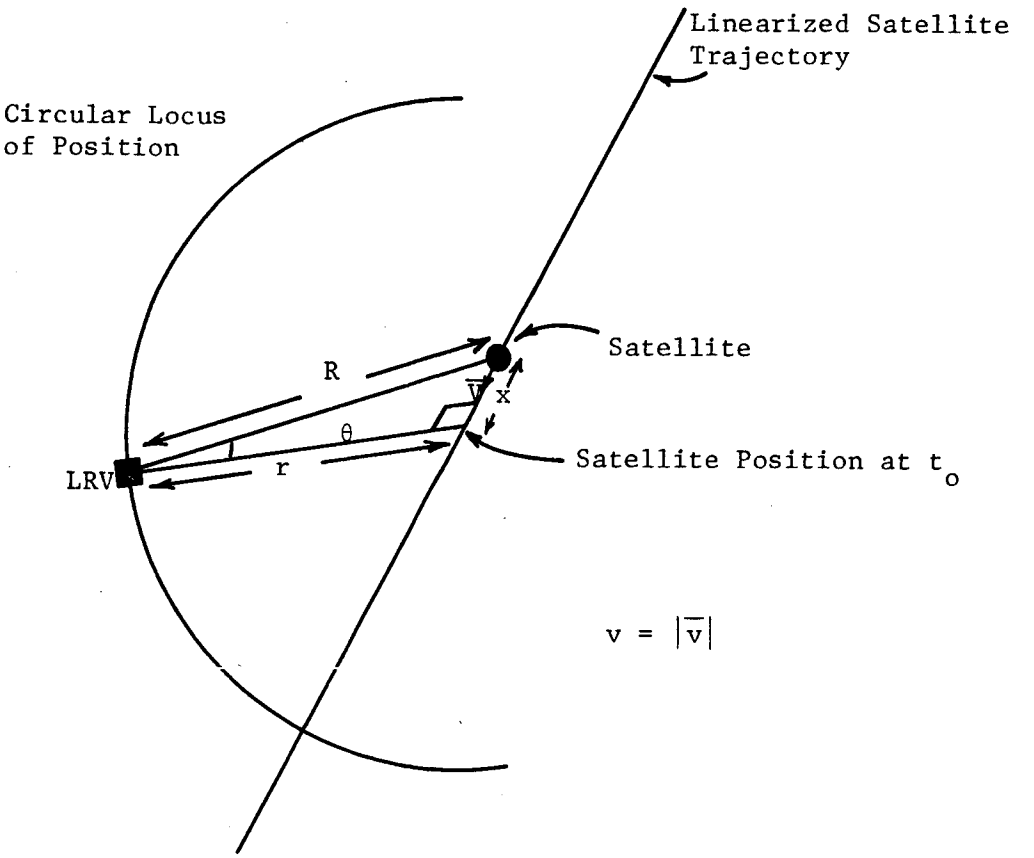

Geometry for Position Fix Using Satellite Range Rate

Fig. 6-10

The relation between R_o and $\ddot{R}$ at $t = t_o$ is (see Appendix E, Section E-2).

$$R_o = \frac{V^2}{\ddot{R} \mid t = t_o}$$

Since it is assumed that the satellite orbital parameters are known, the position and velocity of the satellite at t_o is assumed to be known. Therefore, the last equation establishes a circular locus of position of radius R_o for the LRV. The plane of this circle contains the position of the satellite at t_o and is normal to the satellite trajectory at this point. This circular locus of position intersects the lunar surface at two points, one of which is the measured LRV position. Information from the dead reckoning navigator is used to select the intersection that is the LRV position.

Sensitivity Analysis

An imperfection, a bias, in the doppler radar will cause the measured range rate, $\dot{R}'$, to differ from the actual range rate.

$$\dot{R}' = \dot{R} + \Delta\dot{R}$$

The effect of $\Delta\dot{R}$ will cause an error in the radius of the locus of position.

$$e_r = R_o \left[\sec^3 \left(\frac{\Delta\dot{R}}{V}\right) - 1\right]$$

The detailed derivations of the equations are in Appendix E, Section E-2.

If the satellite orbital radius is 1838 km, 100 km above the lunar surface, then V = 8250 km/sec. Reference 4 gives 20 km/hr. as the nominal three sigma bias for doppler measurements of satellite range rate. If these numbers are used with an assumed value of 200 km for R_o, the range from the satellite to the LRV, then the circular locus of position is erroneously shifted 0.485 km. The error in the estimation of the locus of position radius is only 0.017 km.

This arbitrary selected example indicates that this scheme can be used to determine the LRV position relative to the satellite with greater accuracy than is offered by either of the celestial sighting schemes.

Position Fix Computation

The equations of position fix for this scheme are derived in Appendix F, Section F-2, and repeated below.

$$x = x' \sin a + y' \cos a \cos b + z' \sin a \cos b$$

$$y = -x' \cos a + y' \sin a \cos b + z' \sin a \sin b$$

$$z = -y' \sin b + z' \cos b$$

where x', y', and z' are solved from the following equations

$$\{x' + R \cos L_s \cos(\lambda_s + a)\}^2 + \{z' - R[\cos L_s \sin b \sin(\lambda_s + a) + \sin L_s \cos b]\}^2 = R_o^2$$

$$y' = R[\cos L_s \cos b \sin(\lambda_s + a) - \sin L_s \sin b]$$

$$x'^2 + y'^2 + z'^2 = r^2$$

Here x, y, and z are the same lunar coordinates that were defined in Section 6-3. The x', y', and z' axes are so defined that y' is in the direction of the satellite's velocity, x' is perpendicular to y' and in the xy plane. z' is perpendicular to both x' and y' in accordance with right-hand rule. (See Fig. 6-11).

6-7. Navigation Satellite Scheme III - Angles Between Line of Sight (LOS) and Local Vertical

Position fixing schemes that use angle tracking of a navigational satellite are geometrically related to the concepts discussed under celestial sightings. Now the artificial lunar satellite serves as a very close-by celestial neighbor. The closeness of this new "celestial" body causes some of the angles defined by its position to be more sensitive to the LRV position than angles defined by the position of other celestial bodies. In this respect the satellite is superior to the sun, earth, and other planets as a celestial reference.

There are at least two ways to establish a position fix by angle tracking a satellite as it passes overhead.

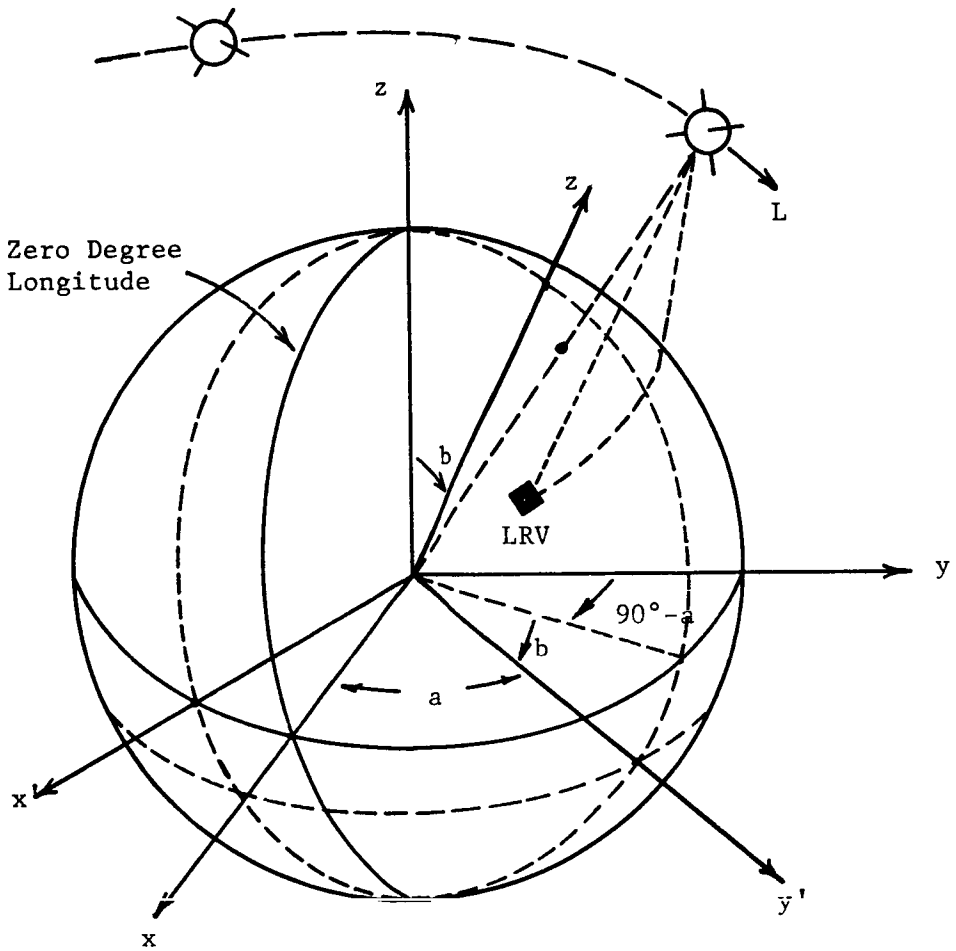

Definition of Coordinates, A Supplement to Figs. 6-9 and 6-10

Fig. 6-11

1. Measure at two instants the angle between the local vertical and the LOS from the LRV to the satellite.
2. Measure at two instants the angle between a known stellar direction and the LOS from the LRV to the satellite.

Either of these sets of measurements will provide a position fix relative to the known satellite position. The position fix established by each of these schemes has a sensitivity to measurement errors that is characteristic of the geometry of the particular angles measured. The method of establishing a position fix and its sensitivity to measurement errors for both of the angle tracking schemes will be examined below. The first scheme is described in this section; the second scheme will be described in Section 6-8.

Measuring the angle between the local vertical and the LOS from the LRV to the satellite establishes a circular locus of position on the lunar surface. Two angle-measurements at two different times during the same satellite pass provides two different circular locus of position (Fig. 6-12). These two circles have two intersections. The estimated LRV position is at the intersection selected by dead reckoning data.

Sensitivity Analysis

The relation between changes in the LRV position and changes in the angles measured for this scheme is also developed in Appendix E, Section E-3, and repeated below

$$\begin{pmatrix} \Delta q_1 \\ \Delta q_2 \end{pmatrix} = \begin{pmatrix} \frac{R_1}{P_1^2}\cot q_1 \sin\beta_1 - \frac{1}{r} & 0 \\ \cos\alpha\left(\frac{R_2}{P_2^2}\cot q_2 \sin\beta_2 - \frac{1}{r}\right) & \sin\alpha\left(\frac{R_2}{P_2^2}\cot q_2 \sin\beta_2 - \frac{1}{r}\right) \end{pmatrix} \begin{pmatrix} \Delta r_\ell \\ \Delta r_m \end{pmatrix}$$

or

$$\begin{pmatrix} \Delta r_\ell \\ \Delta r_m \end{pmatrix} = \begin{pmatrix} \frac{P_1^2}{R_1 \cot q_1 \sin\beta_1 - \frac{P_1^2}{r}} & 0 \\ \frac{-P_1^2 \cot\alpha}{R_1 \cos q_1 \sin\beta_1 - \frac{P_1^2}{r}} & \frac{P_2^2}{\sin\alpha\left(R_2 \cot q_2 \sin\beta_2 - \frac{P_2^2}{r}\right)} \end{pmatrix} \begin{pmatrix} \Delta q_1 \\ \Delta q_2 \end{pmatrix}$$

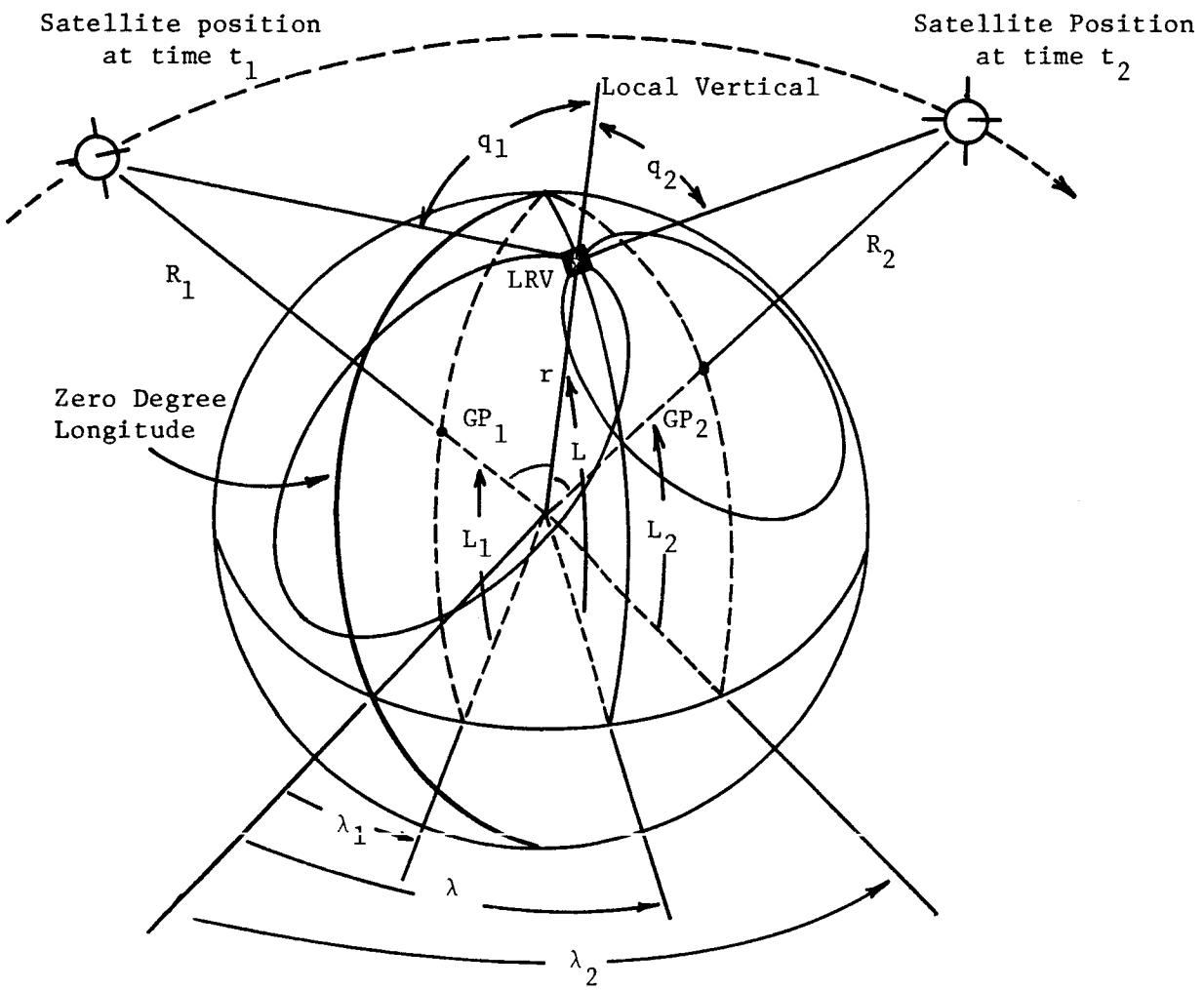

Known: - Lunar radius r.

- Satellite's orbit with respect to the moon, thus know GP_1, GP_2, R_1, and R_2

Measured: Ranges q_1 and q_2

Position Fix by Two Elevation Angles of the Satellite

Fig. 6-12

The meaning of the variables are illustrated in Fig. 6-13.

Position Fix Computation

The equations of position fix are derived in Appendix F, Section F-3, and repeated below:

$$\lambda_2 - \lambda_1 = \cos^{-1}\left(\frac{\cos\phi_1 - \sin L_1 \sin L}{\cos L_1 \cos L}\right) + \cos^{-1}\left(\frac{\cos\phi_2 - \sin L_2 \sin L}{\cos L_2 \cos L}\right)$$

$$\lambda = \lambda_1 + \cos^{-1}\left(\frac{\cos\phi_1 - \sin L_1 \sin L}{\cos L_1 \cos L}\right)$$

The meaning of the variables are shown in Fig. 6-12.

These two equations can be solved for λ and L, the LRV's lunar longitude and latitude.

6-8. Navigation Satellite Scheme IV - Angles Between Satellite LOS and a Stellar Direction

The position fixing scheme that measures the angles between a stellar direction and the LOS from the LRV to two different positions of a satellite is the scheme that is geometrically similar to the celestial fix that uses an earth landmark and two stellar directions. The navigation satellite replaces the earth landmark. The relatively short distance between the LRV and the satellite causes the desirable increase in sensitivity of measured angle to the LRV position.

The angle measured between a stellar direction and the direction to a satellite establishes in space a conical locus of position. A second, similar locus of position for the LRV can be established by measuring the angle between the same stellar direction and the direction to the satellite at a later time during the same pass. The computed LRV position is at one of the mutual intersections of these two cones and the lunar sphere. The proper intersection is selected by a priori information. The scheme is shown in Fig. 6-14.

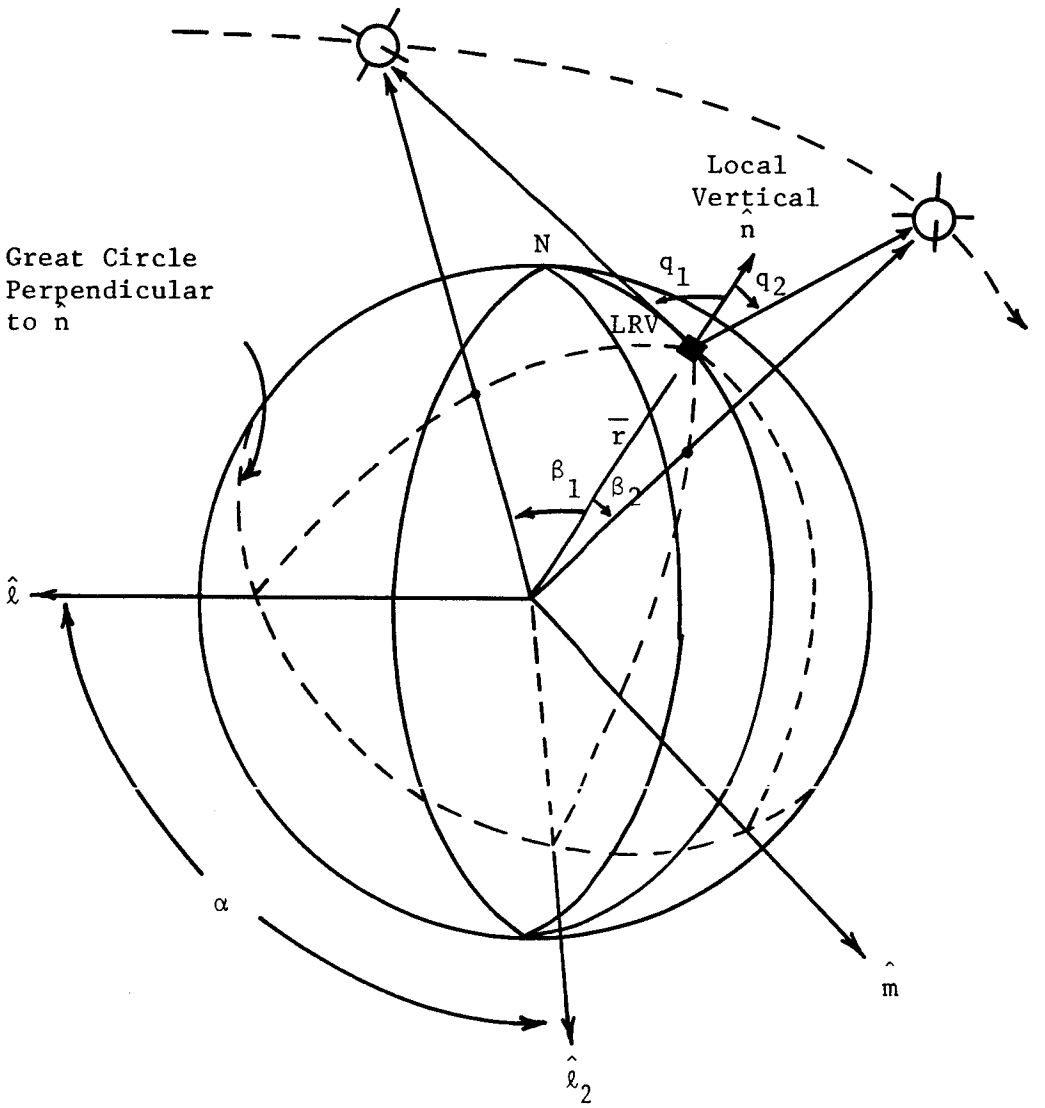

Geometry for Position Fix Using a Satellite and Local Vertical

Fig. 6-13

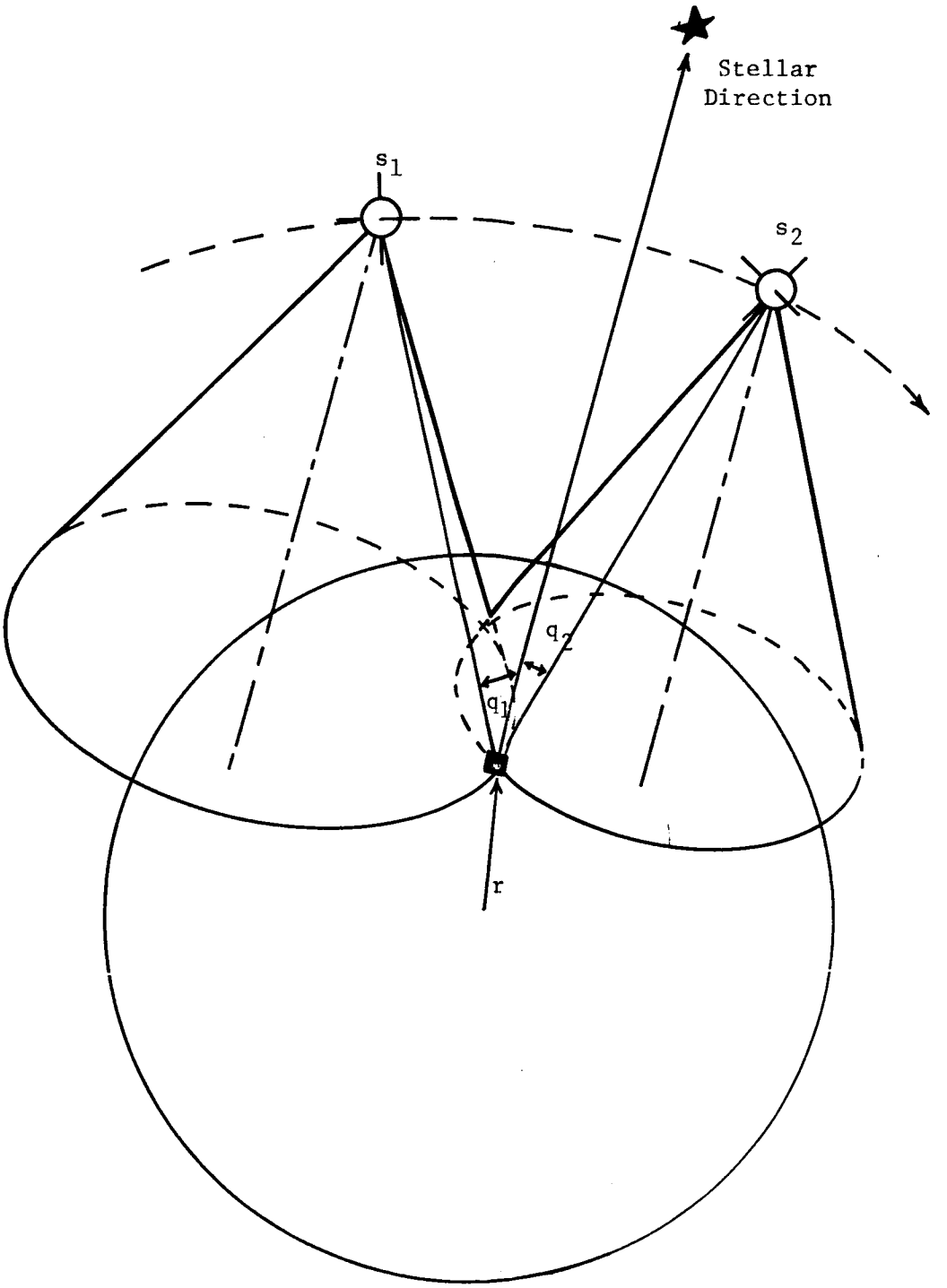

Position Fix by Two Satellite LOS's and a Stellar Direction

Fig. 6-14

Sensitivity Analysis

The relation between changes in the LRV position and changes in the angles measured is developed in Appendix E, Section E-4, and repeated below. The meaning of the variables is illustrated in Fig. 6-15.

$$\begin{pmatrix} \Delta q_1 \\ \Delta q_2 \end{pmatrix} = \begin{pmatrix} \frac{1}{P_1 \sin q_1}(\sin\gamma + \cos E_1 \cos q_1 \cos\alpha_1) & \frac{\cos E_1 \cos q_1 \sin\alpha_1}{P_1 \sin q_1} \\ \frac{1}{P_2 \sin q_2}(\sin\gamma + \cos E_2 \cos q_2 \cos\alpha_2) & \frac{\cos E_2 \cos q_2 \cos\alpha_2}{P_2 \sin q_2} \end{pmatrix} \begin{pmatrix} \Delta r_\ell \\ \Delta r_m \end{pmatrix}$$

or

$$\begin{pmatrix} \Delta r_\ell \\ \Delta r_m \end{pmatrix} = \frac{1}{\sin\gamma(\cos E_2 \cos q_2 \sin\alpha_2 - \cos E_1 \cos q_1 \sin\alpha_1)}$$

$$\begin{pmatrix} P_1 \sin q_1 \cos E_1 \cos q_2 \sin\alpha_2 & -P_2 \sin q_2 \cos E_1 \cos q_1 \sin\alpha_1 \\ -P_1 \sin q_1 (\sin\gamma + \cos E_2 \cos q_2 \cos\alpha_2) & P_2 \sin q_2 (\sin\gamma + \cos E_1 \cos q_1 \sin\alpha_1) \end{pmatrix} \begin{pmatrix} \Delta q_1 \\ \Delta q_2 \end{pmatrix}$$

Position Fix Computation

The equations for position fix are derived in Appendix F, Section F-4, and repeated below.

$$x = x' \sin\lambda_s + y' \sin L_s \cos\lambda_s + z' \cos L_s \cos\lambda_s$$

$$y = -x' \cos\lambda_s + y' \sin L_s \sin\lambda_s + z' \cos L_s \sin\lambda_s$$

$$z = -y' \cos L_s + z' \sin L_s$$

where x', y', and z' are solved from the following equations.

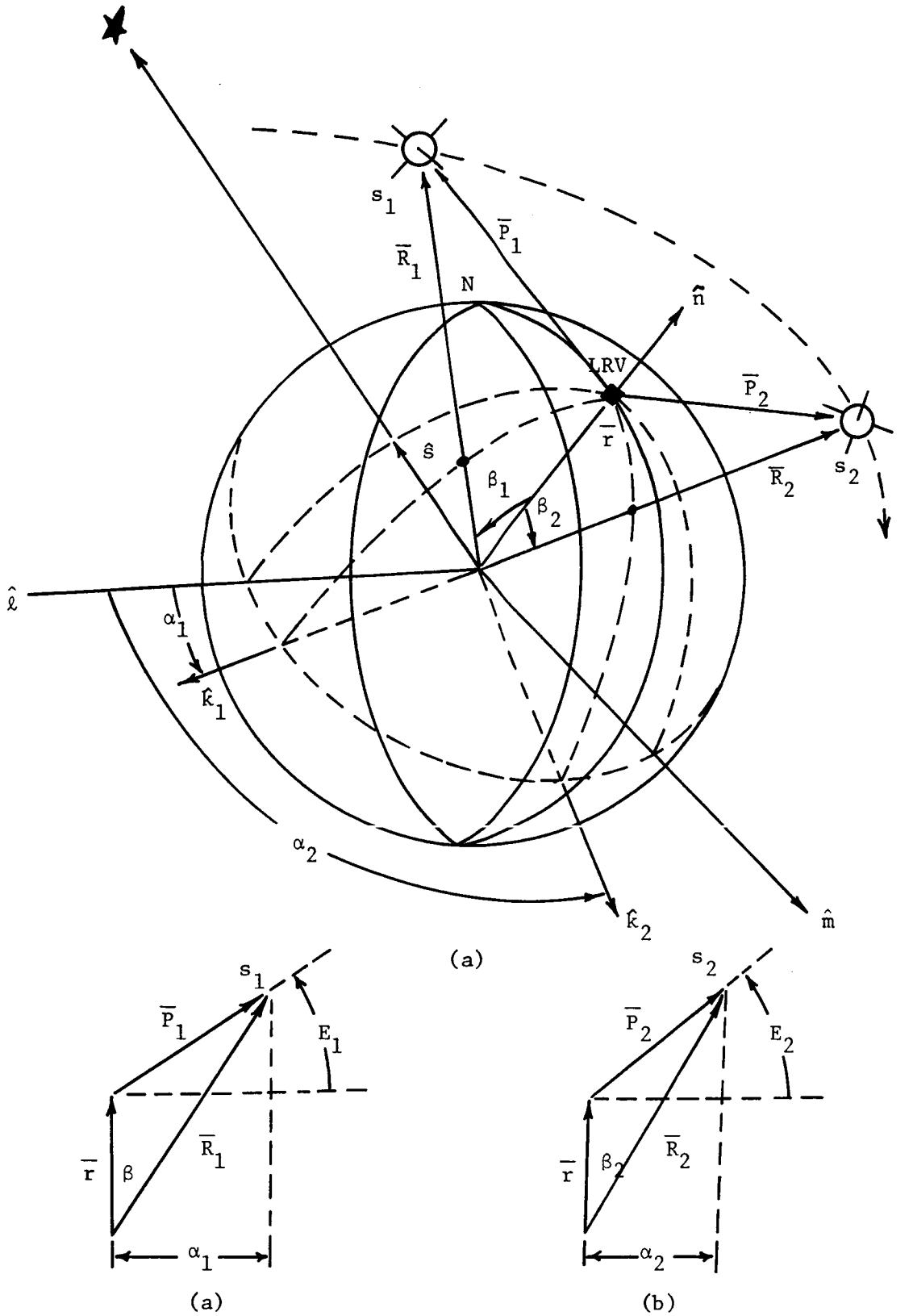

Geometry for Position Fix Using Satellite and Stellar Direction

Fig. 6-15

$$\{x' - (r + R_1)\ \mathrm{cosL}_1\ \sin(\lambda_s - \lambda_1)\}^2$$

$$+ \{y' - (r + R_1)[\mathrm{cosL}_1\ \mathrm{sinL}_s\ \cos(\lambda_s - \lambda_1) - \mathrm{sinL}_1\ \mathrm{cosL}_s]\}^2$$

$$= \{z' - (r + R_1)[\mathrm{cosL}_1\ \mathrm{cosL}_s\ \cos(\lambda_s - \lambda_1) + \mathrm{sinL}_1\ \mathrm{sinL}_s]\}^2 \tan^2 q_1$$

$$\{x' - (r + R_2)\ \mathrm{cosL}_2\ \sin(\lambda_s - \lambda_2)\}^2$$

$$+ \{y' - (r + R_2)[\mathrm{cosL}_2\ \mathrm{sinL}_s\ \cos(\lambda_s - \lambda_1) - \mathrm{sinL}_2\ \mathrm{cosL}_s]\}^2$$

$$= \{z' - (r + R_2)[\mathrm{cosL}_2\ \mathrm{cosL}_s\ \cos(\lambda_s - \lambda_2) + \mathrm{sinL}_2\ \mathrm{sinL}_s]\}^2 \tan^2 q_2$$

$$x'^2 + y'^2 + z'^2 = r^2$$

Here x, y, and z are the same lunar coordinates that were defined in Section 6-3.

x', y', and z' are so defined that the z'-axis is directed along the stellar direction; the x'-axis is perpendicular to z' and in the xy plane; the y'-axis is perpendicular to both x' and y' in accordance with the right-hand rule. The meaning of the variables is shown in Fig. 6-16.

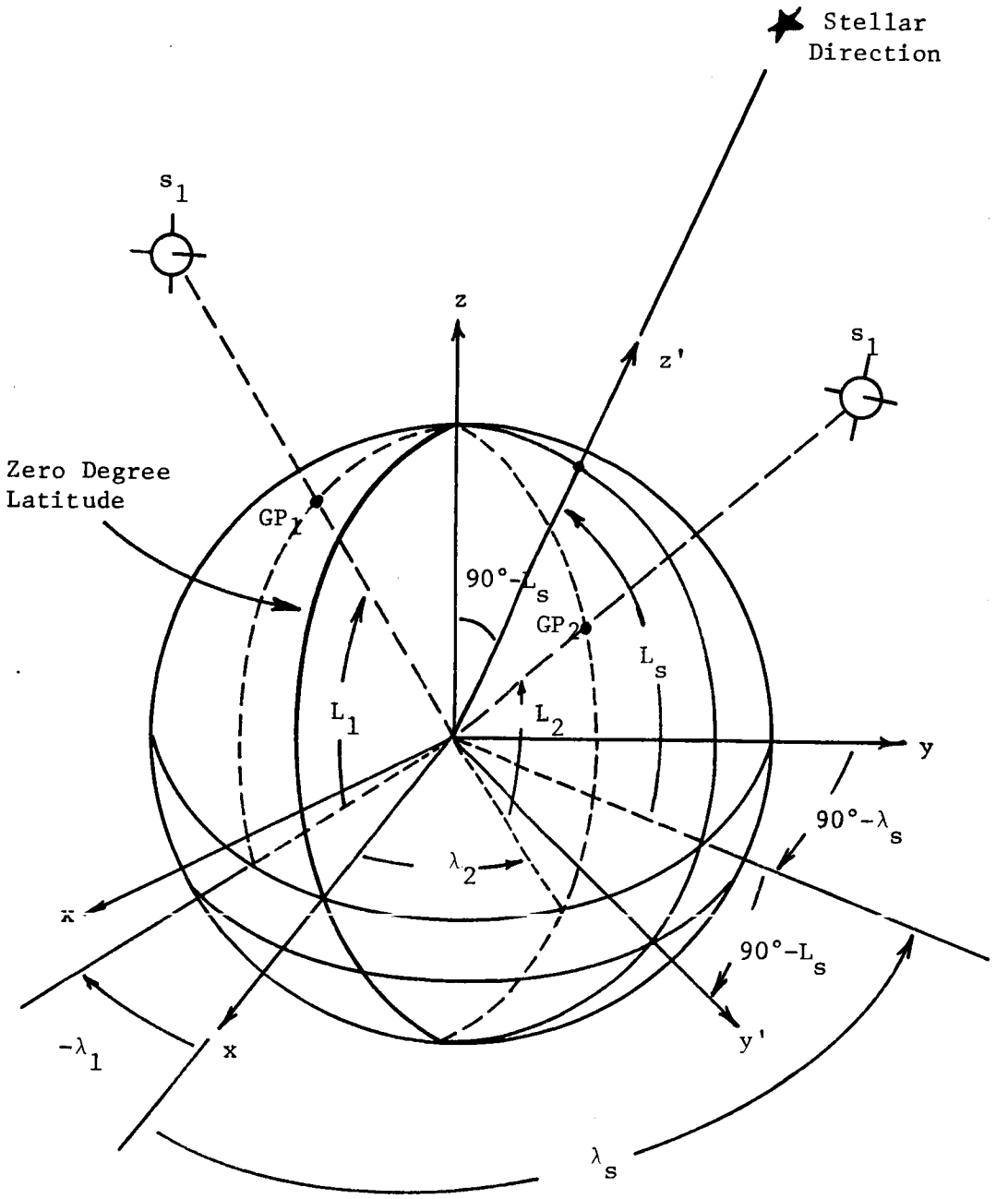

Definition of Coordinates, A Supplement to Figs. 6-14 and 6-15

Fig. 6-16

CHAPTER 7

NAVIGATION TECHNIQUES BASED ON LANDMARK SIGHTINGS

7-1. Navigation Using Landmarks

Although navigation using landmarks is an old art, most of the known techniques are not suitable for LRV navigation due to many considerations such as reliability, weight of hardware, required time for each fix, accuracy, and convenience. New techniques are therefore needed to supplement the old techniques.

Several new techniques of landmark navigation are presented in this chapter. All techniques involve only angle measurements. The use of angle measurements only is very attractive since the required equipment is generally much lighter and simpler than ranging equipment. Because of the simplicity of the equipment, the schemes can be used to guide astronauts to walk back to LEM in case the LRV is disabled.

Two types of landmark navigation are presented here. The first type makes use of landmarks with known position and the second type includes schemes using landmarks whose positions are not known. Most techniques reported in this chapter are believed to be original.

7-2. Landmarks with Known Position

Two assumptions are made for this section: 1) The position of each landmark is known with respect to a given lunar coordinate system, and 2) Only an angle measurement device is used. The first assumption amounts to having a map of landmarks. The computation required for navigation can either be performed by time sharing the on-board computer or handled by an earth-based computer via telemetry.

In the following sections, the measurement geometry and analytics are first presented, then the error sources and approaches to improve the navigation accuracy are discussed. Two rules concerning the selection of landmarks based on results of the sensitivity analysis are given. Techniques of using redundant measurements to improve the position determination are also presented and compared.

Known Azimuth Reference

If there is no noise of any kind involved in the measurement, two landmarks are needed to obtain a fix when the azimuth reference is known and three are needed when the azimuth reference is not known.

Referring to Fig. 7-1, let (x_1, y_1) and (x_2, y_2) be the known positions of two landmarks, and (x, y) be unknown position of the LRV. Since the azimuth reference is known, the angles θ_1 and θ_2, which are measured from the azimuth reference to the lines of sight from the LRV to two landmarks, can be measured.

Two equations representing the lines of sight are

$$\frac{y - y_1}{x - x_1} = \tan \theta_1 = m_1$$

$$\frac{y - y_2}{x - x_2} = \tan \theta_2 = m_2 \qquad (7\text{-}1)$$

Rearranging the equations and using matrix notation, (8-1) becomes

$$\begin{bmatrix} -m_1 & 1 \\ -m_2 & 1 \end{bmatrix} \begin{bmatrix} x \\ y \end{bmatrix} = \begin{bmatrix} b_1 \\ b_2 \end{bmatrix} \qquad (7\text{-}2)$$

where

$$b_i = y_i - m_i x_i , \quad (i = 1, 2) \qquad (7\text{-}3)$$

Thus the LRV position is given by

$$\begin{bmatrix} x \\ y \end{bmatrix} = \begin{bmatrix} -m_1 & 1 \\ -m_2 & 1 \end{bmatrix}^{-1} \begin{bmatrix} b_1 \\ b_2 \end{bmatrix} \qquad (7\text{-}4)$$

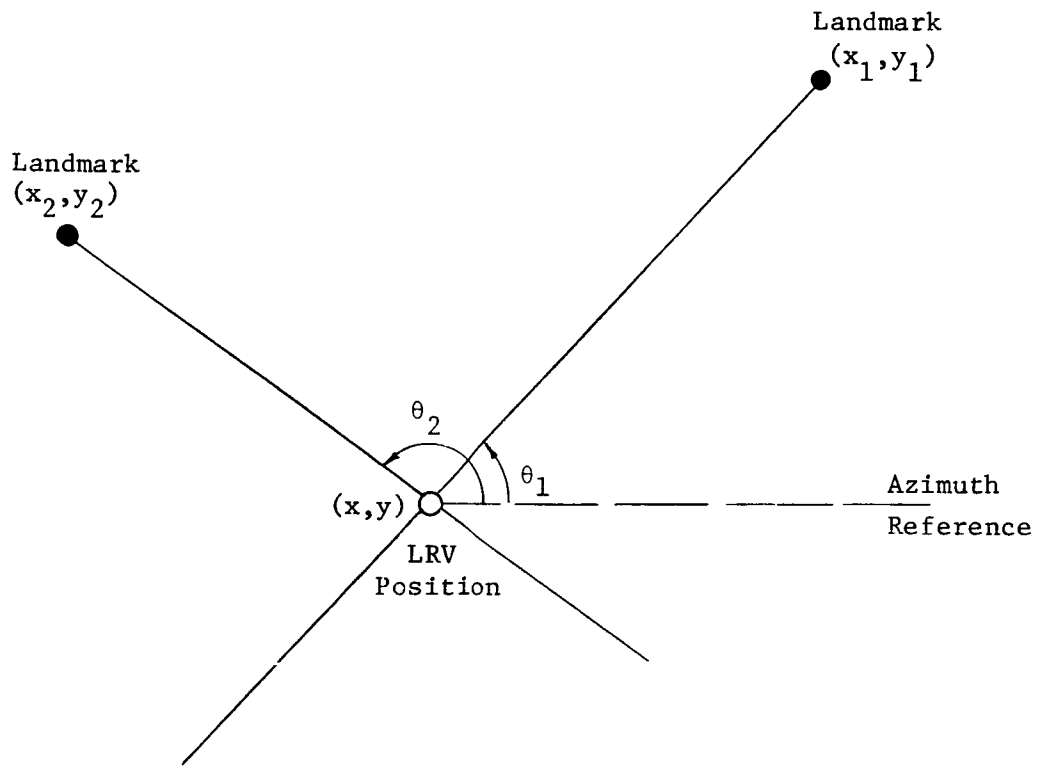

Navigation Using Two Landmarks

Fig. 7-1

Unknown Azimuth Reference

Using similar notation the geometry of the position fix using three landmarks but no azimuth reference is depicted in Fig. 7-2. The angles, β_1, β_2, and β_3 are measured from an arbitrarily chosen reference direction and α is the angle between this reference direction and the unknown azimuth reference. The equations of three lines of sight are

$$\frac{y - y_i}{x - x_i} = \tan (\alpha + \beta_i), \quad (i = 1, 2, 3) \qquad (7\text{-}5)$$

These three equations can be solved for three unknowns x, y, and α.

An alternate way of using three landmarks is to measure any two angles between the lines of sight as shown in Fig. 7-3. Since landmark positions are known, each angle measurement determines an equation of circle passing through two landmarks and the LRV position. Another angle measurement produces an equation of a second circle. One of the intersections of these two circles is the LRV position which can be solved from these two equations.

Error Consideration

In practice perfect measurements can hardly be obtained due to unavoidable errors. The possible error sources are:

1. Human sighting errors
2. Landmark position errors
3. Instrument errors
4. Computation errors

The effects of the first three error sources can be reduced by the proper choice of landmarks and by the use of redundant landmarks. The computation errors are caused by rounding off numerical numbers in the computer computation. In the following development we shall ignore computation errors.

Sensitivity Analysis

To have a feel of how various errors affects the accuracy of the position fix let us first solve (7-1) explicitly.

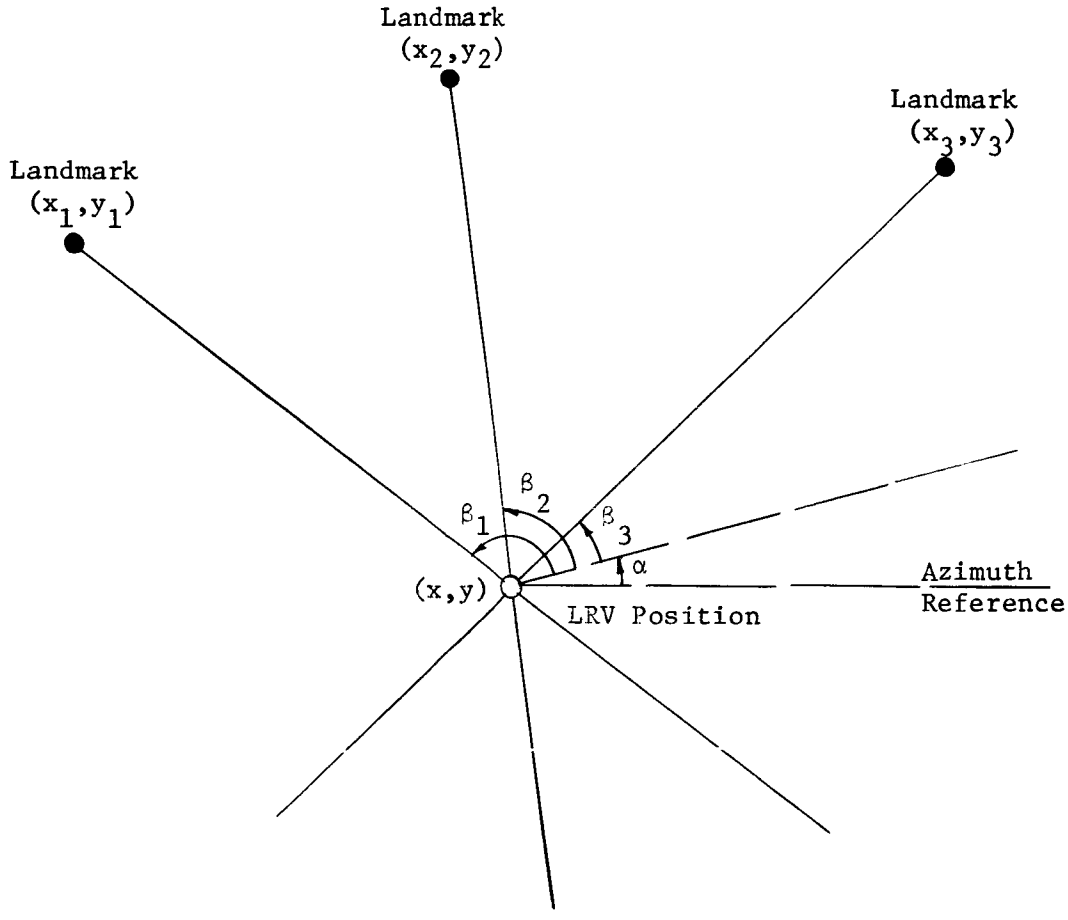

Navigation Using Three Landmarks

Fig. 7-2

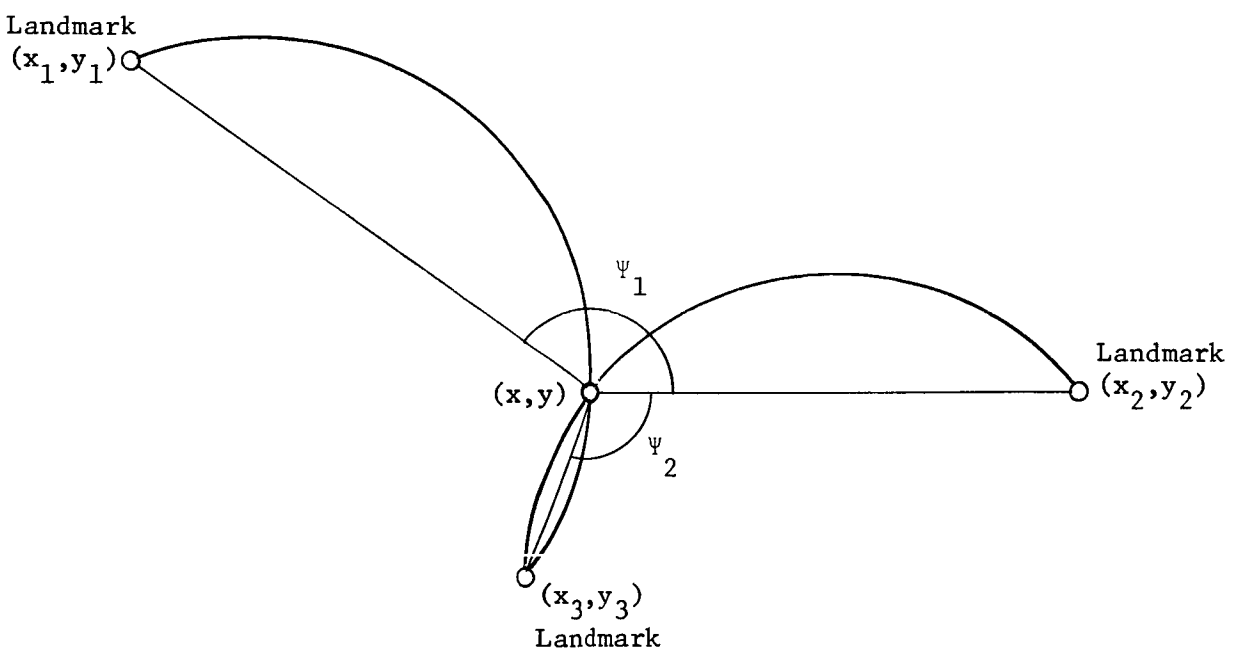

Navigation Using Three Landmarks

Fig. 7-3

$$x = \frac{m_1 x_1 - m_2 x_2 + y_2 - y_1}{m_1 - m_2}$$

$$y = \frac{m_1 m_2 (x_1 - x_2) + m_1 y_2 - m_2 y_1}{m_1 - m_2} \qquad (7\text{-}6)$$

Taking partial derivatives of (7-6) with respect to m_i, x_i, and y_i for i = 1, 2 gives the following twelve sensitivity functions.

$$\left.\begin{aligned}
\frac{\partial y}{\partial m_1} &= \frac{m_2 (y_1 - y_2) - m_2^2 (x_1 - x_2)}{(m_1 - m_2)^2} \\
\frac{\partial y}{\partial m_2} &= \frac{m_1 (y_2 - y_1) - m_1^2 (x_2 - x_1)}{(m_2 - m_1)^2} \\
\frac{\partial x}{\partial m_1} &= \frac{(y_1 - y_2) - m_2 (x_1 - x_2)}{(m_1 - m_2)^2} \\
\frac{\partial x}{\partial m_2} &= \frac{(y_2 - y_1) - m_1 (x_2 - x_1)}{(m_2 - m_1)^2}
\end{aligned}\right\} \qquad (7\text{-}7)$$

$$\left.\begin{aligned}
\frac{\partial y}{\partial y_1} &= \frac{m_2}{m_2 - m_1} \\
\frac{\partial y}{\partial y_2} &= \frac{m_1}{m_1 - m_2} \\
\frac{\partial y}{\partial x_1} &= \frac{m_1 m_2}{m_1 - m_2}
\end{aligned}\right\}$$

$$\left.\begin{aligned}
\frac{\partial y}{\partial x_2} &= \frac{m_2 m_1}{m_2 - m_1} \\
\frac{\partial x}{\partial y_1} &= \frac{1}{m_2 - m_1} \\
\frac{\partial x}{\partial y_2} &= \frac{1}{m_1 - m_2} \\
\frac{\partial x}{\partial x_1} &= \frac{m_1}{m_1 - m_2} \\
\frac{\partial x}{\partial x_2} &= \frac{m_2}{m_2 - m_1}
\end{aligned}\right\} \qquad (7\text{-}8)$$

Notice that when $m_1 = m_2$ all activities become infinite. This is the singular case when two lines of sight coincide. Thus it is desirable to select landmarks such that $m_2 - m_1$ be as large as possible. Thinking along this way we have the following rule

> Rule 1: Select the landmarks such that the sighting lines intersecting at the LRV divide the 360° horizontal field of view, as nearly as possible, into equal parts.

The following figure shows the ideal angle separation for cases of two and three lines. Equation (7-7) also reveals that to make the sensitivities small with respect to the slope measurements it is desirable to keep $x_1 - x_2$ and $y_1 - y_2$ small. Constrained by Rule 1, this means that the closer the two landmarks are to the LRV position the better. Generalizing this idea we have a second rule.

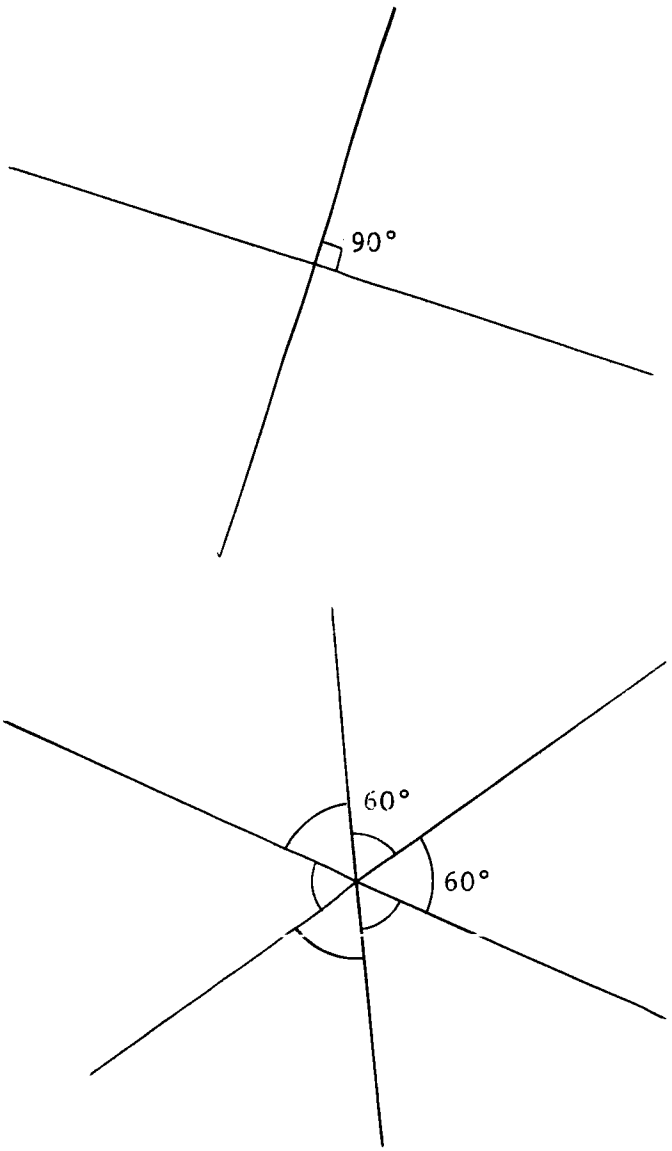

Preferred Angles Between Lines

Fig. 7-4

Rule 2: If n landmarks are used, then among all the landmarks satisfying Rule 1, choose those n nearest to the LRV position.

Redundant Measurements

Aside from reducing errors at error sources, the effect of errors can be reduced by making redundant measurements and then applying certain statistical data reduction techniques to arrive at an optimum position fix. Four data reduction concepts will be discussed. They are:

1. Arithmetic mean,
2. Least square distance regression,
3. Least square solution error regression,
4. Sequential estimation (Kalman filtering).

The first three methods do not make use of statistical properties of errors. Each of them is as good as the others when error statistics is not known. When the statistics of errors are given, the last method would give better results. All methods will be applied to an example.

Consider how n equations resulted from n landmark sightings.

$$\begin{pmatrix} -m_1 & 1 \\ -m_2 & 1 \\ \cdot & \cdot \\ \cdot & \cdot \\ \cdot & \cdot \\ \cdot & \cdot \\ \cdot & \cdot \\ -m_n & 1 \end{pmatrix} \begin{pmatrix} x \\ y \end{pmatrix} = \begin{pmatrix} b_1 \\ b_2 \\ \cdot \\ \cdot \\ \cdot \\ \cdot \\ \cdot \\ b_n \end{pmatrix} \tag{7-9}$$

where $n > 2$ and $b_i = y_i - m_i x_i$. In vector form we have

$$A \underline{z} = \underline{b} \tag{7-10}$$

where

$$\underline{z} = \begin{pmatrix} x \\ \\ y \end{pmatrix}$$

$$A = \begin{pmatrix} -m_1 & 1 \\ -m_2 & 1 \\ . & . \\ . & . \\ . & . \\ . & . \\ -m_n & 1 \end{pmatrix}$$

$$\underline{b} = \begin{pmatrix} b_1 \\ b_2 \\ . \\ . \\ . \\ . \\ b_n \end{pmatrix}$$

All under-barred lower case letters denote vectors and capital letters denote matrices. The set of n equations will in general give $\frac{n!}{(n-2)!2!}$ inconsistent solutions. One of the four data reduction concepts can be used to give an improved unique solution.

Arithmetic Mean

Solving two of the n equations in (7-9) at a time we have

$$\underline{z}_{ij} = \begin{bmatrix} x \\ y \end{bmatrix} = A_{ij}^{-1} \underline{b}_{ij} , \quad \begin{matrix} i,j=1,2,---n \\ i < j \end{matrix} \tag{7-11}$$

where A_{ij} is a 2 x 2 matrix formed by the i^{th} and the j^{th} rows of A, and $\underline{b}_{ij}$ is a 2-vector formed by the i^{th} and the j^{th} elements of $\underline{b}$. The arithmatic mean of $\underline{z}_{ij}$ is therefore,

$$\hat{\underline{z}} = \begin{bmatrix} x \\ \hat{y} \end{bmatrix} = \frac{(n-2)!2!}{n!} \sum_{\substack{ij \\ i<j}} \underline{z}_{ij} \tag{7-12}$$

Least Square Distance Regression

In this regression technique, the position $\underline{z}$ is selected to minimize the sum of the squares of distance from the selected position to each of the set of different solution given by (7-11). That is we want to minimize

$$I_1 = \sum_{\substack{ij \\ i<j}} (\hat{\underline{z}} - A_{ij}^{-1} \underline{b}_{ij})^T (\hat{\underline{z}} - A_{ij}^{-} \underline{b}_{ij}) \tag{7-13}$$

Taking the derivation of (7-13) with respect to $\underline{z}$ and setting the result to zero gives

$$\hat{\underline{z}} = \frac{(n-2)!2!}{n!} \sum_{\substack{ij \\ i<j}} A_{ij}^{-} \underline{b}_{ij} \tag{7-14}$$

which is simply the arithmetic mean, the same as (7-12).

Least Square Solution Error Regression

Write (7-10) as

$$A \underline{z} - \underline{b} = o. \tag{7-15}$$

No simple $\underline{z}$ can be found to satisfy this equation. Instead, any selected $\underline{z}$ will result in a solution error

$$\varepsilon = A\,\underline{z} - \underline{b}$$

The criterion is to choose a $\underline{z}$ such that

$$I_2 = \varepsilon^T \varepsilon = (A\underline{z} - \underline{b})^T (A\underline{z} - \underline{b}) \qquad (7\text{-}16)$$

is minimized. Taking the gradient of (7-16) with respect to $\underline{z}$ and setting the result to zero gives

$$\nabla I = A^T (A\underline{z} - \underline{b}) = o \qquad (7\text{-}17)$$

Solving for $\underline{z}$, yields

$$\hat{\underline{z}} = (A^T A)^{-1} A_T\, \underline{b} \qquad (7\text{-}18)$$

Kalman Estimation

If the statistics of the measurement uncertainities are known, a sequential estimation based on the Kalman filtering principle can be employed to yield the LRV position.

The format of the discrete Kalman filter is first reviewed. The set of equations describing the sequential operation of the Kalman filter is given by

$$\hat{\underline{x}}_k = \hat{\underline{x}}_{k-1} + K_k\,[\underline{y}_k - H_k\,\hat{\underline{x}}_{k-1}],\ k=1,2,\text{---} \qquad (7\text{-}19)$$

$$K_k = [P_{k-1}^{-1} + H_k^T R_k H_k]^{-1} H_k^T R^{-1} \qquad (7\text{-}20)$$

$$P_{k+1} = P_k - P_k H_{k+1}^T [R_{k+1} + H_{k+1} P_k H_{k+1}^T]^{-1} H_{k+1} P_k \qquad (7\text{-}21)$$

where $\hat{\underline{x}}_k$ is the estimate of the desired vector $\underline{x}_k$, $\underline{y}_k$ is a vector representing the observed quantities and is related to $\underline{x}_k$ through the measurement equation.

$$\underline{y}_k = H_k\,\underline{x}_k + \underline{n}_k \qquad (7\text{-}22)$$

The vector $\underline{n}_k$ represents observation noise whose covariance matrix is R_k. H_k is a matrix relating the desired quantities to the observed quantities. P_k is the covariance matrix of the estimation error, $e_k = x_k - \hat{x}_k$. The quantities $\underline{\hat{x}}_o$ and P_o needed for starting the sequential computation are obtained from the statistics of $\underline{x}_o$. Now we shall formulate the landmark navigation problem into the Kalman filter format.

The observed quantity in our problem is the angle θ_i and the desired are LRV coordinates x and y. They are related by the nonlinear relationship

$$\theta_i = \tan^{-1} \frac{y - y_i}{x - x_i} \tag{7-23}$$

It is assumed that the observation error is not severe so the linearization of (7-23) about the initially estimated LRV position is acceptable for describing the perturbation relationships among variables. Differentiating (7-23) gives the perturbation equation

$$d\theta_i = - \frac{y - y_i}{r_i^2} dx + \frac{x - x_i}{r_i^2} dy \tag{7-24}$$

where $r_i = \sqrt{(x-x_i)^2 + (y-y_i)^2}$. Thus the measurement equation corresponding to (7-22) is

$$\Delta\theta_i = \underbrace{\begin{pmatrix} \frac{y - y_i}{r_i^2} & \frac{x - x_i}{r_i^2} \end{pmatrix}}_{H_i} \begin{pmatrix} \Delta x \\ \Delta y \end{pmatrix} + n_i \tag{7-25}$$

where the noise n_i, representing the error in angle measurement, has a known variance of R and a mean of zero.

The initial estimate $\hat{x}_o$ of the LRV position can be obtained by making two initial angle measurements θ_{o1} and θ_{o2} and then solving the equation.

$$\frac{\hat{y}_o - y_{o1}}{\hat{x}_o - x_{o2}} = \tan \theta_{o1} \tag{7-26a}$$

$$\frac{\hat{y}_o - y_{o2}}{\hat{x}_o - x_{o2}} = \tan \theta_{o2} \qquad (7\text{-}26b)$$

where (x_{o1}, y_{o1}) and (x_{o2}, y_{o2}) are the positions of two landmarks. Therefore,

$$\hat{x}_o = \frac{\tan\theta_{o1}\, x_{o1} - \tan\theta_{o2}\, x_{o2} + y_{o2} - y_{o1}}{\tan\theta_{o1} - \tan\theta_{o2}}$$

(7-27)

$$\hat{y}_o = \frac{\tan\theta_{o1}\, \tan\theta_{o2}\, (x_{o1} - x_{o2}) + \tan\theta_{o1}\, y_{o2} - \tan\theta_{o2}\, y_{o1}}{\tan\theta_{o1} - \tan\theta_{o2}}$$

To obtain P_o, we first differentiate (7-27) with respect to angles θ_{o1} and θ_{o2}.

$$\Delta\hat{x}_o = \frac{[(x_{2o}-x_o)\tan\theta_{o2} + y_{o1}-y_{o2}]\sec^2\theta_{o1}\, \Delta\theta_{o1} + [(x_{o1}-x_{o2})\tan\theta_{o1}+y_2-y_1]\sec^2\theta_{o2}\Delta\theta_{o2}}{(\tan\theta_{o1} - \tan\theta_{o2})^2}$$

(7-28)

$$\Delta\hat{y}_o = \frac{[(x_{o2}-x_{o1})\tan\theta_{o2}+y_{o1}-y_{o2}]\tan\theta_{o2}\, \sec^2\theta_{o1}\Delta\theta_{o1}+[(x_{o1}-x_{o2})\tan\theta_{o1}+(y_{o2}-y_{o1})\tan\theta_1\sec^2\theta_{o2}\Delta\theta_{o2}}{(\tan\theta_{o1} - \tan\theta_{o2})^2}$$

In vector form,

$$\begin{bmatrix} \Delta\hat{x}_o \\ \Delta\hat{y}_o \end{bmatrix} = A \begin{bmatrix} \Delta\theta_{o1} \\ \Delta\theta_{o2} \end{bmatrix} \qquad (7\text{-}29)$$

where

$$A = \begin{bmatrix} \dfrac{[(x_{o2}-x_{o1})\tan\theta_{o2}+y_{o1}-y_{o2}]\sec^2\theta_{o1}}{(\tan\theta_{o1}-\tan\theta_{o2})^2} & \dfrac{[(x_{o1}-x_{o2})\tan\theta_{o1}+y_{o2}-y_{o1}]\sec^2\theta_{o2}}{(\tan\theta_{o1}-\tan\theta_{o2})^2} \\ \dfrac{[(x_{o2}-x_{o1})\tan\theta_{o2}+y_{o1}-y_{o2}]\tan\theta_{o2}\sec^2\theta_{o1}}{(\tan\theta_{o1}-\tan\theta_{o2})^2} & \dfrac{[(x_{o1}-x_{o2})\tan\theta_{o1}+y_{o2}-y_{o1}]\tan\theta_{o1}\sec^2\theta_{o2}}{(\tan\theta_{o1}-\tan\theta_{o2})^2} \end{bmatrix}$$

Then compute P_o from

$$P_o = \begin{bmatrix} \Delta\hat{x}_o \\ \Delta y_o \end{bmatrix} [\Delta\hat{x}_o \quad \Delta\hat{y}_o] = AQA^T \qquad (7\text{-}31)$$

where Q is the covariance matrix of $\begin{bmatrix} \Delta\theta_{o1} \\ \Delta\theta_{o2} \end{bmatrix}$ which is assumed known.

The computation procedure for the Kalman estimation can now be listed as follows:

1. From the two initial angle measurements θ_{o1} and θ_{o2} calculate the initial estimate of LRV position $(\hat{x}_o, \hat{y}_o)$ using (7-27), and obtain the initial error covariance matrix P_o using (7-28).

2. To each redundant angle measurement θ_k corresponding to landmark No. k, compute

$$\hat{\theta}_k = \tan^{-1} \frac{\hat{y}_o - y_k}{\hat{x}_o - \bar{x}_k}$$

$$\Delta\theta_k = \theta_k - \hat{\theta}_k$$

$$r_k^2 = (\hat{x}_{k-1} - \bar{x}_k)^2 + (\hat{y}_{k-1} - \bar{y}_k)^2$$

$$H_k = \left(\frac{\hat{y}_{k-1} - \overline{Y}_k}{\Gamma_k^2} \quad \frac{\hat{x}_{k-1} - \overline{X}_k}{\Gamma_k^2} \right)$$

$$P_k = P_{k-1} - P_{k-1} H_k^T \left[R + H_k P_{k-1} H_k^T \right]^{-1} H_k P_{k-1}$$

$$K_k = \left(P_{k-1}^{-1} + H_k^T R H_k \right)^{-1} H_k^T R_k^{-1}$$

3. Compute the h-th correction from

$$\begin{pmatrix} \Delta\hat{x}_k \\ \Delta\hat{y}_k \end{pmatrix} = \begin{pmatrix} \Delta\hat{x}_{k-1} \\ \Delta\hat{y}_{k-1} \end{pmatrix} + \left(K_k \quad \Delta\theta_k - H_k \right) \begin{pmatrix} \Delta\hat{x}_{k-1} \\ \Delta\hat{y}_{k-1} \end{pmatrix}$$

4. Compute the h-th corrected LRV position from

$$\hat{x}_k - \hat{x}_o + \Delta\hat{x}_k \qquad (\Delta\hat{x}_o = o)$$

$$\hat{y}_k = \hat{y}_o + \Delta\hat{y}_k \qquad (\Delta\hat{y}_o = o)$$

5. If a (k+1)-th angle measurement is made repeat step 2 to 5 for the (k+1)-th corrected LRV position.

7-3. Landmarks Whose Positions are not Known

The lunar coordinates of the LRV cannot be determined by observing landmarks whose positions are not indicated on the available lunar maps. However, it is possible to use these observations to locate the LRV on an unscaled map of the lunar surface. This technique can be used to guide the LRV to return to any or all of the previously visited sights, including the original starting point at the LEM.

When a reference direction is available, two landmarks within visible range are enough to guide the LRV. When a reference direction is not available, three landmarks are needed. These two cases will be presented separately in the following discussion.

Use of a Reference Direction

When a reference direction is available, two landmarks are sufficient to guide the LRV to a previously visited site. Consider the situation shown in Fig. 7-5. Here the navigator is given a reference direction and two landmarks whose positions are not known. The reference direction might be defined by the solar direction, a stellar direction, or the direction to a landmark on earth. The following equations will enable the navigator to return from his present position to his initial position using only angle measurements.

Various solutions to this problem can be devised. The special advantage of the scheme described here is that it provides the steering direction which enables the LRV to move from its present position to the initial position in a straight line. This feature allows the navigator to return quickly and to conserve energy.

Let the initial angles of the landmark direction measured from the reference direction be α_o and β_o, while the present angles are α_1 and β_1 as shown in Fig. 7-5.

In order to determine the return direction the navigator must move the LRV a short distance in any direction away from the present position as shown in Fig. 7-6. He must measure the angles θ and ϕ before the movement, and measure the angles θ' and ϕ' after the movement. Then the proper steering angle, α_1, can be determined from equations (7-32) and (7-33). The angle α_1 is defined in Fig. 7-7.

$$K = \frac{\sin\phi' \sin(\theta' - \theta) \sin(\beta_1 - \beta_o)}{\sin\theta' \sin(\phi' - \phi) \sin(\alpha_1 - \alpha_o)} \tag{7-32}$$

$$\gamma_1 = \tan^{-1} \frac{K\sin\alpha_o - \sin\beta_o}{K\cos\alpha_o + \cos\beta_o} \tag{7-33}$$

The derivation of these equations is in Appendix G.

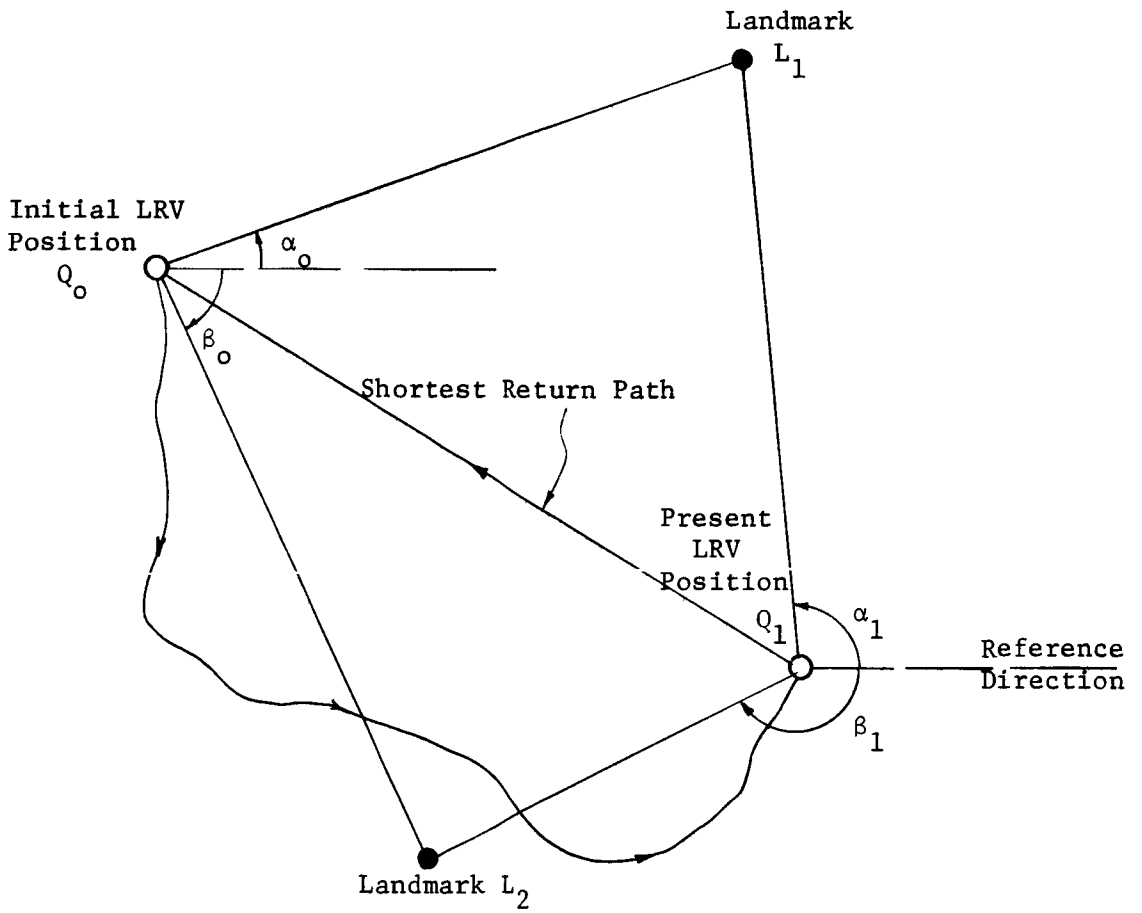

Navigation Using Two Unknown Landmarks

Fig. 7-5

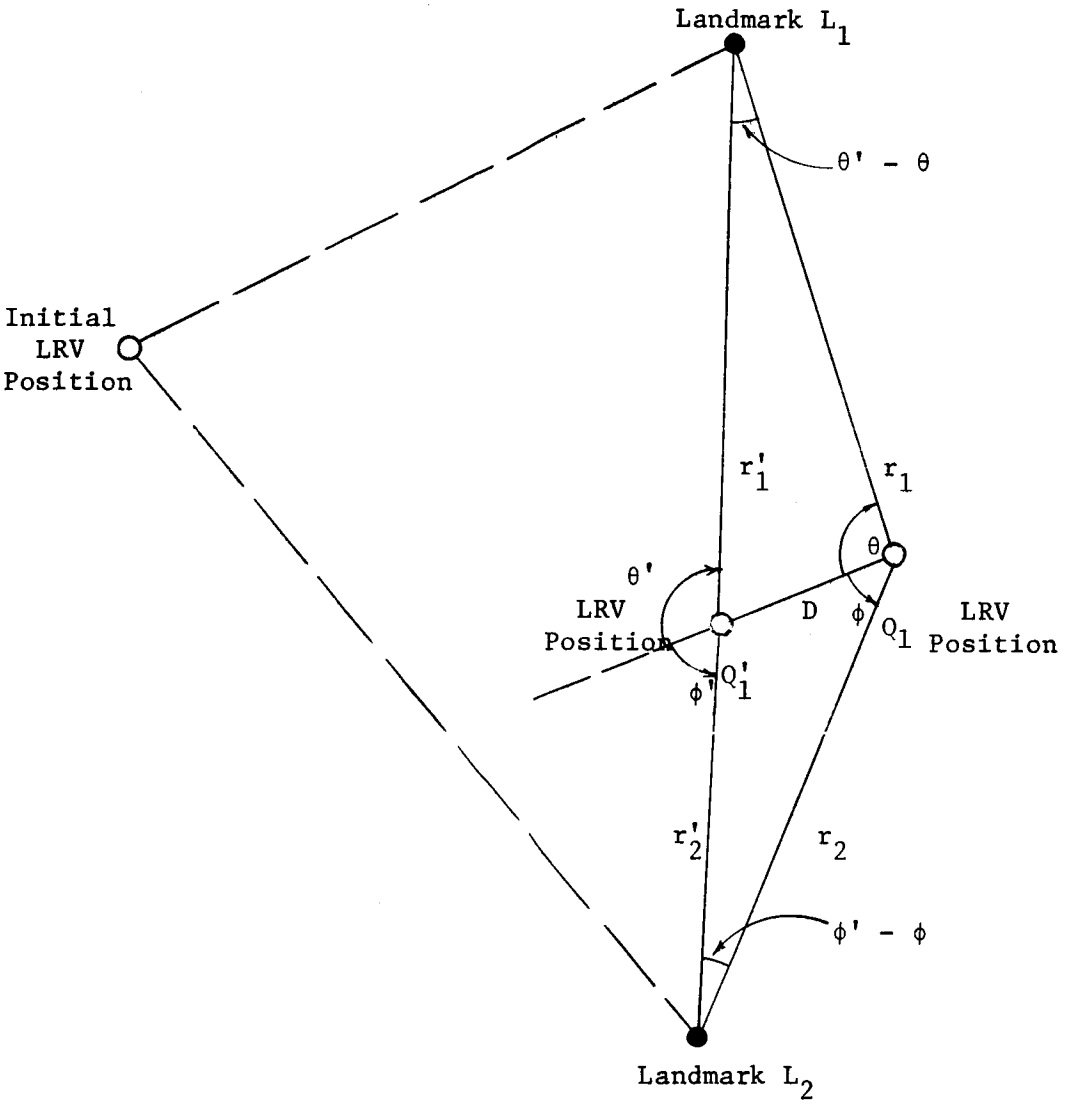

Determination of $\frac{r_1}{r_2}$ Ratio

Fig. 7-6

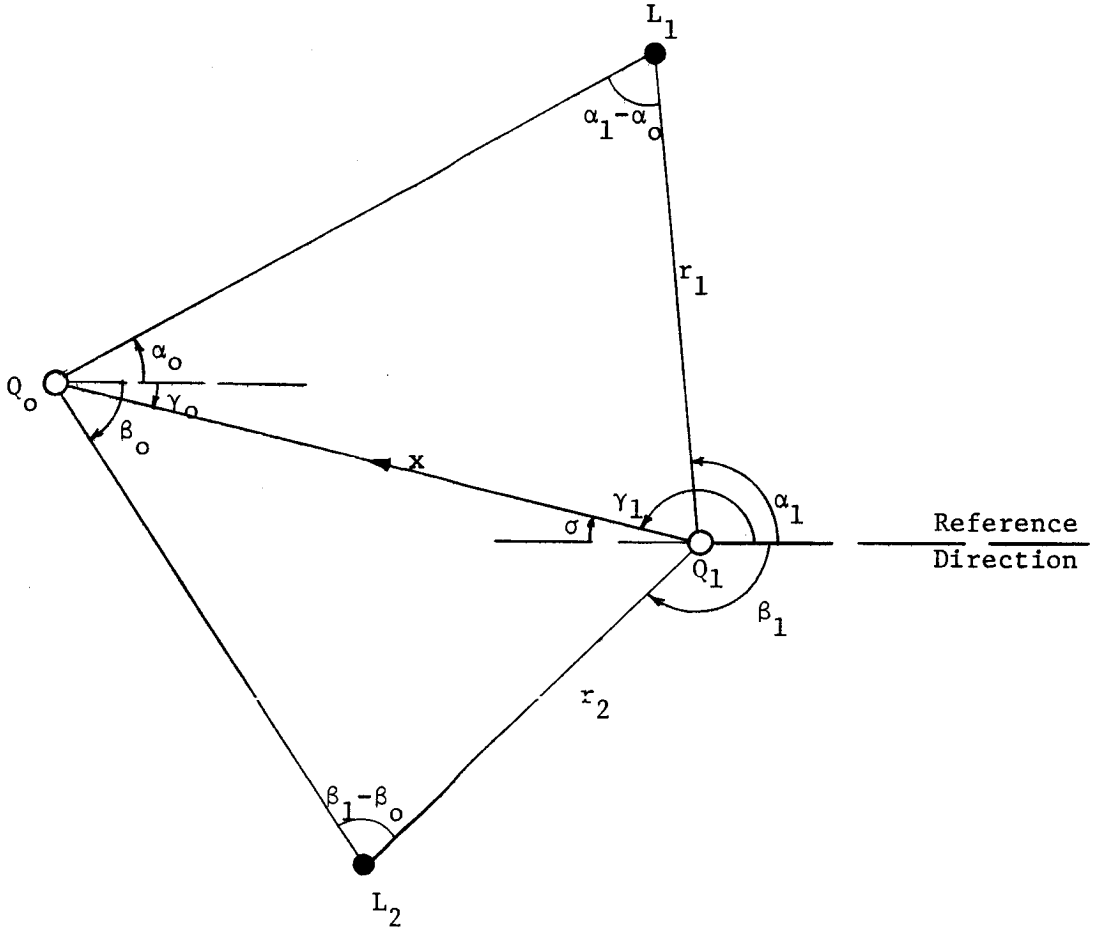

Navigation Using Two Unknown Landmarks

Fig. 7-7

Notice that in (7-33), to each given arctangent two values of γ_1 can be found. This ambiguity will be resolved in the continued study.

Reference Direction Not Available

When a reference direction is not available three landmarks are required to guide the LRV back to its initial position. Fig. 7-8 depicts the geometry of the problem and defines all angles. The direction of the shortest return path is given by the angle γ_1. Notice the reference of each angle measurement and the direction of positive angle.

The present problem is: given the measured angles α_o and β_o between lines joining the initial LRV position and landmarks, and also angles α_1 and β_1 at the present LRV position, how can the angle γ_1 for the shortest return path be determined.

The angle γ_1 is given by

$$\gamma_1 = \tan^{-1} \frac{k_2 \sin A \sin B - k_3 \sin \alpha_1 \sin C}{k_2 \sin B (\cos A - k_3 \cos C) + k_3 \sin C(k_2 \cos B - \cos \alpha_1)} \qquad (7\text{-}34)$$

where

$$\left.\begin{aligned} A &= \alpha_1 + \beta_1 \\ B &= \alpha_1 - \alpha_o \\ C &= \alpha_1 - \alpha_o + \beta_1 - \beta_o \end{aligned}\right\} \qquad (7\text{-}35)$$

$$\left.\begin{aligned} k_2 &= \frac{R_2}{R_1} \\ k_3 &= \frac{R_3}{R_1} \end{aligned}\right\} \qquad (7\text{-}36)$$

The ratios k_2 amd k_3 can be determined by the technique similar to the determination of $(\frac{r_2}{r_1})$ in Appendix G. If the LRV is moved a short distance in any direction at the starting end as shown in Fig. 7-9, then

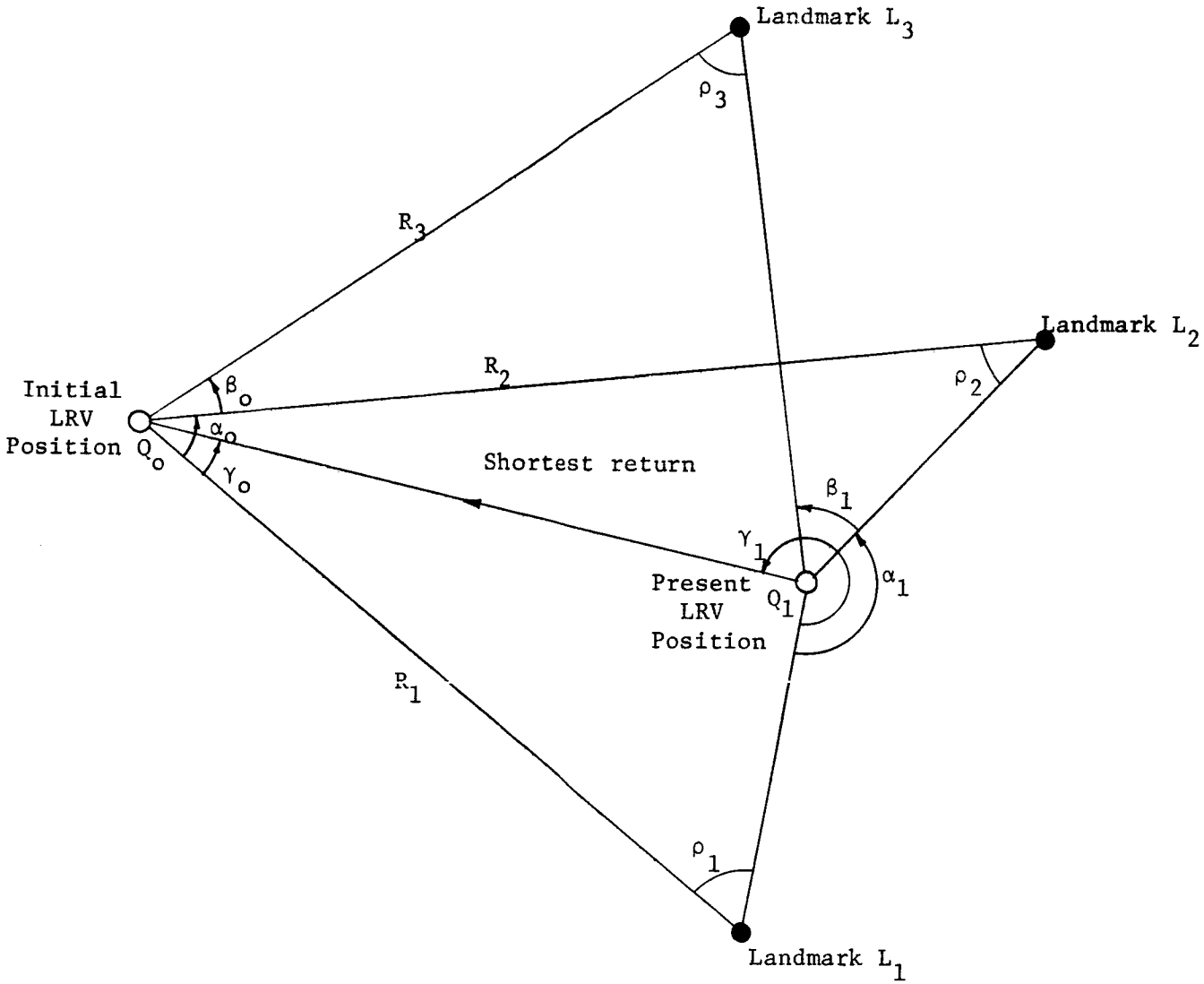

Navigation Using Three Unknown Landmarks

Fig. 7-8

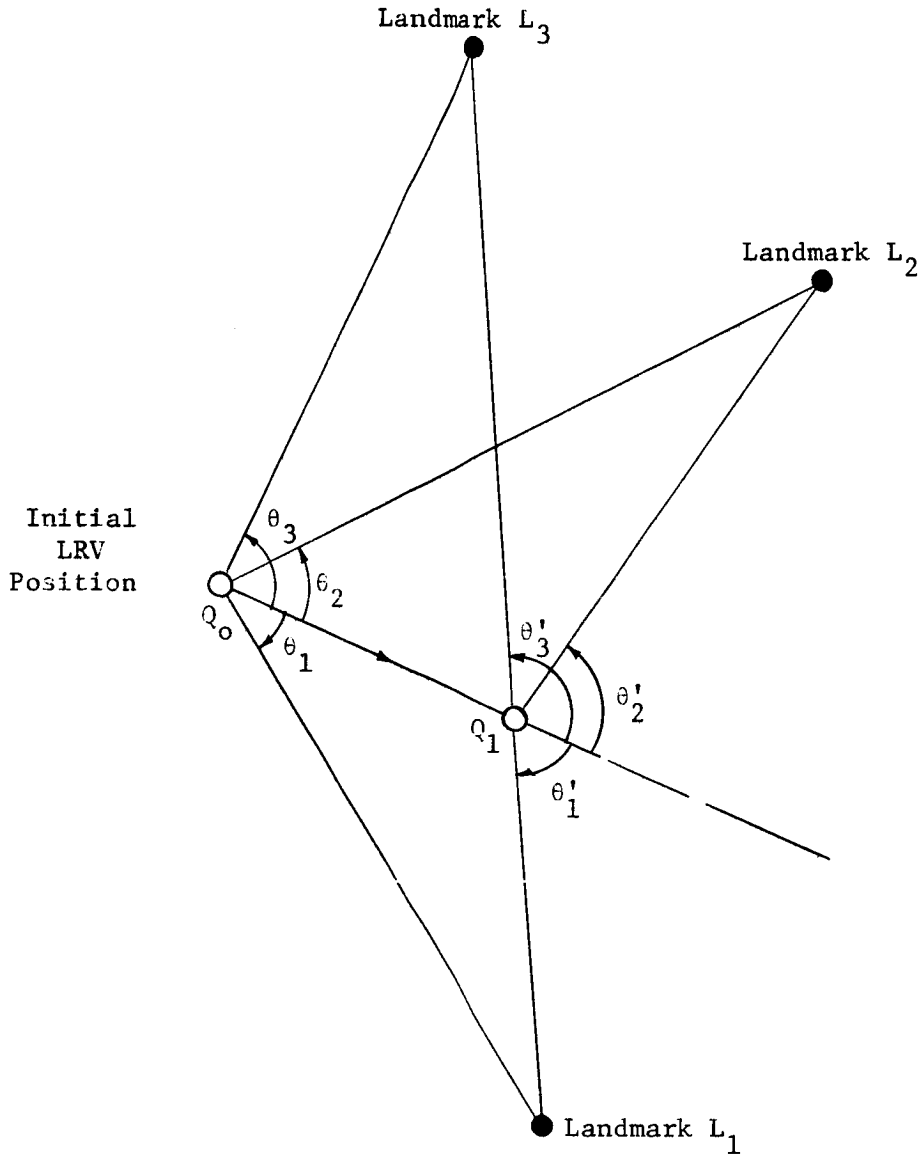

Determination of $\frac{R_2}{R_1}$ and $\frac{R_3}{R_1}$ Ratios

Fig. 7-9

$$k_2 = \frac{R_2}{R_1} = \frac{\sin \theta_2' \sin (\theta_1' - \theta_1)}{\sin \theta_1' \sin (\theta_2' - \theta_2)} \tag{7-37}$$

$$k_3 = \frac{R_3}{R_1} = \frac{\sin \theta_3' \sin (\theta_1' - \theta_1)}{\sin \theta_1' \sin (\theta_3' - \theta_3)} \tag{7-38}$$

All above equations are derived in Appendix G.

As in the case of last section, the value of γ_1 given by (7-34) is not unique. This ambiguity will be resolved in the continued study.

7.4. An Example

Consider the case where landmark positions are known. The true position of the LRV is at x = y = o. Ten angle measurements are made to ten different landmarks whose positions are known. The landmark positions and the corresponding angle measurements are shown below.

Landmark Position		Measured angle
X (KM)	Y (KM)	(degree)
2	1	26.7047
4	-2	-26.5795
-2	8	103.8340
-5	-2	202.0022
6	8	53.1393
2	5	68.2511
-6	6	135.0673
5	-6	-50.3190
-6	-10	239.1266
-5	1	168.6730

It is known a priori that the measured values of the angles are contaminated with noise having a mean of zero and a variance of 0.01. The techniques discussed above are used to obtain the estimates and the results are listed in Table 7-1 and plotted in Fig. 7-10. Fortran programs used to compute these estimates are included in Appendix H.

Arithmetic mean:

$x = 0.0021546$ KM $y = 0.00531784$ KM

Least Square Solution Error Regression

$x = 0.015$ KM $y = 0.001$ KM

Kalman estimation

$x_o = 0.0070807$ KM	$y_o = 0.0024522$
$x_1 = -0.0044727$	$y_1 = -0.0063779$
$x_2 = -0.0064793$	$y_2 = -0.0036411$
$x_3 = -0.0058166$	$y_3 = -0.0035441$
$x_4 = -0.0015173$	$y_4 = -0.0025585$
$x_5 = +0.0016975$	$y_5 = -0.0011890$
$x_6 = +0.0068746$	$y_6 = +0.0009305$
$x_7 = +0.0032268$	$y_7 = 0.0002596$
$x_8 = 0.0018305$	$y_8 = -0.0006101$

Result of the Example

Table 7-1

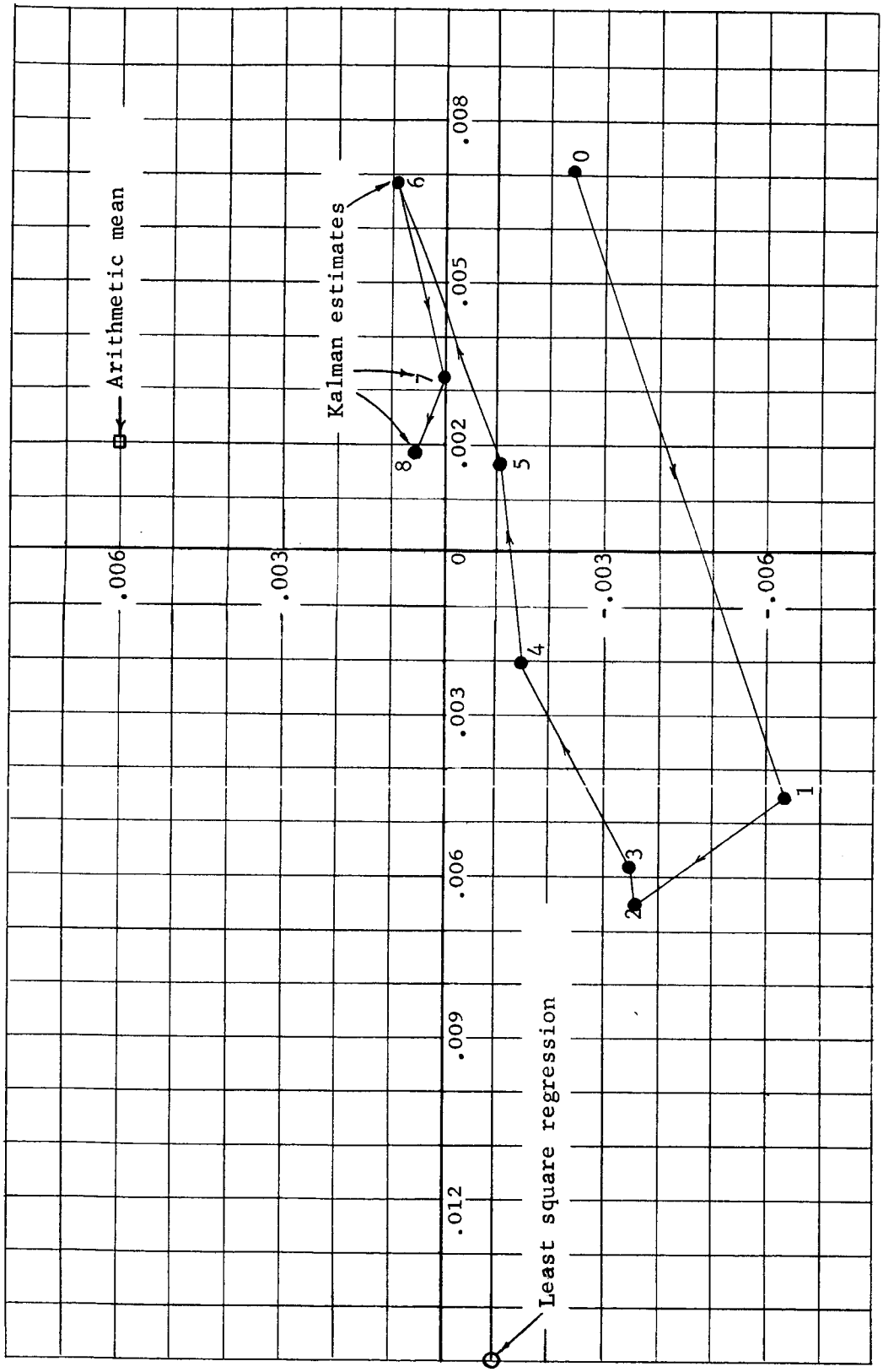

Estimated LRV Positions

Fig. 7-10

CHAPTER 8

DLRV NAVIGATION SYSTEMS AND THEIR COMPARISON

8-1. General

The organization of the total DLRV navigation system is dictated by the DLRV mission requirements. To have continuous navigation, which is needed for vehicle guidance, a dead reckoning navigator must be part of the total system. However, for a long mission period the errors that accumulate with time when a dead reckoning navigator is used would be prohibitively large. Some type of position fix scheme must be employed to periodically update the position estimate provided by the dead reckoning system.

In this chapter comparison will be made among dead reckoning navigators and among position fix schemes. A base line total system will be proposed as a standard for comparison.

8-2. Dead Reckoning Navigators

Two kinds of measurements are involved in a dead reckoning navigator, namely the orientation and the distance measurements. Various combinations of these two kinds of measurement devices give many different dead reckoning navigators.

Orientation Measurement Devices

Table 8-1 presents a list of seven candidate orientation measurement devices for DLRV. Advantages and disadvantages of each device are discussed in the "Remark" column.

All devices, except the gimbaled platform, are attractive for DLRV application in certain respects. The gimbaled platform is simply too heavy and too bulky. Although the pure odometer device is not precise enough to be part of the main navigator, it is very attractive as a back-up, especially for complementing the sun-sensor when the latter is shadowed.

Orientation Measurement Device	Vertical Measurement	Azimuth Measurement	Remarks
1. Gyro-Gyro	Vertical Gyro	Directional Gyro	Adv: - Does not require solar line of sight - Can be made insensitive to lateral acceleration Disadv: - Heavier than systems 2, 3, and 4 - Drift in directional gyro
2. Pendulum-Gyro	Pendulum*	Directional Gyro	Adv: - Light weight - Does not require solar line of sight Disadv: - Drift in directional gyro - Sensitivity to lateral acceleration can be minimized but not completely eliminated
3. Gyro-Sun-Sensor	Vertical Gyro	Sun-Sensor	Adv: - Light weight - Reliable and drift free azimuth sensor - Can be made insensitive to lateral acceleration Disadv: - Vulnerable to shadowing
4. Pendulum Sun-Sensor	Pendulum*	Sun-Sensor	Adv: - Very light weight - Both sensors are drift free Disadv: - Vulnerable to shadowing - Sensitivity to lateral acceleration can be minimized but not completely eliminated
5. Strapdown Platform Unit	No direct vertical and azimuth measurements. Angular rates are measured.		Adv: - Lighter than gimbaled platform - Good precision Disadv: - High computation requirements
6. Gimbaled Platform Unit	Platform is stabilized by gyro outputs.		Adv: - Good precision Disadv: - Too heavy and too bulky for DLRV application
7. Pure Odometer Device	None	Differential of Odometer Outputs	Adv: - Extreme simplicity, no extra sensor needed - An attractive back-up for temporary navigation Disadv: - Not precise because of no vertical reference - Wheel slip causes permanent heading error

*This includes the use of accelerometers as a pendulum.

Orientation Measurement Devices

Table 8-1

Distance Measurement Devices

Two most attractive distance measurement devices for DLRV application are the odometer and the accelerometer. The comparison of the two is given in Table 8-2.

Dead Reckoning Navigators

Table 8-3 lists the fourteen dead reckoning navigators that are generated by combining the seven orientation measurement techniques of Table 8-1 with the two distance measurement techniques of 8-2. It is noted in Table 8-3 that some of these combinations are attractive for the DLRV mission while others are unreasonable combinations.

8-3 Position Fix Navigators

Position fix schemes have been studied that are based on sightings of three different kinds of references: natural celestial bodies, lunar satellites, and lunar landmarks. Table 8-4 lists some of the basic advantages and disadvantages of these three position fixing concepts.

8-4 Base-Line Navigation Package

Here a base-line navigation package, including both dead reckoning and position fix systems, will be selected as a standard for comparison for any candidate schemes for DLRV navigation. In order to provide a good base line for comparison, this package has been conservatively selected as an approach that will meet the essential navigation requirements and not require any extraordinary support devices. It should be emphasized that the selected base line system is not necessarily the best system.

The dead reckoning portion of the base line package is number I1 in table 8-3. This dead reckoning navigator uses a directional gyro and a vertical gyro to determine the LRV orientation and an odometer to measure distance.

Those dead reckoning combinations that use a solar directional reference were discarded because the base-line system should be operative even when shadowed. In order to qualify a dead reckoning package that uses a solar sensor for

Devices	Remarks
I. Odometer	Advantages: - No extra sensor needed since an odometer is already built into each wheel assembly - Not affected by gravitational acceleration Disadvantages: - Wheel slips cause measurement error
II. Accelerometer	Advantages: - Not affected by wheel slips Disadvantages: - Gravitational acceleration must be subtracted using measured orientation - More sensitive to bias due to double integration

Distance Measurement Devices

Table 8-2

Distance Orien-tation	I Odometer	II Accelerometer and Integrators
1 Gyro-Gyro	I1 (Base-line System)	II1
2 Pendulum-Gyro	I2	II2
3 Gyro-Sun-Sensor	I3 - Need back-up when shadowed	II3 - Need back-up when shadowed
4 Pendulum-Sun-Sensor	I4 - Need back-up when shadowed - Lightest system	II4 - Need back-up when shadowed
5 Strapdown Platform	I5 - More computation required	II5 - More computation required
6 Gimbaled Platform	I6 - Too heavy and too bulky	II6 - Accelerometers are mounted on the platform to eliminate resolving accelero-meter signals
7 Odometers	I7 - Using same odometers - Back-up for System I3 or I4	II7 - Back-up for System II3 or I4.

Comments for Dead Reckoning Navigators

Table 8-3

Navigator	Remarks
Use of Celestial Bodies	Advantage: - Stars are already available Disadvantage: - Very sensitive to measurement error
Use of Lunar Satellites	Advantages: - Less sensitive to measurement error as compared to celestial navigation - May take the advantage of the lunar scientific satellite if there will be one. Disadvantages: - Very expensive if need to provide a lunar satellite just for LRV navigation - Need to know accurately the orbital elements of lunar satellites
Use of Landmarks	Advantages: - Least sensitive to measurement error due to the short distance between landmarks and LRV - Very reliable when landmarks are available - Simple hardware Disadvantage: - Landmarks may not be available

Position Fix Navigators

Table 8-4

the DLRV, it will be necessary to demonstrate that this temporary loss of directional reference can meet the mission requirements as well as the base line system.

Similarly, systems that use pendulous vertical sensors were discarded. In order to qualify a dead reckoning package that uses a pendulum it will be necessary to demonstrate that the pendulum swinging does not seriously degrade the navigation accuracy.

Odometers are selected to measure distance because they appear to be the simplest and most reliable way to do the job.

The position fix portion of the base-line system must be based on the concept of sighting natural celestial bodies. The base-line system cannot depend on satellites or landmarks. It cannot depend on satellites because it is uncertain whether it will be possible to provide this type of artificial reference. The base-line position fix scheme cannot depend on lunar landmarks because it is uncertain whether the lunar terrain will be so hospitable as to provide navigator with a dependable supply of distinguishable landmarks.

CHAPTER 9

SUMMARY AND RECOMMENDATIONS

This chapter contains a brief summary of this report and recommendations for further research activities.

9-1. Summary

The requirements of continuous and high precision navigation for the DLRV dictates that both dead reckoning and position fix navigators be employed. A detail study of various navigation components, dead reckoning navigators, position fix navigators, and navigation systems was made. Many technical problems were discovered and solutions to them were suggested. Several most important results contained in this report are summarized here.

Two sets of dead reckoning navigation equations are given. The second set is an approximation of the first, and is very satisfactory when the excursion range between updates is small.

In principle, a pure odometer navigator can be constructed to measure both the heading angle of and the distance traveled by the DLRV on a smooth level surface. The system is not suitable as a primary dead reckoning navigator because of its high vulnerability to wheel slip. Extending its range of application beyond the level surface is not recommended. However, the pure odometer navigator is very attractive as a temporary back-up, especially for complementing the solar sensing device to eliminate the shadowing difficulty.

Because of their simplicity and light weight odometers seem to be the best for distance measurement. But, the conventional way of processing odometer signals has serious pitfalls. Techniques for correct mechanization were developed.

Analysis shows that a properly damped pendulous inclinometer can satisfactorily provide a vertical reference. An inclinometer is much lighter and consumes less power than a vertical gyro.

Five different arrangements for using solar sensors as a heading indicator were proposed, and the required computations were also developed.

Two celestial position fix schemes and four lunar satellite position fix schemes were investigated. Their sensitivity analyses and computation equations were developed. Better position determination can be achieved using a lunar satellite at the expense of system complexity and the installation of a satellite. On the other hand, celestial navigation, though less accurate, is much more economical.

Several new techniques of using lunar landmarks for position fixing were developed. All techniques require only angle measurements. The techniques are very attractive for two reasons. First, the distance between landmarks and the LRV are much shorter than those between stars or satellite and the LRV. Therefore, the error sensitivity due to equipment imperfections is much smaller. Secondly, in general, the angle measuring device is much simpler than a ranging device. Therefore, for the determination of the LRV position on a lunar map, position fix using landmarks is probably the best. Furthermore, when many landmarks are available, redundant measurements can easily be made to improve the navigation accuracy.

Comparisons were made among various sensors, navigators, and navigation systems. A base-line, total navigation system was proposed and is intended only as a comparison standard. The system consists of a celestial navigator for position fixing and a dead reckoning navigator for continuous navigation. The dead reckoning navigator includes a vertical gyro and a directional gyro for orientation measurement and odometers for distance measurement.

Since aerospace industries are constantly working to improve various navigation equipment and since the slow-down of Apollo Application Program will allow more time for hardware improvement, this study did not try to single out a particular navigation system as the best for the DLRV application.

9-2. Recommendations for Further Research

Besides yielding many new results the research reported here also generated many new concepts which deserve further investigation. A thorough study of these concepts will prepare a foundation for an economical development of a better DLRV navigation system. Continued research activity in this direction is strongly recommended. Four most important problems are described briefly in this section.

Position Fix Using Landmarks

From the viewpoint of performance reliability, crew safety, and simplicity of the equipment, the DLRV navigation should take the advantage of lunar landmarks whenever they are available. Continuing research is needed to further study and refine the new concepts advanced in this report. Details to be investigated include:

1. The removal of the heading angle ambiguities associated with navigation schemes using unknown landmarks.
2. A sensitivity analysis for each proposed landmark navigation scheme.
3. The development of an efficient policy for discarding old landmarks and picking up new landmarks as the DLRV moves along.
4. A study of the feasibility of using the proposed schemes as primary position fix navigators and as back-up navigators.
5. Investigation of the hardware required for each scheme.
6. A critical comparison of the landmark navigation approach to other navigation approaches for the DLRV application.

Optimum Combination of Dead Reckoning and Position Fix Data

In this report, dead reckoning and position fixing systems have been discussed separately. The position fix system has been treated as something that will be used periodically to update the continuous dead reckoning system. No attention has been directed to the details of this updating procedure.

The most straightforward updating procedure would be to reset the dead reckoning navigator to the location indicated by the position fix scheme whenever a position fix is obtained. This approach to the problem implies the assumption that the position fix information is perfect and that the dead reckoning information is useless. Fortunately, this is not the true situation. When the dead reckoning system has been operating for a long period of time since its last updating, its position estimate will become imprecise because of biases in the sensors. Nevertheless, this dead reckoning estimate still contains some

information about the vehicle location and this information should not be wasted.

A better way to combine these two types of navigation data would be to recognize that neither the dead reckoning nor the position fix data is perfect and to treat them accordingly. The satistical properties of the dead reckoning and position fix navigation errors can be estimated by considering the type and the quality of the sensors that are used. Once the statistical properties of the navigation errors for the dead reckoning and position fixing schemes are estimated, a procedure can be devised to combine the dead reckoning and position fix data in a manner that will minimize the probable navigation error. The Kalman filtering formulation can be used to produce an optimal way to cimbine the two sets of data. In reference 26 this problem is studied as it applies to navigation of ships at sea.

The following is a list of problems which need to be studied:

1. Development of techniques for optimum instrumentation by first performing the analytical study keeping in mind the practical constraints imposed by the navigation hardware.
2. Study the additional instrumentation and data processing required.
3. Evaluating the performance of the developed techniques by performing a simulation study using practical hardware data.
4. Comparing the merits of all developed techniques.

It should be pointed out that the results obtained from this study can easily be incorporated into any chosen navigation system consisting of dead reckoning and position fix navigators, since the major effort of the optimum instrumentation is in data processing and instrument adjustment.

DLRV's Total Navigation, Guidance, and Control System

Since navigation, guidance, and control are intimately related, a study should be made to consider the best combination of the three subsystems into an integrated, total system. Among the items needed to be studied are:

1. Compatibility
2. Mobility
3. Maneuvability and ease of operation

4. Overall reliability
5. Total power consumption
6. Others

Satellite Navigation

Although a DLRV navigation using lunar satellite is an expensive one, its prospect indeed warrants further research and development of the concept. Experience with Navy's TRANSIT system indicates that satellite navigation approach may be important in achieving the kind of position determination accuracy desired by scientists. The preliminary investigation has shown that given the orbital elements of the satellites, satellite navigation is more accurate than the known celestial navigation. It is very possible that scientists will need lunar satellites for scientific objectives. Under this condition it would be very convenient for NASA to share these satellites for navigation purposes.

The points that need to be studied in satellite navigation include:

1. The concepts
2. The required operation efforts such as tracking, ranging, angle measuring, etc.
3. The required data processing effort and how to do it.
4. The required on-board and earth-based equipment.

REFERENCES

1. J. R. Scull, Spacecraft, Guidance, and Control, Vol. IV of Space Technology, NASA SP-68, National Aeronautics and Space Administration, 1966.
2. R. H. Battin, Astronautical Guidance, McGraw-Hill Book Co., New York, 1964.
3. R. B. Kershner, "Status of the Navy Navigation Satellite System," Practical Space Application, Vol. 21 of Advances in the Astronautical Science Series, American Astronautical Society, 1967.
4. J. T. Broadbent, R. B. Odden, T. T. Trexler, and J. J. Vary, "Lunar Navigation Study Final Report," Vol. I, Bendix Aerospace System Division, Bendix Corporation, December 1966.
5. J. C. Hung, "A Study of Navigation Systems for Dual-Mode Lunar Roving Vehicle," Midterm Report for NASA Contract NAS8-24858, Systems Research, Department of Electrical Engineering, The University of Tennessee Nov. 1969.
6. N. Bowditch, American Practical Navigator, U. S. Navy Hydrographic Office Publication No. 9, U. S. Government Printing Office, Washington, D. C., 1962.
7. B. Dutton, Navigation and Nautical Astronomy, 9th Ed., U. S. Navy Institute, Annapolis, Maryland.
8. C. Broxmeyer, Inertial Navigation Systems, McGraw-Hill Book Co., 1964.
9. V. D. Andreev, Theory of Inertial Navigation, (Ttanslated from Russian), NASA TT F-564, U. S. Department of Commerce, 1969.
10. L. M. Vorobev, Spacecraft Navigation, (Translated from Russian), NASA TT F-564, U. S. Department of Commerce, 1966.
11. R. R. Newton, "The U. S. Navy Doppler Geodetic System and Its Observational Accuracy," Philosophical Transactions of the Royal Society of London, A, 262, pp. 50-66, 1967.
12. W. H. Guier and G. C. Weittenback, "A Satellite Doppler Navigation System," Proc. IRE, Vol. 48, pp. 507-516, 1960.
13. Tables of Computed Altitude and Azimuth, U. S. Navy H. O. Publication No. 214, Volumes 1-9.
14. American Ephemeris and Nautical Almanac, U. S. Government Printing Office, Washington, D. C.
15. M. Kayton and W. R. Fried, Avionics Navigation Systems, John Wiley and Sons, New York, 1969.
16. G. R. Macomber and M. Fermandez, Inertial Guidance Engineering, Prentice-Hall, Inc., Englewood Cliffs, New Jersey, 1962.
17. C. S. Draper, W. Wrigley, and J. Hovorka, Inertial Guidance, Pergamon Press, New York, 1960.
18. C. L. McClure, Inertial Guidance, Prentice-Hall, Inc., Englewood Cliffs, New Jersey, 1960.
19. Dictionary of Technical Terms for Aerospace Use, NASA SP-7, U. S. Government Printing Office, Washington, D. C., 1965.
20. The Rand Corporation, A Million Random Digits with 100,000 Normal Deviates, The Free Press, New York, 1955.

21. J. D. Irwin and J. C. Hung, "A Study of Optimum Discrete Estimators," Final Report for NASA Contract NAS8-11183, Control Theory Group, Department of Electrical Engineering, The University of Tennessee, November 1966.

22. J. S. Miller and J. C. Hung, "An Analysis of A Navigation Scheme for MLRV," Proceedings of the 8th Annual IEEE Region III Convention, pp. 145-152, November 1969.

23. J. E. Bennett and J. C. Hung, "Statistical Techniques for LRV Navigation Using Landmarks," To Appear.

24. J. E. Bennett and J. C. Hung, "Navigation and Guidance Using Landmarks with Unknown Positions," To Appear.

25. C. B. Solloway, "Elements of the Theory of Orbit Determination," EPD-255, Jet Propulsion Laboratory, December 1964.

26. B. E. Bona and R. J. Smay, "Optimum Reset of Ship's Inertial Navigation System," Transactions on Aerospace and Electronic Systems, IEEE, Vol. AES-2, No. 4, pp. 409-414, 1966.

27. F. Ayres, Jr., Trigonometry, Chapters 20-24, Schaum's Outline Series, McGraw-Hill Book Co., New York, 1954.

28. R. E. Anderson, "Satellite Navigation and Communication for Merchant Ships," Navigation, Journal of the Institute of Navigation, Vol. 14, No. 2, pp. 127-141, 1967.

29. L. M. Keane, "Recent Progress in Navigation Satellites," Navigation, Journal of the Institute of Navigation, Vol. 15, No. 4, pp. 415-423, 1968-1969.

30. E. Wall, "A Dead-Reckoning Land Vehicle Navigation System," Navigation, Journal of the Institute of Navigation, Vol. 12, No. 1, pp. 77-89, 1965.

31. W. J. Reilly and K. N. Satyendra, "Space Navigation by Self-Contained Means," Navigation, Journal of the Institute of Navigation, Vol. 9, No. 3, pp. 211-219, 1962.

32. J. W. Little, "An Engineering Approach to the Mathematics of Celestial Navigation," Navigation, Journal of the Institute of Navigation, Vol. 14, No. 3, pp. 239-248, 1967.

33. H. Buell, "Doppler, Inertial, and Doppler-Inertial Techniques," Navigation, Journal of the Institute of Navigation, Vol. 11, No. 3, pp. 250-259, 1964.

34. Maj. R. A. Briggs, USAF, "On the Accuracy of Celestial MPP's in Air Navigation," Navigation, Journal of the Institute of Navigation, Vol. 15, No. 4, pp. 431-435, 1968-1969.

35. M. A. Iacona, "Navigation in Oceanography," Navigation, Journal of the Institute of Navigation, Vol. 15, No. 3, pp. 244-256, 1968.

36. A. G. Mourad and N. A. Frazier, "Improving Navigational Systems Through Establishment of a Marine Geodetic Range," Navigation, Journal of the Institute of Navigation, Vol. 14, No. 2, pp. 187-194, 1967.

37. R. Y. Pei, "Instantaneous Impact Point Analysis," Navigation, Journal of the Institute of Navigation, Vol. 14, No. 2, pp. 195-204, 1967.

38. W. T. McDonald and Dr. R. G. Stern, "Space Navigation," Navigation, Journal of the Institute of Navigation, Vol. 14, No. 4, pp. 416-433, 1967-1968.

39. C. Broxmeyer and D. MacKinnon, "Terminal Phase Navigation," Navigation, Journal of the Institute of Navigation, Vol. 15, No. 4, pp. 424-430, 1968-1969.

APPENDIX A

COMPUTATION OF NAVIGATION ERROR FOR PURE ODOMETER SYSTEM USED ON A TILTED PLANE

The pure odometer navigation system described in Section 4-1 will accurately compute the LRV coordinates along the axes of the tilted surface. Errors occur because the navigation system output is interpreted as being the LRV coordinates along the level axes. The following equations give the x and y coordinates of the LRV as functions of α, β, and the x' and y' coordinates.

$$x = \frac{x' \cos \alpha}{\sqrt{1 - \sin^2 \alpha \sin^2 \beta}}$$

$$y = \left[y' - x' \frac{\sin \alpha \sin \beta}{\sqrt{1 - \sin^2 \alpha \sin^2 \beta}} \right] \cos \beta$$

The navigation error that is caused by using this pure odometer navigation system on a tilted surface is the difference between the LRV coordinates in the tilted plane and the coordinates in the level plane. Therefore,

$$\varepsilon_x = x' - x$$

$$= x' \left[\frac{1 - \cos \alpha}{\sqrt{1 - \sin^2 \alpha \sin^2 \beta}} \right]$$

$$\varepsilon_y = y' - y$$

$$= y' - \left[y' - \frac{x' \sin \alpha \sin \beta}{\sqrt{1 - \sin^2 \alpha \sin^2 \beta}} \right] \cos \beta$$

APPENDIX B

DERIVATIONS OF EXPRESSIONS FOR GIMBAL ANGLES FOR TWO-DEGREE-OF-FREEDOM GYROS

The coordinates of the fixed S2 coordinate system are related to the coordinates of the vehicle referenced S1 coordinate system by the following equation.

$$\begin{pmatrix} i_1 \\ j_1 \\ k_1 \end{pmatrix} = \begin{pmatrix} A \end{pmatrix} \begin{pmatrix} i_2 \\ j_2 \\ k_2 \end{pmatrix} \qquad \text{(B-1)}$$

where the elements of [A] are

$$a_{11} = \cos\theta \cos\Psi$$

$$a_{12} = \sin\theta$$

$$a_{13} = -\sin\Psi \cos\theta$$

$$a_{21} = \sin\theta \sin\Psi - \cos\phi \sin\theta \cos\Psi$$

$$a_{22} = \cos\theta \cos\phi$$

$$a_{23} = \cos\phi \sin\theta \sin\Psi + \sin\phi \cos\Psi$$

$$a_{31} = \sin\theta \cos\Psi \sin\phi + \sin\Psi \cos\phi$$

$$a_{32} = -\cos\theta \sin\phi$$

$$a_{33} = \cos\phi \cos\Psi - \sin\phi \sin\theta \sin\Psi$$

Fig. 5-11 in the text shows that the sides of the inner gimbal angles are the sides between one coordinate of the S1 system and a second coordinate in the S2 system. Consequently the cosines of the inner gimbal angles are simply the element from the matrix A that is the direction cosine between those two coordinates. This means that the cosine of the inner gimbal angle is a_{mn} where

m is 1, 2, or 3 depending on whether the side of the angle that is a S1 coordinate is $\hat{i}_1$, $\hat{j}_1$, or $\hat{k}_1$.
n is 1, 2, or 3 depending on whether the side of the angle that is a S2 coordinate is $\hat{i}_2$, $\hat{j}_2$, or $\hat{k}_2$.

The cosines of the outer gimbal angles are more complex and the derivation of these expressions is also more complex. Fig. 5-11 shows that one of the sides of the outer gimbal angle is a coordinate of the S1 coordinate system and that the other side is a direction defined by the vector cross product of one coordinate in the S1 system and one coordinate in the S2 system.

As an example the procedure for determining the cosine of the outer gimbal angle will be demonstrated for arrangement 1. The cosines of the outer gimbal angles for the other systems are obtained in the same way.

In arrangement 1 the outer gimbal angle is between $\hat{i}_1$ and the direction defined by $\hat{k}_1 \times \hat{i}_2$. From Equation B-1

$$\hat{i}_2 = \cos\theta \cos\Psi \hat{i}_1 + (\sin\phi \sin\Psi - \cos\phi \sin\theta \cos\Psi) \hat{j}_1$$

$$+(\sin\theta \cos\Psi \sin\phi + \sin\Psi \cos\phi) \hat{k}_1$$

It follows that $\hat{k}_1 \times \hat{i}_2 = (\cos\phi \sin\theta \cos\Psi - \sin\phi \sin\Psi) \hat{i}_1$

$$+ \cos\theta \cos\Psi \hat{j}_1$$

The cosine of the outer angle between $\hat{i}_1$ and $(\hat{k}_1 \times \hat{i}_2)$ is

$$\cos(OA) = \frac{\hat{i}_1 \cdot (\hat{k}_1 \times \hat{i}_2)}{\left|(\hat{k}_1 \times \hat{i}_2)\right|} .$$

Therefore,

$$\cos(OA) = \frac{\cos\phi \sin\theta \cos\Psi - \sin\phi \sin\Psi}{(\cos\phi \sin\theta \cos\Psi - \sin\phi \sin\Psi)^2 + (\cos\Psi \cos\theta)^2} .$$

APPENDIX C

DERIVATION OF SENSITIVITY EQUATIONS FOR CELESTIAL POSITION FIXES

C-1. Sensitivity Equations for Position Fix Using an Earth Landmark and Two Stellar Directions

An $\hat{i}$, $\hat{m}$, $\hat{n}$ coordinate system is defined with $\hat{n}$ along the LRV's local vertical, $\hat{m}$ perpendicular to $\hat{n}$ and on the great circle determined by the LRV position and GP_E, and $\hat{l}$ completing the right-hand triplet.

From the geometry of Figure 6-2 it is possible to write

$$P \cos q_1 = \bar{P} \cdot \hat{s}_1$$

$$= (\bar{R} - \bar{r}) \cdot \hat{s}_1$$

Differentiating this equation gives

$$\cos q_1 \, \Delta P - P \sin q_1 \, \Delta q_1 = - \dot{s}_1 \cdot \Delta \bar{r} \qquad \text{(C-1)}$$

From the law of cosines

$$P^2 = R^2 + r^2 - 2rR \cos\beta$$

Differentiating this equation produces

$$2P \, \Delta P = 2rR \sin\beta \, \Delta\beta$$

Then

$$\Delta P = \frac{Rr}{P} \sin\beta \, \Delta\beta \qquad \text{(C-2}$$

For small changes in β

$$\Delta B = - \frac{\Delta \bar{r} \cdot \hat{m}}{r} \qquad \text{(C-3)}$$

Combining (C-1), (C-2), and (C-3) gives

$$\frac{R}{P} \cos q_1 \sin\beta \, \Delta \bar{r} \cdot \hat{m} + P \sin q_1 \, \Delta q_1 = \Delta \bar{r} \cdot \hat{s}_1 \qquad \text{(C-4)}$$

$\hat{s}_1$ can be resolved along $\hat{l}$, $\hat{m}$, and $\hat{n}$ as follows

$$\hat{s}_1 = \sin\gamma_1 \cos\alpha_1 \hat{\ell} + \sin\gamma_1 \sin\alpha_1 \hat{m} + \cos\gamma_1 \hat{n} \qquad \text{(C-5)}$$

Substituting (C-5) into (C-4) gives

$$\frac{R}{P} \cos q_1 \sin\beta \, \Delta\bar{r} \cdot \hat{m} + P \sin q_1 \Delta q_1 =$$

$$\Delta\bar{r} \cdot (\sin\gamma_1 \cos\alpha_1 \hat{\ell} + \sin\gamma_1 \sin\alpha_1 \hat{m}) \qquad \text{(C-6)}$$

(C-6) can be solved for Δq_1

$$\Delta q_1 = \frac{1}{P\sin q_1} [\sin\gamma_1 \cos\alpha_1 \hat{\ell} + (\sin\gamma_1 \sin\alpha_1 - \frac{R}{P} \cos q_1$$

$$\sin\beta) \hat{m} + \cos\gamma_1 \hat{n}] \cdot \Delta\bar{r}$$

$$= \frac{1}{P\sin q_1} [\sin\gamma_1 \cos\alpha_1 \Delta r_\ell + (\sin\gamma_1 \sin\alpha_1 - \frac{R}{P} \cos q_1 \sin\beta)\Delta r_m] \qquad \text{(C-7)}$$

Similarly

$$\Delta q_2 = \frac{1}{P\sin q_2} [\sin\gamma_2 \cos\alpha_2 \Delta r_\ell$$

$$+ (\sin\gamma_2 \sin\alpha_2 - \frac{R}{P} \cos q_2 \sin\beta)\Delta r_m] \qquad \text{(C-8)}$$

(C-7) and (C-8) can be expressed in matrix form

$$\begin{pmatrix} \Delta q_1 \\ \Delta q_2 \end{pmatrix} = \begin{bmatrix} \frac{\sin\gamma_1 \cos\alpha_1}{P \sin q_1} & \frac{1}{P\sin q_1} (\sin\gamma_1 \sin\alpha_1 - \frac{R}{P} \cos q_1 \sin\beta) \\ \frac{\sin\gamma_2 \cos\alpha_2}{P \sin q_2} & \frac{1}{P\sin q_2} (\sin\gamma_2 \sin\alpha_2 - \frac{R}{P} \cos q_2 \sin\beta) \end{bmatrix} \begin{pmatrix} \Delta r_\ell \\ \Delta r_m \end{pmatrix}$$

The inverse relation is

$$\begin{pmatrix} \Delta r_\ell \\ \Delta r_m \end{pmatrix} = \frac{1}{\sin\gamma_1 \sin\gamma_2 \sin(\alpha_2 - \alpha_1) + \frac{R}{P} \sin\beta \, (\cos q_1 \sin\gamma_2 \cos\alpha_2 - \cos q_2 \sin\gamma_1 \cos\alpha_1)}$$

$$\begin{bmatrix} P \sin q_1 (\sin\gamma_1 \sin\alpha_2 - \frac{R}{P} \cos q_2 \sin\beta) & -P \sin q_2 (\sin\gamma_1 \sin\alpha_1 - \frac{R}{P} \cos q_1 \sin\beta) \\ -P \sin q_1 \sin\gamma_2 \cos\alpha_2 & P \sin q_2 \sin\gamma_1 \cos\alpha_1 \end{bmatrix}$$

$$\begin{bmatrix} \Delta q_1 \\ \Delta q_2 \end{bmatrix}$$

C-2. Sensitivity Equations for Position Fix Using Two Stellar Directions and the Local Vertical

A $\hat{l}$, $\hat{m}$, $\hat{n}$ coordinate system is defined as shown in Fig. 6-6. $\hat{n}$ is the LRV's local vertical. $\hat{l}$ is in the $\hat{n}$ $\hat{s}_1$ plane and is perpendicular to $\hat{n}$. $\hat{m}$ completes the right-hand triplet.

q_1 is the angle between $\hat{s}_1$ and $\bar{r}$. Therefere,

$$r \cos q_1 = \bar{r} \cdot \hat{s}_1$$

Differentiating this equation gives

$$- r \sin q_1 \, \Delta q_1 = \Delta\bar{r} \cdot \hat{s}_1 \qquad \text{(C-9)}$$

For small changes of q_1

$$- \Delta q_1 = \frac{1}{r} \, \Delta\bar{r} \cdot \hat{m}$$

$\hat{s}_1$ can be resolved along $\hat{l}$ and $\hat{n}$ as follows.

$$\hat{s}_1 = \sin q_1 \, \hat{\ell} + \cos q_1 \, \hat{n} \qquad \text{(C-10)}$$

Substituting (C-9) into (C-10) produces

$$\Delta q_1 = - \frac{1}{r \sin q_1} (\sin q_1 \, \hat{\ell} + \cos q_1 \, \hat{n}) \cdot \Delta\bar{r}$$

But $\Delta\bar{r}$ is perpendicular to $\hat{n}$ so

$$\Delta q_1 = -\frac{1}{r}\Delta r_\ell \qquad \text{(C-11)}$$

Similarly

$$r\cos q_2 = \bar{r}\cdot\hat{s}_2$$

Differentiating both sides and resolving $\hat{s}_2$ gives

$$\Delta q_2 = -\frac{1}{r}(\cos\alpha\,\Delta r_\ell + \sin\alpha\,\Delta r_m) \qquad \text{(C-12)}$$

(C-11) and (C-12) can be written in matrix form.

$$\begin{pmatrix} \Delta q_1 \\ \Delta q_2 \end{pmatrix} = \begin{pmatrix} -\frac{1}{r} & 0 \\ -\frac{1}{r}\cos\alpha & -\frac{\sin\alpha}{r} \end{pmatrix} \begin{pmatrix} \Delta r_\ell \\ \Delta r_m \end{pmatrix}$$

Consequently

$$\begin{pmatrix} \Delta r_\ell \\ \Delta r_m \end{pmatrix} = \begin{pmatrix} -r & 0 \\ r\cot\alpha & -r\csc\alpha \end{pmatrix} \begin{pmatrix} \Delta q_1 \\ \Delta q_2 \end{pmatrix}$$

APPENDIX D

DERIVATION OF POSITION FIX EQUATIONS FOR CELESTIAL POSITION FIX SCHEMES

D-1. Position Fix Equations Using Earth Landmark and Two Stellar Directions

An x', y', z' coordinate system is defined in Fig. 6-3. The z'-axis points toward star number 1.

$$x' = x \sin\lambda_1 - y \cos\lambda_1$$

$$y' = x \cos\lambda_1 \sin L_1 + y \sin\lambda_1 \sin L_1 - z \cos L_1 \qquad \text{(D-1)}$$

$$z' = x \cos\lambda_1 \cos L_1 + y \sin\lambda_1 \cos L_1 + z \sin L_1$$

The equation of the cone with the center line directed along the z'-axis, the vertex at the center of the moon, and the cone angle q_1 is

$$x'^2 + y'^2 = z'^2 \tan^2 q_1 \qquad \text{(D-2)}$$

Substituting (D-1) into (D-2) gives the equation of the cone in xyz-coordinate system:

$$[x \sin\lambda_1 - y \cos\lambda_1]^2 + [x \cos\lambda_1 \sin L_1 + y \sin\lambda_1 \sin L_1 - z \cos L_1]^2$$

$$= [x \cos\lambda_1 \cos L_1 + y \sin\lambda_1 \cos L_1 + z \sin L_1]^2 \tan^2 q_1$$

Then the equation of the cone with its vertex at the landmark on earth is

$$[(x - x_E)\sin\lambda_1 - (y - y_E)\cos\lambda_1]^2 + [(x - x_E)\cos\lambda_1 \sin L_1 + (y - y_E)\sin\lambda_1 \sin L_1$$

$$-(z - z_E)\cos L_1]^2 = [(x - x_E)\cos\lambda_1 \cos L_1 + (y - y_E)\sin\lambda_1 \cos L_1 + z \sin L_1]^2 \tan^2 q_2$$

(D-3)

Similarly the equation of the cone with center line directed along the stellar direction #2, with cone angle q_2, and with vertex at the landmark on earth is

$$[(x - x_E)\sin\lambda_2 - (y - y_E)\cos\lambda_2]^2 + [(x - x_E)\cos\lambda_2 \sin L_2 + (y - y_E)\sin\lambda_2 \sin L_2$$

$$-(z - z_E)\cos L_2]^2 = [(x - x_E)\cos\lambda_1 \cos L_2 + (y - y_E)\sin\lambda_2 \cos L_2 + z \sin L_2]^2 \tan^2 q_2$$

(D-4)

After simple manipulation (D-3) and (D-4) become

$$(x - x_E)^2(1 - \cos^2 L_1 \cos^2\lambda_1 \sec^2 q_1) + (y - y_E)^2(1 - \cos^2 L_1 \sin^2\lambda_1 \sec^2 q_1)$$

$$+ (z - z_E)^2(1 - \sin^2 L_1 \sec^2 q_1) + (x - x_E)(y - y_E)\sin 2\lambda_1 (2 - \cos^2 L_1 \sec^2 q_1)$$

$$-(y - y_E)(z - z_E)\sin 2L_1 \sin\lambda_1 \sec^2 q_1 - (z - z_E)(x - x_E)\sin 2L_1 \cos\lambda_1 \sec^2 q_1 = 0$$

(D-5)

$$(x - x_E)^2(1 - \cos^2 L_2 \cos^2\lambda_2 \sec^2 q_2) + (y - y_E)^2(1 - \cos^2 L_2 \sin^2\lambda_2 \sec^2 q_2)$$

$$+ (z - z_E)^2(1 - \cos^2 L_2 \sec^2 q_2) + (x - x_E)(y - y_E)\sin 2\lambda_2 (2 - \cos^2\lambda_2 \sec^2 q_2)$$

$$-(y - y_E)(z - z_E)\sin 2L_2 \sin\lambda_2 \sec^2 q_2 - (z - z_E)(x - x_E)\sin 2L_2 \cos\lambda_2 \sec^2 q_2 = 0$$

(D-6)

The equation of the moon's surface is

$$x^2 + y^2 + z^2 = r^2 \qquad \text{(D-7)}$$

The LRV coordinates, x, y, and z can be determined by simultaneous solution of (D-5), (D-6), and (D-7). Note that the coordinates of the landmark on earth are

$$x_E = R \cos\lambda_E \cos L_E$$

$$y_E = R \cos L_E \sin\lambda_E$$

$$z_E = R \sin L_E$$

where R is the distance from moon center to the earth landmark.

The LRV lunar latitude, L, and its lunar longitude, λ, can be determined from the following equations.

$$L = \sin^{-1} \frac{R}{z}$$

$$\lambda = \sin^{-1} \left(\frac{y}{R \cos L} \right)$$

D-2. Position Fix Equations Using Two Stellar Directions and Local Vertical

With the geometry of Fig. 6-5 the spherical trigonometry law of cosines gives the following relations.

$$\cos q_1 = \cos(90° - L_1)\cos(90° - L) + \sin(90° - L_1)\sin(90° - L)\cos(\lambda - \lambda_1)$$

$$= \sin L_1 \sin L + \cos L_1 \cos L \cos(\lambda - \lambda_1)$$

$$\cos q_2 = \cos(90° - L_2)\cos(90° - L) + \sin(90° - L_2)\sin(90° - L)\cos(\lambda_2 - \lambda)$$

$$= \sin L_2 \sin L + \cos L_2 \cos L \cos(\lambda_2 - \lambda)$$

These equations can be solved to produce

$$\lambda - \lambda_1 = \cos^{-1} \left(\frac{\cos q_1 - \sin L_1 \sin L}{\cos L_1 \cos L} \right) \qquad \text{(D-8)}$$

$$\lambda_2 - \lambda = \cos^{-1} \left(\frac{\cos q_2 - \sin L_2 \sin L}{\cos L_2 \cos L} \right) \qquad \text{(D-9)}$$

Combining (D-8) and (D-9) gives

$$\lambda_2 - \lambda_1 = \cos^{-1} \left(\frac{\cos q_1 - \sin L_1 \sin L}{\cos L_1 \cos L} \right) + \cos^{-1} \left(\frac{\cos q_2 - \sin L_2 \sin L}{\cos L_2 \cos L} \right) \qquad \text{(D-10)}$$

or

$$\cos(\lambda_2 - \lambda_1) = \left(\frac{\cos q_1 - \sin L_1 \sin L}{\cos L_1 \cos L} \right) \left(\frac{\cos q_2 - \sin L_2 \sin L}{\cos L_2 \cos L} \right) - \frac{\sqrt{\cos^2 L_1 \cos^2 L - (\cos q_1 - \sin L_1 \sin L)^2}\sqrt{\cos^2 L_2 \cos^2 L - (\cos q_2 - \sin L_2 \sin L)^2}}{\cos L_1 \cos L_2 \cos^2 L} \qquad \text{(D-10)}$$

(D-10) and (D-11) are transcendental equations in L. Either of these two equations can be solved to determine L. Then either (D-8) or (D-9) can be used to determine λ and thus complete the determination of the LRV lunar coordinates.

APPENDIX E

DERIVATION OF SENSITIVITY EQUATIONS FOR SATELLITE POSITION FIX SCHEMES

E-1. Sensitivity Equations for Position Fix Using LRV to Satellite Range

A $\hat{l}$, $\hat{m}$, $\hat{n}$ coordinate system is shown in Fig. 6-7. $\hat{n}$ is the LRV's local vertical; $\hat{l}$ is in the $\bar{r}$ $\bar{R}$ plane and is perpendicular to $\hat{n}$; $\hat{m}$ completes the right-hand triplet.

Using the geometry of Fig. 6-7, the law of cosines gives

$$q_1^2 = R_1^2 + r^2 - 2rR_1 \cos\beta_1$$

Differentiating this gives

$$2q_1 \Delta q_1 = 2rR_1 \sin\beta_1 \Delta\beta_1$$

or

$$\Delta q_1 = \frac{rR_1 \sin\beta_1 \Delta\beta_1}{q_1} \qquad \text{(E-1)}$$

In Fig. 6-6

$$R_1 \sin\beta_1 = q_1 \cos E_1 \qquad \text{(E-2)}$$

Substituting (E-2) into (E-1) gives

$$\Delta q_1 = r \cos E_1 \Delta\beta_1 \qquad \text{(E-3)}$$

For small changes of β_1

$$\Delta\beta_1 = \frac{\Delta\bar{r} \cdot \hat{\ell}}{r} \qquad \text{(E-4)}$$

Substituting (E-4) into (E-3) produces

$$\Delta q_1 = \cos E_1 \, \hat{\ell} \cdot \Delta\bar{r}$$

$$= \cos E_1 \, \Delta r_\ell \qquad \text{(E-5)}$$

Similarly

$$q_2^2 = R_2^2 + r^2 - 2rR_2 \cos\beta_2$$

Differentiating this equation

$$2q_2 \, \Delta q_2 = 2rR_2 \sin\beta_2 \, \Delta\beta_2$$

or

$$\Delta q_2 = \frac{rR_2 \sin\beta_2}{q_2} \, \Delta\beta_2 \qquad \text{(E-6)}$$

From Fig. 6-6

$$R_2 \sin\beta_2 = q_2 \cos E_2 \qquad \text{(E-7)}$$

Putting (E-7) into (E-6) gives

$$\Delta q_2 = r \cos E_2 \, \Delta\beta_2 \qquad \text{(E-8)}$$

But

$$\hat{\ell}_2 = \hat{\ell} \cos\alpha + \hat{m} \sin\alpha$$

Now

$$\Delta\beta_2 = \frac{\Delta\bar{r} \cdot \ell_2}{r} = \frac{1}{r} [\cos\alpha \, \hat{\ell} + \sin\alpha \, \hat{m}] \cdot \Delta\bar{r} \qquad \text{(E-9)}$$

Combining (E-9) and (E-8) gives

$$\Delta q_2 = \cos E_2 \, [\cos\alpha \, \hat{\ell} + \sin\alpha \, \hat{m}] \cdot \Delta\bar{r}$$

$$\doteq \cos E_2 \cos\alpha \, \Delta r_\ell + \cos E_2 \sin\alpha \, \Delta r_m \qquad \text{(E-10)}$$

(E-5) and (E-10) can be written in matrix form

$$\begin{bmatrix} \Delta q_1 \\ \Delta q_2 \end{bmatrix} = \begin{bmatrix} \cos E_1 & 0 \\ \cos E_2 \cos\alpha & \cos E_2 \sin\alpha \end{bmatrix} \begin{bmatrix} \Delta r_\ell \\ \Delta r_m \end{bmatrix}$$

Conversely

$$\begin{bmatrix} \Delta r_\ell \\ \Delta r_m \end{bmatrix} = \begin{bmatrix} \sec E_1 & 0 \\ -\cot\alpha \sec E_1 & \sec E_2 \csc\alpha \end{bmatrix} \begin{bmatrix} \Delta q_1 \\ \Delta q_2 \end{bmatrix}$$

As the sighting azimuthal separation approaches 90° and the sighting elevations approach zero; then the above equation goes to simply

$$\begin{pmatrix} \Delta r_{\ell} \\ \Delta r_{m} \end{pmatrix} = \begin{pmatrix} 1 & o \\ o & 1 \end{pmatrix} \begin{pmatrix} \Delta q_1 \\ \Delta q_2 \end{pmatrix}$$

E-2. Sensitivity Equations for Position Fix Using LRV to Satellite Range Rate

This scheme uses a doppler radar to measure the range rate between the LRV and an overhead satellite. It is assumed that the satellite trajectory is known as a function of time. The instant of closest approach of the satellite to the LRV is indicated when the doppler beat goes to zero. This fixes the LRV position in a plane that is normal to the satellite trajectory and contains the position of the satellite at the instant of closest approach.

An imperfection, a bias, in the doppler radar will cause the wrong instant of time to be identified as the instant of closest approach. Consequently, the planar locus of the LRV position will be erroneously shifted along the satellite trajectory.

The following equations will give the size of the error as a function of the size of the radar bias. From Fig. 6-10 it can be seen that

$$\dot{R} = \frac{vx}{R} = \frac{vx}{\sqrt{R_o^2 + x^2}}$$

If the doppler bias is $\Delta\dot{R}$, then the measured range rate, $\dot{R}'$, will be

$$\dot{R}' = \dot{R} + \Delta\dot{R} = \frac{vx}{\sqrt{R_o^2 + x^2}} + \Delta\dot{R}$$

The instant of closest approach is indicated when $\dot{R}'$ is zero. The actual value of x at the indicated instant of closest approach is the size of the erroneous shift of the planar locus of position. Thus the size of this error can be determined by setting the previous equation to zero. Then

$$x\Big|_{\dot{R}' = o} = + R_o \sqrt{\frac{\Delta\dot{R}^2}{v^2 - \Delta\dot{R}^2}} \qquad \text{(E-11)}$$

If $v >> \Delta\dot{R}$ then

$$x\Big|_{\dot{R}' = o} = + R_o \frac{\Delta\dot{R}}{v}$$

x is negative before the instant of closest approach and positive after the instant of closest approach.

In addition to establishing a planar locus of position by measuring the instant when the doppler beat goes to zero, this scheme also establishes a circular locus in this plane. The circle is centered about the satellite position at the indicated instant of closest approach. The radius of the circle, R'_o, is computed as a function of the second derivative of range measured at the indicated instant of closest approach.

$$R'_o = \frac{v^2}{\ddot{R}'\Big|_{\dot{R}' = o}} \qquad \text{(E-12)}$$

However, the bias in the range rate measurement will not change the measured second derivative of range. So

$$\ddot{R}'\Big|_{\dot{R}' = o} = \ddot{R}\Big|_{\dot{R}' = o}$$

The second derivative of the range can be computed for this constant velocity satellite from Fig. 6-10.

$$R^2 = R_o^2 + x^2$$

$$2R\dot{R} = 2xv$$

$$R\ddot{R} + \dot{R}^2 = v^2$$

$$\ddot{R} = \frac{v^2 - \dot{R}^2}{R}$$

Now (E-12) becomes

$$R'_o = \frac{v^2 \, R|_{\dot{R}' = o}}{v^2 - \dot{R}^2|_{\dot{R}' = o}} = \frac{v^2 \left(R_o^2 + \dfrac{R_o^2 \, \Delta\dot{R}^2}{v^2 - \Delta\dot{R}^2} \right)^{1/2}}{v^2 - \Delta\dot{R}^2}$$

$$= \frac{v^2 \, [R_o v]}{(v^2 - \Delta\dot{R}^2)^{3/2}}$$

Finally, the error in the computed radius of the circle is e_R.

$$e_R = R_o - R_o'$$

$$= R_o \left[1 - \frac{v^3}{(v^2 - \Delta\dot{R}^2)^{3/2}} \right]$$

E-3. Sensitivity Equations for Position Fix Using the Angle Between the Direction to the Satellite and the Local Vertical

Fig. 6-13 shows an $\hat{l}$, $\hat{m}$, $\hat{n}$ coordinate system. $\hat{n}$ is the LRV's local vertical. $\hat{l}$ is in the $\hat{n}$ $\overline{R}_1$ plane and is perpendicular to $\hat{n}$. $\hat{m}$ completes the right-handed triplet.

In Fig. 6-13

$$P_1 \, r \cos q_1 = \overline{P}_1 \cdot \overline{r}$$

Differentiating gives

$$r \cos q_1 \, \Delta P_1 - r P_1 \sin q_1 \, \Delta q_1 = \overline{P}_1 \cdot \Delta\overline{r} + \overline{r} \cdot \Delta\overline{P}_1 \quad \text{(E-13)}$$

Also

$$\overline{R}_1 = \overline{r} + \overline{P}_1$$

Since $\overline{R}_1$ will not be changed when the LRV moves,

$$0 = \Delta\overline{r} + \Delta\overline{P}_1$$

or

$$\Delta\overline{P}_1 = - \Delta\overline{r}$$

For small changes in $\bar{r}$, $\Delta\bar{r}$ is normal to $\bar{r}$ so that

$$\bar{r} \cdot \Delta\bar{P}_1 = - \bar{r} \cdot \Delta\bar{r} = o \qquad \text{(E-14)}$$

Substituting (E-14) into (E-13) gives

$$r \cos q_1 \, \Delta P_1 - rP_1 \sin q_1 \, \Delta q_1 = \bar{P}_1 \cdot \Delta\bar{r}$$

or

$$\Delta q_1 = \frac{r \cos q_1 \, \Delta P_1 - \bar{P}_1 \cdot \Delta\bar{r}}{rP_1 \sin q_1} \qquad \text{(E-15)}$$

From law of cosine of plane trigonometry,

$$P_1^2 = R_1^2 + r^2 - 2R_1 \, r \cos\beta_1$$

Differentiating gives

$$2P_1 \, \Delta P_1 = 2R_1 \, r \sin \beta_1 \, \Delta\beta_1 \qquad \text{(E-16)}$$

or

$$\Delta P_1 = \frac{R_1 \, r \sin\beta_1 \, \Delta\beta_1}{P_1}$$

For small changes in $\bar{r}$

$$\Delta\beta_1 = \frac{\Delta\bar{r} \cdot \hat{\ell}}{r} \qquad \text{(E-17)}$$

$\bar{P}_1$ can be resolved along $\hat{\ell}$ and $\hat{n}$.

$$\bar{P}_1 = P_1 \, (\sin q_1 \, \hat{\ell} + \cos q_1 \, \hat{n}) \qquad \text{(E-18)}$$

Substituting (E-17) into (E-16) gives

$$\Delta P_1 = \frac{R_1 \sin\beta_1 \, \Delta\bar{r} \cdot \hat{\ell}}{P_1} \qquad \text{(E-19)}$$

Substituting (E-18) and (E-19) into (E-15) gives

$$\Delta q_1 = \frac{\dfrac{r \cos q_1 \, R_1 \sin \beta_1 \, \Delta\bar{r} \cdot \hat{\ell}}{P_1} - P_1 \, (\sin q_1 \, \hat{\ell} + \cos q_1 \, \hat{n}) \cdot \Delta\bar{r}}{rP_1 \sin q_1}$$

$$= \left(\frac{R_1}{P_1^2} \cot q_1 \sin \beta_1 - \frac{1}{r}\right) \Delta\bar{r} \cdot \hat{\ell} - \frac{1}{r} \cot q_1 \, \Delta\bar{r} \cdot \hat{n}$$

$$= \left(\frac{R_1}{P_1^2} \cot q_1 \sin \beta_1 - \frac{1}{r}\right) \Delta\bar{r} \cdot \hat{\ell}$$

$$= \left(\frac{R_1}{P_1^2} \cot q_1 \sin \beta_1 - \frac{1}{r}\right) \Delta r_\ell \qquad \text{(E-20)}$$

where

$$\Delta\bar{r} \cdot \hat{n} = o$$

$$\Delta\bar{r} \cdot \hat{\ell} = \Delta r_\ell$$

Similarly

$$\Delta q_2 = \left(\frac{R_2}{P_2^2} \cot q_2 \sin\beta_2 - \frac{1}{r}\right) \Delta\bar{r} \cdot \hat{\ell}_2$$

but

$$\hat{\ell}_2 = \hat{\ell} \cos \alpha + \hat{m} \sin \alpha$$

so that

$$\Delta q_2 = \left(\frac{R_2}{P_2^2} \cot q_2 \sin \beta_2 - \frac{1}{r}\right) (\cos\alpha \, \Delta r_\ell + \sin\alpha \, \Delta r_m) \qquad \text{(E-21)}$$

(E-20) and (E-21) can be written in matrix form.

$$\begin{pmatrix} \Delta q_1 \\ \Delta q_2 \end{pmatrix} = \begin{pmatrix} \frac{R_1}{P_1^2} \cot q_1 \sin \beta_1 - \frac{1}{r} & o \\ \cos\alpha\left(\frac{R_2}{P_2^2} \cot q_2 \sin \beta_2 - \frac{1}{r}\right) & \sin\alpha\left(\frac{R_2}{P_2^2} \cot q_2 \sin \beta_2 - \frac{1}{r}\right) \end{pmatrix} \begin{pmatrix} \Delta r_\ell \\ \Delta r_m \end{pmatrix}$$

The inverse relation is

$$\begin{pmatrix} \Delta r_\ell \\ \Delta r_m \end{pmatrix} \begin{pmatrix} \frac{P_1^2}{R_1 \cot q_1 \sin \beta_1 - \frac{P_1^2}{r}} & o \\ \frac{-P_1^2 \cot \alpha}{R_1 \cos q_1 \sin \beta_1 - \frac{P_1^2}{r}} & \frac{P_2^2}{\sin\alpha(R_2 \cot q_2 \sin\beta_2 - \frac{P_2^2}{r})} \end{pmatrix} \begin{pmatrix} \Delta q_1 \\ \Delta q_2 \end{pmatrix}$$

E-4. Sensitivity Equations for Position Fix Using Angles Between Directions to a Satellite and a Stellar Direction

First it is necessary to name some of the angles in Fig. 6-15.

q_1 is the angle between $\hat{s}$ and $\overline{P}_1$.

q_2 is the angle between $\hat{s}$ and $\overline{P}_2$.

γ is the angle between $\hat{s}$ and $\hat{\ell}$.

In Fig. 6-15

$$P_1 \cos q_1 = \overline{P}_1 \cdot \hat{s} \tag{E-22}$$

But

$$\overline{P}_1 = \overline{R}_1 - \overline{r}$$

Combing (E-22) and (E-23) gives

$$P_1 \cos q_1 = (\overline{R}_1 - \overline{r}) \cdot \hat{s}$$

$$= \overline{R}_1 \cdot \hat{s} - \overline{r} \cdot \hat{s}$$

Differentiating gives

$$\cos q_1 \, \Delta P_1 - P_1 \sin q_1 \, \Delta q_1 = - \hat{s} \cdot \Delta\overline{r}$$

or

$$\Delta q_1 = \frac{\cos q_1 \, \Delta P_1 + \hat{s} \cdot \Delta\overline{r}}{P_1 \sin q_1} \tag{E-24}$$

because $\Delta\overline{R}_1 = o$ for any displacement of LRV.

In Fig. 6-15

$$P_1^2 = r^2 + R_1^2 - 2rR_1 \cos \beta_1$$

Differentiating produces

$$2P_1 - \Delta P_1 = 2rR_1 \sin \beta_1 \, \Delta\beta_1$$

or

$$\Delta P_1 = \frac{rR_1 \sin \beta_1}{P_1} \Delta\beta_1 \tag{E-25}$$

From Fig. 6-15(b) we see

$$R_1 \sin \beta_1 = a_1 = P_1 \cos E_1$$

Substituting (E-26) into (E-25) gives

$$\Delta P_1 = r \cos E_1 \, \Delta\beta_1$$

For small changes in β_1

$$\Delta\beta_1 = \frac{\Delta\bar{r} \cdot \hat{k}_1}{r}$$

But

$$\hat{k}_1 = \cos \alpha_1 \, \hat{\ell} + \sin \alpha_1 \, \hat{m}$$

So

$$\Delta\beta_1 = \frac{1}{r} \Delta\bar{r} \cdot (\cos \alpha_1 \, \hat{\ell} + \sin \alpha_1 \, \hat{m})$$

and

$$\Delta P_1 = r \cos E_1 \, \Delta\beta_1$$

$$= \cos E_1 \, (\cos \alpha_1 \, \hat{\ell} + \sin \alpha_1 \, \hat{m}) \cdot \Delta\bar{r}$$

$$= \cos E_1 \cos \alpha_1 \, \Delta r_\ell + \cos E_1 \sin \alpha_1 \, \Delta r_m \qquad \text{(E-27)}$$

Also,

$$\hat{s} = \sin \gamma \, \hat{\ell} + \cos \gamma \, \hat{n}$$

$$\hat{s} \cdot \Delta\bar{r} = (\sin \gamma \, \hat{\ell} + \cos \gamma \, \hat{n}) \cdot \Delta\bar{r}$$

$$= \sin \gamma \, \Delta r_\ell \qquad \text{(E-28)}$$

Substituting (E-27) and (E-28) into (E-24) gives

$$\Delta q_1 = \frac{\cos q_1 \cos E_1 \, (\cos \alpha_1 \, \Delta r_\ell + \sin \alpha_1 \, \Delta r_m) + \sin \gamma \, \Delta r_\ell}{P_1 \sin q_1}$$

$$= \frac{1}{P_1 \sin q_1} [(\cos q_1 \cos E_1 \cos \alpha_1 + \sin \gamma) \, \Delta r_\ell + \cos q_1 \cos E_1 \sin \alpha_1 \, \Delta r_m] \qquad \text{(E-29)}$$

Similarly

$$\Delta q_2 = \frac{1}{P_2 \sin q_2} [(\cos q_2 \cos E_2 \cos \alpha_2 + \sin \gamma) \Delta r_\ell + \cos q_2 \cos E_2 \sin \alpha_2 \, \Delta r_m] \qquad \text{(E-30)}$$

(E-29) and (E-30) can be written in matrix form.

$$\begin{pmatrix} \Delta q_1 \\ \Delta q_2 \end{pmatrix} = \begin{pmatrix} \frac{1}{P_1 \sin q_1}(\sin\gamma + \cos E_1 \cos q_1 \cos\alpha_1) & \frac{\cos E_1 \cos q_1 \sin\alpha_1}{P_1 \sin q_1} \\ \frac{1}{P_2 \sin q_2}(\sin\gamma + \cos E_2 \cos q_2 \cos\alpha_2) & \frac{\cos E_2 \cos q_2 \sin\alpha_2}{P_2 \sin q_2} \end{pmatrix} \begin{pmatrix} \Delta r_\ell \\ \Delta r_m \end{pmatrix}$$

The inverse relation is

$$\begin{pmatrix} \Delta r_\ell \\ \Delta r_m \end{pmatrix} = \frac{\begin{pmatrix} P_1 \sin q_1 \cos E_2 \cos q_2 \sin\alpha_2 & -P_2 \sin q_2 \cos E_1 \cos q_1 \sin\alpha_1 \\ -P_1 \sin q_1 (\sin\gamma + \cos E_2 \cos q_2 \cos\alpha_2 & P_2 \sin q_2 (\sin\gamma + \cos E_1 \cos q_1 \cos\alpha_1 \end{pmatrix} \begin{pmatrix} \Delta q_1 \\ \Delta q_2 \end{pmatrix}}{\sin\gamma(\cos E_2 \cos q_2 \sin\alpha_2 - \cos E_1 \cos q_1 \sin\alpha_1)}$$

APPENDIX F

DERIVATION OF EQUATIONS FOR POSITION FIX USING SATELLITE POSITION FIX SCHEMES

F-1. Position Fix Equations Using Satellite Range

The geometry for this position fix scheme is shown in Fig. 6-8. The law of cosines provides the following two expressions for cos β_1 and cos β_2.

$$\cos \beta_1 = \frac{r^2 + (r + R_1)^2 - q_1^2}{2r\,(r + R_1)}$$

$$\cos \beta_2 = \frac{r^2 + (r + R_2)^2 - q_2^2}{2r\,(r + R_2)}$$

The next equations come from the law of cosines of spherical trigonometry

$$\cos \beta_1 = \cos (90 - L) \cos (90 - L_1) + \sin (90 - L) \sin (90 - L_1) \cos (\lambda - \lambda_1)$$

$$= \sin L \sin L_1 + \cos L \cos L_1 \cos (\lambda - \lambda_1)$$

$$\cos \beta_2 = \cos (90 - L) \cos (90 - L_2) + \sin (90 - L) \sin (90 - L_2) \cos (\lambda_2 - \lambda)$$

$$= \sin L \sin L_2 + \cos L \cos L_2 \cos (\lambda_2 - \lambda)$$

This pair of equations can be manipulated to produce (F-1) and (F-2)

$$\lambda - \lambda_1 = \cos^{-1} \left(\frac{\cos \beta_1 - \sin L_1 \sin L}{\cos L_1 \cos L} \right) \qquad \text{(F-1)}$$

$$\lambda - \lambda_2 = \cos^{-1} \left(\frac{\cos \beta_2 - \sin L_2 \sin L}{\cos L_2 \cos L} \right) \qquad \text{(F-2)}$$

Adding (F-1) and (F-2) gives

$$\lambda_2 - \lambda_1 = \cos^{-1} \frac{\cos \beta_1 - \sin L \sin L_1}{\cos L \cos L_1} + \cos^{-1} \frac{\cos \beta_2 - \sin L \sin L_2}{\cos L \cos L_2}$$

or

$$\cos(\lambda_2 - \lambda_1) = \frac{\cos\beta_1 - \sin L \sin L_1}{\cos L \cos L_1} \quad \frac{\cos\beta_2 - \sin L \sin L_2}{\cos L \cos L_2} -$$

$$\frac{[\cos^2 L \cos^2 L_1 - (\cos\beta_1 - \sin L \sin L_2)^2][\cos^2 L \cos^2 L - (\cos\beta_2 - \sin L \sin L_2)^2]}{\cos^2 L \cos L \cos L}$$

Equation (F-3) or (F-4) can be solved for L. Then this value of L can be used in (F-1) or (F-2) to determine λ.

F-2. Position Fix Equations Using Satellite Range Rate

Let the satellite velocity vector at the indicated instant of closest approach have an angle a with respect to the x axis and have an angle b with respect to the xy plane. Define a new x'y'z' coordinate system as shown in Fig. 6-11. The y' axis is parallel to the satellite velocity at the indicated instant of closest approach.

$$\begin{aligned} x' &= x \sin a - y \cos a \\ y' &= x \cos a \cos b + y \sin a \cos b - z \sin b \\ z' &= x \cos a \sin b + y \sin a \sin b + z \cos b \end{aligned} \qquad \text{(F-5)}$$

$$\begin{aligned} x &= x' \sin a + y' \cos a \cos b + z' \sin a \cos b \\ y &= -x' \cos a + y' \sin a \cos b + z' \sin a \sin b \\ z &= -y' \sin b + z' \cos b \end{aligned} \qquad \text{(F-6)}$$

where xyz are lunar coordinates. The coordinates of the satellite in xyz-coordinate system:

$$x_s = R \cos L_s \cos \lambda_s, \quad y_s = R \cos L_s \sin \lambda_s, \quad z_s = R \sin L_s \qquad \text{(F-7)}$$

Here R is the distance from the center of the moon to the satellite.

Combining (F-7) and (F-5) gives the coordinates of the satellite in the x'y'z' system.

$$x'_s = - R \cos L_s \cos (\lambda_s + a)$$

$$y'_s = R [\cos L_s \cos b \sin (\lambda_s + a) - \sin L_s \sin b]$$

$$z'_s = R [\cos L_s \sin b \sin (\lambda_s + a) + \sin L_s \cos b]$$

The LRV is located somewhere on a circle in a plane parallel to the x'z' plane. This circle is centered about the position of the satellite at the indicated instant of closest approach. The circle's radius, R_o, is computed from the measured derivative of range rate. The equations for this circle are

$$(x' - x'_s)^2 + (z' - z'_s)^2 = R_o^2$$

$$y' = y'_s$$

or

$$\{x' + R\cos L_s \cos(\lambda_s + a)\}^2 + \{z' - R[\cos L_s \sin b \sin(\lambda_s + a) + \sin L_s \cos b]\}^2 = R_o^2 \quad \text{(F-8)}$$

$$y' = R [\cos L_s \cos b \sin (\lambda_s + a) - \sin L_s \sin b]$$

The equation for the lunar surface is

$$x'^2 + y'^2 + z'^2 = r^2$$

The moon's radius is r.

Simultaneous solution of (F-8), (F-9), and (F-10) gives the LRV coordinates in the x'y'z' system. Then (F-6) can be used to determine the coordinates in the xyz system. Finally the next equations can be used to compute the LRV's lunar latitude and longitude.

$$x = r \cos L \cos \lambda$$

$$y = r \cos L \sin \lambda$$

$$z = r \sin L$$

F-3. Position Fix Equations Using the Angles Between the LRV to Satellite Line of Sight and the Local Vertical

The geometry for this scheme is shown in Fig. 6-12. The angles q_1 and q_2 will be assumed to be less than 90° since the satellite can be observed only when it is above the horizon.

$$\frac{r}{\sin (q_1 - \phi_1)} = \frac{r + R_1}{\sin (180^\circ - q_1)} = \frac{r + R_1}{\sin q_1}$$

$$\frac{r}{\sin (q_2 - \phi_2)} = \frac{r + R_2}{\sin (180^\circ - q_2)} \quad \frac{r + R_2}{\sin q_2}$$

$$\phi_1 = q_1 - \sin^{-1}(\frac{r}{r + R_1} \sin q_1)$$

$$\phi_2 = q_2 - \sin^{-1}(\frac{r}{r + R_2} \sin q_2)$$

From the law of cosine of the Spherical Trigonometry:

$$\cos \phi_1 = \cos (90^\circ - L_1) \cos (90^\circ - L) + \sin (90^\circ - L_1) \sin (90^\circ - L) \cos (\lambda - \lambda_1)$$

$$= \sin L_1 \sin L + \cos L_1 \cos L \cos (\lambda - \lambda_1)$$

$$\cos \phi_2 = \cos (90^\circ - L_2 \cos (90^\circ - L) + \sin (90^\circ - L_2) \sin (90^\circ - L) \cos (\lambda_2 - \lambda)$$

$$= \sin L_2 \sin L + \cos L_2 \cos L \cos (\lambda_2 - \lambda)$$

or

$$\lambda - \lambda_1 = \cos^{-1} (\frac{\cos \phi_1 - \sin L_1 \sin L}{\cos L_1 \cos L}) \qquad \text{(F-11)}$$

$$\lambda_2 - \lambda = \cos^{-1} (\frac{\cos \phi_2 - \sin L_2 \sin L}{\cos L_2 \cos L}) \qquad \text{(F-12)}$$

Combining (F-11) and (F-12) gives

$$\lambda_2 - \lambda_1 = \cos^{-1} (\frac{\cos \phi_1 - \sin L_1 \sin L}{\cos L_1 \cos L}) + \cos^{-1} (\frac{\cos \phi_2 - \sin L_2 \sin L}{\cos L_2 \cos L}) \qquad \text{(F-13)}$$

or

$$\cos (\lambda_2 - \lambda_1) = (\frac{\cos \phi_1 - \sin L_1 \sin L}{\cos L_1 \cos L})(\frac{\cos \phi_2 - \sin L_2 \sin L}{\cos L_2 \cos L}) -$$

$$\frac{\sqrt{\cos^2 L_1 \cos^2 L - (\cos \phi_1 - \sin L_1 \sin L)^2}\ \sqrt{\cos^2 L_2 \cos^2 L - (\cos \phi_2 - \sin L_2 \sin L)^2}}{\cos L_1 \cos L_2 \cos^2 L} \qquad \text{(F-14)}$$

(F-13) or (F-14) can be solved for L. Then (F-11) or (F-12) can be used to determine λ.

F-4. Position Fix Equations Using the Angles Between the LPV to Satellite Line of Sight and/or a Stellar Direction

The geometry for this scheme is shown in Fig. 6-16. The coordinates of S_1 and S_2, the positions of the satellite at two different times, can be written from Fig. 6-16.

$$\text{Coordinates of } S_1: \quad x_1 = (r + P_1) \cos L_1 \cos \lambda_1$$

$$y_1 = (r + R_1) \cos L_1 \sin \lambda_1$$

$$z_1 = (r + R_1) \sin L_1$$

$$\text{Coordinates of } S_2: \quad x_2 = (r + R_2) \cos L_2 \cos \lambda_2$$

$$y_2 = (r + R_2) \cos L_2 \sin \lambda_2$$

$$z_2 = (r + R_2) \sin L_2$$

Fig. 6-16 also shows an x'y'z' coordinate system. The z' axis is along the stellar direction.

$$x' = x \sin \lambda_s - y \cos \lambda_s$$

$$y' = x \cos \lambda_s \sin L_s + y \sin \lambda_s \sin L_s - z \cos L_s \qquad \text{(F-15)}$$

$$z' = x \cos \lambda_s \cos L_s + y \sin \lambda_s \cos L_s + z \sin L_s$$

$$x = x' \sin \lambda_s + y' \sin L_s \cos \lambda_s + z' \cos L_s \cos \lambda_s$$

$$y = -x' \cos \lambda_s + y' \sin L_s \sin \lambda_s + z' \cos L_s \sin \lambda_s \qquad \text{(F-16)}$$

$$z = -y' \cos L_s + z' \sin L_s$$

The coordinates of S_1 and S_2 in the x'y'z' system are as follows. Coordinates of S_1:

$$x_1' = (r + P_1) \cos L_1 \sin (\lambda_s - \lambda_1)$$

$$y_1' = (r + R_1)[\cos L_1 \sin L_s \cos (\lambda_s - \lambda_1) + \sin L_1 \cos L_s]$$

$$z_1' = (r + R_1)[\cos L_1 \cos L_s \cos (\lambda_s - \lambda_1) + \sin L_1 \sin L_s]$$

Coordinates of S_2:

$$x_2' = (r + R_2) \cos L_2 \sin (\lambda_s - \lambda_2)$$

$$y_2' = (r + R_2)[\cos L_2 \sin L_s \cos (\lambda_s - \lambda_2) - \sin L_2 \cos L_s]$$

$$z_2' = (r + R_2)[\cos L_2 \cos L_s \cos (\lambda_s - \lambda_2) + \sin L_2 \sin L_s]$$

The following equations describe two cones with vertices at S_1 and S_2 and axes along the stellar directions. The LRV is at the mutual intersection of these cones and the lunar surface.

$$(x' - x_1')^2 + (y' - y_1')^2 = (z' - z_1')^2 \tan^2 q_1$$

$$(x' - x_2')^2 + (y' - y_2')^2 = (z' - z_2')^2 \tan^2 q_2$$

or

$$\{x' - (r+R_1)\cos L_1 \sin(\lambda_s-\lambda_1)\}^2 + \{y'-(r+R_1)[\cos L_1 \sin L_s \cos(\lambda_s-\lambda_1)-\sin L_1 \cos L_s]\}^2$$

$$-\{z' [(r+R_1)\cos L_1 \cos L_s \cos(\lambda_s-\lambda_1) + \sin L_1 \sin L_s]\}^2 \tan^2 q_1 \qquad \text{(F-17)}$$

$$\{x' - (r+R_2)\cos L_2 \sin(\lambda_s-\lambda_2)\}^2 + \{y'-(r+R_2)[\cos L_2 \sin L_s \cos(\lambda_s-\lambda_1)-\sin L_2 \cos L_s]\}^2$$

$$=\{z'-[(r+R_2)\cos L_2 \cos L_s \cos(\lambda_s-\lambda_2) + \sin L_2 \sin L_s]\}^2 \tan^2 q_2 \qquad \text{(F-18)}$$

The next equation describes the lunar surface.

$$x'^2 + y'^2 + z'^2 = r^2 \qquad \text{(F-19)}$$

Simultaneous solution of (F-17), (F-18), and (F-19) gives the LRV coordinates in the x'y'z' system. Then (F-15) will give the coordinates in the xyz system. Finally the following equations can be used to compute the LRV's lunar latitude and longitude.

$$x = r \cos L \cos \lambda$$

$$y = r \cos L \sin \lambda$$

$$z = r \sin L$$

APPENDIX G

DERIVATION OF EQUATIONS FOR NAVIGATION USING UNKNOWN LANDMARKS

G-1. Navigation Using Two Unknown Landmarks

Referring to Fig. 7-8 and applying the law of sines to triangles $\Delta Q_o Q_1 L_1$ and $\Delta Q_o Q_1 L_2$ gives

$$\frac{x}{\sin(\alpha_1 - \alpha_o)} = \frac{r_1}{\sin(\alpha_o + \sigma)}$$

$$\frac{x}{\sin(\beta_1 - \beta_o)} = \frac{r_2}{\sin(\beta_o - \sigma)} .$$

Taking the ratio of these two equations gives

$$\frac{\sin(\beta_1 - \beta_o)}{\sin(\alpha_1 - \alpha_o)} = \frac{r_1}{r_2} \frac{\sin(\beta_o - \sigma)}{\sin(\alpha_o + \sigma)} .$$

Substituting $\sigma = 180 - \gamma_1$ into this equation,

$$\frac{\sin(\beta_1 - \beta_o)}{\sin(\alpha_1 - \alpha_o)} \frac{r_1}{r_2} \frac{\sin(\beta_o + \gamma_1)}{\sin(\alpha_o - \gamma_1)} . \qquad \text{(G-1)}$$

Eq. (G-1) can be solved for γ_1 which is the direction of the shortest return path.

$$1 = \tan^{-1} \frac{K \sin \alpha_o - \sin \beta_o}{K \cos \alpha_o + \cos \beta_o} \qquad \text{(G-2)}$$

where

$$K = \frac{r_2 \sin(\beta_1 - \beta_o)}{r_1 \sin(\alpha_1 - \alpha_o)} . \qquad \text{(G-3)}$$

The navigator must move the LRV a short distance in any direction away from the present position as shown in Fig. 7-7. Using the law of sines in triangles $\Delta Q_1 Q' L_1$ and $\Delta Q_1 Q_1' L_2$ of Fig. 7-7 gives

$$\frac{\sin(\theta' - \theta)}{D} = \frac{\sin(180 - \theta')}{r_1}$$

$$= \frac{-\sin\theta'}{r_1}$$

$$\frac{\sin(\phi' - \phi)}{D} = \frac{\sin(180 - \phi')}{r_2}$$

$$= \frac{-\sin\phi'}{r_2} \quad .$$

Dividing the first equation by the second,

$$\frac{\sin(\theta' - \theta)}{\sin(\phi' - \phi)} = \frac{r_2}{r_1} \frac{\sin\theta'}{\sin\phi'} \quad .$$

Therefore,

$$\frac{r_2}{r_1} = \frac{\sin\phi' \sin(\theta' - \theta)}{\sin\theta' \sin(\phi' - \phi)} \quad . \qquad \text{(G-4)}$$

Similarly

$$\frac{r_2'}{r_1'} = \frac{\sin\phi \sin(\theta' - \theta)}{\sin\theta \sin(\phi' - \phi)} \qquad \text{(G-5)}$$

Combining (G-3) and (G-4) gives

$$K = \frac{\sin\phi' \sin(\theta' - \theta) \sin(\beta_1 - \beta_o)}{\sin\theta' \sin(\phi' - \phi) \sin(\alpha_1 - \alpha_o)} \quad . \qquad \text{(G-6)}$$

Eq. (G-6) was

$$\gamma_1 = \tan^{-1} \frac{K\sin\alpha_o - \sin\beta_o}{K\cos\alpha_o + \cos\beta_o}$$

These are the two equations needed for navigation using two unknown landmarks.

G-2. Navigation Using Three Unknown Landmarks

Referring to Fig. 7-9 and applying the law of sine to triangles $\Delta Q_o Q_1 L_1$,

$\Delta Q_o Q_1, L_2$, and $\Delta Q_o Q_1 L_3$ gives

$$\frac{x}{\sin \rho_1} = \frac{-R_1}{\sin \gamma_1} \qquad \text{(G-7)}$$

$$\frac{x}{\sin \rho_2} = \frac{K_2 R_1}{\sin (\gamma_1 - \alpha_1)} \qquad \text{(G-8)}$$

$$\frac{x}{\sin \rho_3} = \frac{K_1 R_1}{\sin (\gamma_1 - \alpha_1 - \beta_1)} \quad . \qquad \text{(G-9)}$$

But,

$$\rho_1 = \gamma_1 - \gamma_o - 180°$$

$$\rho_2 = 180 - \alpha_o + \gamma_o - \gamma_1 + \alpha_1$$

$$\rho_3 = 180 - \alpha_o - \beta_o + \gamma_o - \gamma_1 + \alpha_1 + \beta_1$$

so (G-7), (G-8), and (G-9) become

$$\frac{x}{\sin (\gamma_1 - \gamma_o)} = \frac{R_1}{\sin \gamma_1} \qquad \text{(G-10)}$$

$$\frac{x}{\sin (\overline{\gamma_1 - \gamma_o} - \overline{\alpha_1 - \alpha_o})} = \frac{K_2 R_1}{\sin (\gamma_1 - \alpha_1)} \qquad \text{(G-11)}$$

$$\frac{x}{\sin (\overline{\gamma_1 - \gamma_o} - \overline{\beta_1 - \beta_o} - \overline{\alpha_1 - \alpha_o})} = \frac{K_3 R_1}{\sin (\gamma_1 - \alpha_1 - \beta_1)}. \qquad \text{(G-12)}$$

Dividing (G-10) first by (G-11) and then by (G-12), and rearranging terms, yields

$$\cos (\alpha_1 - \alpha_o) - \frac{1}{K_2} (\cos\alpha_1 - \cot\gamma_1 \cos\alpha_1) = \cot (\gamma_1 - \gamma_o) \sin (\alpha_1 - \beta_o) \qquad \text{(G-13)}$$

$$\cos (\alpha_1 - \alpha_o + \beta_1 - \beta_o) - \frac{1}{K_3} [\cos (\alpha_1 + \beta_1) - \cot \gamma_1 \sin (\alpha_1 + \beta_1)]$$

$$= \cot (\gamma_1 - \gamma_o) \sin (\alpha_1 - \alpha_o + \beta_1 - \beta_o) \qquad \text{(G-14)}$$

By dividing (G-13) by (G-14) the factor cos $(\gamma_1 - \gamma_o)$ is eliminated and the result can be solved for γ_1, the angle for straight line return.

$$\gamma_1 = \tan^{-1} \frac{K_2 \sin A \sin B - K_3 \sin \alpha_1 \sin C}{K_2 \sin B(\cos A - K_3 \cos C) + K_3 \sin C (K_2 \cos B - \cos \alpha_1)} \qquad \text{(G-15)}$$

where

$$A = \alpha_1 + \beta_1$$

$$B = \alpha_1 - \alpha_o$$

$$C = \alpha_1 - \alpha_o + \beta_1 - \beta_o$$

$$K_2 = \frac{R_2}{R_1}$$

$$K_3 = \frac{R_3}{R_1}$$

APPENDIX H

FORTRAN PROGRAMS FOR SECTION 7-4

(AN EXAMPLE)

1. ARITHMATIC MEAN

```
      DIMENSION ALF(10),AX(10),AY(10),X(10),Y(10),TAN(10)
      PRINT 103
  103 FORMAT(1H1,9X,10HINPUT DATA///)
      DO 201 I=1,10
      READ 202,X(I),Y(I),ALF(I)
  202 FORMAT(2F6.1,F9.4)
      ALF(I)=ALF(I)/57.3
      B=ALF(I)
      TAN(I)=SIN(B)/COS(B)
  201 PRINT 204,X(I),Y(I),ALF(I),TAN(I)
  204 FORMAT(4X,2F7.1,4X,F15.8,4X,F15.8/)
      PRINT 220
  220 FORMAT(1H1,9X,6HOUTPUT///)
      TX=0.0
      TY=0.0
      M=0
      N=1
  205 M=M+1
      N=N+1
      IF(M.EQ.10) GO TO 206
      DO 207 I=N,10
      DE=TAN(M)-TAN(I)
      TR=Y(I)-X(I)*TAN(I)
      TS=Y(M)-X(M)*TAN(M)
      AX(I)=(TR-TS)/DE
      AY(I)=(TR*TAN(M)-TS*TAN(I))/DE
      TX=TX+AX(I)
      TY=TY+AY(I)
  207 PRINT 209,X(I),Y(I),AX(I),AY(I)
  209 FORMAT(4X,2F7.1,4X,E15.8,4X,F15.8/)
      GO TO 205
  206 AMX=TX/45.0
      AMY=TY/45.0
      PRINT 208,AMX,AMY
  208 FORMAT(10X,F15.8,4X,E15.8)
      CALL EXIT
      END
```

2. LEAST SQUARE SOLUTION ERROR REGRESSION

```
      DIMENSION A(10,2),R(2,2),C(2,10)
      DIMENSION T(2,10),B(10,1),Z(2,1)
      DIMENSION X(10),Y(10),ALPH(10),AE(2,2),AI(2,2)
      DO 4 I=1,10
    2 READ 3,X(I),Y(I),ALPH(I)
    3 FORMAT(2F6.1,F9.4)
      A(I,1)=1.0
      A(I,2)=-TAN(ALPH(I)*3.142/180.0)
    4 B(I,1)=Y(I)-X(I)*TAN(ALPH(I)*3.142/180.0)
      PRINT 6,(X(I),Y(I),ALPH(I),A(I,1),A(I,2),B(I,1),I=1,10
    6 FORMAT (1H0,6E16.9)
      DO 20 I=1,2
      DO 20 J=1,10
   20 C(I,J)=A(J,I)
      DO 21 I=1,2
      DO 21 J=1,2
      R(I,J)=0.0
      DO 21 K=1,10
   21 R(I,J)=R(I,J)+C(I,K)*A(K,J)
      DO 22 I=1,2
      DO 22 J=1,2
   22 AE(I,J)=R(I,J)
      D=AE(1,1)*AE(2,2)-AE(1,2)*AE(2,1)
      AI(1,1)=AE(2,2)/D
      AI(1,2)=-AE(1,2)/D
      AI(2,1)=-AE(2,1)/D
      AI(2,2)=AE(1,1)/D
      DO 23 I=1,2
      DO 23 J=1,10
      T(I,J)=0.0
      DO 23 K=1,2
   23 T(I,J)=T(I,J)+AI(I,K)*C(K,J)
      I=1
      DO 24 J=1,2
      Z(J,I)=0.0
      DO 24 K=1,10
   24 Z(J,I)=Z(J,I)+T(J,K)*B(K,I)
      PRINT 5,(Z(I,1),I=1,2)
    5 FORMAT(1H0,5X,F8.3)
      CALL EXIT
      END
```

3. KALMAN ESTIMATION

```
      DIMENSION P(2,2),PI(2,2),HT(2,1),HTRI(2,1)
      DIMENSION H(1,2),AMI(2,2),HTR(2,1),DCPXY(2,1)
      DIMENSION CKD(2,1),HP(1,2),HPHT(1,1),PHT(2,1)
      DIMENSION DEAF(1,1),DLFHD(1,1),R(1,1),RI(1,1)
      DIMENSION HTRIH(2,2),AM(2,2),CK(2,1),HD(1,1)
      DIMENSION PB(2,1),PBHP(2,2),BM(1,1),BMI(1,1)
      DIMENSION L(2),M(2),PA(2,2),AE(2,2)
      READ 1,X1,Y1,X2,Y2,ALFI,ALFII
    1 FORMAT(4F6.1,2F9.4)
      ALF1=ALFI/57.3
      ALF2=ALFII/57.3
      TAN1=SIN(ALF1)/COS(ALF1)
      TAN2=SIN(ALF2)/COS(ALF2)
      PRINT 68,TAN1,TAN2
   68 FORMAT(1H1,3X,E15.8,4X,E15.8/)
      DEN=TAN1-TAN2
      TR1=Y2-X2*TAN2
      TR2=Y1-X1*TAN1
      CPX2=(TR1-TR2)/DEN
      CPY2=(TR1*TAN1-TR2*TAN2)/DEN
      PRINT 2,CPX2,CPY2
    2 FORMAT(4X,E15.8,4X,E15.8/)
      A=((X2-X1)*TAN2-(Y2-Y1))/(DEN*COS(ALF1))**2
      B=((Y2-Y1)-(X2-X1)*TAN1)/(DEN*COS(ALF2))**2
      AP=((X2-X1)*TAN2-(Y2-Y1))*TAN2/(DEN*COS(ALF1))**2
      BP=((Y2-Y1)-(X2-X1)*TAN1)*TAN1/(DEN*COS(ALF2))**2
      P(1,1)=0.01*(A**2+B**2)
      P(1,2)=0.01*(A*AP+B*BP)
      P(2,1)=P(1,2)
      P(2,2)=0.01*(AP**2+BP**2)
      PA(1,1)=P(1,1)
      PA(1,2)=P(1,2)
      PA(2,1)=P(2,1)
      PA(2,2)=P(2,2)
      D1=PA(1,1)*PA(2,2)-PA(1,2)*PA(2,1)
      IF(D1.EQ.0.0) GO TO 45
      PI(1,1)=PA(2,2)/D1
      PI(1,2)=-PA(1,2)/D1
      PI(2,1)=-PA(2,1)/D1
      PI(2,2)=PA(1,1)/D1
      DO 33 J=1,2
   33 PRINT 123,PI(J,1),PI(J,2)
  123 FORMAT(4X,2E15.8)
      DO 11 I=1,2
   11 PRINT 3,P(I,1),P(I,2)
    3 FORMAT(4X,2E15.8)
      R(1,1)=0.01
      RI(1,1)=1.0/R(1,1)
```

```
      DCPXY(1,1)=0.0
      DCPXY(2,1)=0.0
   88 READ 4,X,Y,ALFME,K
    4 FORMAT(2F6.1,F9.4,I1)
      IF(K.EQ.9) GO TO 99
      ALFM=ALFME/57.3
      AY=Y-CPY2
      AX=X-CPX2
      ALFC=ATAN2(AY,AX)
      PRINT 22,AX,AY,ALFC
   22 FORMAT(1H1,3X,3E15.8/)
      IF(ALFME.GT.180.0) ALFM=(-360.0+ALFME)/57.3
      DALF=ALFM-ALFC
      DIFD=(ALFM-ALFC)*57.3
      PRINT 58,DALF,DIFD
   58 FORMAT(4X,E15.8,2X,E15.8/)
      SMLR=SQRT(AX**2+AY**2)
      H(1,1)=SIN(ALFC)/SMLR
      H(1,2)=-COS(ALFC)/SMLR
      HT(1,1)=H(1,1)
      HT(2,1)=H(1,2)
      DO 81 I=1,2
   81 HTRI(I,1)=HT(I,1)*RI(1,1)
      HTRIH(1,1)=HTRI(1,1)*H(1,1)
      HTRIH(1,2)=HTRI(1,1)*H(1,2)
      HTRIH(2,1)=HTRI(2,1)*H(1,1)
      HTRIH(2,2)=HTRI(2,1)*H(1,2)
      DO 82 I=1,2
      DO 82 J=1,2
   82 AM(I,J)=PI(I,J)+HTRIH(I,J)
      DO 9 I=1,2
      DO 9 J=1,2
    9 AE(I,J)=AM(I,J)
      D2=AE(1,1)*AE(2,2)-AE(1,2)*AE(2,1)
      IF(D2.EQ.0.0) GO TO 47
      AMI(1,1)=AE(2,2)/D2
      AMI(1,2)=-AE(1,2)/D2
      AMI(2,1)=-AE(2,1)/D2
      AMI(2,2)=AE(1,1)/D2
      PRINT 64,HTRIH(1,1),HTRIH(1,2),AMI(1,1),AMI(1,2)
   64 FORMAT(4X,E15.8,2X,E15.8,2X,E15.8,2X,E15.8/)
      PRINT 66,HTRIH(2,1),HTRIH(2,2),AMI(2,1),AMI(2,2)
   66 FORMAT(4X,E15.8,2X,E15.8,2X,E15.8,2X,E15.8//)
      DO 83 I=1,2
   83 HTR(I,1)=HT(I,1)*RI(1,1)
      DO 84 I=1,2
   84 CK(I,1)=AMI(I,1)*HTR(1,1)+AMI(I,2)*HTR(2,1)
      HD(1,1)=H(1,1)*DCPXY(1,1)+H(1,2)*DCPXY(2,1)
      DLFHD(1,1)=DALF-HD(1,1)
      DO 85 I=1,2
   85 CKD(I,1)=CK(I,1)*DLFHD(1,1)
```

```
      DO 86 I=1,2
   86 DCPXY(I,1)=CKD(I,1)+DCPXY(I,1)
      HP(1,1)=H(1,1)*P(1,1)+H(1,2)*P(2,1)
      HP(1,2)=H(1,1)*P(1,2)+H(1,2)*P(2,2)
      HPHT(1,1)=HP(1,1)*HT(1,1)+HP(1,2)*HT(2,1)
      BM(1,1)=R(1,1)+HPHT(1,1)
      BMI(1,1)=1.0/BM(1,1)
      PHT(1,1)=P(1,1)*HT(1,1)+P(1,2)*HT(2,1)
      PHT(2,1)=P(2,1)*HT(1,1)+P(2,2)*HT(2,1)
      DO 89 I=1,2
   89 PB(I,1)=PHT(I,1)*BMI(1,1)
      PBHP(1,1)=PB(1,1)*HP(1,1)
      PBHP(1,2)=PB(1,1)*HP(1,2)
      PBHP(2,1)=PB(2,1)*HP(1,1)
      PBHP(2,2)=PB(2,1)*HP(1,2)
      DO 19 I=1,2
      DO 19 J=1,2
   19 P(I,J)=P(I,J)-PBHP(I,J)
      PRINT 5,DCPXY(1,1),DCPXY(2,1)
    5 FORMAT(4X,E15.8,2X,E15.8/)
      PRINT 44,P(1,1),P(1,2)
   44 FORMAT(4X,E15.8,2X,E15.8/)
      PRINT 29,P(2,1),P(2,2)
   29 FORMAT(4X,E15.8,2X,E15.8///)
      GO TO 88
   45 PRINT 39
   39 FORMAT(20X,21HD=0 PI CANNOT PERFORM)
      GO TO 99
   47 PRINT 49
   49 FORMAT(20X,22HD=0 AMI CANNOT PERFORM)
   99 PRINT 77
   77 FORMAT(1H1,20HEND OF JOB THANK YOU)
      CALL EXIT
      END
C FORM OF INPUT DATA X1,Y1,X2,Y2,ALFI,ALFII
   2.0    1.0    4.0   -2.0   26.7047 -26.5795
C FORM OF INPUT DATA X(K),Y(K),ALFME(K),K
  -2.0    8.0 103.8340
  -5.0   -2.0 202.0022
   6.0    8.0  53.1393
   2.0    5.0  68.2511
  -6.0    6.0 135.0673
   5.0   -6.0 -50.3190
  -6.0  -10.0 239.1266
  -5.0    1.0 168.6730
```

INPUT DATA

LANDMARK POSITION L1 X = 2.0 Y = 1.0 (KILOMETERS)
L2 X = 4.0 Y = -2.0
L3 X = -2.0 Y = 8.0
L4 X = -5.0 Y = -2.0
L5 X = 6.0 Y = 8.0
L6 X = 2.0 Y = 5.0
L7 X = -6.0 Y = 6.0
L8 X = 5.0 Y = -6.0
L9 X = -6.0 Y = -10.0
L10 X = -5.0 Y = 1.0

MEASURED ANGLE ALPHA 01 = 26.7047 (DEGREES)
02 = -26.5795
1 = 103.8340
2 = 202.0022
3 = 53.1393
4 = 68.2511
5 = 135.0673
6 = 50.3100
7 = 239.1266
8 = 168.6730

RESULTS

ACTUAL POSITION X = 0.0 Y = 0.0

ESTIMATED POSITION BY

1. ARITHMETIC MEAN X = 0.00215 Y = 0.00532

2. LEAST SQUARE SOLUTION REGRESSION
X = -0.015 Y = -0.00

3. KALMAN ESTIMATION
INITIAL ESTIMATION X = 0.00708 Y = -0.00245
SEQUENTIAL ESTIMATION
L1 X = -0.00447 Y = -0.00638
L2 X = -0.00648 Y = -0.00364
L3 X = -0.00582 Y = -0.00354
L4 X = -0.00152 Y = -0.00256
L5 X = 0.00170 Y = -0.00119
L6 X = 0.00687 Y = 0.00093
L7 X = 0.00323 Y = 0.00026
L8 X = 0.00183 Y = -0.00061

DISTRIBUTION LIST

George C. Marshall Space Flight Center
National Aeronautics and Space Administration
Huntsville, Alabama 35812

A&TS-PR-M
A&TS-MS-IL
A&TS-TU
A&TS-MS-I (2)
PD-AP (4) J. Belew, c/o N. Neudatschin, S&E-ASTR-SGN
S&E-ASTR-ZI
S&E-ASTR-SGD (12)
Mr. N. Neudatschin, S&E-ASTR-SGD
Mr. M. Brooks, S&E-ASTR-SG
Mr. W. B. Chubb, S&E-ASTR-SGD
Mr. P. W. Davis, S&E-ASTR-GM
Mr. Z. Thompson, S&E-ASTR-NE
Mr. Wojtalik, S&E-ASTR-S
Mr. J. E. Blanton, S&E-ASTR-SG
Mr. F. B. Moore, S&E-ASTR-DIR
Mr. W. P. Horton, S&E-ASTR-DIR
Mr. R. E. Currie, PD-AP-L
Mr. B. J. Doran, S&E-ASTR-GD
Mr. J. C. Blair, S&E-AERO-GO
Mr. F. L. Vinz, S&E-COMP-S

Auburn University

Dr. J. D. Irwin

The University of Tennessee

Mr. J. S. Miller
Mr. J. E. Bennett
Mr. C. Chen
Mr. H. J. Holley
Dr. J. C. Hung (30)
Dr. J. M. Bailey, Industrial Engineering